

Old Dominion University

ODU Digital Commons

Theses and Dissertations in Biomedical
Sciences


College of Sciences

Spring 1993

Competitive Enzyme Immunoassay by Polyclonal Antibodies Against Organophosphorus Pesticides

Kuo-Lan Wen
Old Dominion University

Follow this and additional works at: https://digitalcommons.odu.edu/biomedicalsciences_etds

 Part of the [Biomedical Engineering and Bioengineering Commons](#), and the [Medical Immunology Commons](#)

Recommended Citation

Wen, Kuo-Lan. "Competitive Enzyme Immunoassay by Polyclonal Antibodies Against Organophosphorus Pesticides" (1993). Doctor of Philosophy (PhD), dissertation, Chemistry and Biochemistry, Old Dominion University, DOI: 10.25777/2n72-6d44
https://digitalcommons.odu.edu/biomedicalsciences_etds/145

This Dissertation is brought to you for free and open access by the College of Sciences at ODU Digital Commons. It has been accepted for inclusion in Theses and Dissertations in Biomedical Sciences by an authorized administrator of ODU Digital Commons. For more information, please contact digitalcommons@odu.edu.

**COMPETITIVE ENZYME IMMUNOASSAY
BY POLYCLONAL ANTIBODIES
AGAINST ORGANOPHOSPHORUS PESTICIDES**

by

Kuo-Lan Wen

B.S. June 1988, National Taiwan University

A Dissertation Submitted to the Faculty of Old
Dominion University and Eastern Virginia Medical
School in Partial Fulfillment of the Degree of

DOCTOR OF PHILOSOPHY

BIOMEDICAL SCIENCE

OLD DOMINION UNIVERSITY

May, 1993

Approved by:

Dr. James H. Yuan, Director //

Dr. Mark S. Elliott

Dr. Gerald J. Pepe

Dr. Lloyd Wolfenbarger, Jr.

ABSTRACT

COMPETITIVE ENZYME IMMUNOASSAY BY POLYCLONAL ANTIBODIES AGAINST ORGANOPHOSPHORUS PESTICIDES

Kuo-Lan Wen
Old Dominion University, 1993
Director: Dr. James H. Yuan

Organophosphorus compounds (OPs) comprise one of the major classes of pesticides in use today because they are highly effective and less toxic. Because of their extensive use, there is a need for monitoring OPs in water and vegetables. Gas chromatography (GC) is the usual method for OPs screening, but it is time-consuming and has the high cost of instrumentation. The goal of this project was to find an easy method which was sensitive and had less instrumentation required to test OPs.

Microwells and microtubes were utilized as the solid-phase immobilization for the development of an enzyme immunoassay for OPs. A sensitive and simple microtube based competition enzyme immunoassay for the quantitative determination of organophosphorus compounds was developed. Malathion (phosphorodithioate), parathion (phosphorothionate), tamaron (phosphorothiolate) and mevinphos (phosphate ester) were chosen as the antigens for the antibody production. Gamma globulins were isolated from whole anti-sera by DEAE-cellulose chromatography. A carbodiimide coupling

method was utilized to prepare the organophosphorus compound-peroxidase conjugates (OP-HRPO). Microtubes coated with antibody were incubated with analyte and OP-HRPO conjugate. The assay was performed within 20 minutes at room temperature, utilizing the competitive reaction of the analyte and the OP-HRPO, which produces more color, when less analyte is present.

Due to the high cross-reactivity of the different OPs to the antibodies and the low cross-reactivity of the different secondary metabolites (dimethyl phosphite, p-nitrophenol, ethyl propionate and methyl isobutyrate) to the antibodies, two of the immunoassay tests were conducted to be nonspecific which enabled them to act as a general screening method for OPs.

The assays of these four classes of OPs when compared to GC had the correlation coefficients ranging from 0.912 to 0.999 in water samples and from 0.949 to 0.999 in vegetable extract screening, which can be adapted to field testing.

The reproducibility of the immunoassay in the detection of OP residues in water and vegetable samples with the percent coefficients of variation (%CV) for the organophosphorus compounds assays ranged from 51.59% to 14.06% at 1 ng/mL and 6.03% to 4.34% at 100 ng/mL. The CVs of 1 ng/mL appeared to be high since they were below or close to the detection limit.

DEDICATION

Dedicated, with love, to my dearest parents

C. J. and Lena L. Wen

whose love, support and encouragement

helped me through the my entire education.

ACKNOWLEDGEMENT

This is to gratefully acknowledge the supervision, guidance and encouragement of Dr. James H. Yuan through the research. I would like to sincerely thank the research committee members, Dr. Mark S. Elliott, Dr. Gerald J. Pepe and Dr. Lloyd Wolfinbarger, Jr. for the hours they spent on reviewing my work and providing the precious suggestions. Thanks is also given to the Institute of Pathology in Taipei for leading me to the world of pesticides and the Institute of Pesticide Residues in Taiwan for helping me through the validation study of the research project.

I especially thank my husband, Michael T. Tseng, and my brother, Kuo-Kuang Wen, and my dearest friend, Sandra B. Ward, for their love and encouragement which helped me through several emotional periods to regain control and finally finish my Ph. D. degree.

The final acknowledgement is to my special friends, Dr. C. K. Chiang, Hui-Mei Tseng, Chin-Ling Hsu, Dr. Tony D. T. and Cheryl L. Chen, and Pi-Hsia Fan for their encouragement and consideration.

TABLE OF CONTENTS

	Page
LIST OF TABLES	iv
LIST OF FIGURES	v
 Chapter	
I. INTRODUCTION	1
A. Background	1
B. Statement of problem	25
II. EXPERIMENTAL	26
A. Materials	26
B. Equipment	27
C. Methods	28
1. Preparation of the microwells for titer assays	28
2. Preparation of DEAE-cellulose resins	28
3. Isolation of gamma globulin fraction from the whole antiserum	29
4. Electrophoresis	29
5. Preparation of the assay solutions	30
6. Preparation of organophosphate-peroxidase	31
7. Preparation of organophosphorus pesticide standard solutions	31
8. Preparation of gamma globulin coated microwells and polystyrene tubes	32
9. The organophosphorus compounds assays procedures . .	33
10. Study of cross reaction	34
11. Assay validation (water and vegetable samples)	34

TABLE OF CONTENTS (Continued)

III. RESULTS	36
A. Preparation of antisera	36
1. Preparation of antigens	36
2. Immunization of rabbit	38
3. Titer assay of the antisera by solid-phase enzyme linked immunosorbent assay	39
4. Isolation of the gamma globulin from the whole anti-serum	40
B. Study of OP assay on the microwells	50
1. Study of the optimal enzyme dilutions for the OP assay	50
2. Study of the optimal concentration of gamma globulin for the microwell coating	56
3. Study of the antigen and OP-HRPO quantitations for malathion, parathion, tamaron and mevinphos in the competitive enzyme immunoassay on microwell immobilization	61
4. Study of the optimal OVA concentrations for malathion, parathion, tamaron and mevinphos in the competitive enzyme immunoassay on microwell immobilization	67
5. Study of the competitive enzyme immunoassays for malathion, parathion, tamaron and mevinphos on microwells	72
C. Study of the parathion and mevinphos assays on disposable cuvettes	77
D. Screening of various brands of polystyrene tubes	81
1. Capacity study of different brands of polystyrene tubes	81
2. Study of parathion and mevinphos assays on polystyrene tubes from Evergreen and Fisher	83

TABLE OF CONTENTS (Continued)

E. Development of the competitive enzyme immunoassay for malathion, parathion, tamaron and mevinphos on microtubes	83
1. Development of the optimal reaction ratio of OP to OP-HRPO	83
2. Study of the optimal enzyme dilution	90
3. Study of the optimal incubation time	97
4. Study of the optimal incubation temperature	97
5. Selection of the incubation solution	106
6. Determination of pH condition of the OP assays	112
7. Study of the relationship of the color development and enzyme-substrate-chromogen results	117
F. Study of the performance characteristics	127
1. Study limit of detections	127
2. Precision study	127
3. Study of the cross reaction	128
a. Study of the cross reaction against the other OPs	128
b. Study of the cross reaction of the metabolite analogues	130
G. Study of the validation of the EIA method	133
1. Study the validation on water samples	133
2. Study the validation on vegetable samples	138
3. Reproducibility study	141
IV. DISCUSSION	144
A. Hapten preparation	145
B. Production and purification of antibody	150
C. Immunoassay	153
D. Sample preparation and analysis	160

TABLE OF CONTENTS (Continued)

LIST OF REFERENCES 164

List of Tables

Table	Page
1. Titer assay studies of anti-malathion, anti-parathion, anti-tamaron and anti-mevinphos sera	45
2. Summary of the assay condition of the homogeneous enzyme immunoassay on microwell immobilization of malathion, parathion, tamaron and mevinphos	78
3. Binding capacity study of different brands of polystyrene tubes	82
4. Summary of the assay condition of the homogeneous enzyme immunoassay on microtube immobilization of malathion, parathion, tamaron and mevinphos	122
5. Precision studies of malathion, parathion, tamaron and mevinphos assays	129
6. Cross reactivity studies of different organophosphorus compounds	131
7. Cross reactivity studies of the metabolites of organophosphorus compounds	134
8. Comparison of the GC and EIA methods for the determination of organophosphorus compounds in water samples	137
9. Comparison of the GC and EIA methods for the determination of organophosphorus compounds in vegetable samples	139
10. Reproducibility of the OPs immunoassay on OP-fortified water and vegetable samples	142

List of Figures

Figure	Page
1. The diagram of mammalian nervous system	6
2. The diagram of insect nervous system	7
3. The hydrolysis scheme of acetylcholine and organophosphorus compounds on acetylcholinesterase	10
4. Principle of Homogeneous enzyme immunoassay: (enzyme-multiplied immunoassay technique, EMIT)	20
5. Heterogeneous enzyme immunoassay: competition principle . . .	22
6. Heterogeneous enzyme immunoassay: non-competition principle	23
7. Structures of four kinds of organophosphorus compounds	37
8. The titer assay study of anti-malathion by solid-phase enzyme linked immunosorbent assay on microwell immobilization . . .	41
9. The titer assay study of anti-parathion by solid-phase enzyme linked immunosorbent assay on microwell immobilization . . .	42
10. The titer assay study of anti-tamaron by solid-phase enzyme linked immunosorbent assay on microwell immobilization . . .	43
11. The titer assay study of anti-mevinphos by solid-phase enzyme linked immunosorbent assay on microwell immobilization . . .	44
12. The elution profile of anti-malathion from DEAE-cellulose ion-exchange chromatography	46
13. The elution profile of anti-parathion from DEAE-cellulose ion-exchange chromatography	47
14. The elution profile of anti-tamaron from DEAE-cellulose ion-exchange chromatography	48

List of Figures (Continued)

15. The elution profile of anti-mevinphos from DEAE-cellulose ion-exchange chromatography	49
16. The electrophoretic patterns of gamma globulins isolated from DEAE-cellulose ion-exchange chromatography	51
17. Optimization of malathion-HRPO dilution in malathion assay in solid-phase enzyme immunoassay on microwell immobilization	52
18. Optimization of parathion-HRPO dilution in parathion assay in solid-phase enzyme immunoassay on microwell immobilization	53
19. Optimization of tamaron-HRPO dilution in tamaron assay in solid-phase enzyme immunoassay on microwell immobilization	54
20. Optimization of mevinphos-HRPO dilution in mevinphos assay in solid-phase enzyme immunoassay on microwell immobilization	55
21. Saturation curve of anti-malathion gamma globulins in malathion assay in solid-phase enzyme immunoassay on microwell immobilization	57
22. Saturation curve of anti-parathion gamma globulins in parathion assay in solid-phase enzyme immunoassay on microwell immobilization	58
23. Saturation curve of anti-tamaron gamma globulins in tamaron assay in solid-phase enzyme immunoassay on microwell immobilization	59
24. Saturation curve of anti-mevinphos gamma globulins in mevinphos assay in solid-phase enzyme immunoassay on microwell immobilization	60

List of Figures (Continued)

25. Study of malathion and malathion-HRPO quantitations for the malathion solid-phase enzyme immunoassay on microwell immobilization	62
26. Study of parathion and parathion-HRPO quantitations for the parathion solid-phase enzyme immunoassay on microwell immobilization	63
27. Study of tamaron and tamaron-HRPO quantitations for the tamaron solid-phase enzyme immunoassay on microwell immobilization	64
28. Study of mevinphos and mevinphos-HRPO quantitations for the mevinphos solid-phase enzyme immunoassay on microwell immobilization	65
29. OVA blocking study of the malathion solid-phase enzyme immunoassay on microwell immobilization	68
30. OVA blocking study of the parathion solid-phase enzyme immunoassay on microwell immobilization	69
31. OVA blocking study of the tamaron solid-phase enzyme immuncassay on microwell immobilization	70
32. OVA blocking study of the mevinphos solid-phase enzyme immunoassay on microwell immobilization	71
33. Standard curve of the malathion solid-phase enzyme immunoassay on microwell immobilization	73
34. Standard curve of the parathion solid-phase enzyme immunoassay on microwell immobilization	74
35. Standard curve of the tamaron solid-phase enzyme immunoassay on microwell immobilization	75
36. Standard curve of the mevinphos solid-phase enzyme immunoassay on microwell immobilization	76

List of Figures (Continued)

37. Standard curve study of parathion solid-phase enzyme immunoassay on disposable cuvette immobilization	79
38. Standard curve studies of mevinphos solid-phase enzyme immunoassay on disposable cuvette immobilization	80
39. Standard curve study of parathion solid-phase enzyme immunoassay on selected polystyrene tubes	84
40. Standard curve study of mevinphos solid-phase enzyme immunoassay on selected polystyrene tubes	85
41. Study of malathion and malathion-HRPO quantitations for the malathion solid-phase immunoassay on microtube immobilization	87
42. Study of parathion and parathion-HRPO quantitations for the parathion solid-phase immunoassay on microtube immobilization	88
43. Study of tamaron and tamaron-HRPO quantitations for the tamaron solid-phase immunoassay on microtube immobilization	89
44. Study of mevinphos and mevinphos-HRPO quantitations for the malathion solid-phase immunoassay on microtube immobilization	91
45. Optimization of enzyme dilution study of malathion-HRPO in the malathion solid-phase enzyme immunoassay on microtube immobilization	93
46. Optimization of enzyme dilution study of parathion-HRPO in the parathion solid-phase enzyme immunoassay on microtube immobilization	94
47. Optimization of enzyme dilution study of tamaron-HRPO in the tamaron solid-phase enzyme immunoassay on microtube immobilization	95

List of Figures (Continued)

48. Optimization of enzyme dilution study of mevinphos-HRPO in the mevinphos solid-phase enzyme immunoassay on microtube immobilization	96
49. Effect of two different incubation time for malathion solid-phase enzyme immunoassay on microtube immobilization	98
50. Effect of two different incubation time for parathion solid-phase enzyme immunoassay on microtube immobilization	99
51. Effect of two different incubation time for tamaron solid-phase enzyme immunoassay on microtube immobilization	100
52. Effect of two different incubation time for mevinphos solid-phase enzyme immunoassay on microtube immobilization	101
53. Effect of three different incubation temperature for the malathion solid-phase enzyme immunoassay on microtube immobilization	102
54. Effect of three different incubation temperature for the parathion solid-phase enzyme immunoassay on microtube immobilization	103
55. Effect of three different incubation temperature for the tamaron solid-phase enzyme immunoassay on microtube immobilization	104
56. Effect of three different incubation temperature for the mevinphos solid-phase enzyme immunoassay on microtube immobilization	105
57. Effect of different incubation buffers for the malathion solid-phase enzyme immunoassay on microtube immobilization	108

List of Figures (Continued)

58. Effect of different incubation buffers for the parathion solid-phase enzyme immunoassay on microtube immobilization	109
59. Effect of different incubation buffers for the tamaron solid-phase enzyme immunoassay on microtube immobilization	110
60. Effect of different incubation buffers for the mevinphos solid-phase enzyme immunoassay on microtube immobilization	111
61. Effect of different incubation pH conditions for the malathion solid-phase enzyme immunoassay on microtube immobilization	113
62. Effect of different incubation pH conditions for the parathion solid-phase enzyme immunoassay on microtube immobilization	114
63. Effect of different incubation pH conditions for the tamaron solid-phase enzyme immunoassay on microtube immobilization	115
64. Effect of different incubation pH conditions for the mevinphos solid-phase enzyme immunoassay on microtube immobilization	116
65. Standard curve of the malathion solid-phase enzyme immunoassay on microtube immobilization	118
66. Standard curve of the parathion solid-phase enzyme immunoassay on microtube immobilization	119
67. Standard curve of the tamaron solid-phase enzyme immunoassay on microtube immobilization	120
68. Standard curve of the mevinphos solid-phase enzyme immunoassay on microtube immobilization	121

List of Figures (Continued)

69. Color development time study in malathion solid-phase enzyme immunoassay on microtube immobilization	123
70. Color development time study in parathion solid-phase enzyme immunoassay on microtube immobilization	124
71. Color development time study in tamaron solid-phase enzyme immunoassay on microtube immobilization	125
72. Color development time study in mevinphos solid-phase enzyme immunoassay on microtube immobilization	126
73. The mixed-anhydride procedure for conjugation of amine-containing hapten to protein	148
74. The carbodiimide procedure for conjugation of nucleophilic hapten to protein	149

Chapter I

INTRODUCTION

A. Background

The worldwide steady expansion of population demands increases in food production, attention to public health, and protection of the environment. Pests harm crops and transmit diseases and thus their control becomes an integral part of the development of every country. Since the invention of dichlorodiphenyl-trichloroethane (DDT) in 1930 [1], the pesticides have changed human life. Because the chemical control of pests has been so successful, there has been an explosive expansion in the development of synthetic organic pesticides. More than a thousand pesticides are in common use. Organochlorine compounds, organophosphorus compounds and carbamates are the most used pesticides around the world.

Organophosphorus compounds are very toxic due to excess stimulation of cholinergic nerves and the inhibition of acetylcholinesterase by the formation of phosphorylated acetylcholinesterase. The hydrophobicity is less than that of the organochlorine compounds, and the half-life in water is less than six weeks; therefore, the tendency to accumulate in the body is very rare. Organochlorine compounds are persistent in soil and most biological media. These compounds tend to accumulate in the adipose tissue since they are highly hydrophobic; however, they produce no toxic effects there. Some of the organochlorine

compounds are less toxic than organophosphorus compounds and carbamates, but the organochlorine compounds have greater potential for chronic toxicity.

The mode of action of the organochlorine compounds is not yet clear.

Different toxic effects were observed with different types of organochlorine compounds primarily due to their differences in chemical structure. For example, DDT, an antecedent of all pesticides, its toxic action is found to block the sodium-potassium channel in the membrane and thus interferes with nerve impulse transmission [2], and also increase estrogen production in birds [3]. Different toxic effects among the isomers of benzene hexachloride (BHC), an organochlorine compound, were observed. The γ -isomer of benzene hexachloride (BHC) can stimulate the mammalian nervous system, resulting in a rise in blood pressure, a fall in the rate of heartbeat and an irregular encephalogram, while β -and δ -isomers of BHC are depressants of the mammalian nervous system and may partially eliminate the effects of the γ -isomer [4].

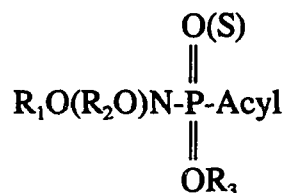
Carbamates, another type of insecticide, are generally less toxic than organophosphorus compounds especially for the dermal exposure. The detoxification of carbamate pesticides, similar to that of organophosphorus compounds, is carried out by the liver microsomal NADPH-dependent mixed-function oxidase. Similar to the action of organophosphorus compounds, the mode of action of the carbamates is the inhibition of acetylcholinesterase by the formation of

carbamylated acetylcholinesterase intermediate [5, 6]. Due to the larger rate constant observed in the reversed hydrolysis of the carbamylated acetylcholinesterase intermediate, the toxicity of carbamates is generally less than that of the organophosphorus compound. This is consistent with the report that the reversal of the carbamylated enzyme has a turnover number five folds of that reported for the organophosphorus compounds (a turnover number of 0.04 per acetylcholinesterase molecule compared to 0.008 of organophosphorus compounds) [7, 8, 9].

Among these three classes of pesticides the organophosphorus compounds are most widely used, especially in the developing and underdeveloped countries. Pesticides are extensively used in agriculture worldwide. Except for the organochlorine compounds, most of these chemicals persist for only a few weeks to several months in the environment. However, as a result of the continuous use of pesticides, appreciable quantities of insecticide residues and their degradation products accumulate in the biota. The monitoring of residues in the environment as well as food products has become an extremely important aspect of insecticide technology and application.

Organophosphorus compounds were first synthesized by Saunders in England and by Schrader in Germany during World War II. Saunders synthesized nerve poisons, including diisopropyl phosphorofluoridate (DFP) [10];

Schrader and his co-workers found insecticidal activity in some organophosphorus compounds of the general formula [11]:



where R_1 , R_2 , and R_3 are alkyl groups, and "acyl" is an inorganic or organic acid radical such as Cl, F, SCN, and CH_3COO . In 1941, Schrader found a systemic insecticide, octamethyl-pyrophosphoramidate (OMPA), which was later named schradan after its discoverer [13]. He also discovered a number of pesticidal organophosphorus esters, including the first practical insecticide named "Bladan," which contained tetraethyl pyrophosphate (TEPP) and was marketed in Germany in 1944. The great advancements in agricultural practice and scientific knowledge on the structural-activity relationship of organophosphorus pesticides were achieved by the discovery of compound No. 605 (parathion, diethyl p-nitrophenyl phosphorothionate) by Schrader in 1944 [10]. Although parathion itself is extremely toxic to mammals as well as to insects, many less toxic pesticides have been developed by slight structural modifications; for instance, chlorthion [13], fenthion [14], and fenitrothion [15] were discovered in 1952, 1958, and 1959, respectively.

More than 50,000 organophosphorus compounds have been synthesized and tested for pesticidal activity. But the number actually employed for this purpose today probably does not exceed three dozen. Organophosphorus pesticides are among the most toxic of all substances that cause poisoning in humans and are also the most frequently encountered insecticide poisons [16].

The inhibitory activity of organophosphorus esters against cholinesterase was first found in 1941 by Adrian and his co-workers [17]. Subsequently, it was reported that the inhibition could be attributed to the phosphorylation of the active site as demonstrated by the reaction of DFP with chymotrypsin [18]. The target of organophosphorus esters inhibition, including nerve gas and pesticides, is acetylcholinesterase, an enzyme which catalyzed the hydrolysis of acetylcholine to form choline and acetate. Acetylcholine is the major transmitter of nerve impulses at the endings of postganglionic parasympathetic nerve fibers, of somatic motor nerves to skeletal muscle, of preganglionic fibers of both parasympathetic and sympathetic nerves, and certain synapses in the central nervous system. The diagrams of mammalian and insect nervous systems are shown on Figures 1 and 2. The receptors of acetylcholine are found widely distributed among various tissues; such as the muscarinic receptors which are on smooth muscle, heart and exocrine glands, the nicotinic receptors which are on the endings of motor nerves of skeletal muscle, autonomic ganglia, and central nervous system. The inhibition of

Figure 1

Diagram of mammalian nervous system.

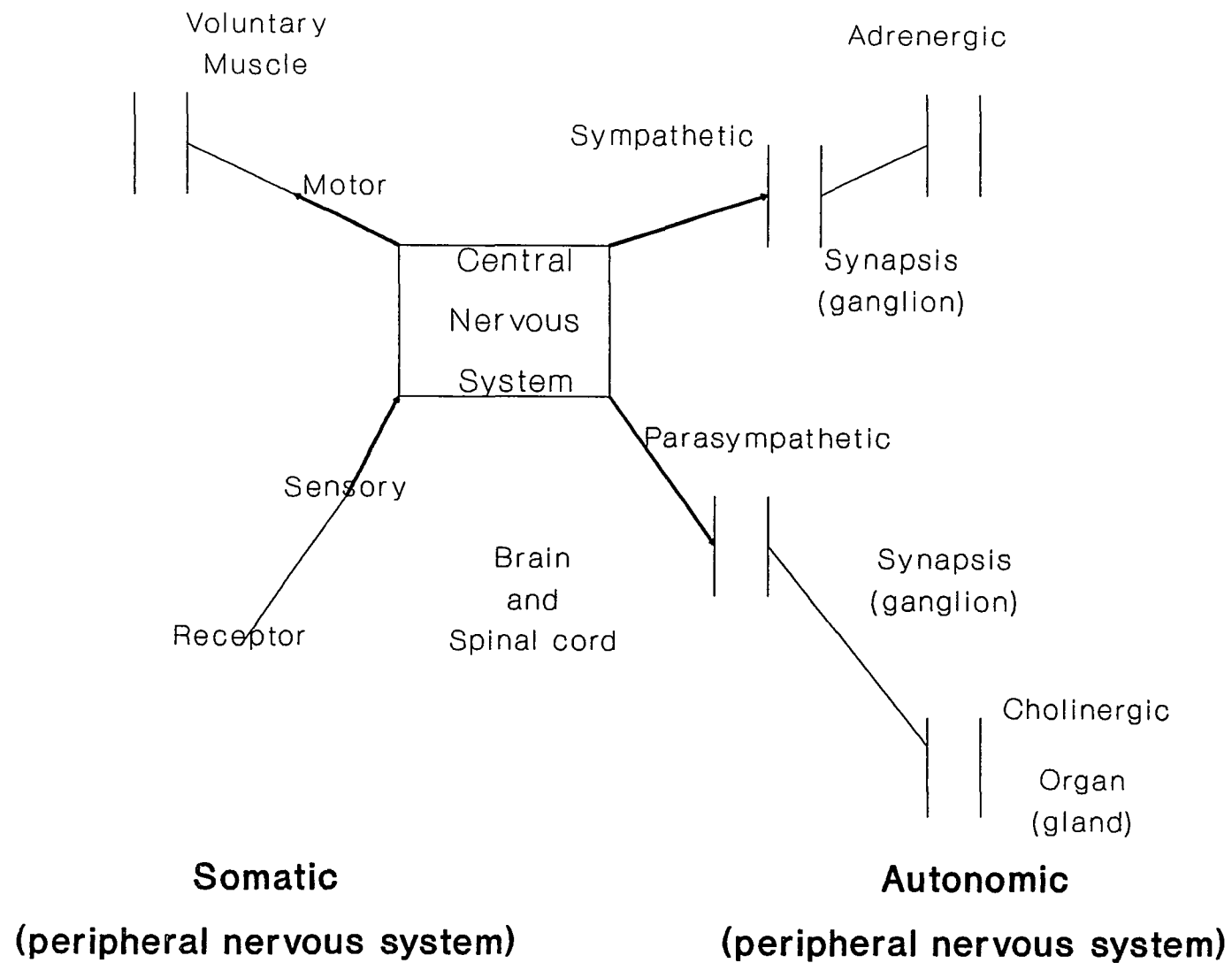
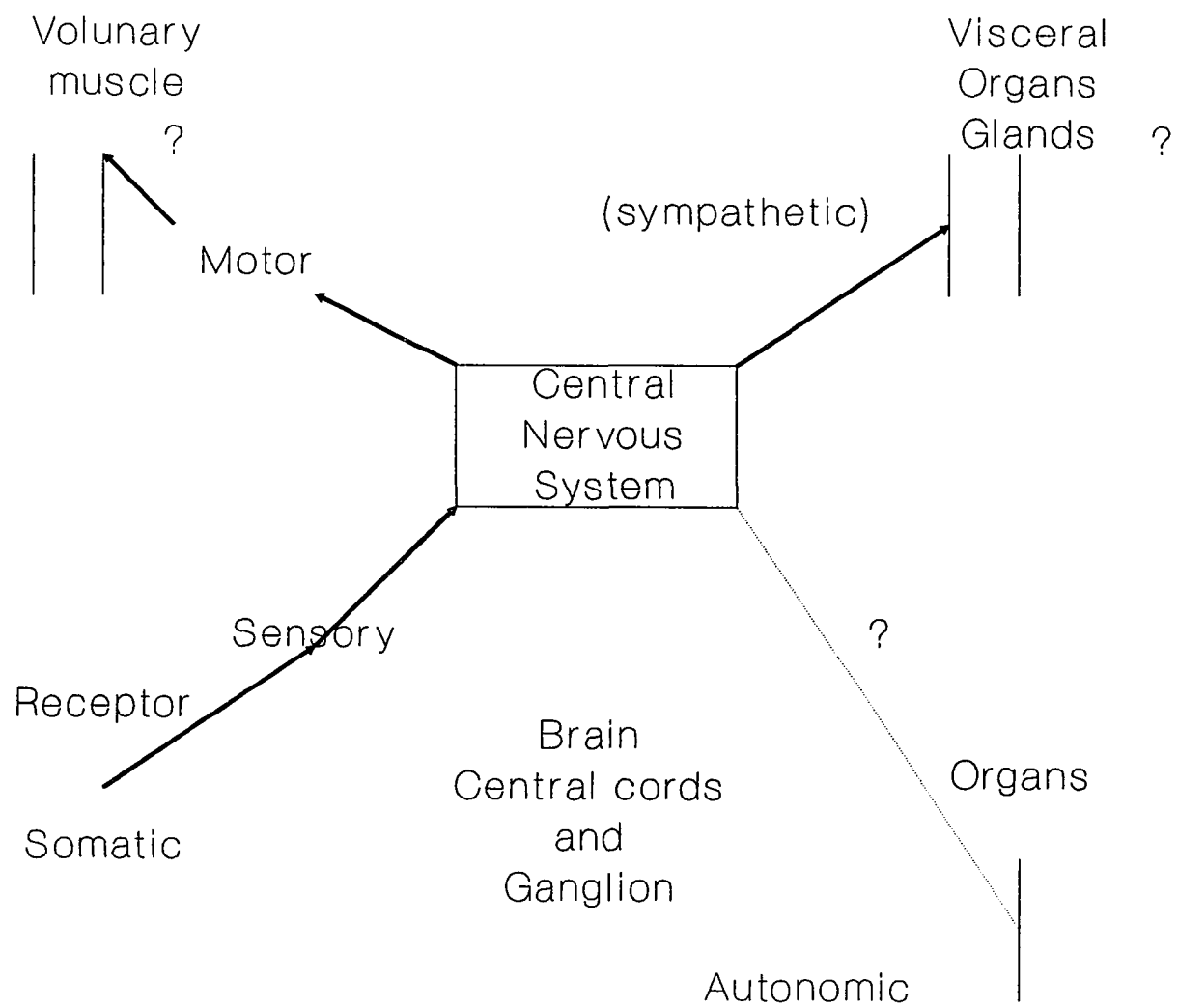


Figure 2
Diagram of insect nervous system.



acetylcholinesterase by organophosphorus pesticides disturbs the normal nervous function and eventually results in the death of animal.

Acetylcholinesterase (E.C.3.1.1.7) and cholinesterase (E.C.3.1.1.8) are cholinesterases which are distinguished from other β esterases by their specific properties to hydrolyze choline esters in preference to other carboxylic esters and to be inhibited by physostigmine (eserine) at low concentrations.

Acetylcholinesterase and cholinesterase differ in specificity toward some substrates while behaving similarly toward others. The acetylcholinesterase acts on acetyl- β -methylcholine, but cannot hydrolyze benzylcholine; while the cholinesterase acts on the latter one but not on the former one. Only choline esters are hydrolyzed by acetylcholinesterase; aryl or alkyl esters are not attacked. This enzyme is also inhibited by its substrate, acetylcholine, if present at concentration above 10^{-2} M [19]. Acetylcholinesterase is found in erythrocytes, lung, spleen, neurons and neuromuscular junctions, and the gray matter of the brain. It is responsible for the prompt hydrolysis of the acetylcholine which is released at the nerve endings to mediate transmission of the neural impulse across the synapse.

Acetylcholinesterase, neither contains nor requires any specific prosthetic group or metal ion although the activity is enhanced with various metal ions such as Ca^{++} and Mg^{++} [20]. The enzyme is known to have one active site with two major binding regions, the anionic site which binds the substrate and

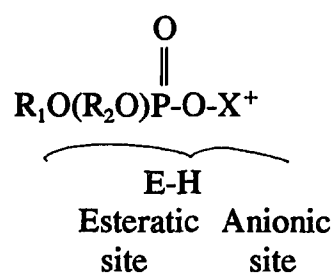
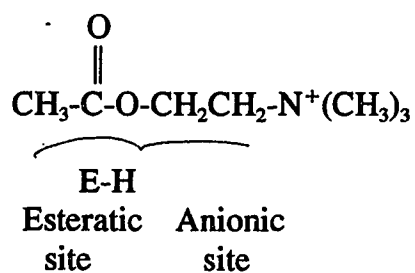
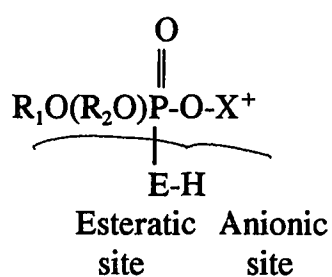
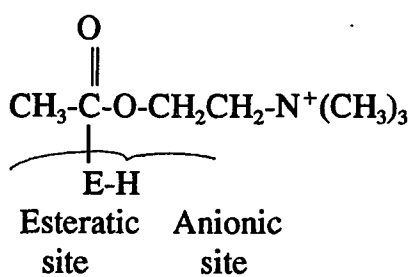
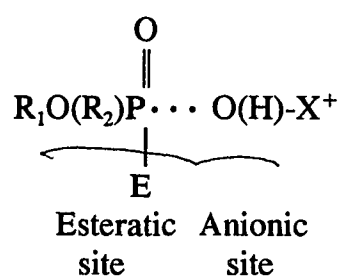
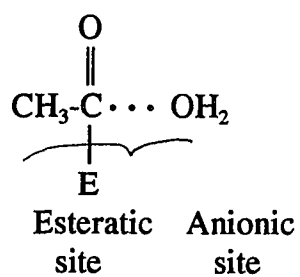
is concerned chiefly with specificity and the esteratic site which hydrolyses the substrate and is mainly responsible for the catalytic process [20]. It is generally accepted that the hydrolysis of choline ester by acetylcholinesterase may be expressed in the following scheme shown in Figure 3. Since organophosphorus compounds mimic the gross molecular shape of the natural substrate, acetylcholine, the process of organophosphorus inhibition of acetylcholinesterase is essentially analogous to the early stage of acetylcholine hydrolysis as illustrated in the following steps.

Step 1: complex formation: the binding of the substrate molecule involves the binding of the quaternary nitrogen group of acetylcholine or the cationic moiety of the organophosphate to the anionic site and the binding of acyl carbon atom of acetylcholine or phosphorus atom of the organophosphate to the esteratic site.

Step 2: acetylation (acetylcholine) or phosphorylation (organophosphate): a hydrogen atom is transferred from the enzyme esteratic site to the choline moiety of acetylcholine (substrate) or O-X part of the inhibitor by hydrogen bond formation, and then the cleavage and rearrangement of the C-O-C (substrate) or P-O-X (inhibitor) part of the molecule take place. It is an acylation in the case of substrate molecule and is a phosphorylation in the case of organophosphorus compound. It is reported that the acylation takes place on a serine-hydroxyl group which was activated by the participation of a histidine

Figure 3

Scheme of hydrolysis of acetylcholine by acetylcholinesterase reactions of the anticholinesterase organophosphorus pesticides.

Step 1**Step 2****Step 3**

imidazole group [21]. It was suggested that the formation of a hydrogen bond between the double-bonded nitrogen of the unprotonated imidazole ring and the hydroxyl group of serine residue may create a partial negative charge on the oxygen of the serine which may attack nucleophilically the carbonyl group of substrate or the phosphoryl group of the inhibitors.

Step 3 : deacetylation or dephosphorylation: in the last step the analogy between acetylcholine and organophosphorus compounds, and the organophosphorus compounds cannot proceed. The process of deacetylation from the enzyme, or sometimes called enzyme recovery, occurs very rapidly; whereas, the dephosphorylation takes place at an extremely slow pace with a turnover number of 300,000 for the acetylcholine and that of 0.008 for the organophosphorus compounds [7, 8, 9]. It is this particular step that makes organophosphorus compounds the powerful acetylcholinesterase inhibitors.

In the study of the hydrolysis of the acetylated enzyme, Krupka [22] showed that one of the two active histidine groups (B2: pK_a 5.5) in the catalytic site of acetylcholinesterase functions in acetylation of serine hydroxyl and is located at 9 Å from the anionic site. Another histidine group (B1: pK_a 6.3) functions in deacetylation and is located within 5 Å from the anionic site [22]. The higher pK_a value of B₁ is probably due to the interaction of the carboxylic acid near the base (within 5 Å). This imidazole group activates a water

molecule to attack the acetyl serine by abstracting a proton in a similar way to the activation of serine-hydroxyl in the acetylation step.

Phosphorylated enzymes can be considered as a kind of phosphate ester that is extremely stable. The stable complex can be slowly recovered upon hydrolysis by water or other nucleophilic agents, such as oxime, only at an early stage. The reaction ultimately yields the original enzyme, and therefore can be called a reactivation. This reactivation process takes place only in the dialkylphosphate vicinity of the organophosphate moiety. The rates of reactivation vary for different alkyl groups and are considered as the reversal of the stability of the formation of phosphorated enzyme complex [23, 24, 25].

The rates of reactivation vary with the basic alkyl groups on the phosphorus:



The rate of acetylcholinesterase inhibition, however, is very much dependent on the first part of the reaction with the phosphate, where the initial affinity of the phosphate for the enzyme is very important. In order to inhibit the acetylcholinesterase molecule, the phosphate molecule must make an electrophilic attack on the active site, possibly the serine hydroxyl group, of the enzyme. Therefore, those substituents which makes phosphate a better electrophilic reagent should improve its anti-acetylcholinesterase activity [26]. It was reported that the degree of electrophilicity of the X substituents as

exemplified by Hammett's σ constant for aromatic compounds closely follows that of anti-acetylcholinesterase activity [27].

The organophosphorus pesticides are believed to act by inhibiting acetylcholinesterase at neuromuscular junctions, autonomic ganglia, and parasympathetic neuron effector junctions [28]. The inhibition of AChE leads to an accumulation of acetylcholine in these sites, resulting in initial over-stimulation and later over depolarization of ACh receptors. Tissue and organ malfunctions reflect these effects of excess ACh. The ability of various organophosphorus compounds to induce acute toxicity varies greatly depending on the structure and formulation and has been shown to be well correlated with the ability of the compound to phosphorylate and inhibit AChE [29]. It has also shown that treatment with organophosphorus compounds stimulates phosphatidylinositol phosphodiesterase and it has been suggested that this may be an additional factor in the inhibition of synaptic transmission in poisoned animal. Levels of phosphatidylinositol phosphodiesterase reflect changes in the metabolism of phosphatidylinositol, which in turn is associated with alterations in the fluidity of cell membranes. It is becoming increasingly apparent that all the signs and symptoms associated with over-exposure to organophosphorus cannot be explained simply by their ability to inhibit AChE [30]. Organophosphorus compounds have also been implicated in another toxic condition unrelated to the inhibition of AChE. This condition, termed

organophosphate-induced-delayed neurotoxicity (OPIDN), is characterized by a delayed (two to three weeks onset), primary involvement of the peripheral limbs and induce hypoesthesia and muscle weakness, coupled with variable reflex abnormalities. The biochemical mechanism is not clear, but it has been suggested that neurotoxic esterase (NTE), a membrane-bound esterase, found in the brain, spinal cord and peripheral nerves may play a role in OPIDN [31]. NTE can be assayed by its ability to hydrolyze phenyl valerate in vitro. The initial reaction is believed to involve the phosphorylation of NTE by an organophosphorus compound. The phosphorylation inhibits the enzymatic activity of NTE, and there is a good correlation between the loss of activity in vitro and the development of clinical signs in vivo [32, 33]. Recently a condition called an "intermediate syndrome" was reported [34]. Signs were first seen 24-96 hours after exposure. The neuromuscular systems is the primary target and associated with a postsynaptic defect. The signs include paresis or paralysis of proximal limbs, cranial nerve deficits, and deficiencies in muscles involved in respiration. It is reported that overexposure to some organophosphorus pesticides can lead to muscle necrosis. Accumulation of acetylcholine at the motor endplate was implicated in overstimulation of receptors leading to a depolarizing paralysis and eventual necrosis of innervated fibers [35]. It was found that long time exposure to organophosphorus pesticides would decrease plasma cholinesterase (ChE) levels significantly,

alteration of the neuromuscular function, and loss of small motor units [36].

There was evidence that OPS may cause biochemical changes in the dopamine, serotonin, and muscarinic neurotransmitter systems [37].

Early analytical methods for organophosphorus compounds were based on acetylcholinesterase inhibition [38], total phosphorus determinations [39], and colorimetric procedures such as the classical Averell-Norris method [40]. By today's standards, these methods lack speed, sensitivity and/or specificity; however, the basic analytical concepts are still widely used. Since a wide range of organophosphorus compounds are used as pesticides, a variety of methods are used in their analysis. Currently, pesticide residue analysis can be summarized into four steps: (a) extraction from the sample matrix, (b) removal of interfering co-extractive, (c) identification and quantitation, and (d) confirmation of presence and identity. Since most of the specimens are from the environment, sample clean-up is very important. The sensitivity increases when more interfering co-extractive are removed. The extraction of pesticides from the sample matrix is generally according to the difference of partition coefficients of each compound in different organic solvents. Higher recovery can be obtained with multiple extraction; however, the solvent waste increases. The interfering co-extractives can be removed by column separation. Generally the samples are passed through the florisil column which can decolorize the sample before the extraction step. The pesticides were isolated by repeated

extraction with organic solvents and centrifugation, which were much more complicated and time-consuming [41, 42, 43, 44]. In 1982, Bushway [45] used Octadecyl reversed-phase silica ($C_{18}RPSiO_2$) Sep-pak cartridges for extraction of azinphos methyl and azinphos methyl oxon before high-performance liquid chromatography analysis. Sep-pak cartridge, which combines the steps of the extraction of the pesticides and removal of the interfering of the co-extractive, is reusable and required less solvent. It can be used to isolate organophosphorus pesticides from biological or environmental samples. The cleaned-extracted sample can then be analyzed by various instrumental methods.

The analysis of residues of organophosphorus pesticides has been aided greatly by the development of gas chromatography (GC) with selective detectors. EPA method 8140 employs three packed columns for the separation of some 21 organophosphorus pesticides combined with liquid-liquid extraction and cleanup separation [46]. There are several detectors which have been used in pesticide residues analysis. Flame ionization detection (FID) which has been most commonly used to detect insecticide residues, has low sensitivity [47]. Electron capture detection (ECD) has a higher sensitivity, around 0.1 pg/sec, and can be used to detect the presence of pesticide residues especially organochlorine pesticides. It was recently demonstrated that the organophosphorus pesticides could also be detected by ECD [48, 49]. Flame photometric detection (FPD) with two filters which can detect phosphorus- and

sulfur-containing compounds simultaneously is used for the determination of organophosphorus pesticides [50], with a detection limit around 250-ng level. Thermionic gas chromatography with a thermionic detection (TSD) provides a rapid and sensitive method to determine the organophosphorus pesticides with detection limits as little as 0.1 ppm ($\mu\text{g/mL}$) [51, 52]. The nitrogen-phosphorus detection is the best detector for the analysis of organophosphorus pesticides [53, 54] since it is only sensitive to nitrogen and phosphorus containing residues. A sensitivity of 10 pg/sec was found for organophosphorus compounds based on photoelectric measurement of the 2535.65 Å atomic phosphorus line [43]. But since it is only sensitivity to nitrogen and phosphorous containing residues, it is a less useful detector in some aspects. Generally, the GC procedure is the most commonly used method for the analysis of the organophosphorus pesticides in the laboratory. But the method is more time consuming, instrument demanding and not suitable for general pesticide residues screening application.

Thin layer chromatography (TLC) procedure has been proposed as a technique for pesticide residue screening. Several procedures have been developed for such purpose. The procedures [55, 56, 57, 58, 59] have been developed and reported for the screening pesticide residues in vegetables, however, these methods still require some degree of instrumentation and laboratory setup.

The analytical methods described above are quantitative and instrumentation required procedures with the exception of TLC all are unsuitable for screening purpose. A new approach using other principle for a rapid screening method for such residues in the non-laboratory environment is urgently needed. Only very recently, an enzyme inhibition method was marketed for the screening of organophosphorus insecticide residues in vegetable. It utilizes the principle of the organophosphorus inhibition of the housefly's acetylcholinesterase as described in the previous section. Unfortunately, this method is not specific with possible crop contamination from other pesticides such as carbamate.

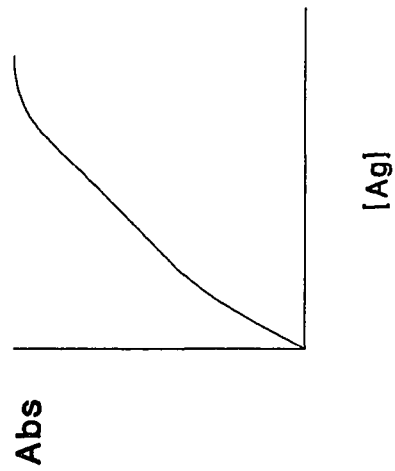
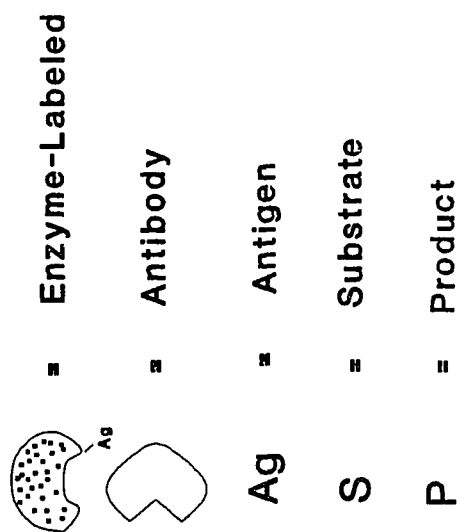
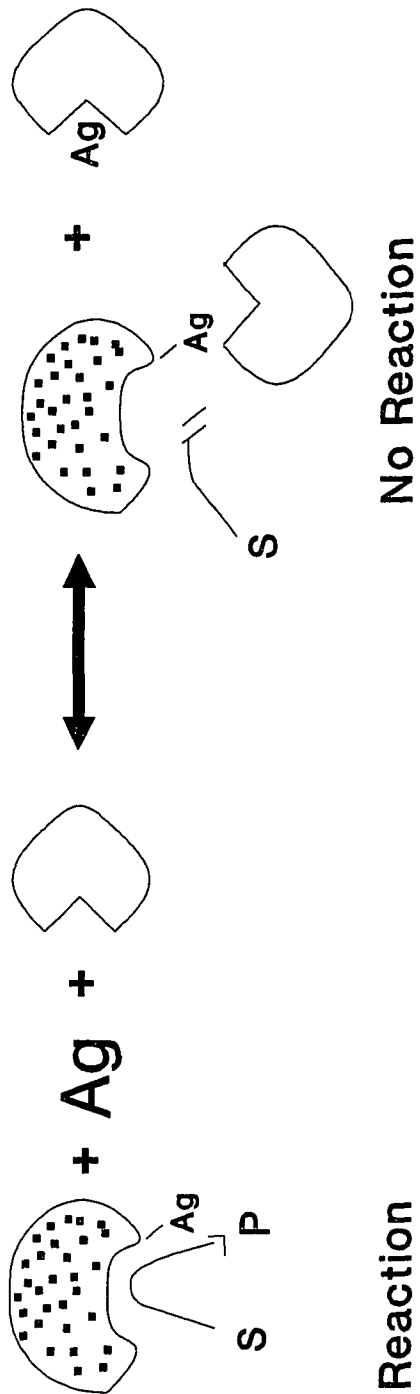
Over the past three decades, there has been tremendous progress in the discovery and development of immunological methods for the quantitative determination of minute amounts of various substances in biological samples. The introduction of competitive protein binding techniques and radioimmunoassay (RIA) have made it possible to measure many hormones, steroids and drugs at extremely low concentration; thus, it provides a new tool for the sensitive assays. Also the immunological reaction provides the essential specificity which is required to measure the specific substances from the complex mixture of biological samples. As these techniques involve the use of radioactive isotopes, analytical laboratories allied to medical sciences are faced with serious problems with waste disposal and the health hazard in the

environment. Enzyme immunoassay (EIA) has essentially solved these problems because no radiation hazard or disposal difficulties are involved with this procedure.

Enzyme immunoassay (EIA) is the developmental successor to radio-immunoassay. There are two types of principles in the enzyme immunoassay, a homogeneous test principle and a heterogeneous test principle. The homogeneous enzyme immunoassay is referred to as the enzyme multiplied immunoassay technique (EMIT) in which the binding of antibody to enzyme-labeled antigen changes the enzyme activity of the label enabling the antibody-bound label to be distinguished from the unbound labeled antigen (Figure 4). This dispenses with the need for phase separation. As there is no need for a bound/free separation step, EMIT is quickly and easily done with automatic equipment. There are other problems which may occur in the homogeneous test. Because it does not need the phase separation, the enzyme activity is liable to interference from the other sample constituents. Inhibition of the enzyme activity results in only small absorbance difference (0.1-0.2 A) between an inhibited reaction and non-inhibited reaction; therefore, measurements are difficult.

The heterogeneous enzyme immunoassay (or ELISA: enzyme linked immunosorbent assays) are those procedures that required the physical separation of the antibody-antigen complex from the unbound constituents in

Figure 4
Principle of homogenous enzyme immunoassay (enzyme-multiplied immunoassay technique, EMIT).



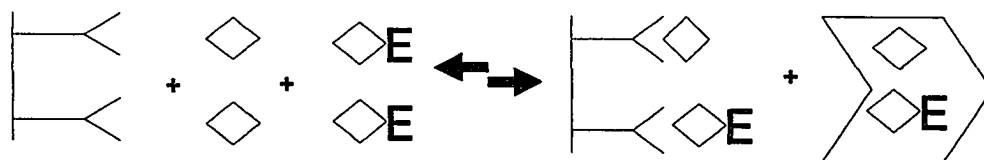
order to determine the enzyme activity associated with free reactant separated from the bound labeled reactant after immunological incubation. ELISA usually have an antibody immobilized on a solid support, and the ligand is labeled with the enzyme. There are two kinds of ELISA that have been already developed: competitive and sandwich.

The principle of the competitive enzyme immunoassay is based on the competition of antigen and enzyme-conjugated antigen to bind the antibody which is pre-coated on the solid phase. The excess of the unbound antigen and the enzyme-conjugated antigen is washed out after the reaction. The substrate of the enzyme is added later and the result can be shown as color developed by the bound-enzyme reaction. Therefore, there is an inverse relationship between the color intensity and the antigen in the sample. The non-competitive enzyme immunoassay, also called sandwich assay, is based on the two-site reaction principle in which enzyme-conjugated antibody binding to the antigen which is captured by an antibody pre-coated on the solid phase. Therefore, more color development represents more antigen in the sample. Because of the two-site reaction principle, the antigen is limited to macromolecule that can provide such binding reaction. Both of these methods are shown on Figure 5 and 6. EIA methods are specific and sensitive, some of these procedures being as sensitive as RIA. Technical manipulations of EIA are simple and the assays are rapid. The variety of labels available may allow multiple simultaneous assays to be

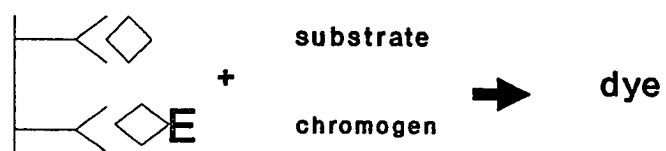
Figure 5

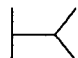
Heterogeneous enzyme immunoassay: competitive principle.


Immunological reaction



Indicator reaction



 **specific antibody**
(coated to tube wall)

 **enzyme-labelled**
antigen

 **antigen**

 **wash step**

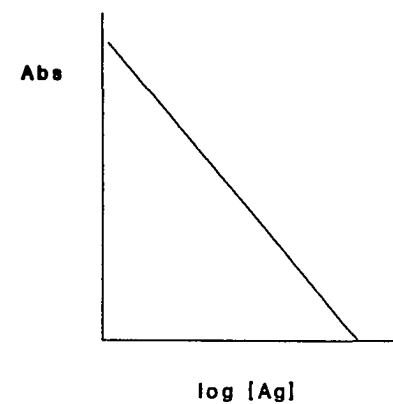
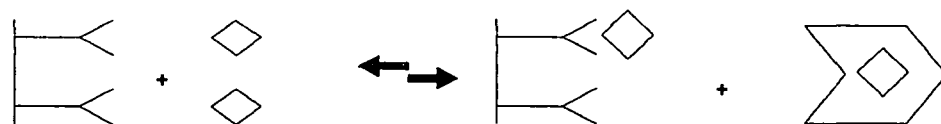


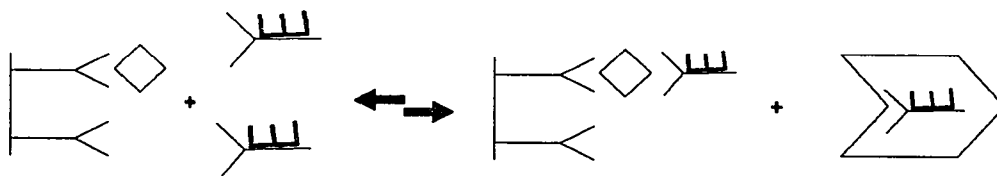
Figure 6

Heterogeneous enzyme immunoassay: non-competitive principle.

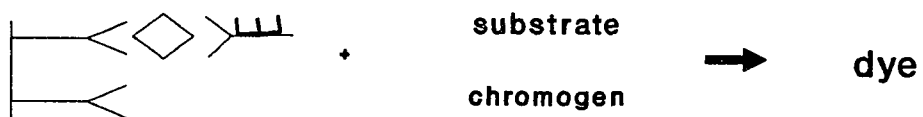
1st immunological reaction





2nd immunological reaction

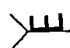


Indicator reaction

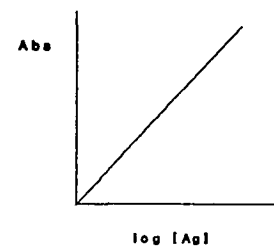


 specific antibody
(coated to tube wall)

 antigen

 enzyme-labelled
antibody

 wash step



performed, and it appears that there is a potential for automation. Recently the EIA method has been applied to the analysis of pesticides [60]. The EIA tests for the analysis of organochlorine pesticide and atrazine, one kind of herbicide, have been carried out successfully [61, 62, 63]. It is felt that the possibility of using EIA as a tool for developing a screening method for organophosphorus insecticide residues should be investigated.

It is well known that different classes of organophosphorus pesticides give different degrees of inhibition of acetylcholinesterase, and the variation of the side chains within the same class of organophosphorus compounds express a great degree of variation in the inhibition of acetylcholinesterase [64]. Moreover, some organophosphorus pesticides were reported not to show any inhibitory effect on acetylcholinesterase [65]. To further complicate the matter, some carbamates were reported to demonstrate an inhibitory effect on acetylcholinesterase [66] and could possibly invalidate the performance of such commercial kits.

Recently, Hunter et al [67] reported on developing monoclonal antibodies against soman, an organophosphorus compound. It is felt that it is possible to use EIA as a tool for screening organophosphorus insecticide residues. There is less than a dozen commonly used organophosphorus pesticides on the market in Taiwan currently, and these can be classified into four classes: (a) phosphorothionate pesticides including parathion, parathion-methyl, and

Primifos-methyl; (b) phosphorodithioate pesticides including malathion, dimethoate (Rogor, Cygon), and Chloropyrifos; (3) phosphorothiolate pesticides including Dementon-S-methyl and methamidophos (Tamaron, Monitor); and (d) phosphate ester pesticides such as mevinphos. It is felt that a practical method using EIA for screening organophosphorus pesticide residues in water can be developed.

B. Statement of problem

The purpose of the research project is to develop a competitive enzyme immunoassay system for organophosphorus pesticides determination. The goals of this study are (a) to prepare the antigens, (b) to produce and characterize the rabbit antisera against the prepared antigens, (c) to develop a simple and quick method to isolate gamma globulin fraction from the whole anti-serum, (d) to determine the optimal concentration of gamma globulin for the solid phase coating, (e) to produce the antigen-enzyme (HRPO) conjugate, (f) to determine the optimal conditions for malathion, parathion, tamaron and mevinphos assays, (g) to study a proper solid phase for the prepared the EIA method, (i) to study the cross reactions, (j) to investigate the performance characteristics of the developed method and compare this method with other methods which have already been developed, and (k) to evaluate the developed method on the validation study on the water and vegetable samples.

Chapter II

EXPERIMENTAL

A. Materials

The following materials were purchased from Sigma: diethylaminoethyl-cellulose (DEAE-cellulose, medium mesh); bovine serum albumin; ovalbumin; horse serum albumin; Freund's complete adjuvant; Freund's incomplete adjuvant; horseradish peroxidase (HRPO), type VI-A; sodium phosphate (monobasic, anhydrous); Trizma base (Tris [hydroxymethyl] aminomethane); 1-ethyl-3(3-dimethylaminopropyl)-carbodiimide HCL (EDC); 3, 3', 5, 5'-tetramethylbenzidine (TMB), urea hydrogen peroxide, and activated charcoal. From Eastman Kodak Co. 1,6-hexanediamine was obtained. Sodium hydroxide pellets and sodium chloride were products of Baker Chemical Co. Citric acid monohydrate, glycerin and polystyrene tubes were supplied by Fisher Scientific Company. Anhydrous sodium sulfate, dichloromethane, anhydrous methyl alcohol, ammonium molybdate, dichloromethane and dimethyl sulfoxide (DMSO) were products of Mallinckrodt, Inc. Ethyl ether was purchased from EM science. Econo-Columns were purchased from Bio-Rad. Spectra/por dialysis tubing (molecular weight cutoff 8,000) was the product of Spectrum Medical Industries, Inc.. Syringes, 1 cc and 3 cc, and needles, 25G1 and 30G1, were purchased from Becton Dickinson and Company. Immunolon I removable strips were products of Dynatech Laboratories. Dimethyl phosphite,

ethyl propionate, methyl isobutyrate and p-nitrophenol were purchased from Aldrich Chemical Company, Inc. Hexane, UV grade, was purchased from Baxter Healthcare Co.. DB-608 capillary GC column was purchased from Altech Co.. The standard organophosphorus compounds were purchased from Chem Service. Malathion, parathion, tamaron and mevinphos were gifts from the Institute of Insecticide, Taipei, Taiwan.

B. Equipment

A Beckman Microzone Electrophoresis Cell model R-101 coupled with an EC-400 power supply was used for protein electrophoresis. High speed centrifugation (15,000 rpm) was performed using a Beckman model JA-21 refrigerated centrifuge equipped with a Beckman JA-20 rotor. A Biotech model EL 307C microplate reader equipped with a 450 nm filter was used for the absorbance reading of the sample on microwell EIA. A Milton Roy spectronic model 1201 UV-visible spectrophotometer was used for the absorbance readings for the assays performed in the polystyrene tubes. All pH measurements were performed with a Corning Digital 110 pH meter with three calibrators at pH 4, 7 and 10. An ISCO model UA-5 Absorbance/Fluorescence monitor coupled with a 10-mm light path flow cell was used for monitoring column effluent. Büchler rotavapor RE 120 rotary evaporator was used for organic solvent aspiration. All gas chromatography measurements were performed on a HP

5850A gas chromatography instrument coupled with a J & W DB-608 capillary column, a Varian model A028 ECD and a HP 3396A integrator.

C. Methods

1. Preparation of the microwells for titer assays

Solid-phase enzyme-linked immunosorbent assay (ELISA) was utilized for the titer assay. Microwells were prepared by coating 5 $\mu\text{g/mL}$ OP-ovalbumin (OVA), 200 μL , in the coating buffer overnight at room temperature. After washing with PBS, the unbound spaces on the polystyrene surface of the microwell were further blocked with 0.3% (w/v) ovalbumin, 200 μL , in coating buffer for two hours at room temperature. The coated microwells were air dried at room temperature, and sealed in a plastic bag. The microwells were stored at 4°C for up to one year before use.

2. Preparation of DEAE-cellulose resins

DEAE-cellulose resin used for the ion-exchange chromatography was prepared according to the following procedure. Fifty grams of DEAE-cellulose were suspended in one liter of 0.1 N HCl and stirred for 10 minutes at room temperature. The resin was then filtered through a 300-mL glass fritted funnel (coarse) and washed with one liter deionized water. The process was repeated with one liter of 0.10 N NaOH and followed with one liter deionized water. After the previous procedure to remove the blocking ions,

which were attached to the resin itself, the resin was equilibrated in 5.0 mM sodium phosphate buffer, pH 6.5 and stored at 4°C.

3. Isolation of gamma globulin fraction from the whole antiserum

For the isolation and purification of the gamma globulin fraction from rabbit antisera, a procedure utilizing DEAE-cellulose ion exchange chromatography was employed [68]. One milliliter of rabbit antiserum (anti-malathion, anti-parathion, anti-tamaron or anti-mevinphos) was diluted to a final volume of 10 mL with 5 mM sodium phosphate buffer, pH 6.5, and dialyzed against four liters of the same buffer for 24 hours at 4°C with three changes of the same buffer. The anti-serum was then applied to a DEAE-cellulose column (1 x 24 cm) which was pre-equilibrated with the same buffer at 4°C. The gamma globulin fraction was eluted from the column with the same buffer and concentrated to approximately 1.0 mL with an Amicon Diaflo system (model 52) equipped with a YM-05 membrane. All operations of chromatographic separation and Diaflo system were performed at 4°C.

4. Electrophoresis

The purity of each of the purified antibodies was analyzed by a Microzone electrophoresis method. The electrophoresis was performed on a cellulose acetate membrane in a Beckman Microzone electrophoresis cell containing sodium barbital buffer (ionic strength 0.075, pH 8.6). The cellulose acetate membrane was first wetted in the electrophoresis buffer (sodium barbital

buffer, ionic strength 0.075, pH 8.6), removed, the excess surface buffer was blotted, and then placed onto the Microzone electrophoresis cell. Samples of the purified antibodies, 10 μ L, were applied to the membrane with the use of an applicator. The electrophoresis was carried out at a constant voltage 250 V for 20 minutes at room temperature. After the electrophoresis, the membrane was removed from the cell and placed in 100 mL fixative/Dye solution, containing 0.2% (w/v) Ponceau-S stain, 3.0% (w/v) trichloroacetic acid and 3.0% (w/v) sulfosalicylic acid in deionized water, for 10 minutes. The background of the staining was rinsed off with three successive washes of 100-mL 5% aqueous acetic acid. The membrane was then agitated in 100 mL full strength alcohol dehydrating solution for one minute, and then placed on a clean glass plate into the clearing solution which was made as 30% reagent grade cyclohexanone in denatured ethanol and agitated for one minute. Finally, the membrane was placed on a glass plate, the excess clearing solution was removed by a gentle squeeze, and then placed in a 100°C oven for 15 minutes. The membrane was then peeled from the glass plate and the purity of the antibodies was identified by the bands shown on the membrane [69].

5. Preparation of the assay solutions

Two solutions, Solutions A (the substrate solution) and B (the chromogen solution), were prepared for the measurement of the peroxidase activity. Solution A contained 2% (w/v) hydrogen peroxide in 0.1 M citric

acid and 0.1 M sodium phosphate, pH 5.0. Solution B was prepared by dissolving 10 mg TMB completely in 1.0 mL DMSO and then diluted to 50 mL with deionized water to a final concentration of 0.2 mg/mL.

6. Preparation of organophosphate-peroxidase (OP-HRPO) conjugate

Horseradish peroxidase (HRPO) and EDC were added to the modified OP, i.e. 1,6-hexadamine elongated malathion, mevinphos, adipic acid elongated tamaron or the diazonium salt of modified parathion, and then incubated at 4°C for an additional five hours. The sample was dialyzed against running water for eight hours at room temperature. To stabilize the HRPO activity, horse serum albumin was added to a final concentration of 10 mg/mL. The sample was further dialyzed at 4°C against phosphate buffered saline, pH 7.4, for 16 hours with one change of the buffer. The prepared OP-HRPO was then stored at -80°C until further use.

7. Preparation of organophosphorus pesticide standard solutions

The organophosphorus pesticides in the commercial samples were first extracted with dichloromethane, five mL, three times and dried with anhydrous sodium sulfate. These organophosphorus pesticides can be dissolved in the dichloromethane because of the hydrophobicity. Dichloromethane was then evaporated to dryness on a rotary evaporator under reduced pressure, and the residue was redissolved in one milliliter of anhydrous methanol. The concentration of purified organophosphorus pesticide was determined by a

modification of the method of Fiske and Subbarow [70]. This modification consisted of using 1 % (w/v) Elon (p-methylaminophenyl sulfate) in 3 % (w/v) sodium bisulfite as the reducing agent. The formation of molybdenum blue was measured spectrophotometrically at 600 nm to provide a determination for phosphate.

A stock solution of each extracted organophosphorus pesticide was prepared by taking 20 mg of each and diluting it with methanol into a 100-mL volumetric flask. Intermediate standard solutions were obtained by pipetting 0.1 mL of stock solution into a 10-mL volumetric flask and using deionized water to bring to volume. Actual working standards were prepared by pipetting 2.5, 5, 10, 25, 50, 125, 250, 1250 and 2500 μ L aliquot from the intermediate standard solutions into a separate 5-mL volumetric flasks and bringing to volume with deionized water. This gave working standards of 1, 2, 4, 10, 20, 50, 100, 500, and 1000 ng/mL [63].

8. Preparation of gamma globulin coated microwells and polystyrene tubes

The concentration of isolated gamma globulin was determined by the absorption at 280 nm using an extinction coefficient, $E_{1\%}$, of 13.5 [72]. The gamma globulins were diluted with coating buffer to 50 ng/mL, 500 ng/mL, 500 ng/mL and 50 ng/mL for malathion, parathion, tamaron and mevinphos, respectively. The gamma solution, 200 μ L each for the microwells

and 500 μL each for the polystyrene tubes, were then incubated at room temperature overnight. The microwells and microtubes were emptied, washed with deionized water ten times, and air dried at room temperature. The coated microwells and polystyrene tubes were sealed in a plastic bag and stored at 4°C for up to one year.

9. The OP assay procedures

The aqueous samples (standard, control or unknown) were added (440 μL for malathion, 300 μL for parathion, 460 μL for tamaron and 300 μL for mevinphos) to specific anti-OP antibody coated microtubes and followed with the appropriate enzyme-conjugate (50 μL for parathion and mevinphos and 10 μL for malathion and tamaron, with 50 fold dilutions for all except 150 fold dilutions for parathion), and deionized water to a total volume of 500 μL . All samples determinations were performed in duplicate. The average was recorded. If it appeared that one of the duplicates was in error, the better of the two was recorded. The mixture was incubated at room temperature for 10 minutes, and the microtubes were emptied and washed with deionized water ten times. Solution A (substrate), 250 μL , and Solution B (chromogen), 250 μL , were added to these microtubes and let stand at room temperature for color development for no more than ten minutes depending on the development of color intensity. After the color developed, 100 μL of 2.0 N sulfuric acid was added to quench the reaction, and the absorbance at 450 nm was measured.

10. Study of cross reaction

Solutions of potentially cross-reacting compounds such as these four chosen OPs, ethyl propionate, dimethyl phosphite, methyl isobutyrate and p-nitrophenol were prepared in deionized water. The assays were performed by comparing the cross-reacting compounds to the standard solutions under the same assay condition.

11. Assay validation

a. the validation assay on water samples

Deionized water, tap water and the water from Elizabeth river were employed as water samples. Different concentrations of organophosphorus compounds were prepared by adding the compound to the water samples to give a final concentration of 0, 1, 5, 10, 50 and 100 ng/mL. The prepared samples were directly employed for EIA, but the samples for GC analysis required further treatment. The samples for GC analysis were extracted with 50 mL of dichloromethane three times, evaporated to dryness, and n-hexane was added to the desired volume. The assays were performed by the comparison of the results under GC and EIA analysis.

b. the validation assay on vegetable samples

Lettuce and spinach were selected as the vegetable samples. The 20 g of the vegetables were homogenized in 200 mL deionized water and then the residues were filtered with a glass funnel. One half of the filtrate was

decolorized with 20 g of activated charcoal at room temperature for 30 minutes. The organophosphorus compounds were added to both the charcoal treated and the crude extract fractions to give a final concentration of 0, 1, 5, 10, 50 and 100 ng/mL. The prepared samples were then employed directly for EIA screening. The samples prepared for GC analysis were prepared differently. To 20 g vegetables, 200 mL of acetone was added and homogenized in a blender at room temperature for 2 minutes. The residue was then removed by filtering on a funnel with glass fiber filter. The filtrate was then decolorized with charcoal by shaking the resultant mixture for 30 minutes at room temperature. The organophosphorus compounds were then added to the filtrates to give a final concentration of 0, 1, 5, 50, and 100 ng/mL, respectively. The acetone fraction was then extracted first with 150 mL, and then twice with 50 mL of dichloromethane. The dichloromethane extracts were pooled and evaporated to dryness on a rotary evaporator under reduced pressure. The residue was reconstituted with n-hexane for GC analysis.

Chapter III

RESULTS

A. Preparation of antisera

1. Preparation of antigens

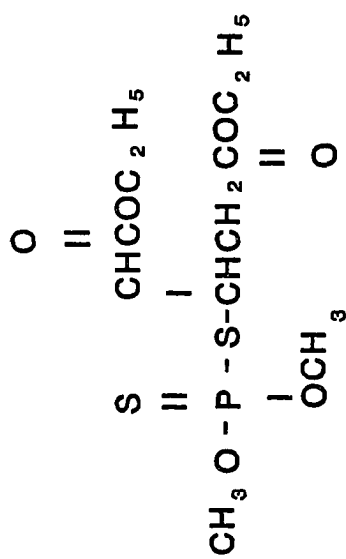
Organophosphorus pesticides are small molecules with molecular weights smaller than 500 daltons. No immune response can be induced by an antigen which has a molecular weight smaller than 10,000 daltons. To eliciting antibody production, they must be conjugated with a carrier protein. As described in the previous section, four commonly used organophosphorus pesticides from four different classes were selected. They were parathion (a phosphorothionate pesticide), malathion (a phosphorodithioate pesticide), tamaron (a phosphorothiolate pesticide), and mevinphos (a phosphate ester pesticide). The formulas of these organophosphorus pesticides are illustrated in Figure 7.

The major difference among these four compounds is in the side chains, and these side chains play the role of the leaving groups in the acetylcholinesterase catalyzed reaction. Taking advantage of this property, the principle of coupling these compounds to the carrier protein, bovine serum albumin (BSA), is the addition of a six carbon alkyl chain as the spacer between the side chain and the BSA molecule. For parathion, the nitro group was first reduced to an amino group and then the amino group was reacted with

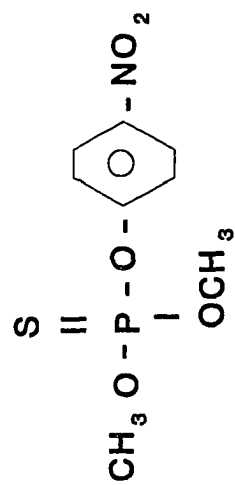
Figure 7

Structures of four kinds of organophosphorus compounds.

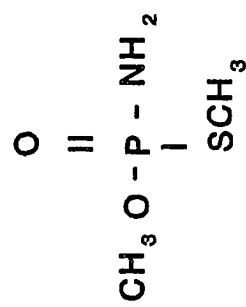
•



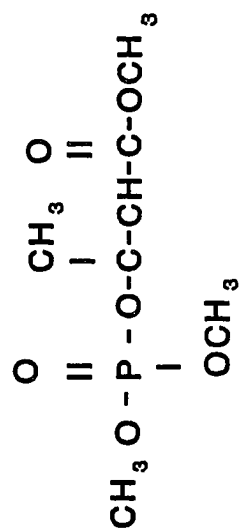
Malathion



Parathion



Tamaron



Mevinphos

nitrous acid to form a diazonium group which in turn reacted with a tyrosine residue of the BSA at a slightly alkaline pH condition [72, 73]. To elicit a higher immune response, the molar ratio of parathion to BSA is ten to one. For malathion and mevinphos, the ester group in each of the side chains was modified into a carboxyl groups by acid hydrolysis and then coupled with 1,6-hexdiamine through a carbodiimide reaction which took place in the presence of EDC at 4°C; the pH was maintained between 5.0-5.5 [74]. In the same manner, the amino group of the six carbon-elongated chain can then be coupled to a carboxyl group of BSA in a ten to one molar ratio through a carbodiimide reaction. For tamaron, adipic acid was directly added to the side chain amino group first and then coupled to BSA in a ten to one molar ratio by the carbodiimide reaction. After the preparation of the antigen, the unconjugated hapten and other chemical by-products were removed by dialysis. The dialysis tubing was selected with a molecular weight cutoff of 8,000.

2. Immunization of the rabbit

For immunization, white rabbits, two to four per group were immunized by the injection of the prepared organophosphorus-BSA (OP-BSA) in complete Freund's adjuvant into the footpads. Three to four booster injections of the immunogen suspended in incomplete Freund's adjuvant were given in two to four week intervals depending on the tolerance of the animals. Control antisera were also obtained by immunizing in a similar manner with

BSA. Blood samples were obtained from the marginal ear vein 10 to 14 days after each booster for titer assay.

3. Titer assay of the antisera by solid-phase enzyme linked immunosorbent assay

Titer is the dilution at which the antibody and antigen combine in a one to one ratio. The higher the titer is; the more antibodies are produced. Solid-phase enzyme-linked immunosorbent assay (ELISA) using the sandwich principle was utilized for titer assay of antisera. The microwells were coated with a specific OP-OVA conjugate which was prepared in a similar fashion as OP-BSA conjugates. Briefly, the modified organophosphorus pesticides which were first elongated with 1,6-hexadamine (for malathion and mevinphos), adipic acid (for tamaron) or modified into a diazonium compound (for parathion) were coupled to OVA in a one to one molar ratio through a carbodiimide reaction. The prepared OP-OVA conjugates were immobilized onto polystyrene microwells in a coating solution. An aliquot of 200 μ L of the serial dilutions of the antisera, before and after purification, in phosphate buffered saline (PBS) was incubated in the prepared organophosphorus pesticide-ovalbumin coated microwells.

The organophosphorus pesticide moiety of the OP-OVA coated on the well provided the basis for immunological attachment of the antibody from the antisera. The immunochemically bound antibody, rabbit IgG, was then reacted

further with goat anti-rabbit IgG-horseradish peroxidase conjugate (IgG-HRPO), an indicator protein. The activity of enzyme, the horseradish peroxidase, of the sandwich reactant (OP-OVA:IgG:anti-IgG-HRPO) was then assayed by the addition of the substrate solution, H_2O_2 in citrate buffer, and the indicator solution; 3, 3', 5, 5'-tetramethylbenzidine (TMB). The titer assay of each of the four antisera are exemplified in the Figures 8-11, and the results obtained from these are summarized in Table 1.

4. Isolation of the gamma globulin from the whole anti-serum

The antiserum was diluted nine folds with 5 mM sodium phosphate buffer, pH 6.5, and then dialyzed against 4.0 liters of 5 mM sodium phosphate buffer, pH 6.5, at 4°C overnight. The sample was then applied to a DEAE-cellulose column (1 x 24 cm) which was pre-equilibrated with the same buffer. The gamma globulin fraction was then eluted with the same buffer in isocratic condition and monitored by its absorption at 280 nm. Figures 12-15 represent the elution profile of anti-malathion, anti-parathion, anti-tamaron and anti-mevinphos fractions from the DEAE-cellulose columns, respectively. Each fraction was then concentrated to about 1.0 mL using an Amicon ultrafiltration system equipped with a YM-05 membrane. The concentration of the purified antibody can be determined by the absorbance at 280 nm and calculated with the use of the extinction coefficient, $E_{1\%}^{1\text{cm}}$ 13.5. The shelf life of the purified gamma globulins is greater than one year if stored at -20°C. The purified

Figure 8

The titer assay study of anti-malathion by solid-phase enzyme linked immunosorbent assay on microwell immobilization. Anti-malathion ranging from 100 to 512,000 folds of dilution were employed. The absorbance was measured at 450 nm.

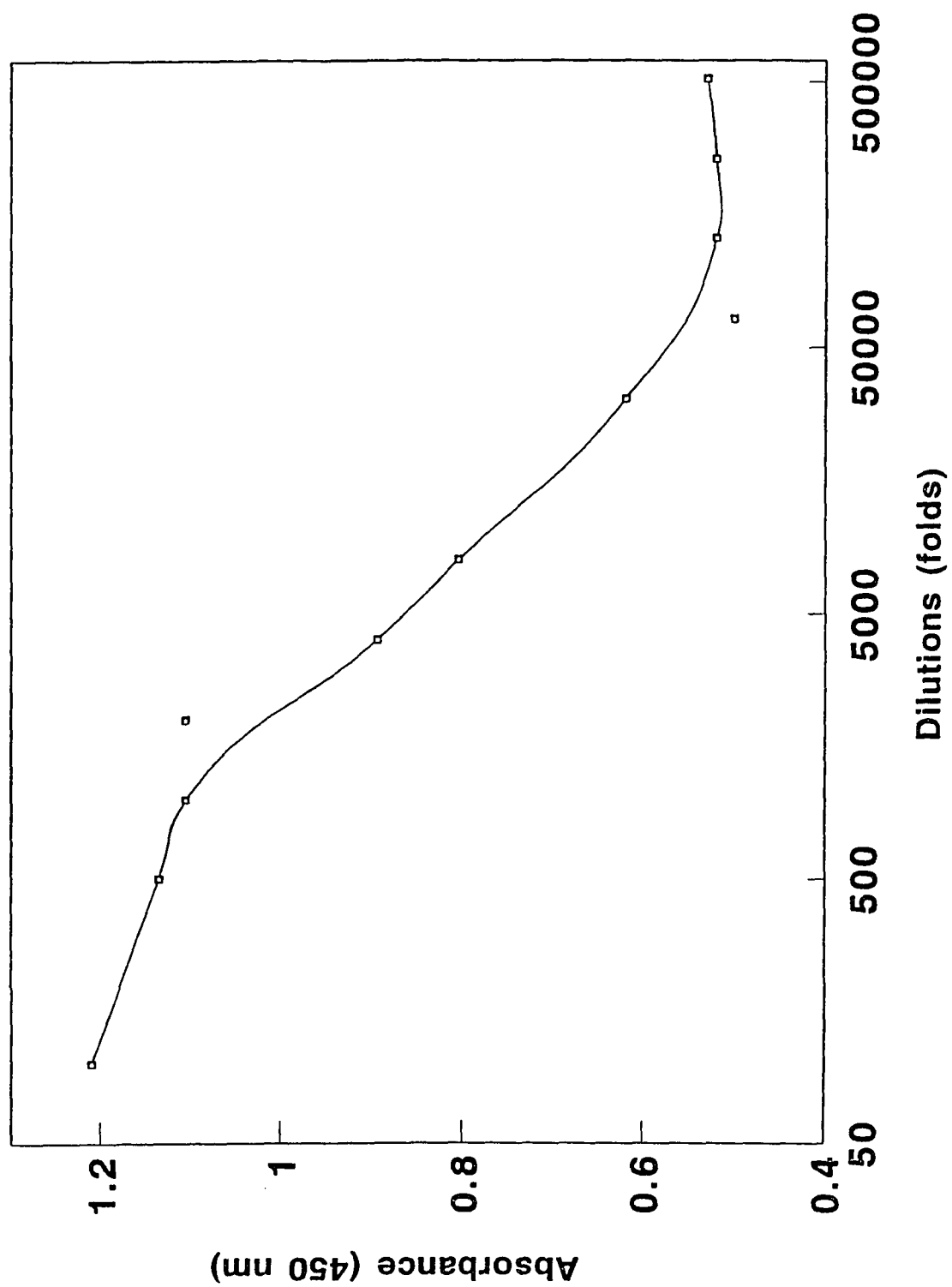


Figure 9

The titer assay study of anti-parathion by solid-phase enzyme linked immunosorbent assay on microwell immobilization. Anti-parathion ranging from 1,000 to 20,480,000 folds of dilution were employed. The absorbance was measured at 450 nm.

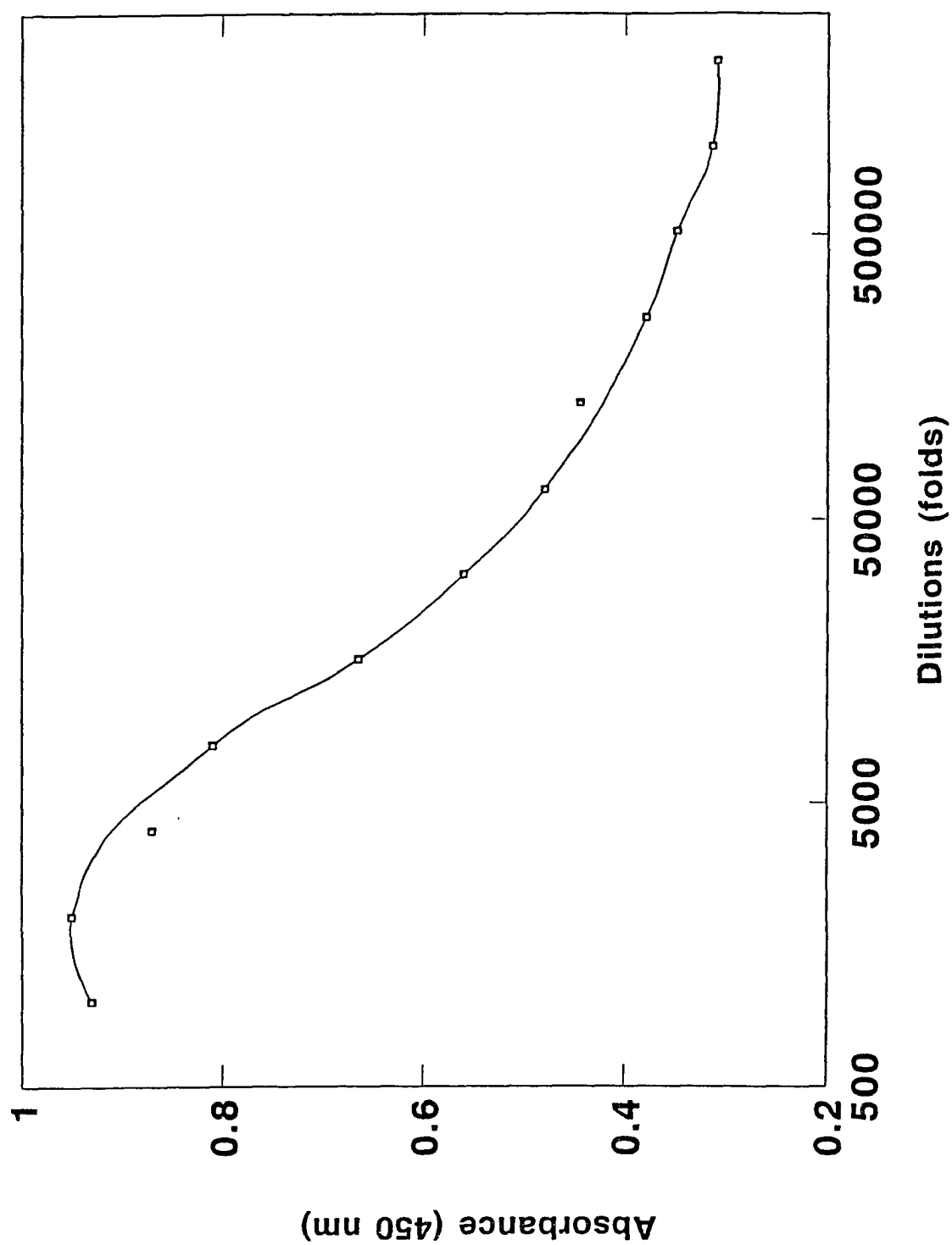


Figure 10

The titer assay study of anti-tamaron by solid-phase enzyme linked immunosorbent assay on microwell immobilization. Anti-tamaron ranging from 100 to 2,048,000 folds of dilution were employed. The absorbance was measured at 450 nm.

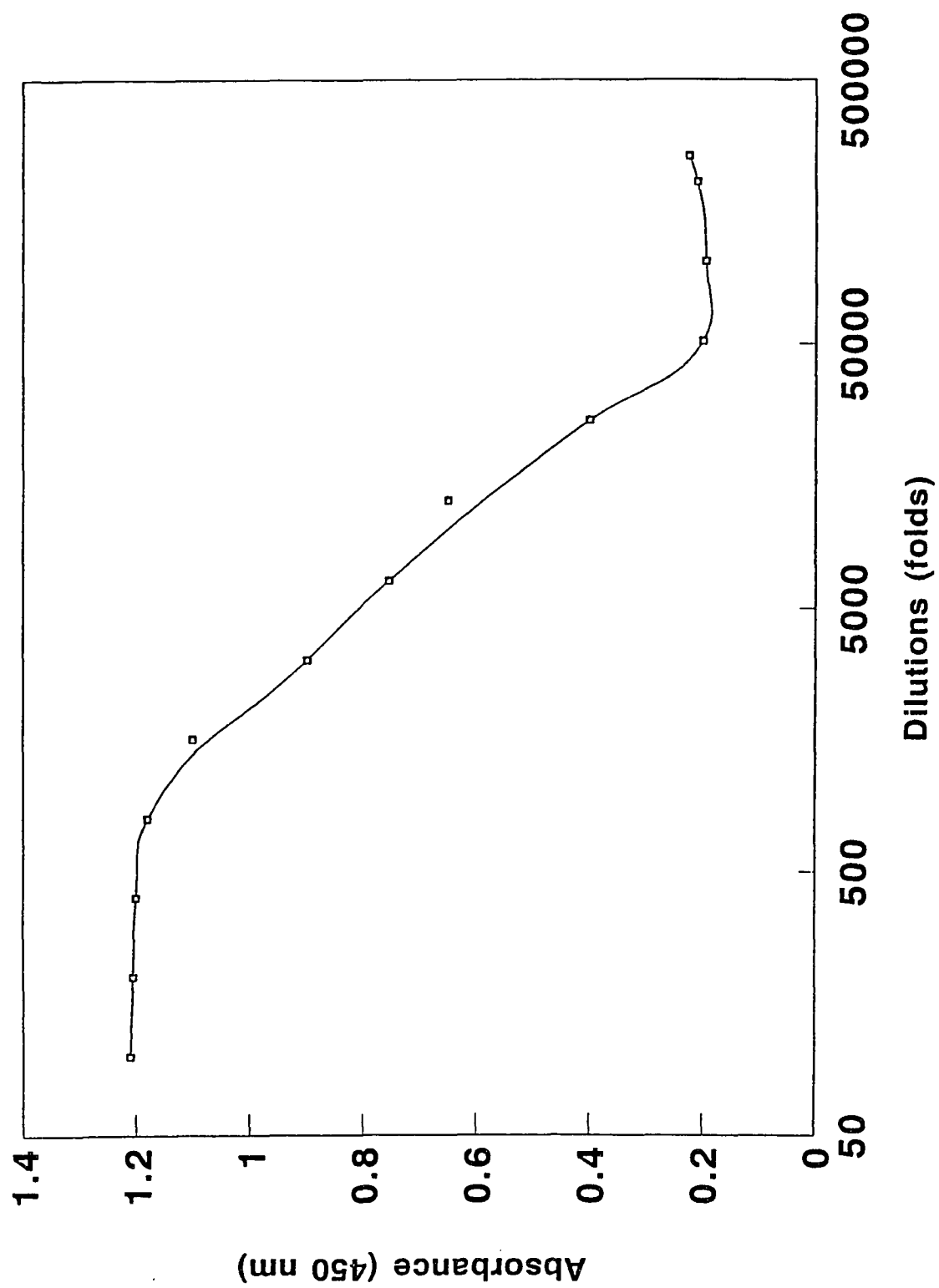


Figure 11

The titer assay study of anti-mevinphos by solid-phase enzyme linked immunosorbent assay on microwell immobilization. Anti-mevinphos ranging from 100 to 512,000 folds of dilution were employed. The absorbance was measured at 450 nm.

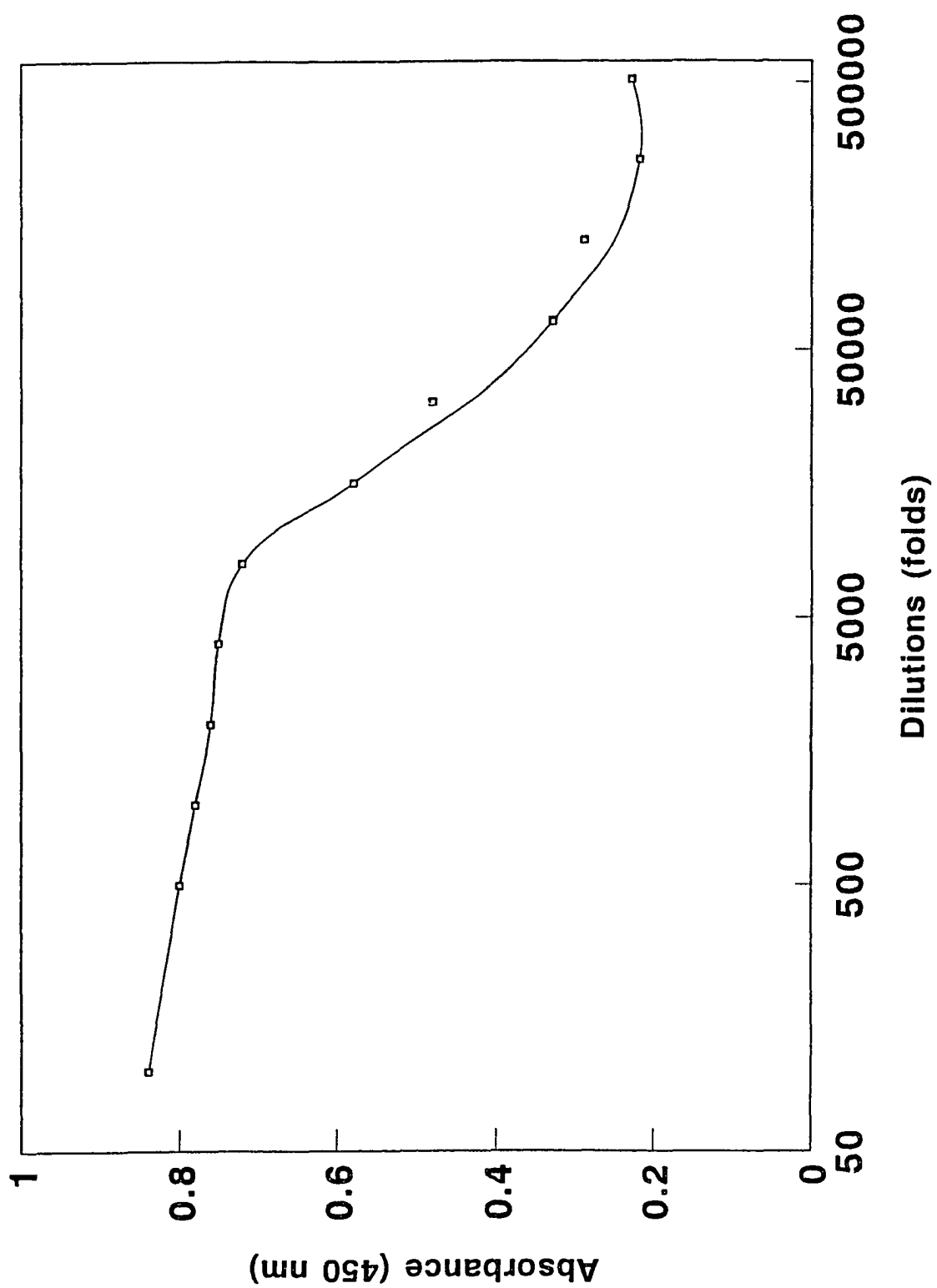


Table 1 Titer assay studies of anti-OP sera

Compound	Titer (folds of dilution)
malathion	10,800
parathion	25,000
tamaron	9,000
mevinphos	35,000

Figure 12

The elution profile of anti-malathion gamma globulin from DEAE-cellulose ion-exchange chromatography. The gamma globulin was eluted from the column with 5.0 mM sodium phosphate buffer (pH 6.5) in an isocratic condition and monitored at 280 nm.

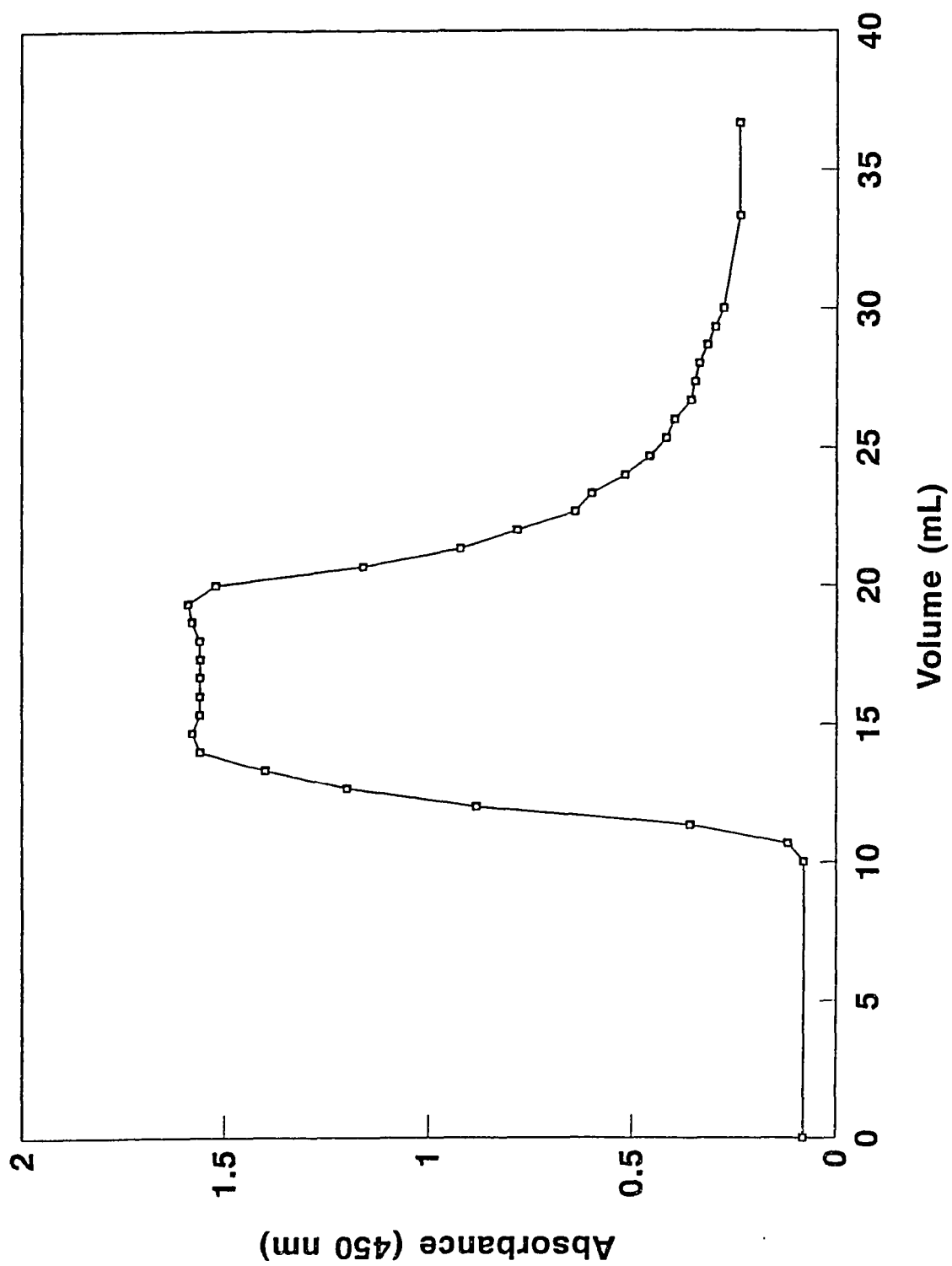


Figure 13

The elution profile of anti-parathion gamma globulin from DEAE-cellulose ion-exchange chromatography. The gamma globulin was eluted from the column with 5.0 mM sodium phosphate buffer (pH 6.5) in an isocratic condition and monitored at 280 nm.

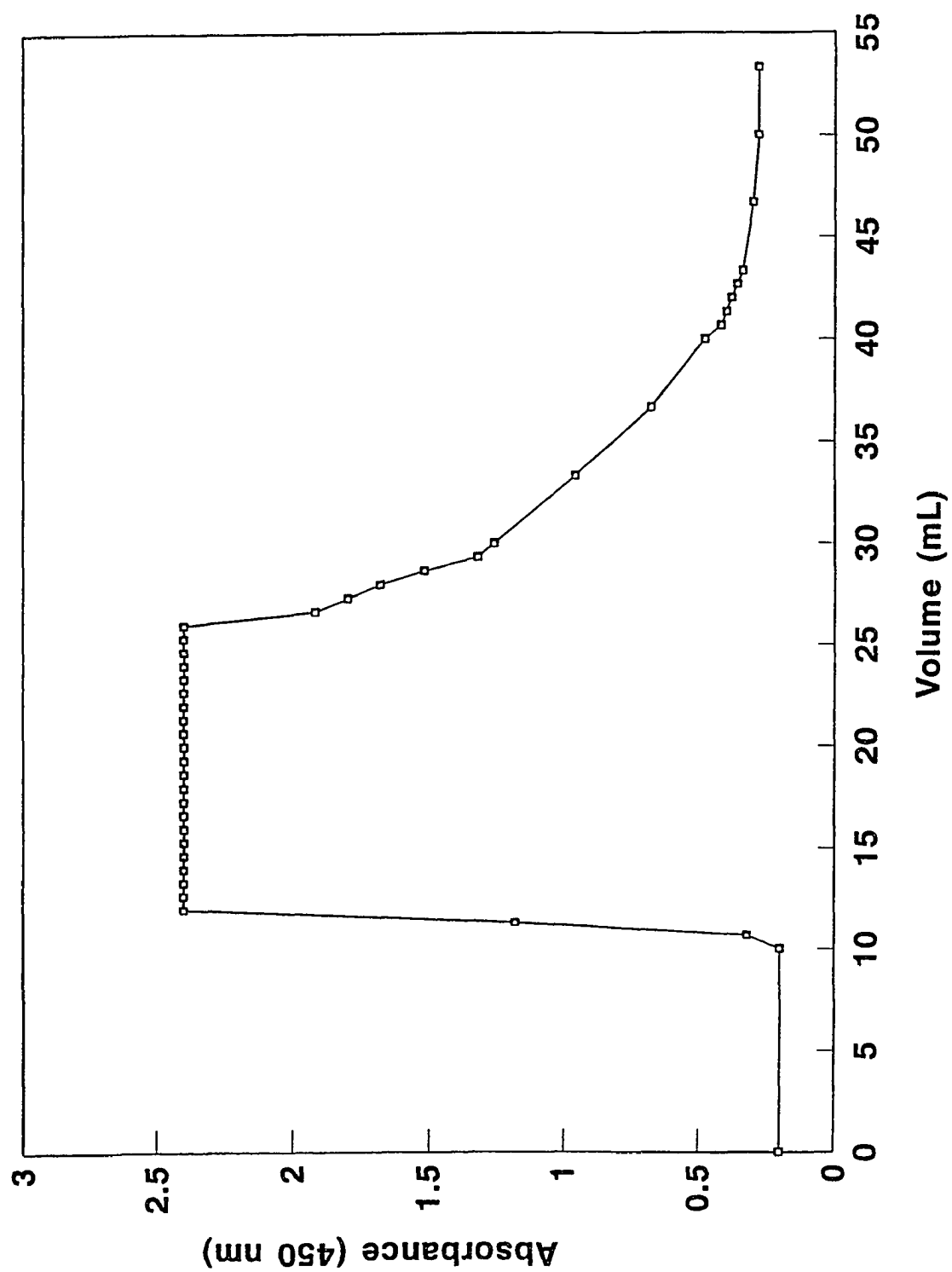


Figure 14

The elution profile of anti-tamaron gamma globulin from DEAE-cellulose ion-exchange chromatography. The gamma globulin was eluted from the column with 5.0 mM sodium phosphate buffer (pH 6.5) in an isocratic condition and monitored at 280 nm.

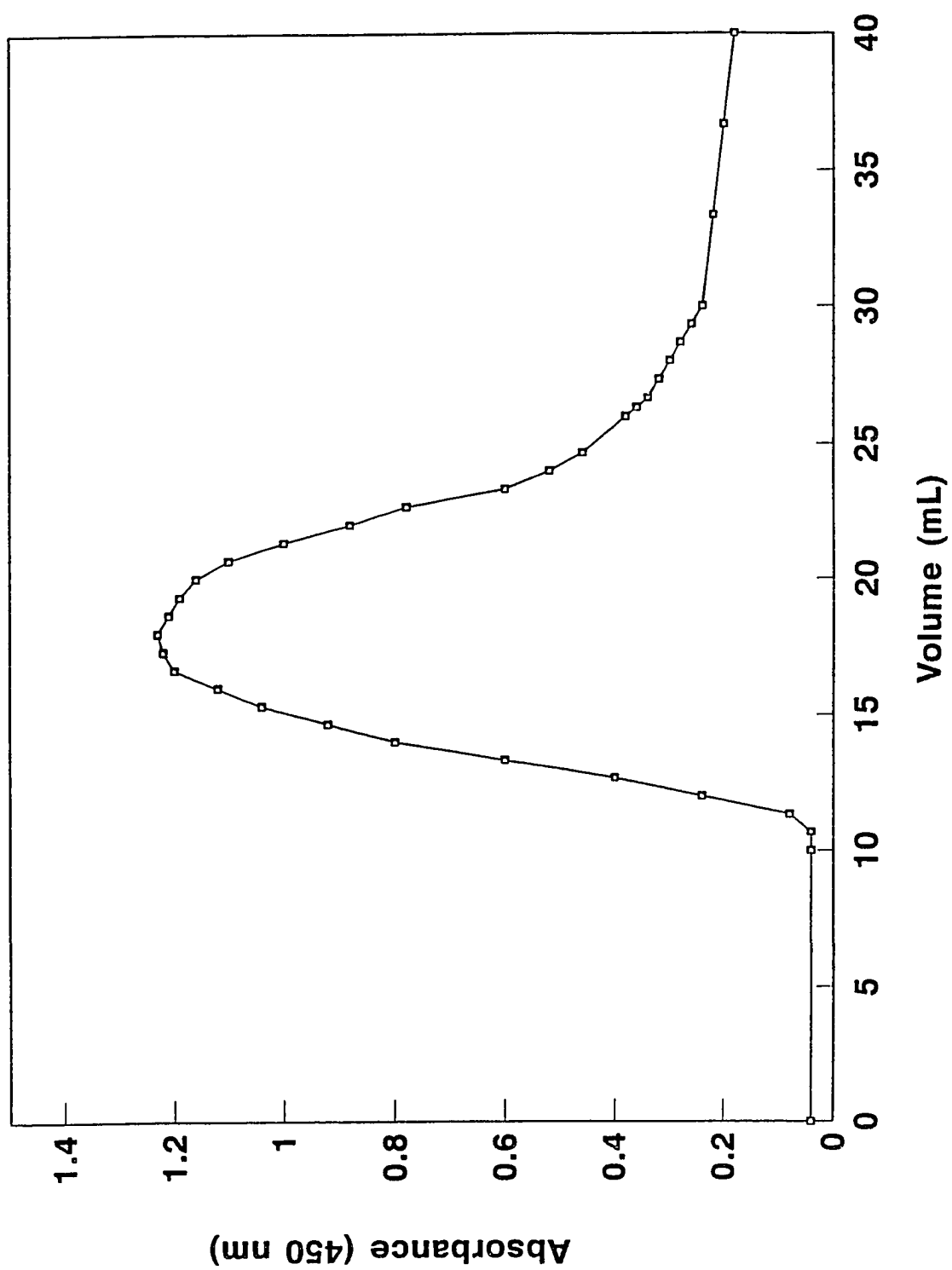
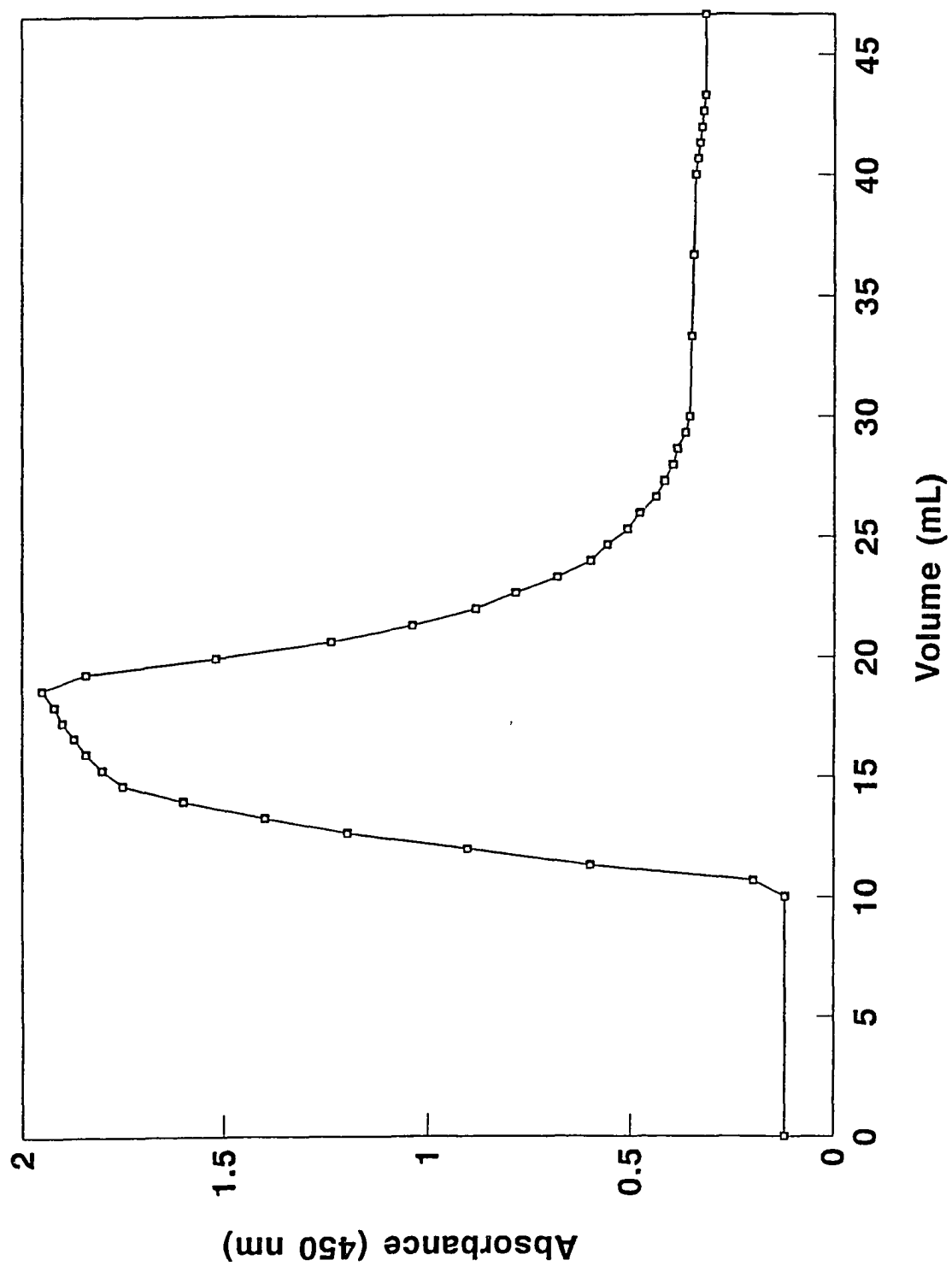


Figure 15

The elution profile of anti-mevinphos gamma globulin from DEAE-cellulose ion-exchange chromatography. The gamma globulin was eluted from the column with 5.0 mM sodium phosphate buffer (pH 6.5) in an isocratic condition and monitored at 280 nm.



gamma globulin fractions were then analyzed by Beckman microzone electrophoresis system using a cellulose acetate membrane and are presented in Figure 16.

B. Study of OP assay on the microwells

1. Study of the optimal enzyme dilutions for the OP assay

In the study of the optimal OP-HRPO dilution for enzyme immunoassay, the OP-HRPO was diluted to 10, 20, 50, 100, 200, 400, 800, 1600 and 3200 fold dilutions in 10 mM PBS, pH 7.4. The original concentrations of OP-HRPO, which were stored at -80°C, were 47.49 mg/mL, 34.83 mg/mL 26.71 mg/mL and 37.95 mg/mL for malathion-HRPO, parathion-HRPO, tamaron-HRPO and mevinphos-HRPO, respectively. To each microwell which was precoated with 1 μ g/well specific OP-OVA, 200 μ L of the different dilutions of OP-HRPO were pipetted and incubated for 60 minutes at room temperature. After incubation the microwells were emptied, washed with deionized water 10 times and dried. For the enzyme activity assay, the same procedure was followed as described in the previous section. The data of the optimal enzyme dilution of these four OP-HRPO are plotted as absorbance at 450 nm versus the fold of dilution of OP-HRPO in semi-log scale as illustrated in Figures 17-20. The optimal dilution of OP-HRPO were

Figure 16

The electrophoretic patterns of the gamma globulins isolated from DEAE-cellulose ion-exchange chromatography. (A), (B), (C) and (D) represent the electrophoretic patterns obtained from isolated anti-malathion, anti-parathion, anti-tamaron and anti-mevinphos gamma globulin fractions.

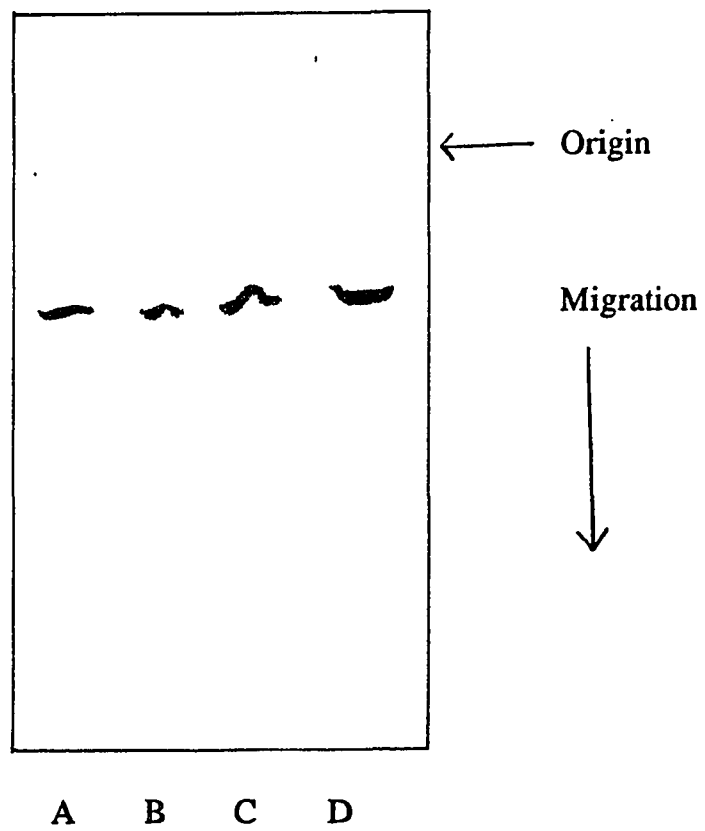


Figure 17

Optimal enzyme dilution study of malathion-HRPO in malathion assay in solid-phase enzyme immunoassay on microwell immobilization. Malathion-HRPO ranging from 100 to 1600 folds of dilution were employed. The absorbance was measured at 450 nm.

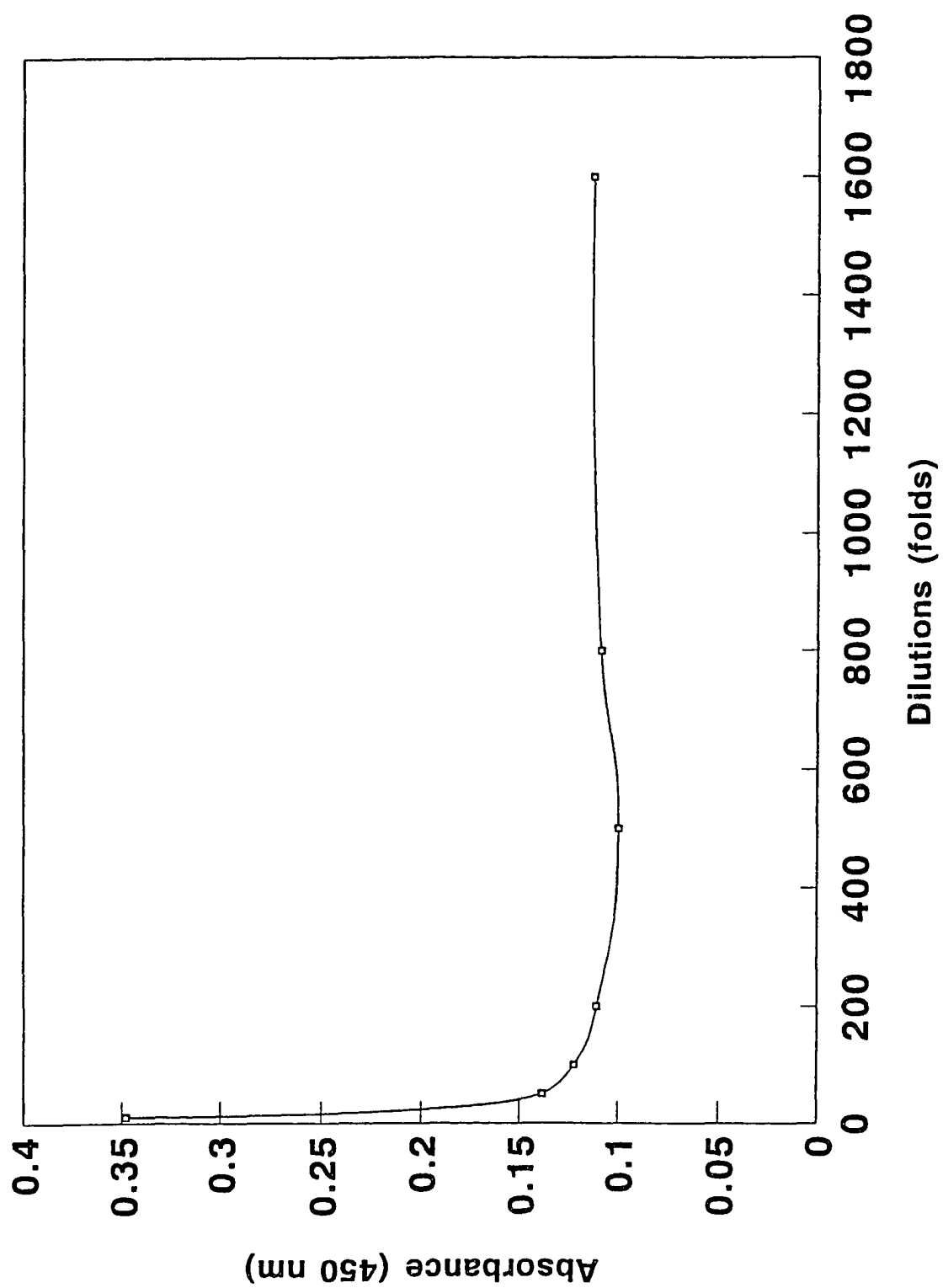


Figure 18

Optimal enzyme dilution study of parathion-HRPO in parathion assay in solid-phase enzyme immunoassay on microwell immobilization. Parathion-HRPO ranging from 10 to 2000 folds of dilution were employed. The absorbance was measured at 450 nm.

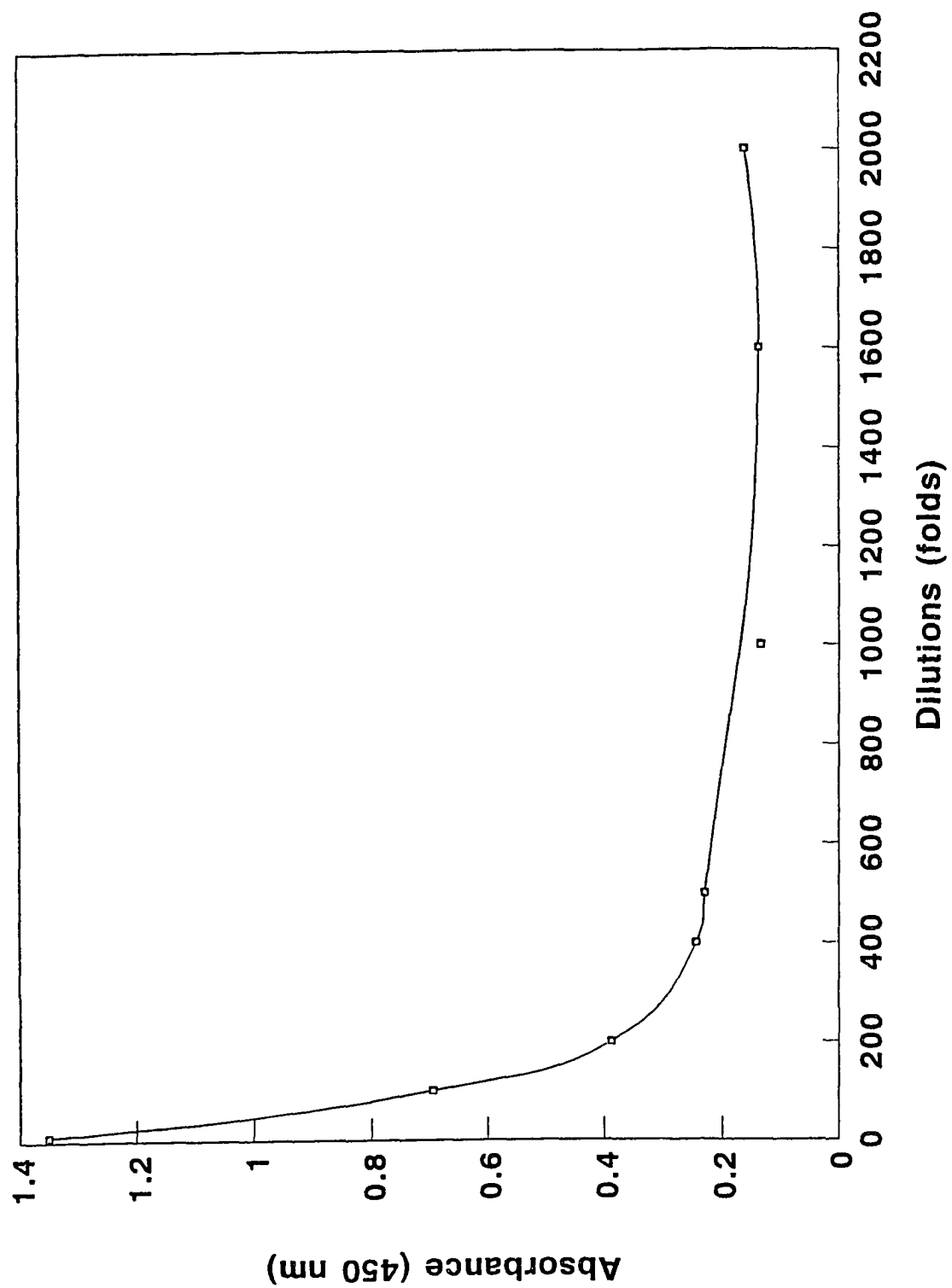


Figure 19

Optimal enzyme dilution study of tamaron-HRPO in tamaron in solid-phase enzyme immunoassay on microwell immobilization. Tamaron-HRPO ranging from 10 to 1000 folds of dilution were employed. The absorbance was measured at 450 nm.

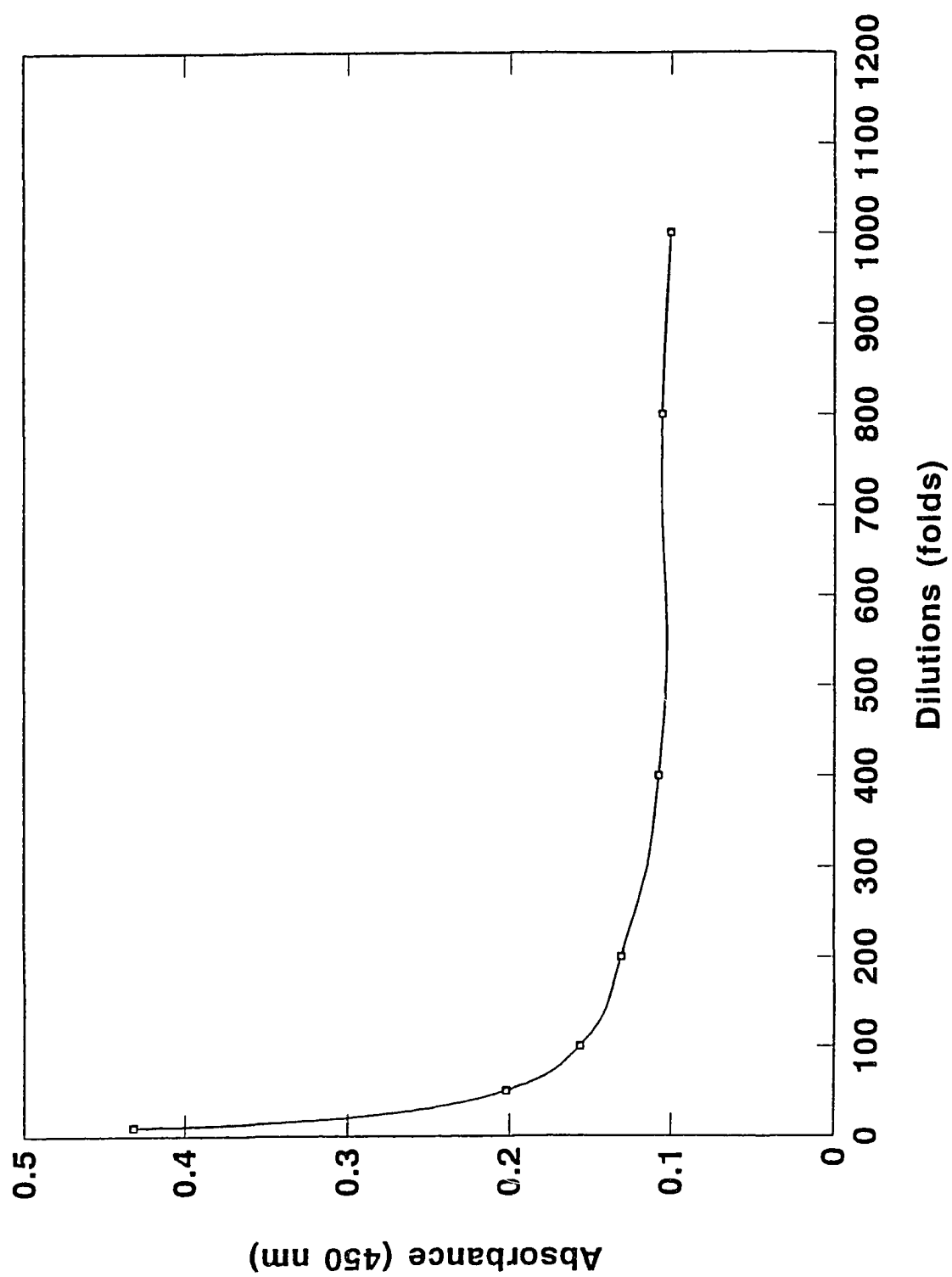
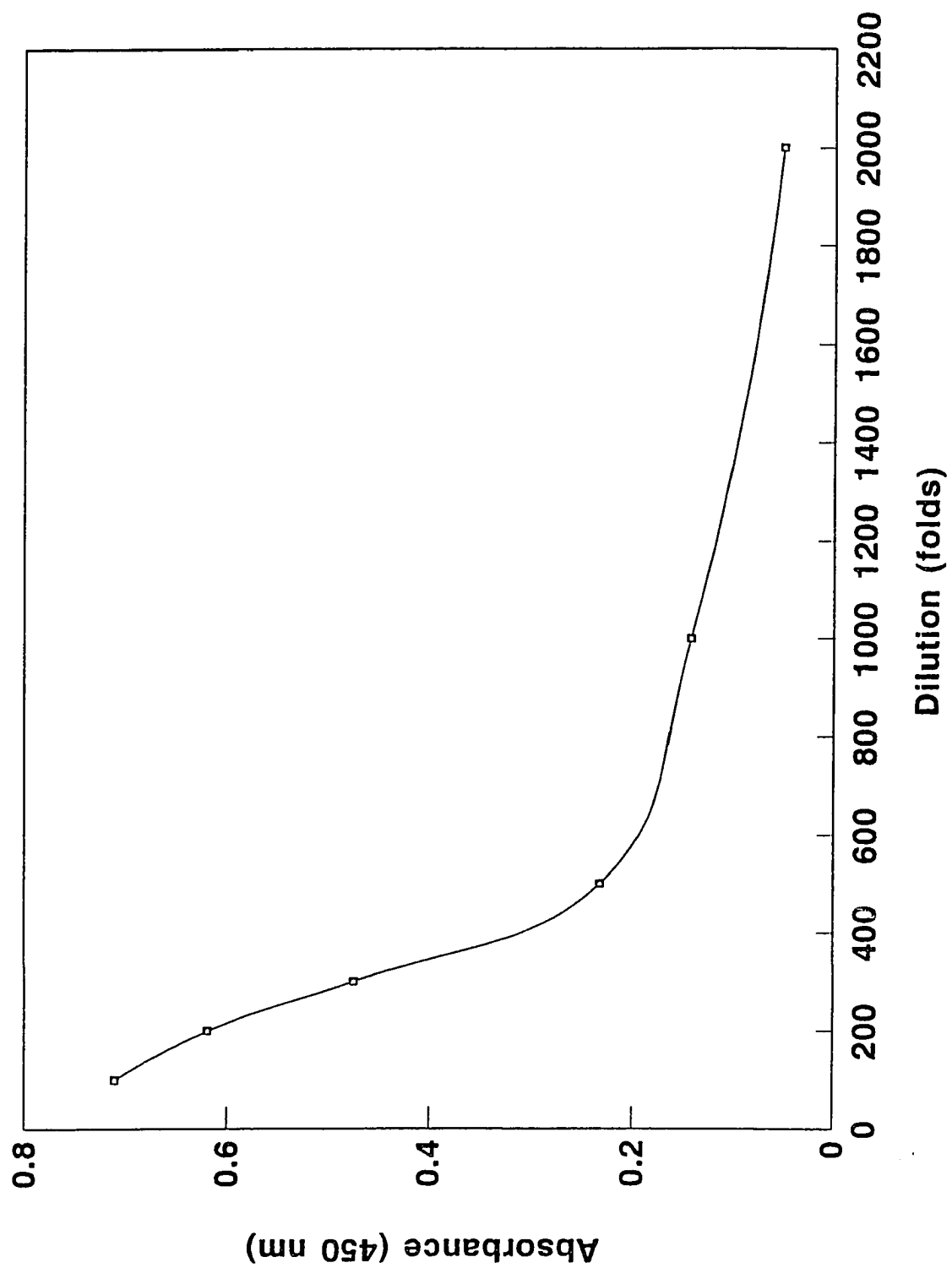


Figure 20

Optimal enzyme dilution study of mevinphos-HRPO in mevinphos assay in solid-phase enzyme immunoassay on microwell immobilization. Mevinphos-HRPO ranging from 100 to 2000 folds of dilution were employed. The absorbance was measured at 450 nm.



determined to be 100, 100, 100, 500 fold dilutions for malathion-HRPO, parathion-HRPO, tamaron-HRPO and mevinphos-HRPO, respectively.

2. Study of the optimal concentrations of gamma globulin for the microwell coating

The concentrations of purified anti-malathion, anti-parathion, anti-tamaron and anti-mevinphos gamma globulins were determined by absorption at 280 nm and calculated by using the extinction coefficient, $E_{1\%}$, 13.5. In the study of the optimal anti-OP gamma globulin concentration for microwell coating, 200 μL of the diluted purified anti-OP gamma globulin was pipetted into the microwells to give 0.1, 0.2, 0.5, 1, 2, 4, 8, 16, 32, 64, 125, 250, 500 and 1000 ng/well. These wells were incubated at room temperature overnight, then emptied, washed with deionized water 10 times and dried. To each microwell, 200 μL of the desired diluted OP-HRPO solution were added and incubated at room temperature for 60 minutes. The microwells were then emptied, washed and the HRPO activity was assayed using the same procedure as described above, and the data obtained are shown in Figures 21-24. The optimal amount of anti-OP gamma globulin for microwell coating was determined to be 10, 100, 100, 10 ng/200 μL /well for anti-malathion, anti-parathion, anti-tamaron and anti-mevinphos, respectively.

Figure 21

Saturation curve of anti-malathion gamma globulin in malathion assay in solid-phase enzyme immunoassay on microwell immobilization. Anti-malathion gamma globulin ranging from 1.0-100 ng/well were used to coat microwells. Experimental conditions for immobilization of the protein to microwells were described in the text. The absorbance was measured at 450 nm.

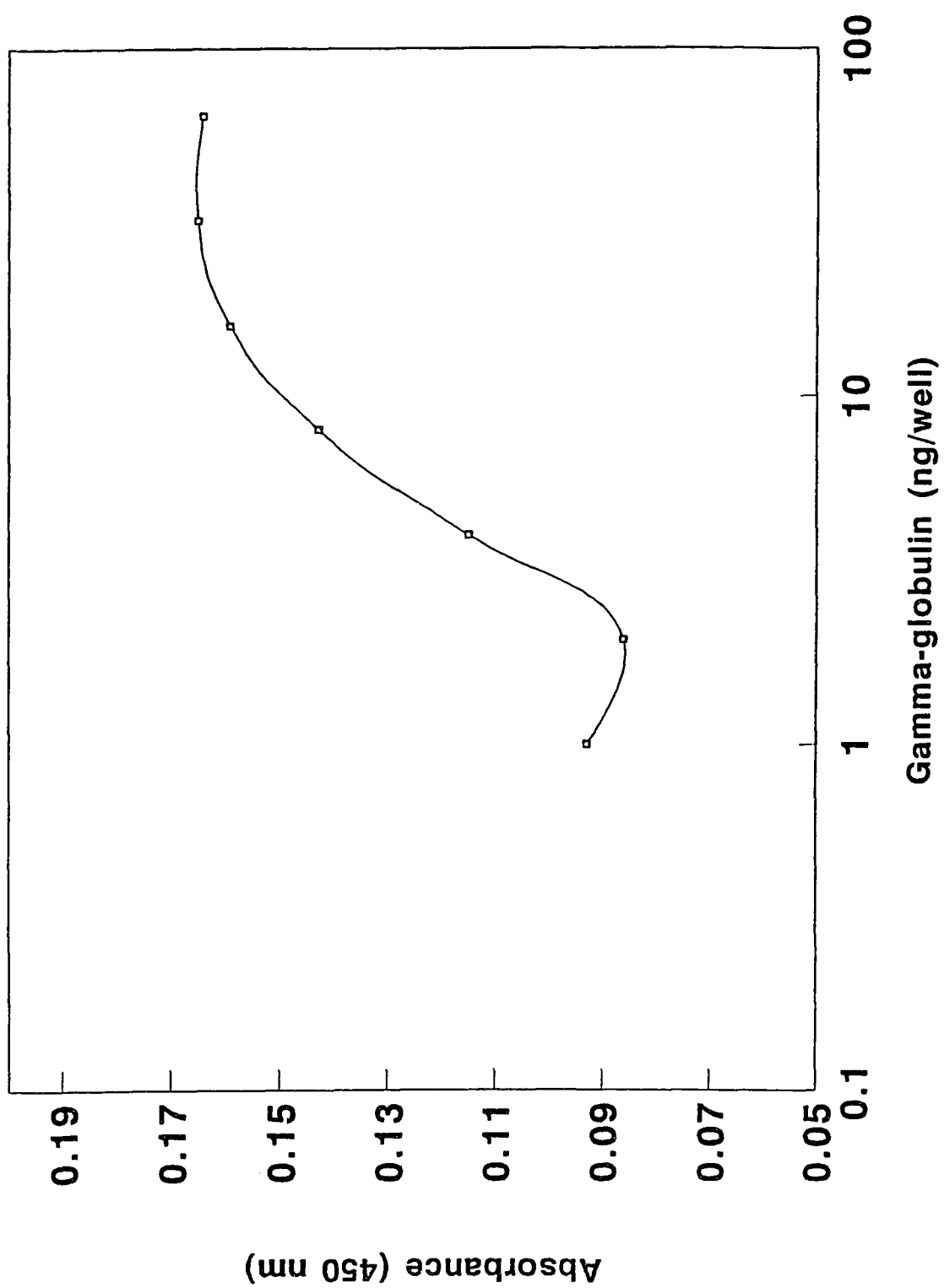


Figure 22

Saturation curve of anti-parathion gamma globulin in parathion assay in solid-phase enzyme immunoassay on microwell immobilization. Anti-parathion gamma globulin ranging from 1.0 to 500 ng/well were used to coat microwells. Experimental conditions for immobilization of the protein to microwells were described in the text. The absorbance was measured at 450 nm.

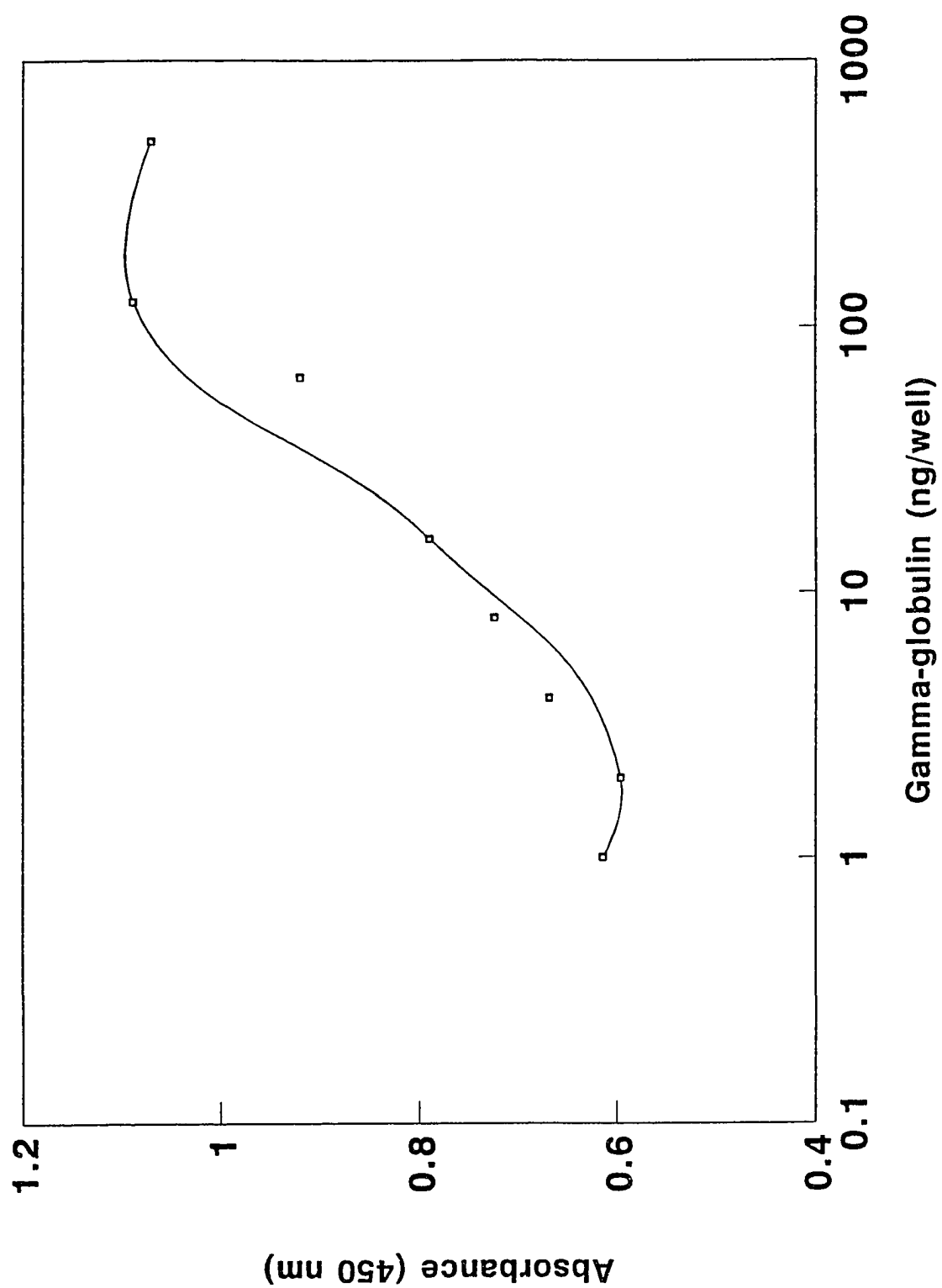


Figure 23

Saturation curve of anti-tamaron gamma globulin in tamaron assay in solid-phase enzyme immunoassay on microwell immobilization. Anti-tamaron gamma globulin ranging from 1.0 to 250 ng/well were used to coat microwells. Experimental conditions for immobilization of the protein to microwells were described in the text. The absorbance was measured at 450 nm.

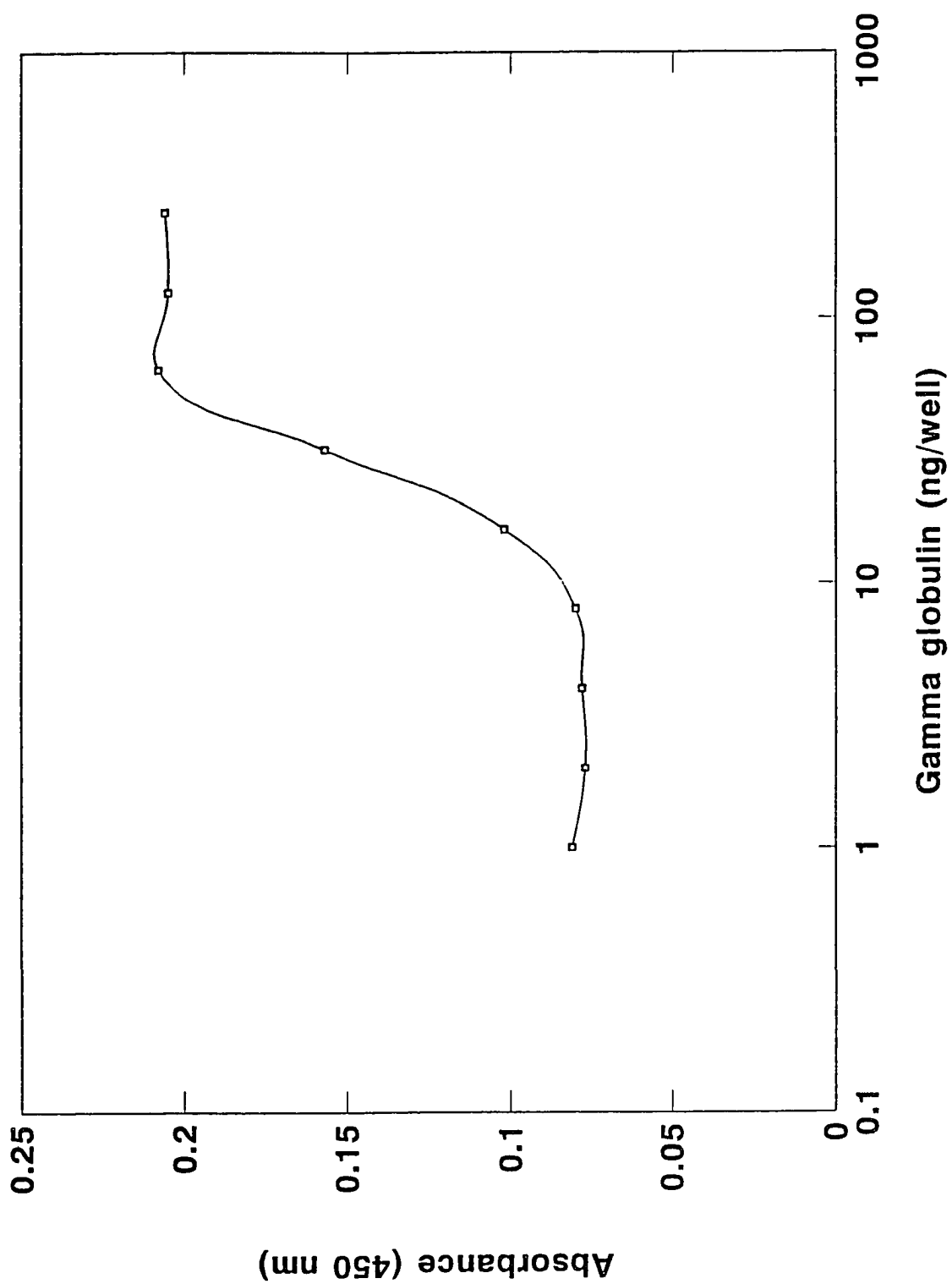
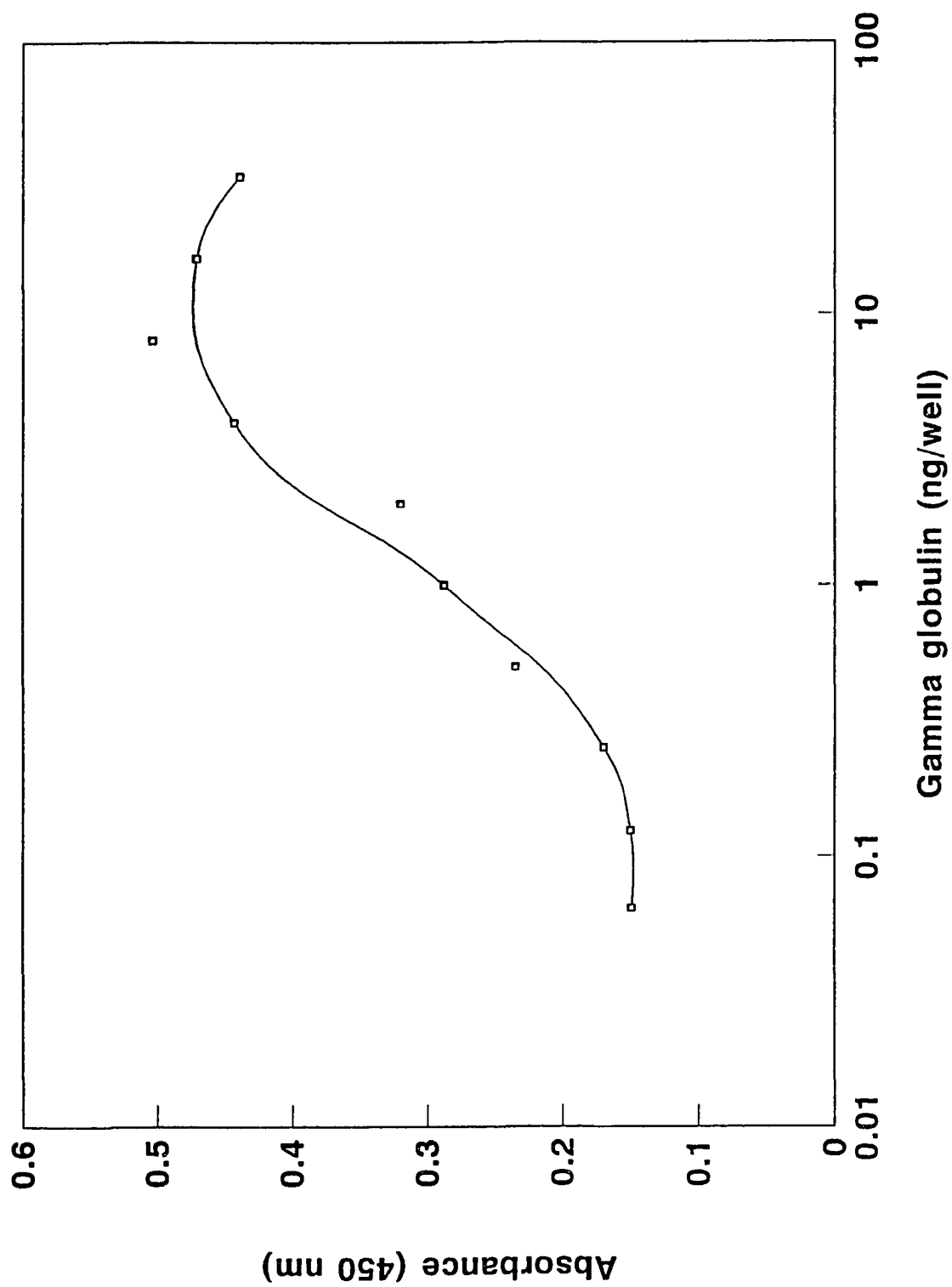


Figure 24

Saturation curve of anti-mevinphos gamma globulin in mevinphos assay in solid-phase enzyme immunoassay on microwell immobilization. Anti-mevinphos gamma globulin ranging from 0.128 – 32 ng/well were used to coat microwells. Experimental conditions for immobilization of the protein to microwells were described in the text. The absorbance was measured at 450 nm.



3. Study of the antigen and OP-HRPO quantitations for malathion, parathion, tamaron and mevinphos in the competitive enzyme immunoassay on microwell immobilization

Into the specific microwells which were precoated with anti-OP at optimal concentration, 200 μL of the mixture of organophosphorus pesticides and OP-HRPO in different ratios were pipetted. Different ratios of the mixture of organophosphorus pesticides and OP-HRPO were tested to construct the best standard curve. The results obtained, shown in Figures 25-28, were plotted in a semi-logarithmic scale of OP concentrations (0 to 15 ng/mL) versus the HRPO activity assayed at 450 nm. Simple regression analysis was used to select to the optimal OP to OP-HRPO ratio. Since the color development shown in the competitive enzyme immunoassay is inverse to the antigen concentration, the regression coefficient, the slope, should be performed as a negative value. The more negative the regression coefficient, the slope, of the regression curve suggests, the higher the sensitivity is.

The ratios of antigen (malathion) to malathion-HRPO were 50 μL to 50 μL , 50 μL to 100 μL , 100 μL to 50 μL , 40 μL to 60 μL , and 60 μL to 40 μL for malathion assay. The result in Figure 25 shows that the ratio of 100 μL to 50 μL , antigen to malathion-HRPO was selected due to the better separation, with a sharp slope of -0.02 compared to -0.012 (50 μL to 50 μL -antigen to malathion-HRPO), -0.003 (40 μL to 60 μL -antigen to malathion-HRPO) and -

Figure 25

Study of malathion and malathion-HRPO quantitations for the malathion solid-phase enzyme immunoassay on microwell immobilization. For the malathion assay, (□) represents 50 μ L analyte and 50 μ L malathion-HRPO; (+) represents 50 μ L analyte and 100 μ L malathion-HRPO; (*) represents 100 μ L analyte and 50 μ L malathion-HRPO; (■) represents 40 μ L analyte and 60 μ L malathion-HRPO; and (x) represents 60 μ L analyte and 40 μ L malathion-HRPO as the assay conditions. The experimental conditions were described in the text. The absorbance was measured at 450 nm. Standard curves of malathion assay in different assay conditions in microwell immobilization as plotted on semi-logarithm scale. The results were plotted as absorbance versus logarithm of malathion concentration.

□: $Y=0.205-0.012x\log(X)$, $r=-0.807$; +: $Y=0.059+0.032x\log(X)$, $r=0.956$
*: $Y=0.160-0.022x\log(X)$, $r=-0.904$; ■: $Y=0.096-0.003x\log(X)$, $r=-0.310$
x: $Y=0.091-0.007x\log(X)$, $r=-0.661$

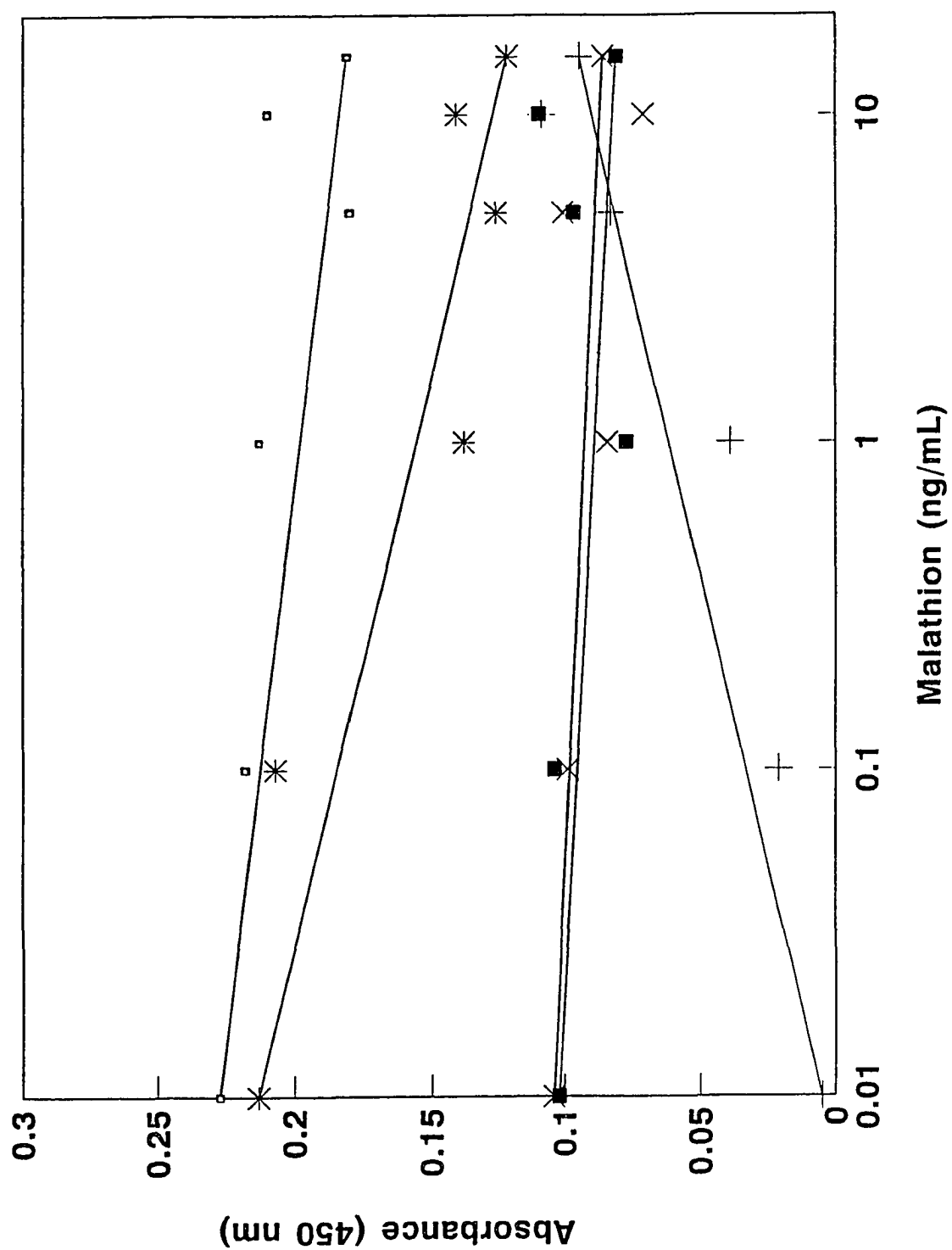


Figure 26

Study of parathion and parathion-HRPO quantitations for the parathion solid-phase enzyme immunoassay on microwell immobilization. For the parathion assay, (\square) represents 50 μ L analyte and 100 μ L parathion-HRPO; ($+$) represents 100 μ L analyte and 50 μ L parathion-HRPO; and (*) represents 50 μ L analyte and 50 μ L parathion-HRPO as the assay conditions. The experimental conditions were described in the text. The absorbance was measured at 450 nm. Standard curves of parathion assay in different assay conditions in microwell immobilization as plotted on semi-logarithm scale. The results were plotted as absorbance versus logarithm of parathion concentration.

\square : $Y=0.224-0.003 \times \log(X)$, $r=-0.409$; $+$: $Y=0.340-0.051 \times \log(X)$, $r=0.961$

*: $Y=0.363-0.065 \times \log(X)$, $r=-0.995$

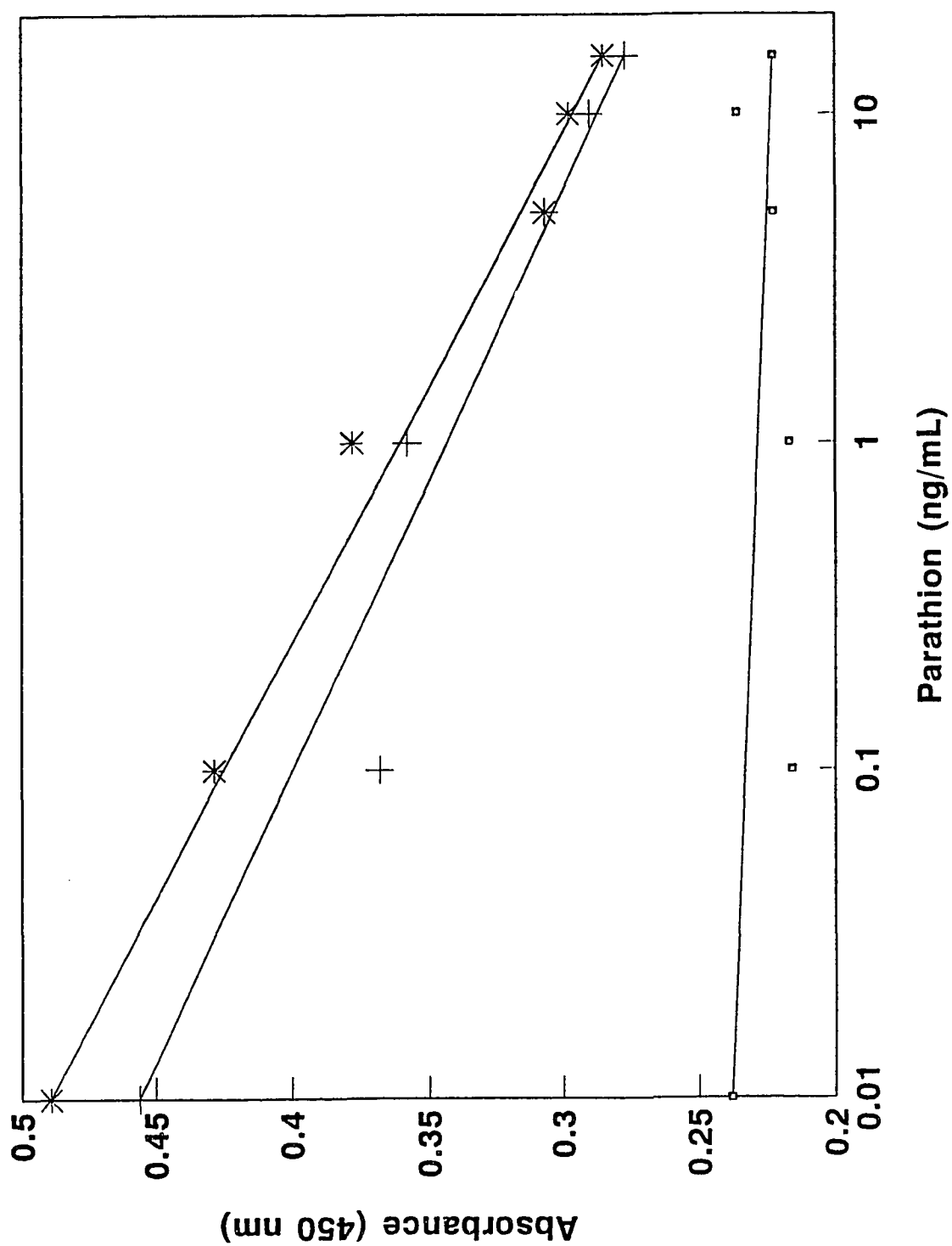


Figure 27

Study of tamaron and tamaron-HRPO quantitations for the tamaron solid-phase enzyme immunoassay on microwell immobilization. For the tamaron assay, (□) represents 50 μ L analyte and 50 μ L tamaron-HRPO; (+) represents 50 μ L analyte and 100 μ L tamaron-HRPO; and (*) represents 100 μ L analyte and 50 μ L tamaron-HRPO as the assay conditions. The experimental conditions were described in the text. The absorbance was measured at 450 nm. Standard curves of tamaron assay in different assay conditions in microwell immobilization as plotted on semi-logarithm scale. The results were plotted as absorbance versus logarithm of tamaron concentration.

□: $Y=0.075-0.020 \times \log(X)$, $r=-0.989$; +: $Y=0.109-0.017 \times \log(X)$, $r=0.882$

*: $Y=-0.291+0.237 \times \log(X)$, $r=0.207$

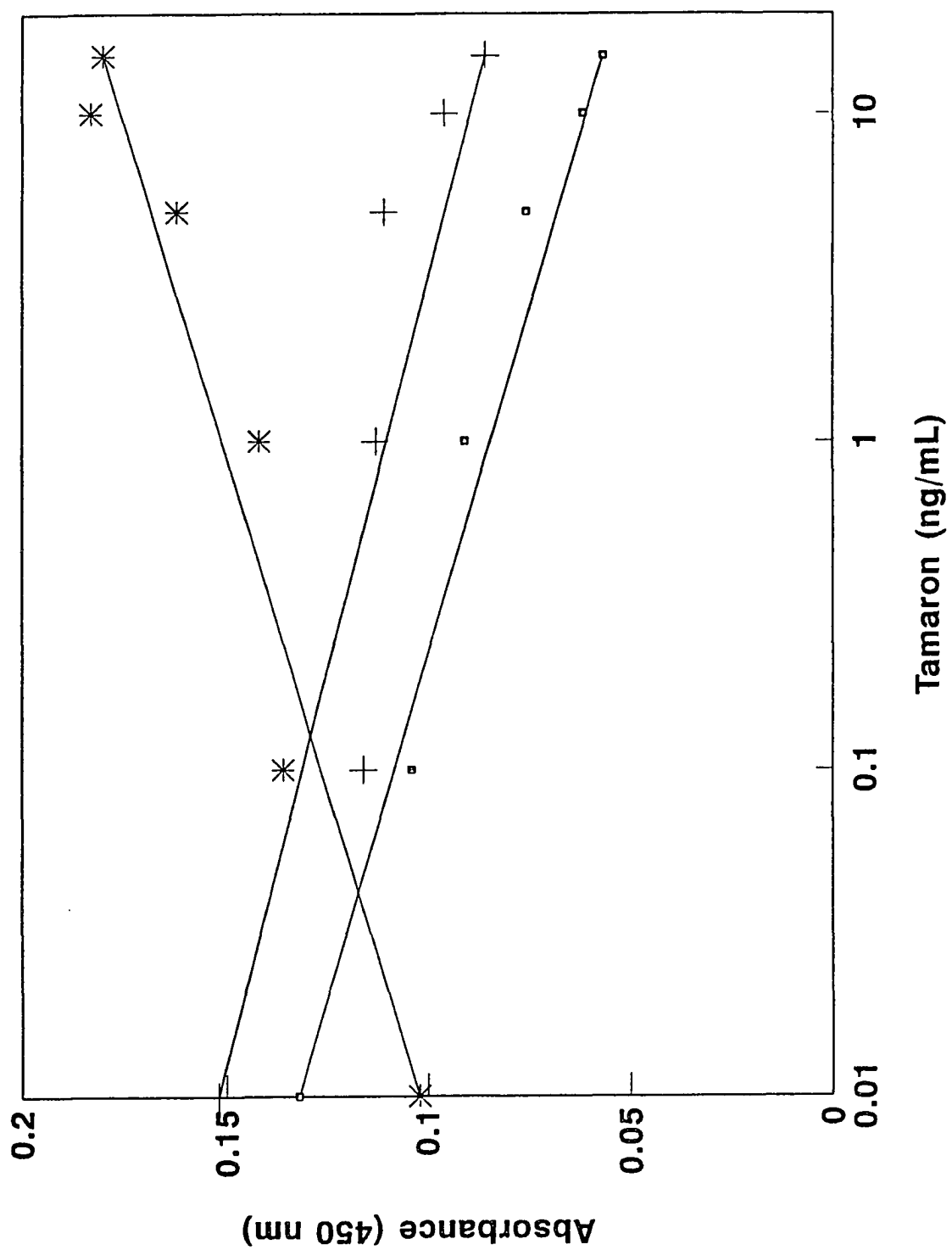
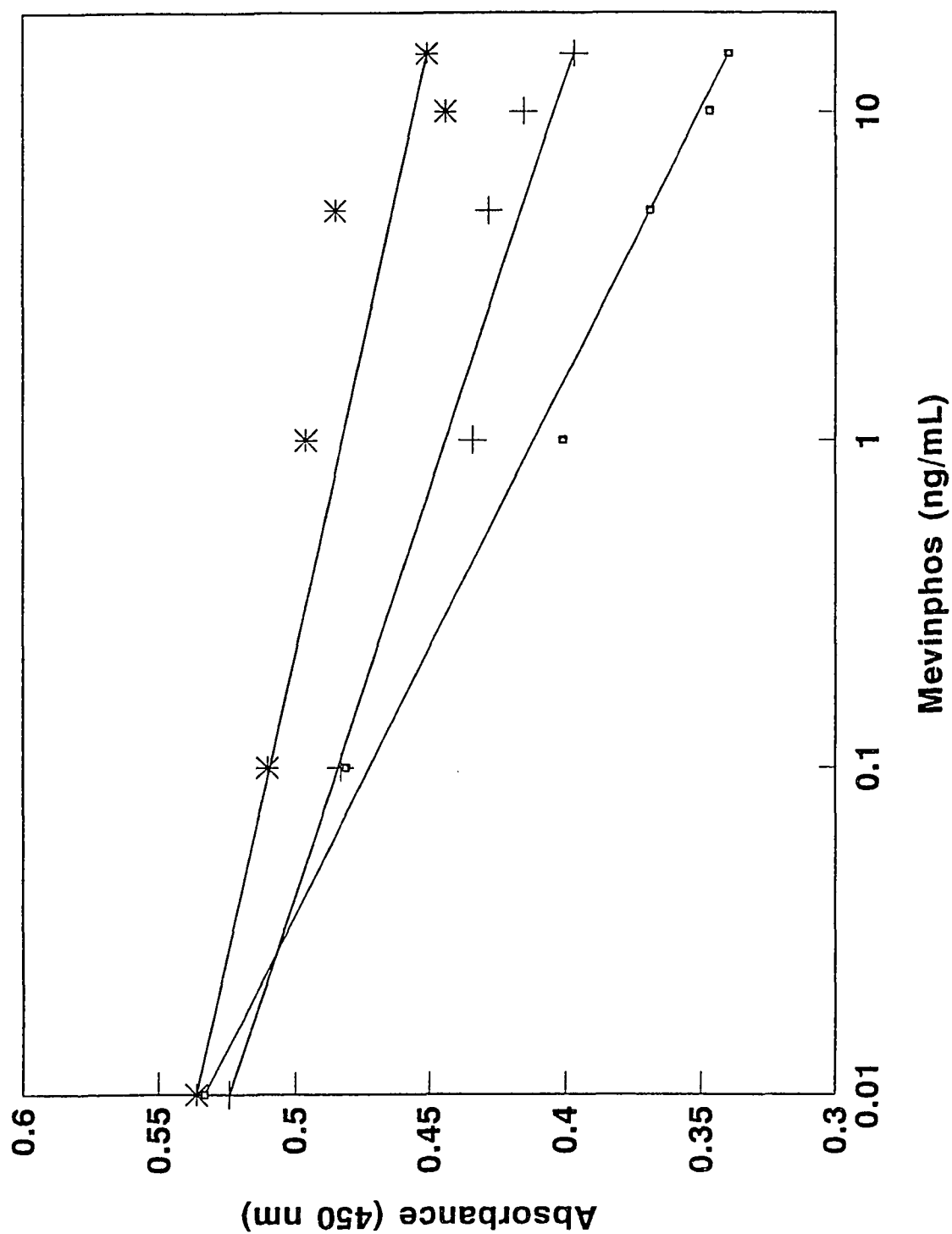


Figure 28

Study of mevinphos and mevinphos-HRPO quantitations for the mevinphos solid-phase enzyme immunoassay on microwell immobilization. For the mevinphos assay, (□) represents 50 μ L analyte and 50 μ L mevinphos-HRPO; (+) represents 50 μ L analyte and 100 μ L mevinphos-HRPO; and (*) represents 100 μ L analyte and 50 μ L mevinphos-HRPO as the assay conditions. The experimental conditions were described in the text. The absorbance was measured at 450 nm. Standard curves of mevinphos assay in different assay conditions in microwell immobilization as plotted on semi-logarithm scale. The results were plotted as absorbance versus logarithm of mevinphos concentration.
□: $Y=0.410-0.061 \times \log(X)$, $r=-0.997$; +: $Y=0.446-0.037 \times \log(X)$, $r=0.987$
*: $Y=0.486-0.026 \times \log(X)$, $r=-0.945$



0.007 (60 μ L to 40 μ L-antigen to malathion-HRPO). The correlation coefficient (r) was -0.904, which is a high correlation.

For parathion assay the ratios of antigen to parathion-HRPO selected were 50 μ L to 50 μ L, 50 μ L to 100 μ L and 100 μ L to 50 μ L. The ratio of 50 μ L to 50 μ L, antigen to parathion-HRPO was selected due to the highest separation, with a slope of -0.065 compared to -0.03 (for 50 μ L to 100 μ L-antigen to parathion-HRPO) and -0.05 (for 100 μ L to 50 μ L-antigen to parathion-HRPO). The correlation coefficient (r) for 50 μ L to 50 μ L (antigen to parathion-HRPO) was -0.995, which is close to -1, the highest correlation. As shown in Figure 26 the antigen to parathion-HRPO of 50 μ L to 50 μ L was the best selection.

The ratios of antigen to tamaron-HRPO studied were 50 μ L to 50 μ L, 50 μ L to 100 μ L and 100 μ L to 50 μ L for tamaron assay. The ratio of 50 μ L to 50 μ L, antigen to tamaron-HRPO was selected due to the highest separation, with a sharpest slope of -0.02 compared to -0.017 (for 50 μ L to 100 μ L-antigen to tamaron-HRPO) and 0.237 (for 100 μ L to 50 μ L-antigen to tamaron-HRPO). The correlation coefficient (r) for 50 μ L to 50 μ L (antigen to tamaron-HRPO) was -0.989 which stood as a very high correlation. The antigen to tamaron-HRPO of 50 μ L to 50 μ L was the best selection as shown in Figure 27.

For mevinphos assay the ratios of antigen to mevinphos-HRPO studied were 50 μ L to 50 μ L, 50 μ L to 100 μ L and 100 μ L to 50 μ L. The ratio of 50

μL to 50 μL , antigen to mevinphos-HRPO was selected due to the highest separation, with a slope of -0.060 compared to -0.037 (for 50 μL to 100 μL -antigen to mevinphos-HRPO) and -0.026 (for 100 μL to 50 μL -antigen to mevinphos-HRPO). Meanwhile, the correlation coefficient (r) for 50 μL to 50 μL (antigen to mevinphos-HRPO) was -0.997, a very high correlation. This suggests that antigen to mevinphos-HRPO of 50 μL to 50 μL is the best selection as shown in Figure 28.

4. Study of the optimal OVA concentrations for malathion, parathion, tamaron and mevinphos in the competitive enzyme immunoassay on microwell immobilization

Once the optimal antigen to OP-HRPO conditions were established, the optimal OVA concentration for blocking the non-specific binding space in the microwells for each OP assay was studied. OVA was added to the antibody pre-coated wells to block the unbound spaces of the microwell to eliminate the non-specific binding interference. The results obtained for the optimal concentration of OVA blocking are shown in Figures 29-32.

The OVA concentrations were studied as 0% and 0.1% OVA blocking for malathion assay. Figure 29 shows that OVA 0.1% was selected due to higher sensitivity which stood for better separation. For parathion assay, shown in Figure 30; 0%, 0.1% and 0.3% OVA were employed. OVA 0.3%

Figure 29

OVA blocking study of the malathion solid-phase enzyme immunoassay on microwell immobilization. (□) and (+) represent 0 and 1 $\mu\text{g/mL}$ OVA blocking the nonspecific sites of the microwell in malathion assay, respectively. The absorbance was measured at 450 nm. Standard curves of malathion assay in different assay conditions in microwell immobilization as plotted on semi-logarithm scale. The results were plotted as absorbance versus logarithm of malathion concentration.

□: $Y=0.412-0.003 \times \log(X)$, $r=-0.109$; +: $Y=0.379-0.004 \times \log(X)$, $r=-0.372$

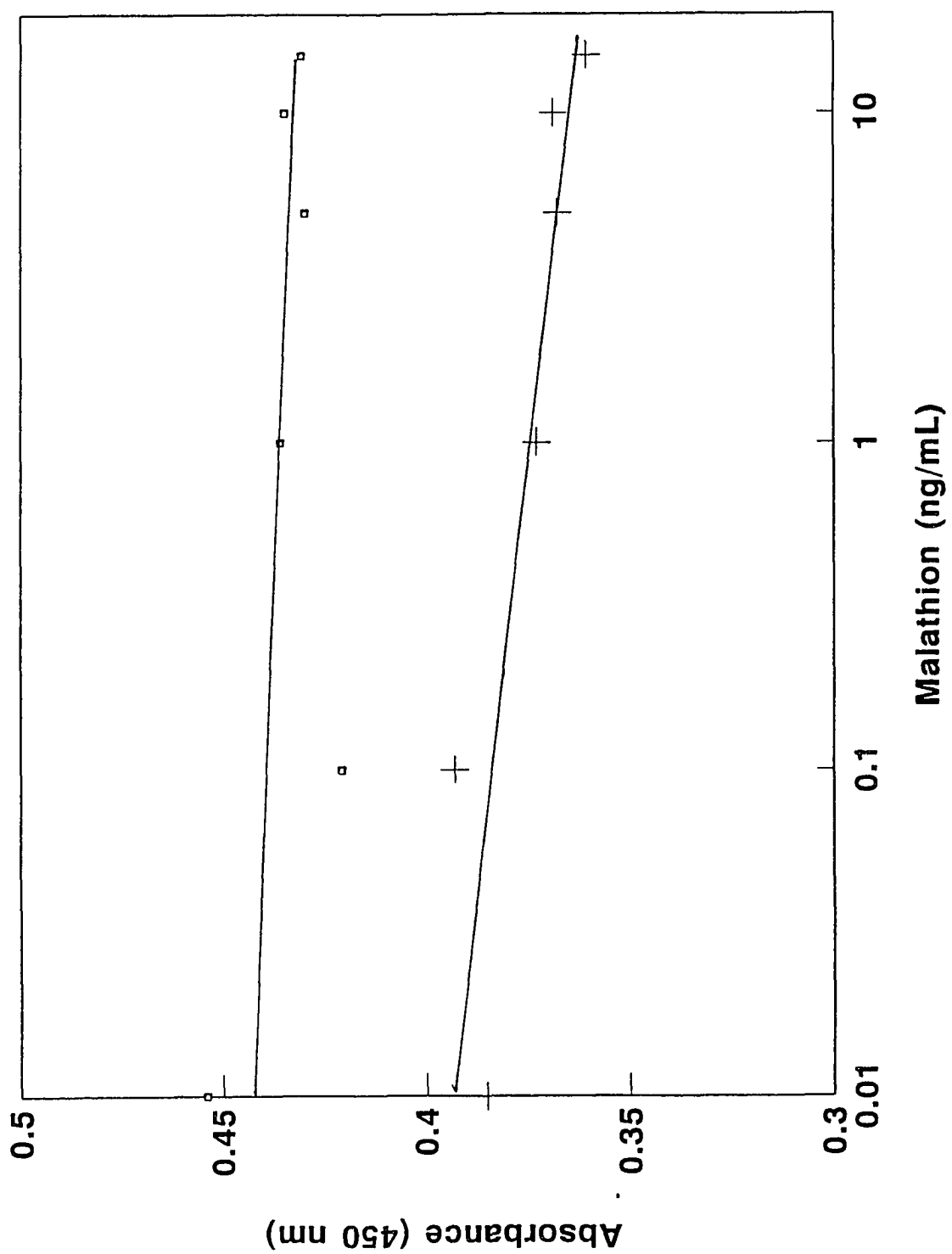


Figure 30

OVA blocking study of the parathion solid-phase enzyme immunoassay on microwell immobilization. (□), (+) and (*) represent 0, 10, 30 $\mu\text{g/mL}$ OVA blocking the nonspecific sites of the microwell in parathion assay, respectively. The absorbance was measured at 450 nm. Standard curves of parathion assay in different assay conditions in microwell immobilization as plotted on semi-logarithm scale. The results were plotted as absorbance versus logarithm of parathion concentration.

□: $Y=0.888-0.036 \times \log(X)$, $r=-0.630$; +: $Y=0.463+0.184 \times \log(X)$, $r=0.960$

*: $Y=0.552-0.023 \times \log(X)$, $r=-0.971$

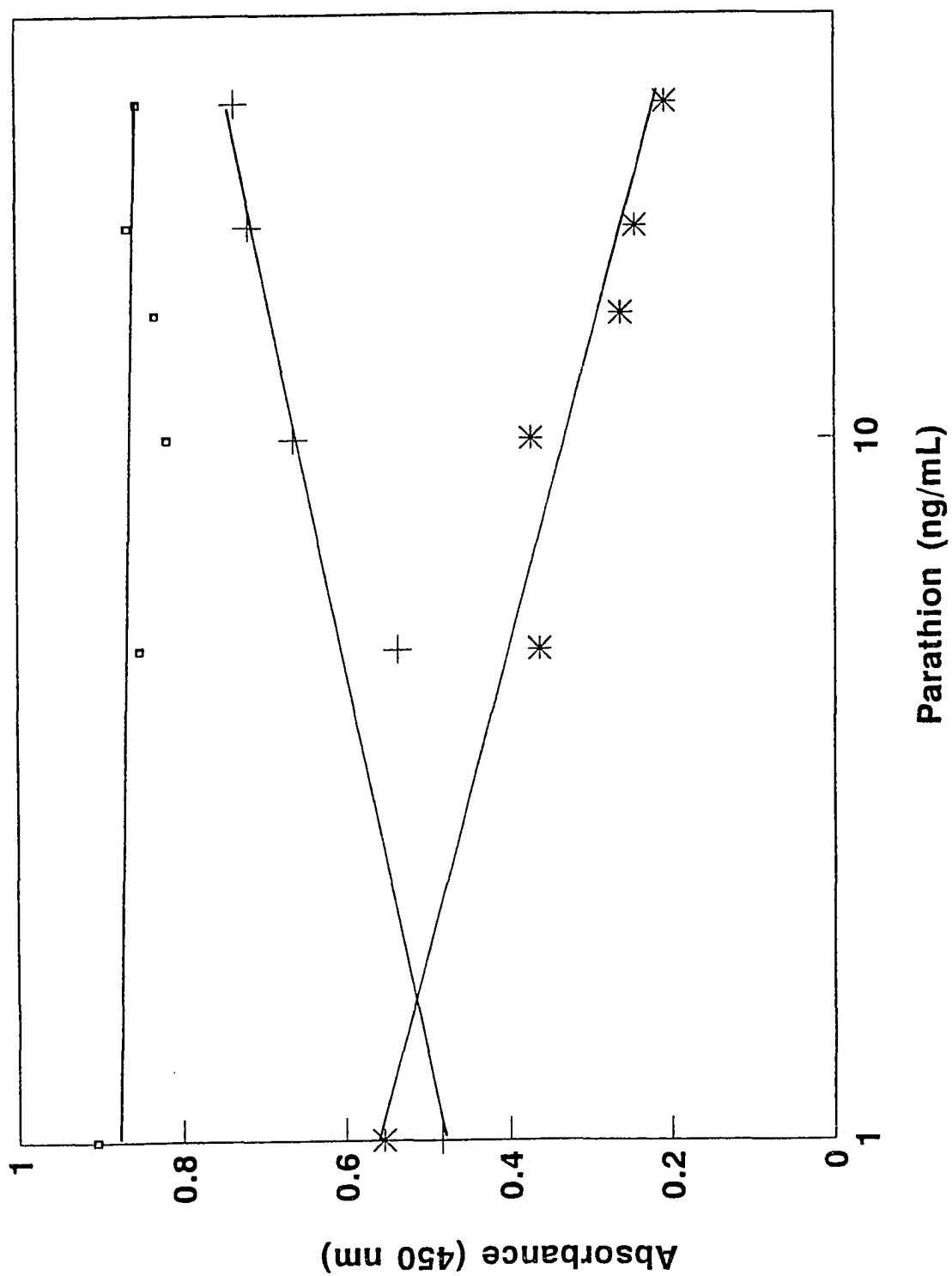


Figure 31

OVA blocking study of the tamaron solid-phase enzyme immunoassay on microwell immobilization. (□) and (+) represent 0 and 1 $\mu\text{g/mL}$ OVA blocking the nonspecific sites of the microwell in tamaron assay, respectively. The absorbance was measured at 450 nm. Standard curves of tamaron assay in different assay conditions in microwell immobilization as plotted on semi-logarithm scale. The results were plotted as absorbance versus logarithm of tamaron concentration.

□: $Y=0.186+0.033 \times \log(X)$, $r=0.691$ (0 ng/mL to 4 ng/mL)

+: $Y=0.179-0.028 \times \log(X)$, $r=-0.953$

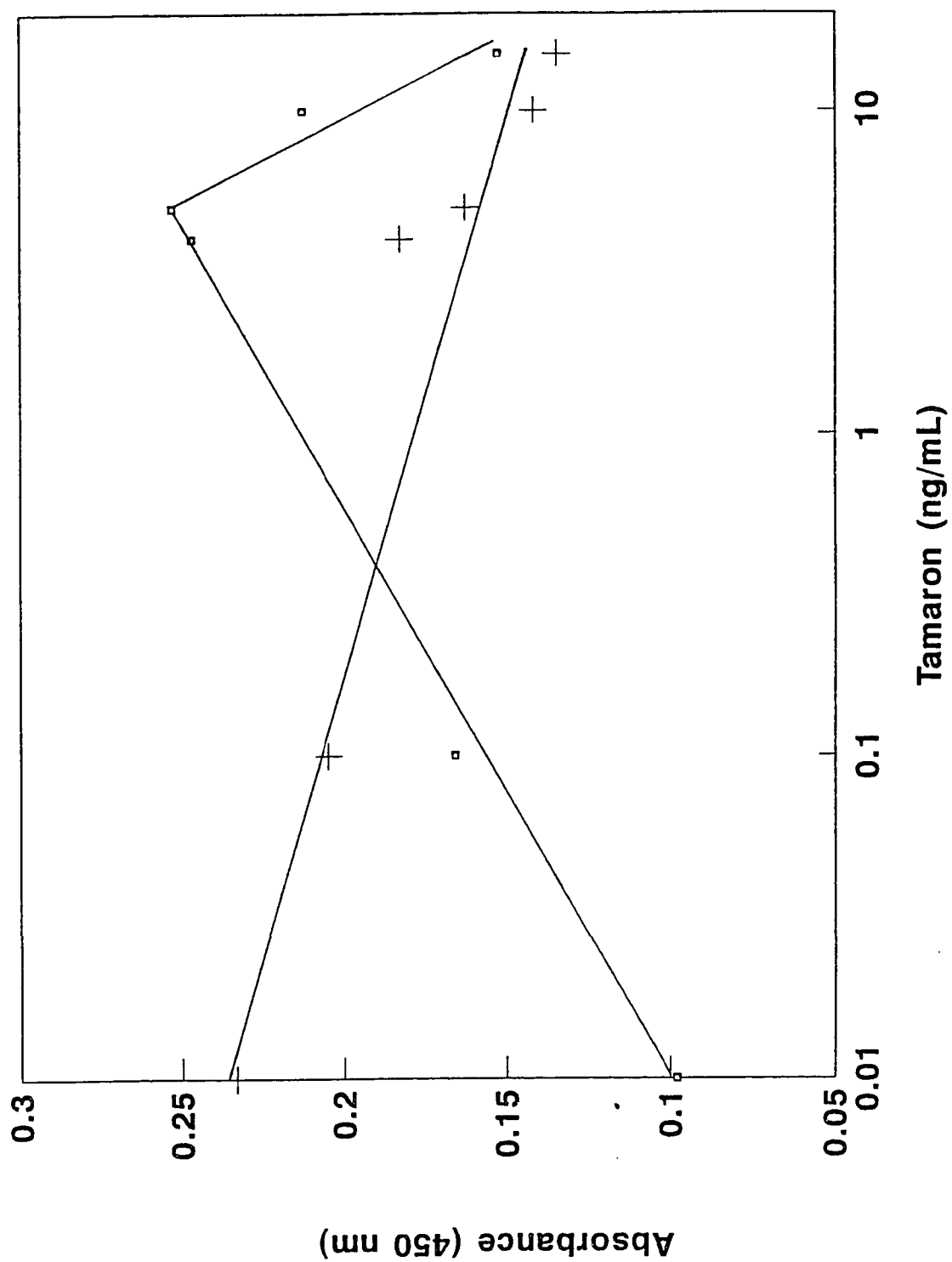
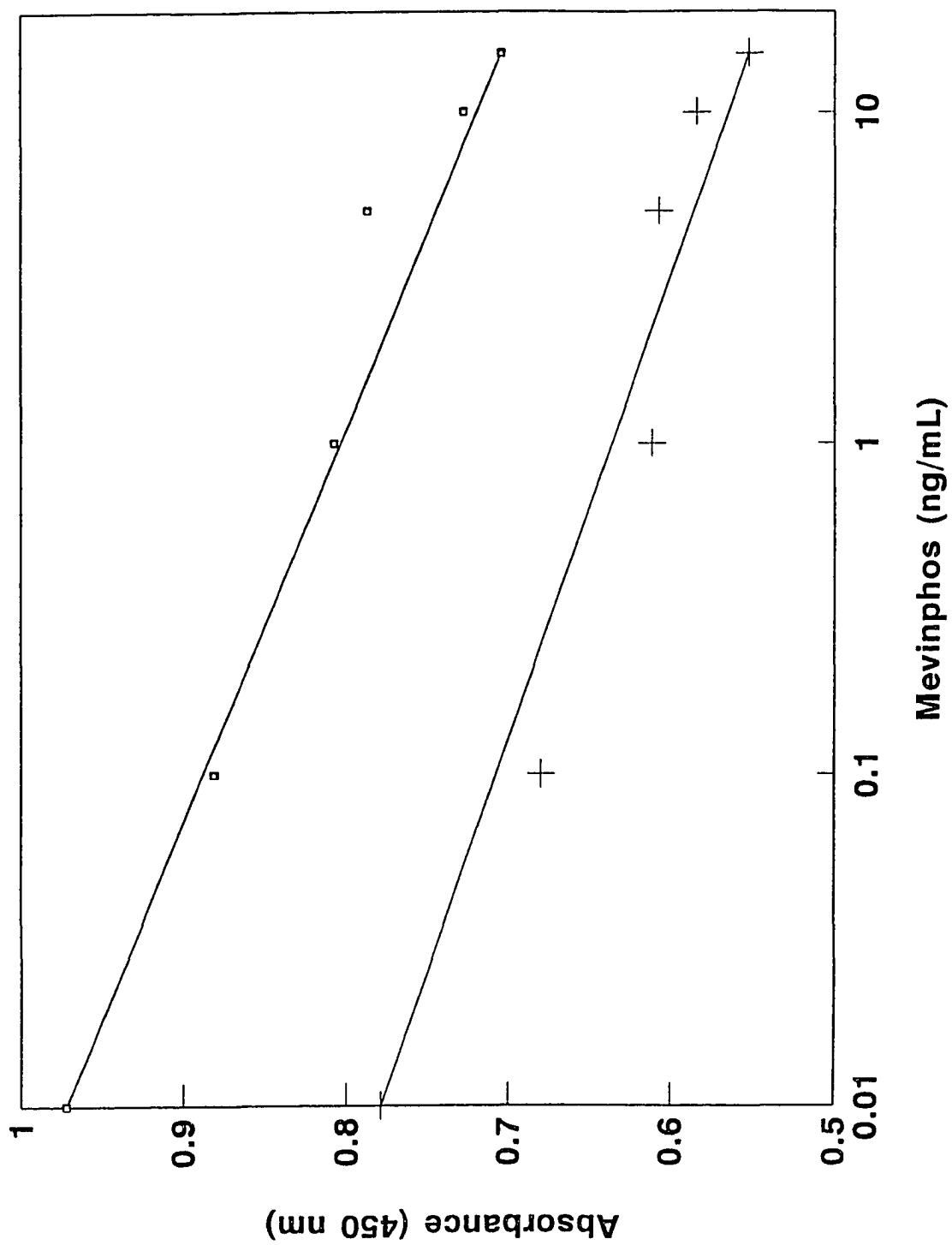


Figure 32

OVA blocking study of the mevinphos solid-phase enzyme immunoassay on microwell immobilization. OVA blocking study of mevinphos assay. (\square) and ($+$) represent 0 and 1 $\mu\text{g/mL}$ OVA blocking the nonspecific sites of the microwell in mevinphos assay, respectively. The absorbance was measured at 450 nm. Standard curves of mevinphos assay in different assay conditions in microwell immobilization as plotted on semi-logarithm scale. The results were plotted as absorbance versus logarithm of mevinphos concentration.
 \square : $Y=0.812-0.078\log(X)$, $r=-0.987$; $+$: $Y=0.723-0.071\log(X)$, $r=-0.667$



was preferred due to highest sensitivity with a regression coefficient of -0.23 and a correlation coefficient of -0.970. OVA concentrations 0% and 10^{-4} % were studied in tamaron and mevinphos assays. The results shown in Figures 31 and 32 suggests that 10^{-4} % OVA and 0% OVA were the choices for tamaron and mevinphos assays, respectively.

5. Study of the competitive enzyme immunoassay for malathion, parathion, tamaron and mevinphos assays in microwell immobilization

The standard curves for the malathion, parathion, tamaron and mevinphos enzyme immunoassays, shown in Figures 33-36 are the result of employing the optimal conditions suggested in the previous sections. The correlation coefficients for these four enzyme immunoassays are -0.987, -0.936, -0.965 and -0.995 for malathion, parathion, tamaron and mevinphos assays, respectively. The accuracy was high in the four assays; however, the sensitivity was low, with the absorbance difference at 450 nm less than 0.3 between the concentrations 0 ng/mL and 10,000. This suggested that the volumes of the small molecules, pesticides with a molecular weight around 300, and the large molecules, pesticide conjugated enzyme with a molecular weight around 50,000, were not large enough for the competitive enzyme immunoassay, and furthermore, the capacity of the microwell did not provide sufficient capacity for higher ratios of the OP and OP-HRPO. Thus larger

Figure 33

Standard curve of the malathion solid-phase enzyme immunoassay on microwell immobilization. The results were plotted as absorbance of peroxidase activity versus logarithm of malathion concentration. ($Y=0.228-0.012 \times \log(X)$, $r=-0.987$)

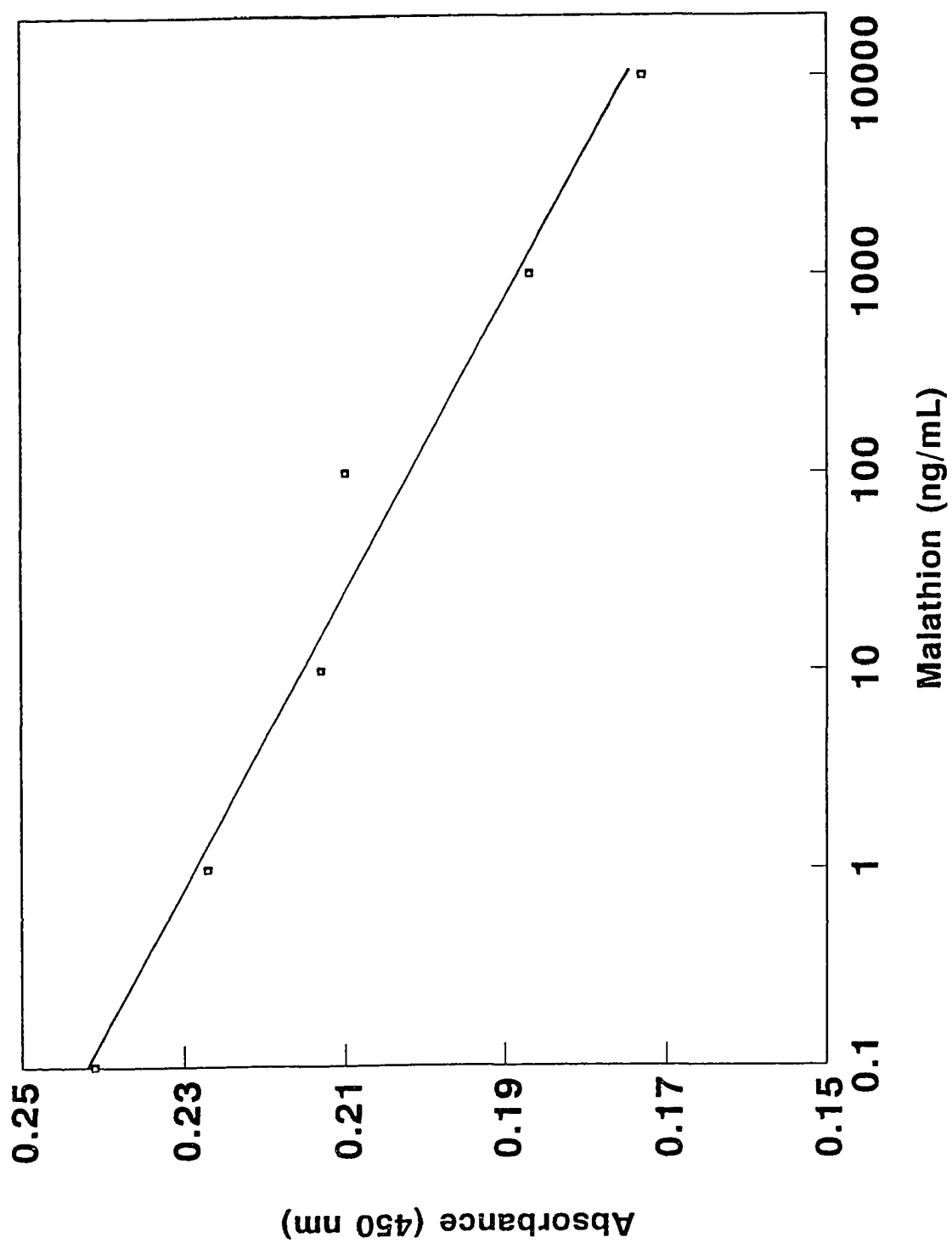


Figure 34

Standard curve of the parathion solid-phase enzyme immunoassay on microwell immobilization. The results were plotted as absorbance of peroxidase activity versus logarithm of parathion concentration. ($Y=0.360-0.027 \times \log(X)$, $r=-0.936$)

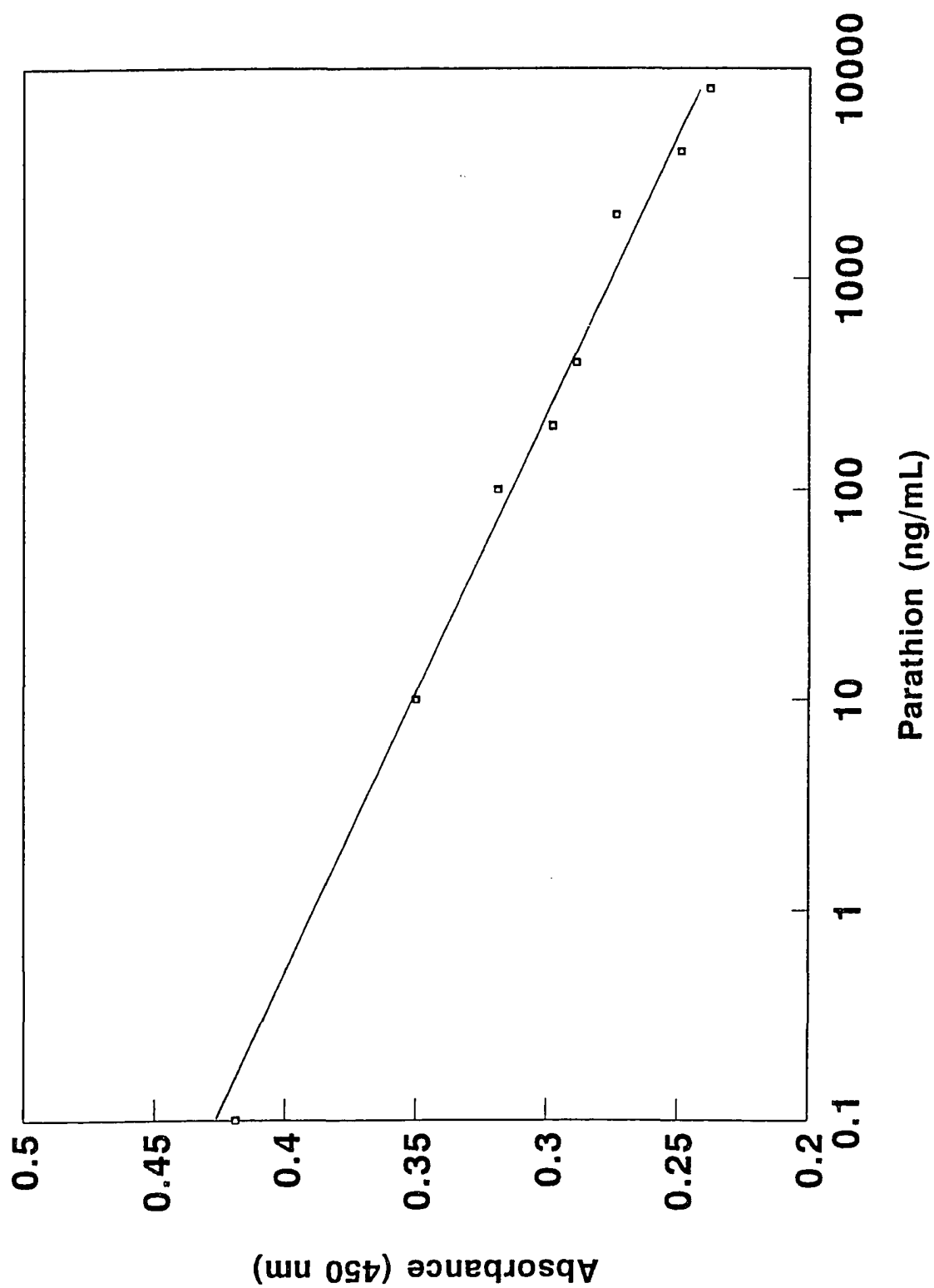


Figure 35

Standard curve of the tamaron solid-phase enzyme immunoassay on microwell immobilization. The results were plotted as absorbance of peroxidase activity versus logarithm of tamaron concentration. ($Y=0.190-0.005 \times \log(X)$, $r=-0.965$)

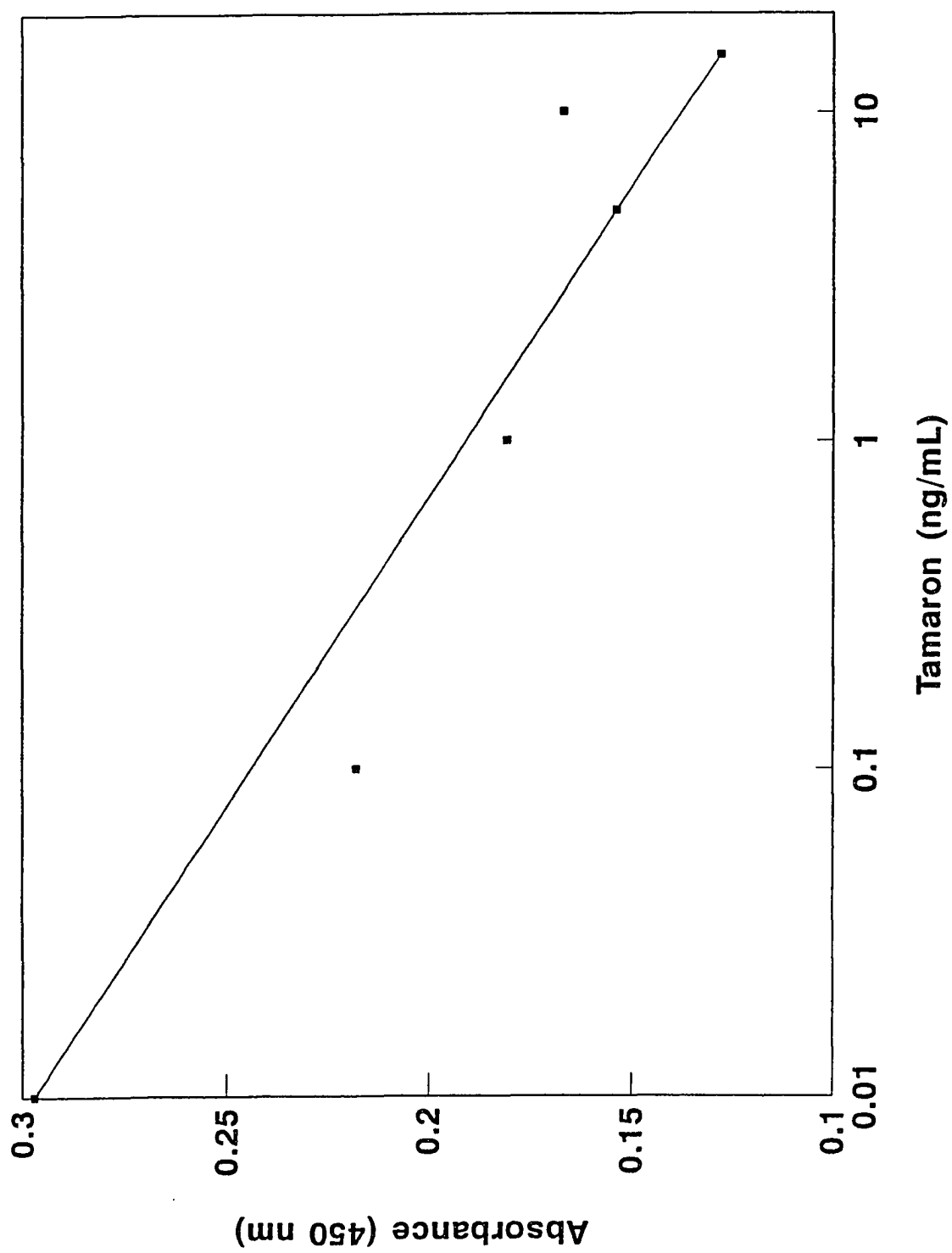
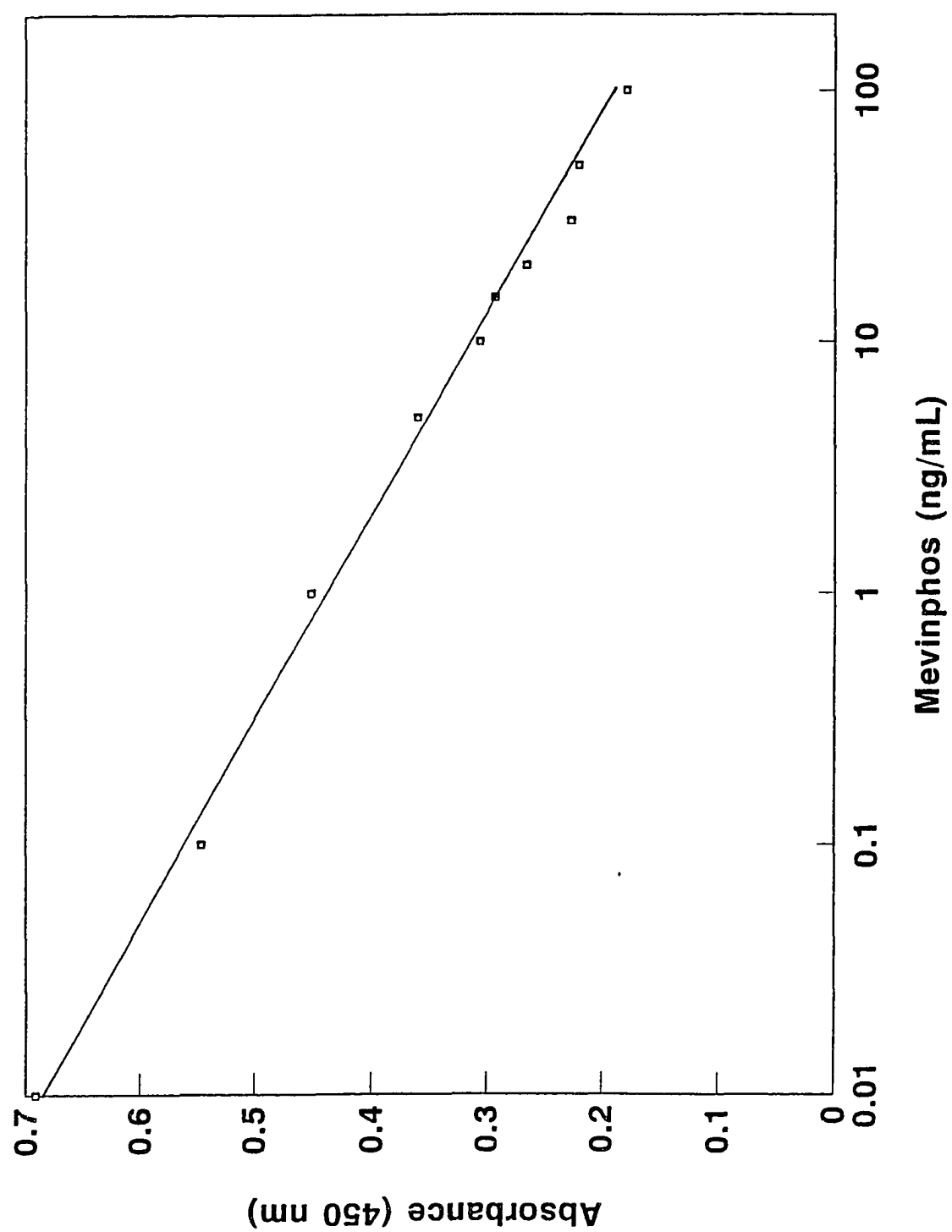


Figure 36

Standard curve of the mevinphos solid-phase enzyme immunoassay on microwell immobilization. The results were plotted as absorbance of peroxidase activity versus logarithm of mevinphos concentration. ($Y=0.434-0.128 \times \log(X)$, $r=-0.995$)



solid-phase matrices were investigated for more sensitive and accurate competitive enzyme immunoassay.

The results of the competitive enzyme immunoassay conditions of these four organophosphorus pesticides are shown on Table 2.

C. Study of the parathion and mevinphos assays on disposable cuvettes

Due to the low absorbance changes in the use of microwell as an EIA solid matrix, and the high OP to OP-HRPO volumes ratio requirements the disposable cuvette which provides a much larger surface (4.25 cm^2 for the 1-mL and 13.97 cm^2 for 3-mL cuvettes) was studied as a possible alternative solid matrix for the OP enzyme immunoassay. Parathion and mevinphos were chosen since they had the best results on the microwell assay. The cuvettes, 1-mL and 3-mL sizes, were precoated with anti-parathion and anti-mevinphos at the desired concentration overnight at room temperature. To the 1-mL and 3-mL cuvettes obtained from Fisher Scientific, $500 \mu\text{L}$ and $1000 \mu\text{L}$ of the OP standards and OP-HRPO mixtures were added. The volume ratio of the OP to OP-HRPO was 2:1 and 1:1 for parathion and mevinphos, respectively. The assays were incubated at room temperature for five minutes. The results are illustrated in Figures 37 and 38, and indicate that the greater surface area and higher capacity of these cuvettes results in increasing the difference of the

Table 2 Summary of the assay condition study of the homogeneous enzyme immunoassay on microwell immobilization of the organophosphorus pesticides

	Malathion	Parathion	Tamaron	Mevinphos
Antibody concentration per well (ng/well) ¹	10	100	100	100
Concentration of OVA blocking (mg/mL) ²	0.001	3.0	0.001	0
Volume of OP standard (μL) ³	100	100	100	50
OP-HRPO concentration (mg/mL) ⁴	0.475	0.116	1.068	0.0759
Volume of OP-HRPO in PBS (μL) ⁵	100	50	100	50
Volume of PBS buffer (μL) ⁶	0	50	0	100
Incubation time (min) ⁷	60	60	60	60
Color Developed time (min) ⁸	60	30	60	20
$\Delta OD_{450\text{ nm}}$ ($A_{0\text{ ng/mL}} - A_{100\text{ ng/mL}}$)	< 0.2	< 0.3	< 0.1	< 0.3

1. The optimal antibody concentration suggested for microwell coating was at the saturation point of antibody saturation curve on microwell immobilization.
2. the optimal OVA concentration recommended for the blocking the non-specific binding sites of the antibody pre-coated microwell to decrease the interference of other proteins or the enzyme binding on the microwells
3. the optimal volume suggested for the enzyme immunoassay of the organophosphorus pesticides
4. the optimal OP-HRPO concentration recommended for the enzyme immunoassay of the organophosphorus pesticides
5. the optimal OP-HRPO volume suggested for the enzyme immunoassay of the organophosphorus pesticides
6. the optimal buffer volume proposed for the enzyme immunoassay of the organophosphorus pesticides
7. the optimal incubation time advised for the competitive reaction of organophosphorus pesticides and OP-HRPO
8. the optimal color development time required for enzyme-substrate-chromogen reaction

Figure 37

Standard curve study of parathion solid-phase enzyme immunoassay on disposable cuvette immobilization. The cuvettes with 1-mL, (\square), and 3-mL, ($+$), capacity were used for antibody immobilization. The absorbance was measured at 450 nm. Standard curves of parathion assay in the same assay condition in different disposable cuvettes as plotted on semi-logarithm scale. The results were plotted as absorbance versus logarithm of parathion concentration.
 \square : $Y=0.711-0.051 \times \log(X)$, $r=-0.996$; $+$: $Y=0.197-0.007 \times \log(X)$, $r=-0.890$

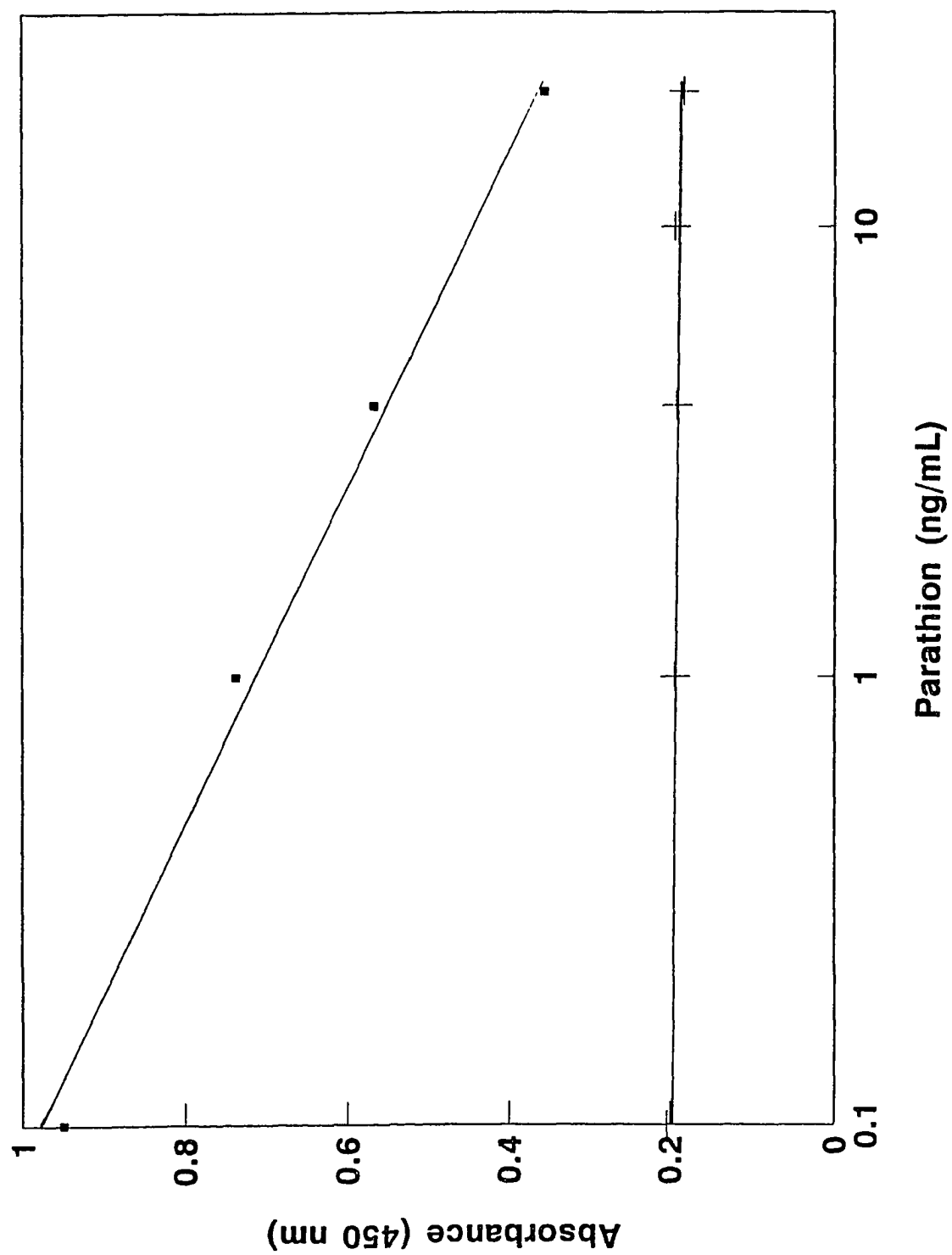
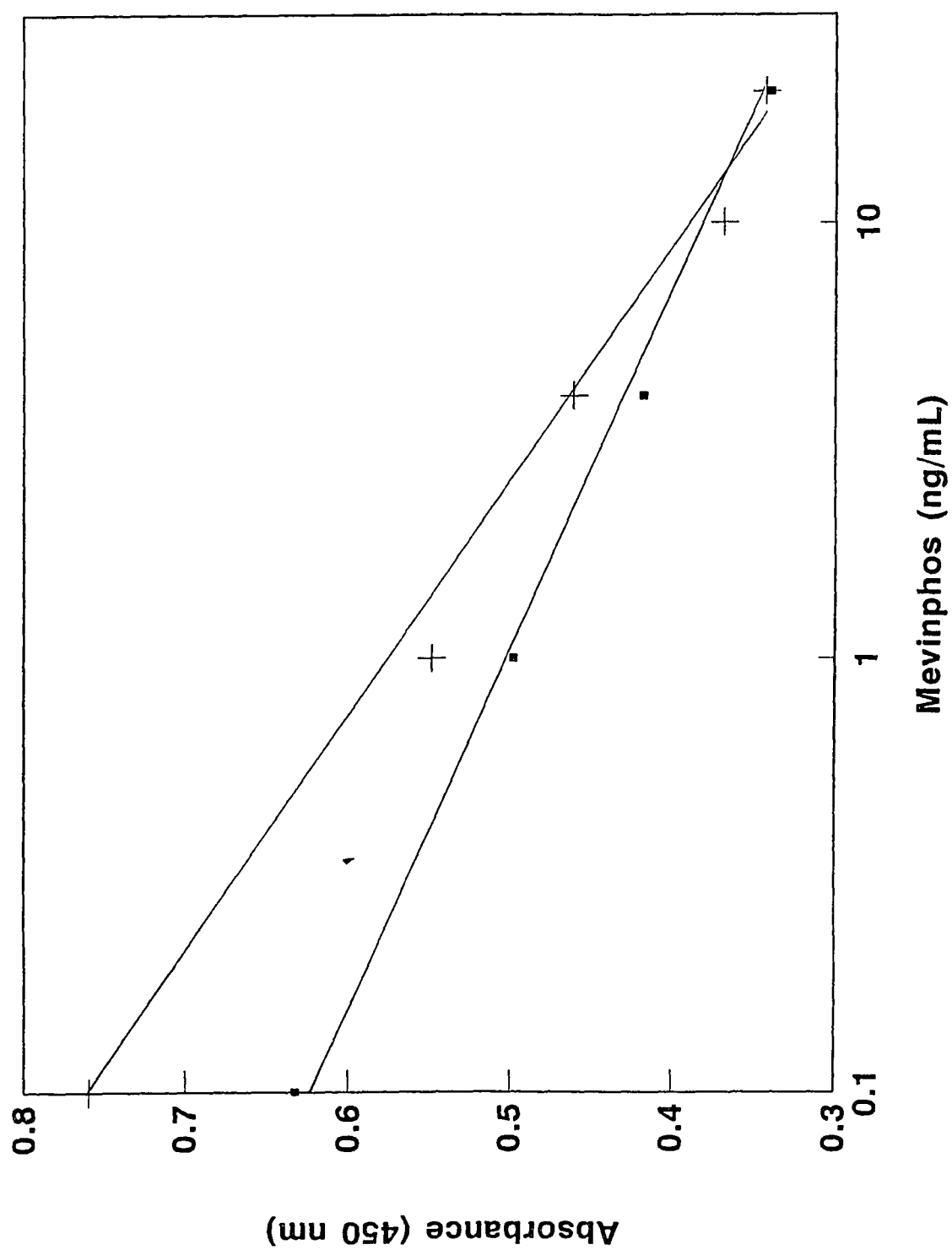


Figure 38

Standard curve study of mevinphos solid-phase enzyme immunoassay on disposable cuvette immobilization. The cuvettes with 1-mL, (\square), and 3-mL, ($+$), capacity were used for antibody immobilization. The absorbance was measured at 450 nm. Standard curves of mevinphos assay in the same assay conditions in disposable cuvettes as plotted on semi-logarithm scale. The results were plotted as absorbance versus logarithm of mevinphos concentration.

\square : $Y=0.342-0.077 \times \log(X)$, $r=-0.410$; $+$: $Y=0.566-0.180 \times \log(X)$, $r=-0.996$



absorbance values to 0.593 and 0.416 for parathion and mevinphos assays when the concentrations differences were as small as 20 ng/mL.

D. Screening of various brands of polystyrene tube

1. Capacity Study of different brands of polystyrene tubes

In addition to the disposable polystyrene cuvettes, various types of polystyrene tubes were also studied as possible alternative solid matrix for the OP enzyme immunoassay, ten different types of small polystyrene tubes were obtained as free samples from Evergreen, Fisher, Scientific Products and Nunc. To each tubes 500 μ L or 1000 μ L of 1 μ g/mL BSA were coated overnight at room temperature, then emptied and air dried. The assays were performed at room temperature for five minutes with the addition of anti-BSA-HRPO conjugate as the indicator protein. They were then emptied, washed and the HRPO activity was assayed.

The enzyme activity of the different polystyrene tubes were studied. At the same concentration of the anti-BSA-HRPO, 50 fold dilution, Evergreen (cat# 240-5704-06) and Fisher (cat# 16-857-67) gave the highest absorbance readings at 450 nm, which indicated more BSA coating on the surface of the polystyrene tubes. These two polystyrene tubes can also utilize more diluted enzyme concentration to reach the saturation point, which was indicated as the enzyme dilution extrapolated in X-axis intercept. The results shown in Table 3

Table 3 Binding capacity study of different brands of polystyrene tubes

Brand	Absorbance at 50 fold dilution of anti-BSA-HRPO ¹	Enzyme dilution extrapolated to X-axis intercept ²
Fisher 14-961-10	6.736	1208.3
Evergreen 240-5704-06	7.104	8.6E9
Fisher 14-961-2	3.848	533.9
Fisher 14-961-3A	2.308	1859.6
Fisher 14-0961-100	2.135	949.1
Fisher 14-0961-8A	5.670	964.5
S/P T-1225-3	8.003	1265.7
Nunc 444202	7.352	3865.0
Nunc 470319	7.375	6028.9
Fisher 09-857-67	8.916	21743.5

1. the absorbance readings at 50 fold dilution of anti-BSA-HRPO for different brands of polystyrene tubes pre-coated with BSA.
2. the minimum dilutions, showing significant sensitivity, of enzyme (anti-BSA-HRPO) involved in the reaction of anti-BSA-HRPO binding BSA.

indicate that the tubes from Evergreen (cat# 240-5704-06) and Fisher (cat# 16-857-67) provide the highest binding capacity.

2. Study of parathion and mevinphos assay on polystyrene tubes from Evergreen and Fisher

The study of parathion and mevinphos assays in polystyrene tubes were carried out in the same fashion as that performed in the disposable polystyrene cuvettes which were pre-coated with anti-OP. The results, shown in Figures 39 and 40, indicate that the tube from Fisher (cat# 16-857-67), which is a microtube, gave the best performance characteristics by providing higher sensitivity, which contributed to better regression coefficients, and accuracy, which resulted in higher correlation coefficients.

E. Development of competitive enzyme immunoassays for malathion, parathion, tamaron and mevinphos on microtubes

1. Study of the optimal reaction ratio of OP to OP-HRPO

Different volume ratios of OP to OP-HRPO diluted with deionized water to a final volume of 500 μ L were carried out in the microtubes with appropriate antibody. The reactions were performed at room temperature, and the incubation time was set as five minutes, which was suggested in the atrazine determination reaction on microtube immobilization [63].

Figure 39

Standard curve study of parathion solid-phase enzyme immunoassay on selected polystyrene tubes. (□) and (+) represent Evergreen 240-5704-06 and Fisher 09-857-67 polystyrene tubes which were precoated with desired concentrations of anti-parathion gamma globulin. The results were plotted as absorbance versus logarithm of parathion concentration. The absorbance was measured at 450 nm.

□: $Y=0.590-0.149 \times \log(X)$, $r=-0.983$; +: $Y=0.367-0.056 \times \log(X)$, $r=-0.862$

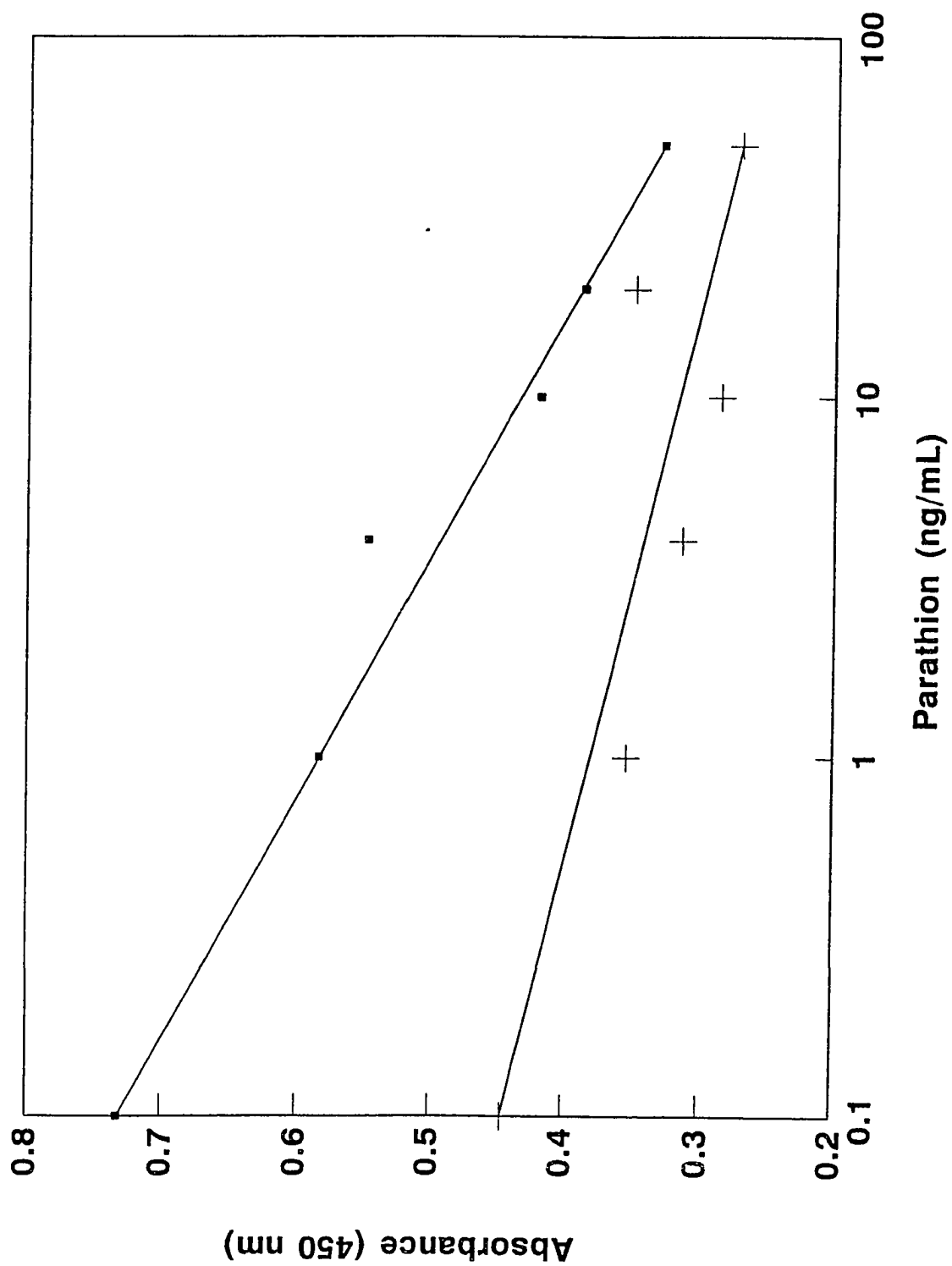
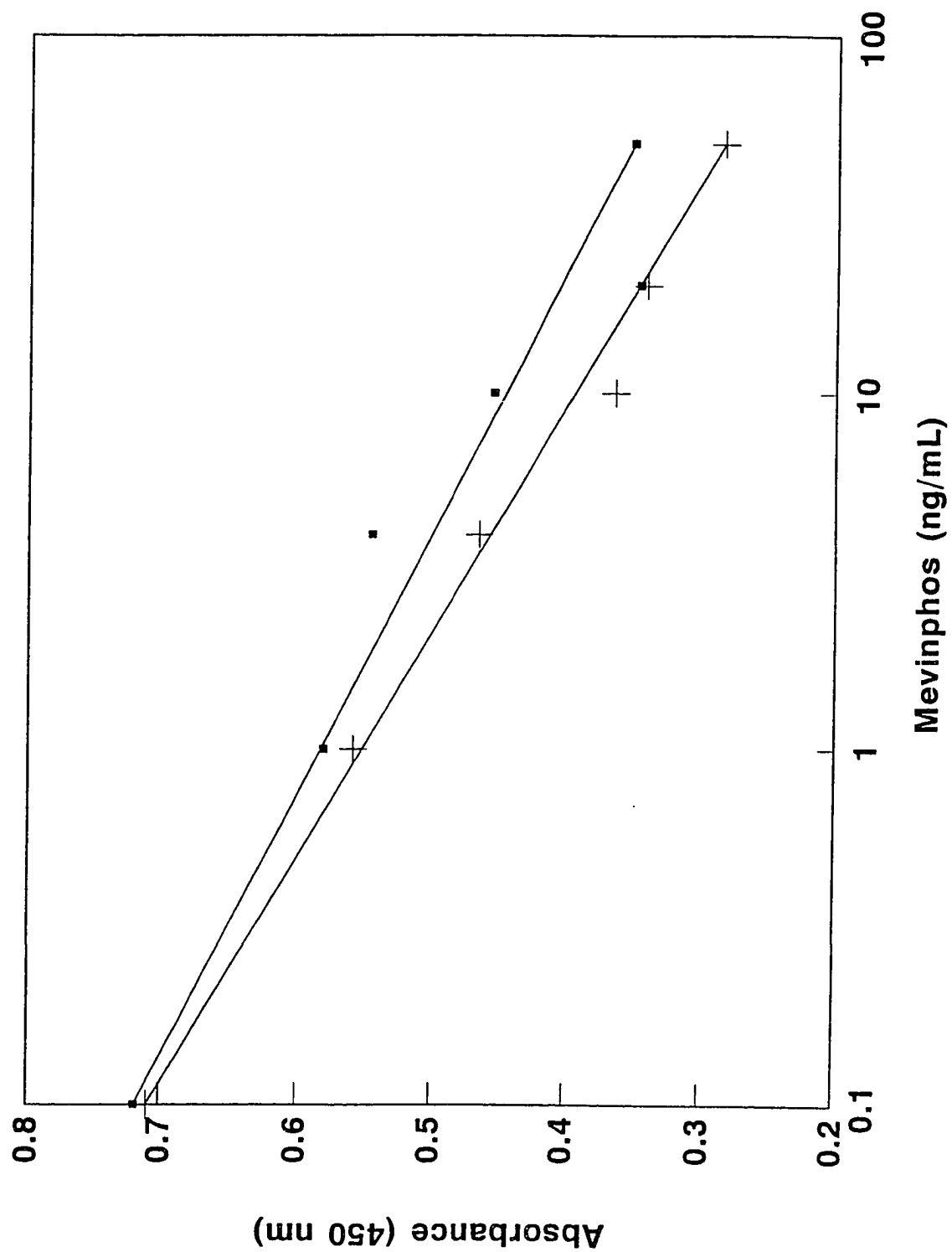


Figure 40

Standard curve study of mevinphos solid-phase enzyme immunoassay in selected polystyrene tubes. (□) and (+) represent Evergreen 240-5704-06 and Fisher 09-857-67 polystyrene tubes which were precoated with desired concentrations of anti-mevinphos gamma globulin. The results were plotted as absorbance versus logarithm of mevinphos concentration. The absorbance was measured at 450 nm.

□: $Y=0.585-0.143 \times \log(X)$, $r=-0.974$; +: $Y=0.551-0.160 \times \log(X)$, $r=-0.996$



The volume ratios of malathion standard solutions, 0 ng/mL to 500 ng/mL, to malathion-HRPO (0.96 mg/mL) were 300 μ L to 50 μ L, 350 μ L to 50 μ L, 400 μ L to 50 μ L, 440 μ L to 10 μ L, and 450 μ L to 10 μ L for malathion assay. The result in Figure 41 shows that the ratio of 440 μ L to 10 μ L, malathion standard solution to malathion-HRPO was selected due to the highest separation, with the largest absorbance difference compared to the other four ratios of the malathion standard and malathion-HRPO mixtures.

The volume ratios of parathion standard solutions, 0 ng/mL to 1000 ng/mL, to parathion-HRPO were prepared as 200 μ L to 50 μ L, 250 μ L to 50 μ L, 300 μ L to 50 μ L and 400 μ L to 50 μ L for parathion assay. The ratio of 300 μ L to 50 μ L, parathion standard solution to parathion-HRPO was selected due to the highest separation within 0 ng/mL and 100 ng/mL within the concentrations of the standard solutions of 0 ng/mL to 1000 ng/mL shown in Figure 42.

The volume ratios of tamaron standard solution, 0 ng/mL to 1000 ng/mL to tamaron-HRPO (0.534 mg/mL) studied were 300 μ L to 50 μ L, 350 μ L to 50 μ L, 400 μ L to 50 μ L, 450 μ L to 10 μ L, and 460 μ L to 10 μ L for tamaron assay. As seen in Figure 43 the ratio of 460 μ L to 10 μ L, tamaron standard to tamaron-HRPO is the best due to the highest separation, within the concentrations of the standard solutions of 0 ng/mL and 1000 ng/mL.

Figure 41

Study of malathion and malathion-HRPO quantitations for the malathion solid-phase enzyme immunoassay on microtube immobilization. The experimental conditions were described in the text. The absorbance differences between 0 ng/mL and 100 ng/mL were measured at 450 nm.

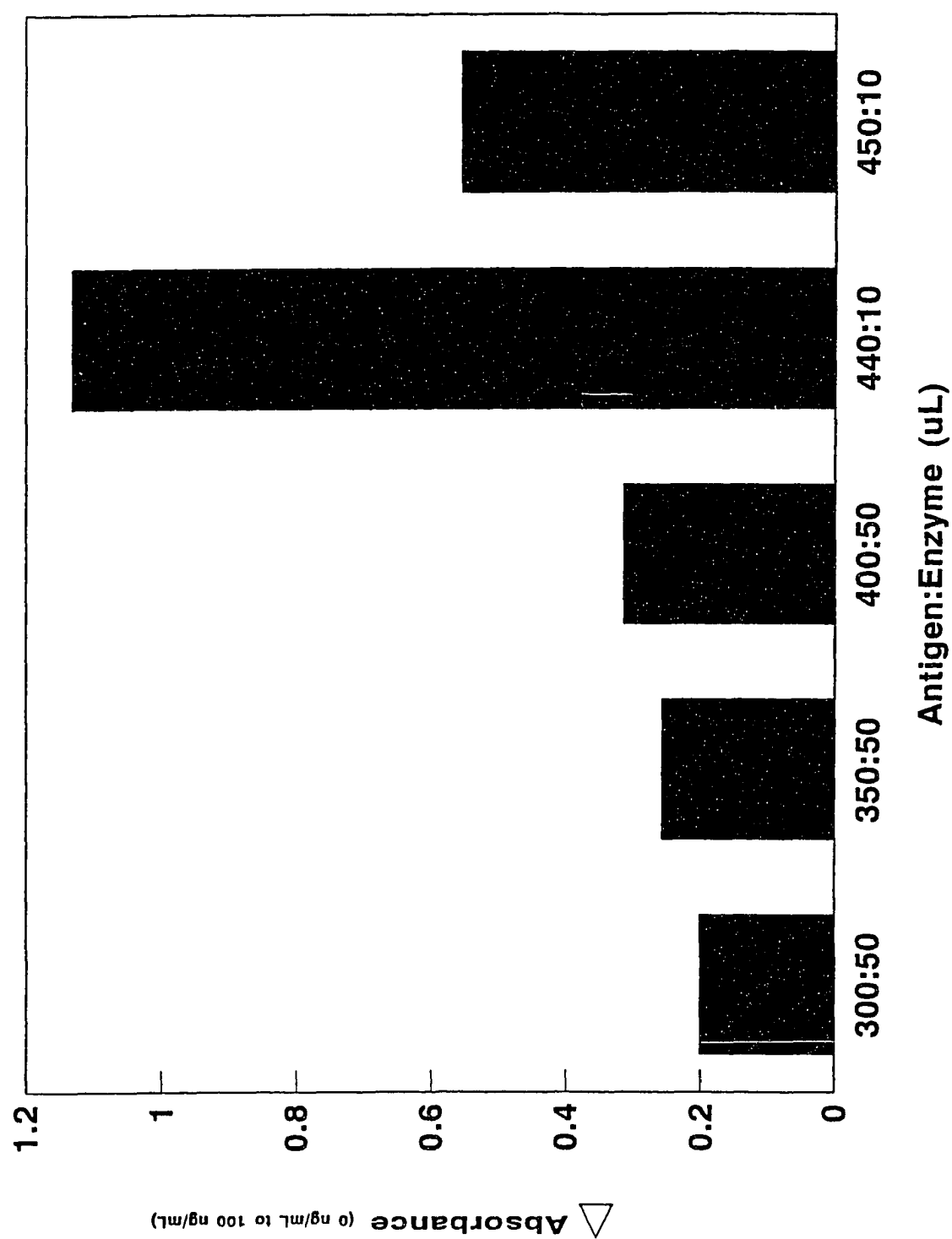


Figure 42

Study of parathion and parathion-HRPO quantitations for the parathion solid-phase enzyme immunoassay on microtube immobilization. The experimental conditions were described in the text. The absorbance difference between 0 ng/mL and 100 ng/mL were measured at 450 nm.

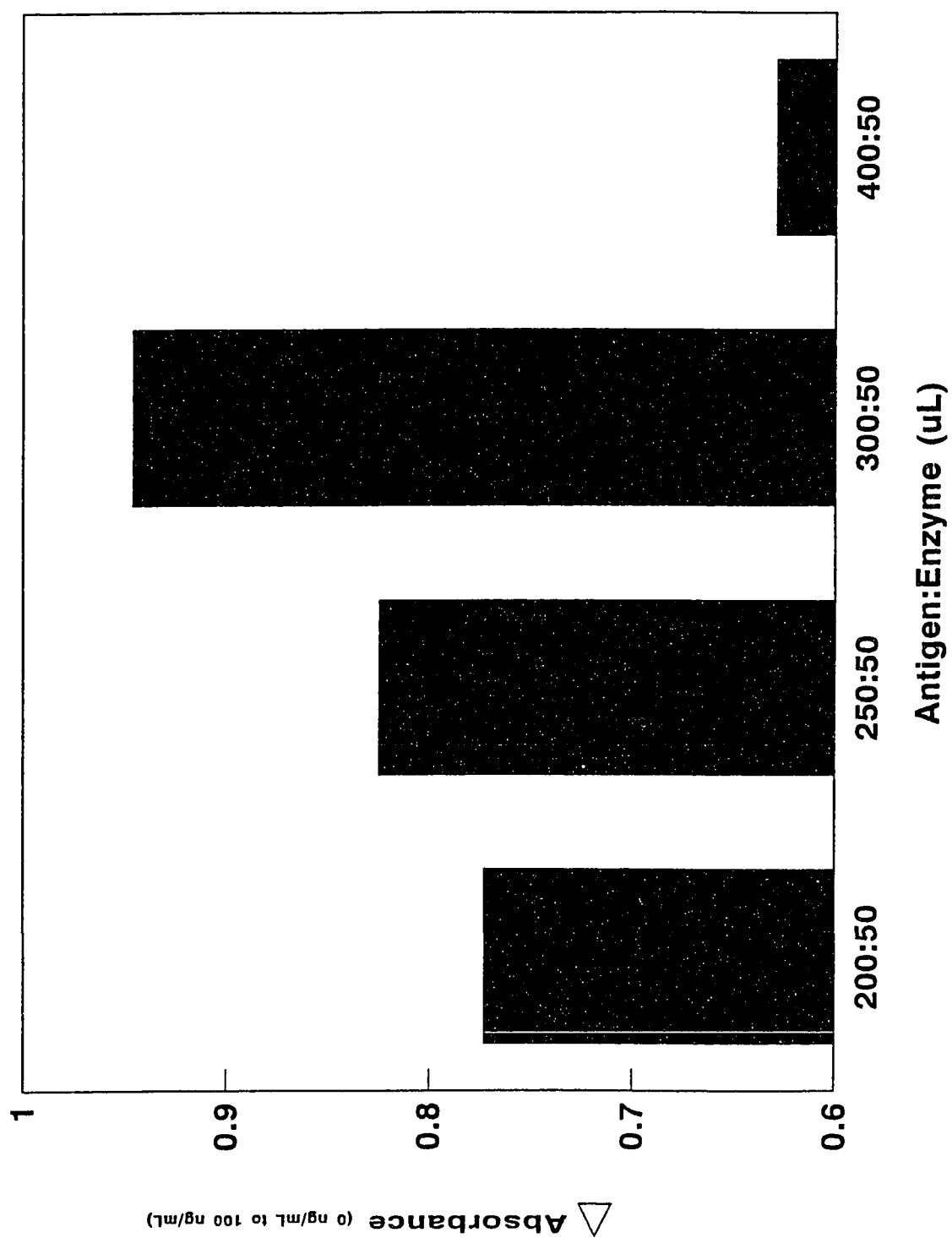
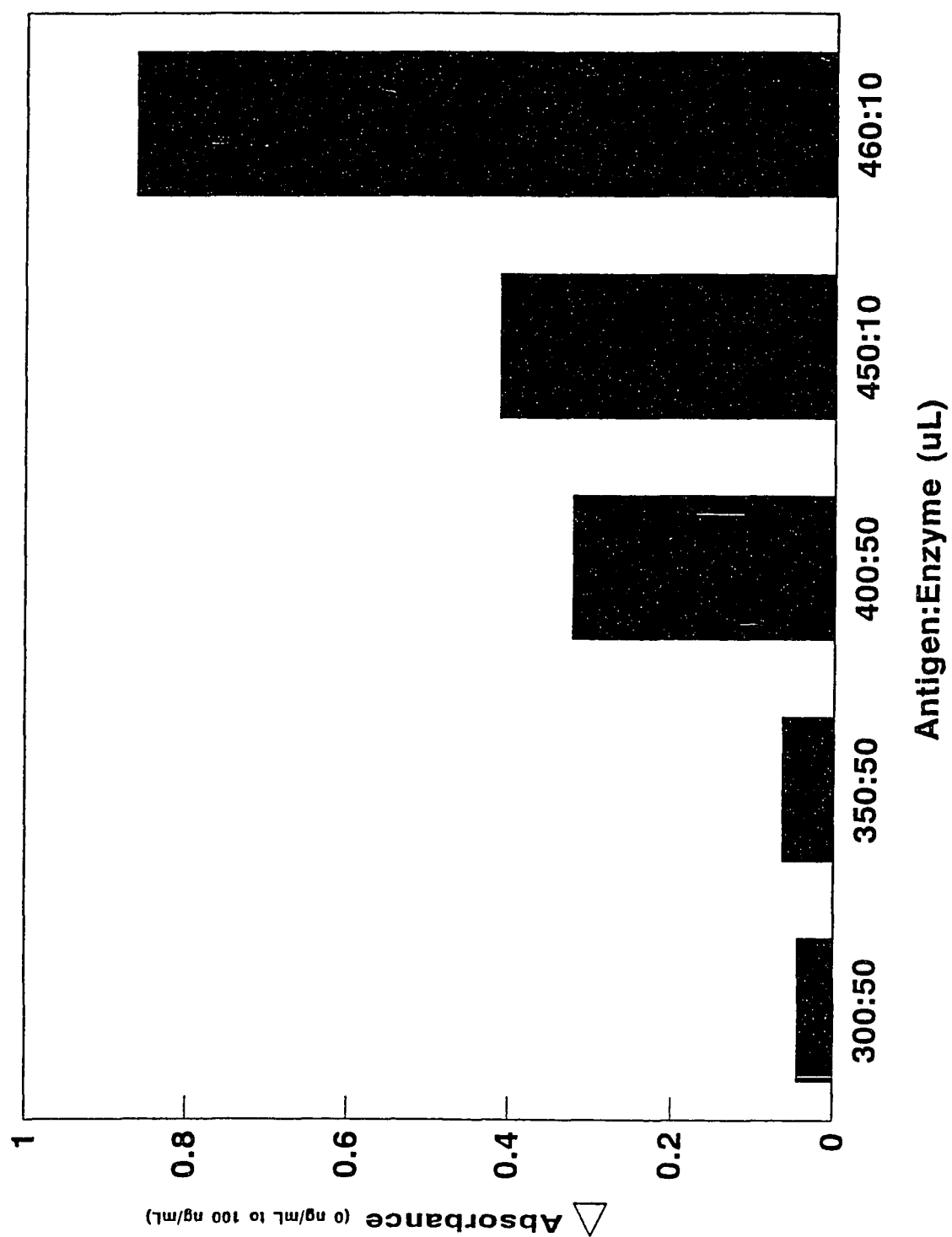


Figure 43

Study of tamaron and tamaron-HRPO quantitations for the tamaron solid-phase enzyme immunoassay on microtube immobilization. The experimental conditions were described in the text. The absorbance difference between 0 ng/mL and 100 ng/mL were measured at 450 nm.



For mevinphos assay the ratios of antigen (mevinphos standard solution, 0 ng/mL to 2000 ng/mL), mevinphos-HRPO (0.759 mg/mL) studied were 125 μ L to 125 μ L, 200 μ L to 100 μ L, 300 μ L to 50 μ L and 400 μ L to 50 μ L. The ratio of 300 μ L to 50 μ L, antigen to mevinphos-HRPO was selected due to the highest separation within the concentrations of the standard solutions of 0 ng/mL to 2000 ng/mL as shown in Figure 44.

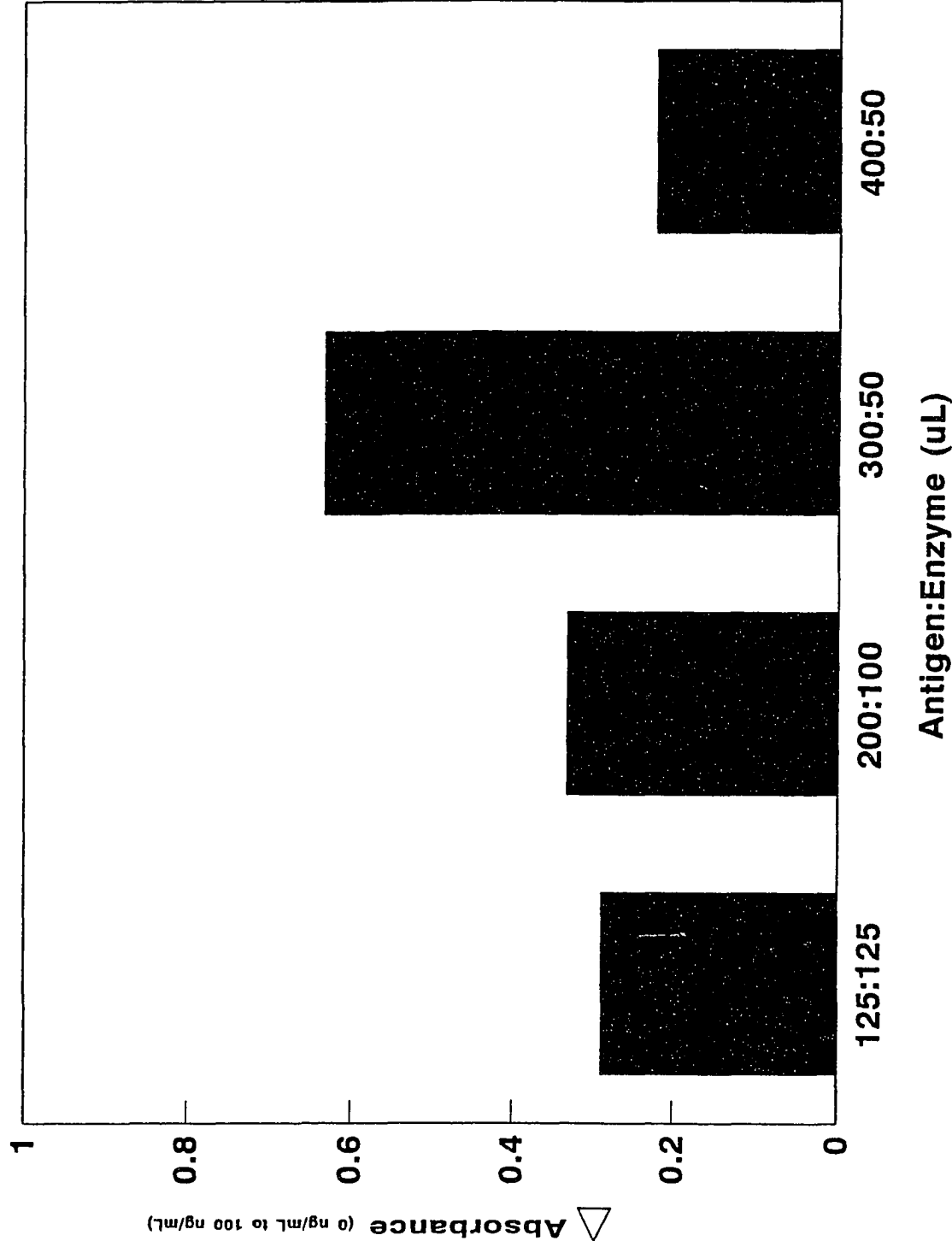
The results shown in Figures 41-44 indicate the best ratios of OP to OP-HRPO for each OP are 440 μ L to 10 μ L (0.96 mg/mL), 300 μ L to 50 μ L (0.23 mg/mL), 460 μ L to 10 μ L (0.53 mg/mL) and 300 μ L to 50 μ L (0.76 mg/mL) for malathion, parathion, tamaron and mevinphos, respectively.

2. Study of the optimal enzyme dilution

Different dilutions of OP-HRPO were prepared for the study of the optimal enzyme dilution for each OP assay. The stock OP-HRPO solutions were prepared as 47.49 mg/mL, 34.80 mg/mL, 26.71 mg/mL and 37.95 mg/mL for malathion-HRPO, parathion-HRPO, tamaron-HRPO and mevinphos-HRPO, respectively. The microtubes with reaction mixture containing appropriate amount of OP and OP-HRPO as described in the former section were incubated at room temperature for five minutes, emptied, and washed. The HRPO activity was then assayed using the same procedure as described previously.

Figure 44

Study of mevinphos and mevinphos-HRPO quantitations for the mevinphos solid-phase enzyme immunoassay on microtube immobilization. The experimental conditions were described in the text. The absorbance difference between 0 ng/mL and 100 ng/mL were measured at 450 nm.



The malathion-HRPO dilutions were prepared as 25, 50 and 75 fold for malathion assay. The results shown in Figures 45 indicate the optimal enzyme dilution for malathion is 50 fold dilution for the highest sensitivity for the malathion standard solutions of concentrations between 0 ng/mL and 100 ng/mL.

The parathion-HRPO dilutions were prepared as 50, 75, 150 and 500 fold dilutions for parathion assay. The results shown in Figures 46 demonstrate that the optimal enzyme dilution for parathion is 150 fold dilution for the highest sensitivity between the parathion standard solutions of concentrations for 0 ng/mL and 100 ng/mL.

The tamaron-HRPO dilutions were prepared as 25, 50 and 75 fold for tamaron assay. The results shown in Figures 47 indicate the optimal enzyme dilution for tamaron is 50 fold dilution for the highest sensitivity for the tamaron standard solutions of concentrations between 0 ng/mL and 100 ng/mL.

The mevinphos-HRPO dilutions were prepared as 25, 50 and 75 fold dilutions for mevinphos assay. The results shown in Figures 48 demonstrate that the optimal enzyme dilution for parathion is 150 fold dilution for the highest sensitivity for the mevinphos standard solutions of the concentrations between 0 ng/mL and 100 ng/mL.

Figure 45

Optimization of enzyme dilution study of malathion-HRPO in the malathion solid-phase enzyme immunoassay on microtube immobilization. For malathion assay, 25, 50 and 75 folds of dilution for malathion-HRPO were studied. The experimental conditions were described in the text. The absorbance differences between 0 ng/mL and 100 ng/mL were measured at 450 nm.

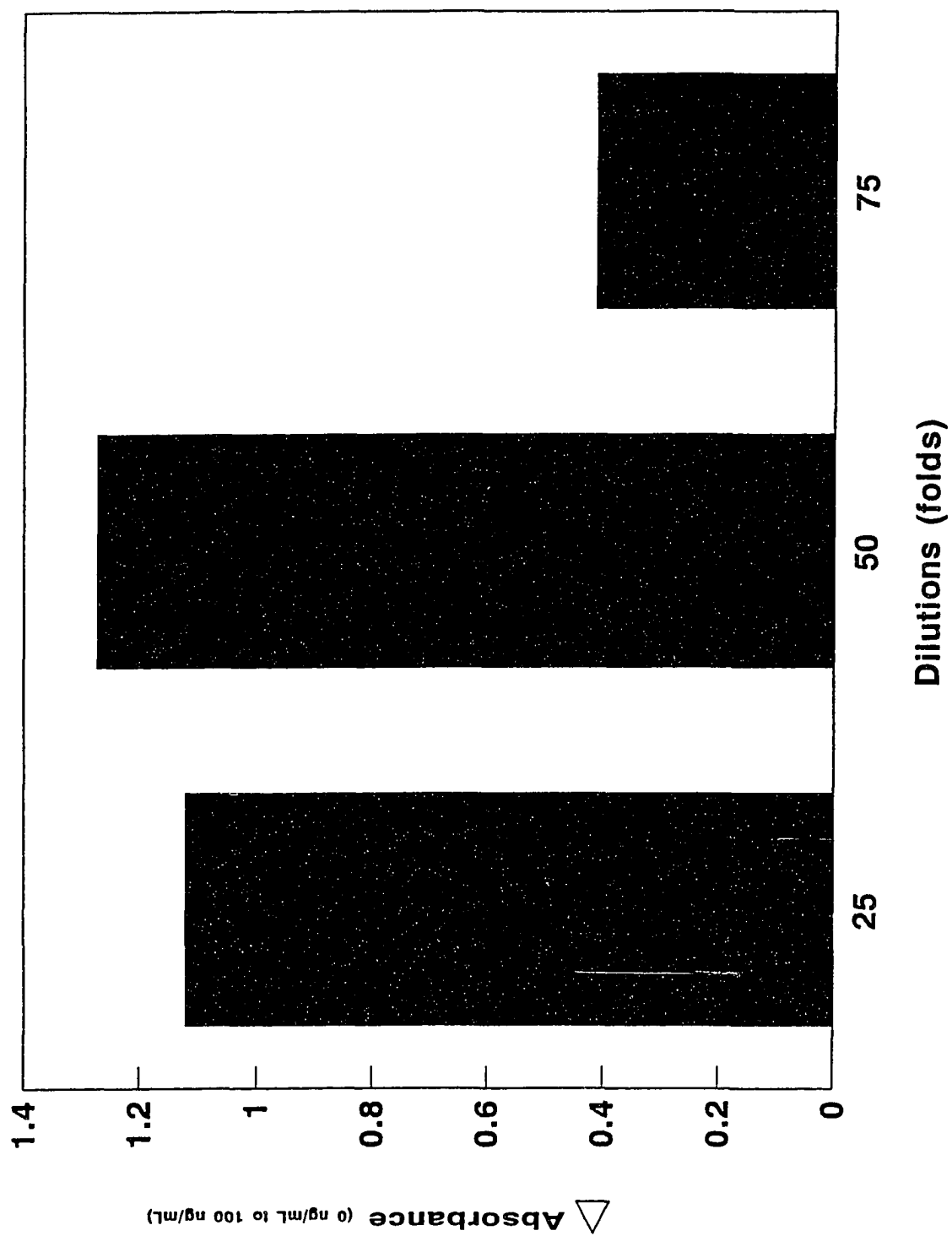


Figure 46

Optimization of enzyme dilution study of parathion-HRPO in the parathion solid-phase enzyme immunoassay on microtube immobilization. For parathion assay, 50, 75, 150, 500 folds of dilution for parathion-HRPO were studied. The experimental conditions were described in the text. The absorbance differences between 0 ng/mL and 100 ng/mL were measured at 450 nm.

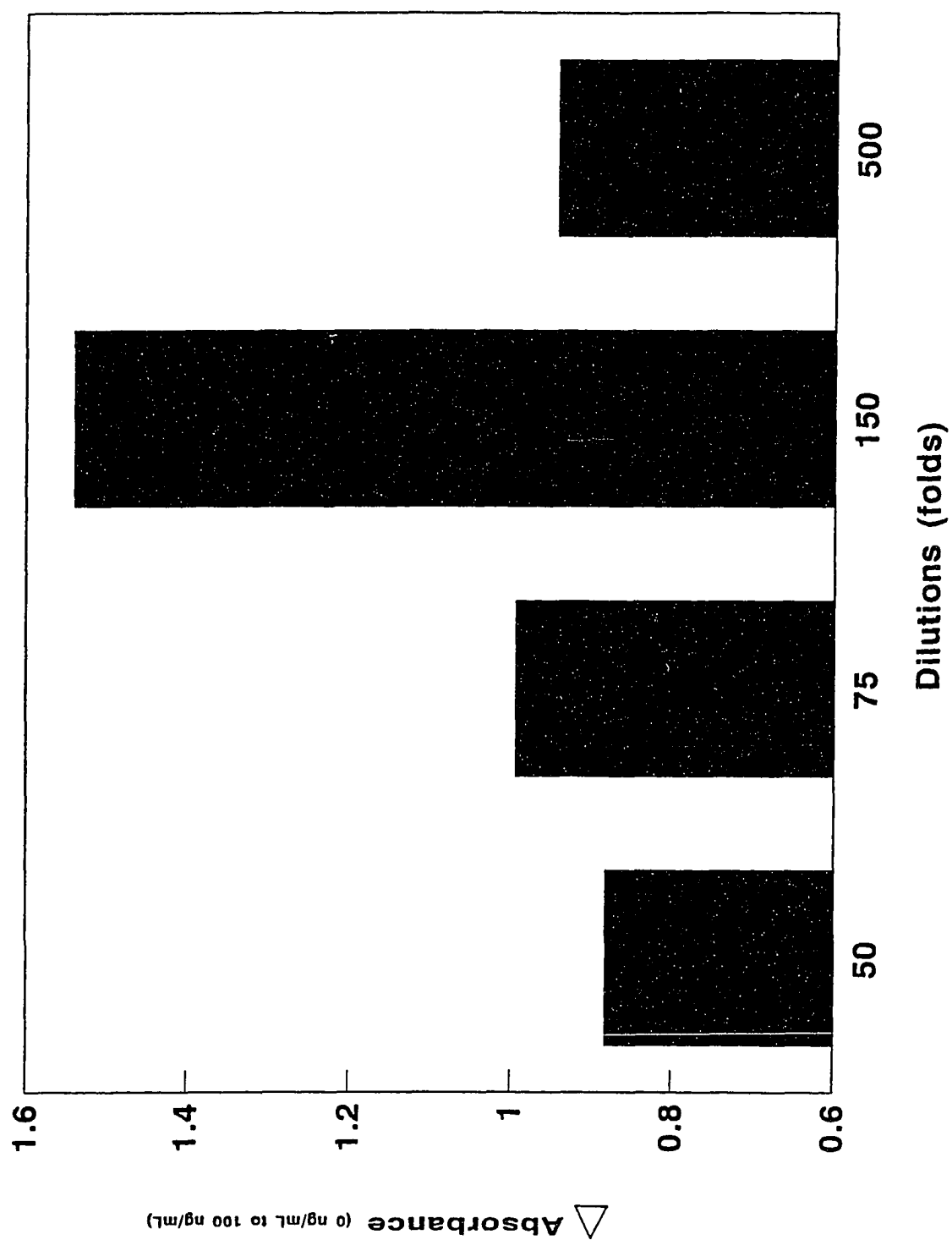


Figure 47

Optimization of enzyme dilution study of tamaron-HRPO in the tamaron solid-phase enzyme immunoassay on microtube immobilization. For tamaron assay, 25, 50 and 75 folds of dilution for tamaron-HRPO were studied. The experimental conditions were described in the text. The absorbance differences between 0 ng/mL and 100 ng/mL were measured at 450 nm.

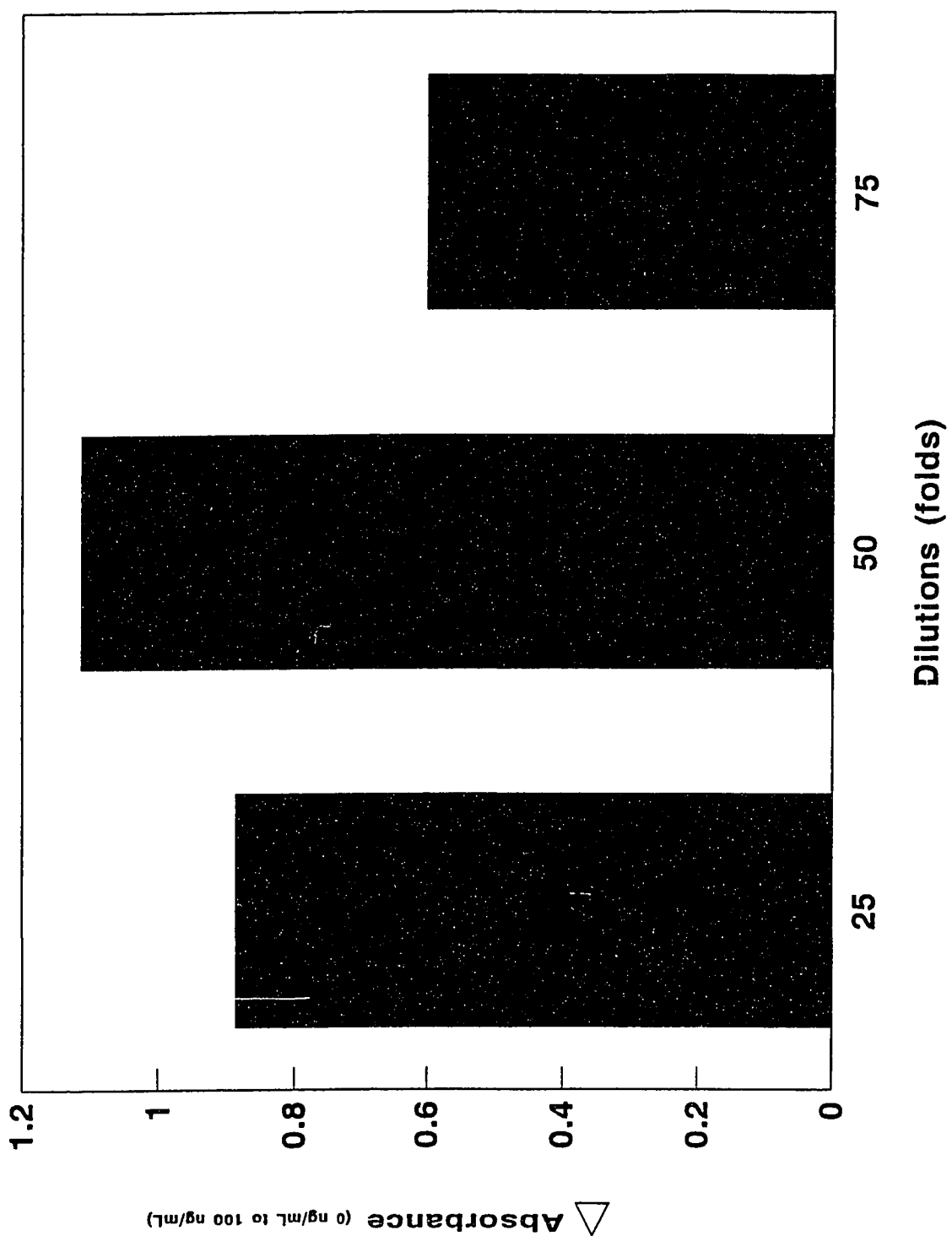
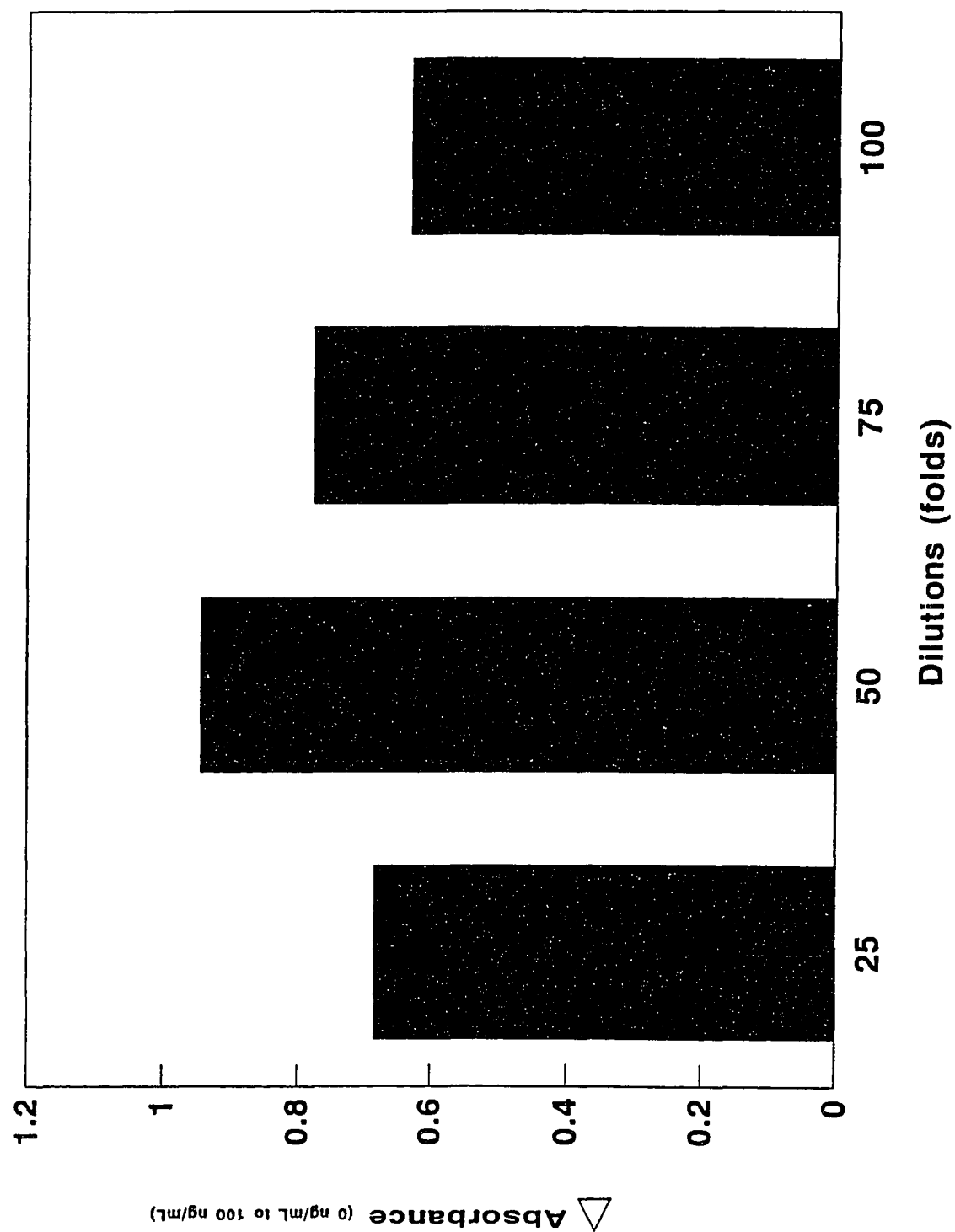


Figure 48

Optimization of enzyme dilution study of mevinphos-HRPO in the mevinphos solid-phase enzyme immunoassay on microtube immobilization. For mevinphos assay, 25, 50, 75, 100 folds of dilution for mevinphos-HRPO. The experimental conditions were described in the text. The absorbance differences between 0 ng/mL and 100 ng/mL were measured at 450 nm.



The optimal enzyme dilution of these four types of OP are 50 fold for all except for parathion. The enzyme dilution for parathion assay appears to be 150 fold dilution.

3. Study of the optimal incubation time

Study to determine the optimal incubation time for the four OP assays were performed at room temperature for five and ten minute incubation time. Figures 49-52 illustrate that ten-minute incubation gave the best separation especially in the lower concentration in all four OP assays. There are no significant differences in the determination of the higher concentration range. It indicates that longer incubation time will enhance the competition between small quantities of the antigen and OP-HRPO and increase the sensitivity.

4. Study of the optimal incubation temperature

The study of the incubation temperature were carried out at 20°C, 30°C and 40°C for ten-minutes incubation. Figures 53-56 show that there is no significant difference in the results obtained for the incubations at 20°C, 30°C and 40°C for malathion, tamaron and mevinphos assays. For the parathion assay, shown in Figure 54, between the concentrations of 0 ng/mL and 100 ng/mL the most separation occurred at 30°C, with poorest separation at 40°C. This indicated that a higher temperature did increase the enzyme activity, but over the melting point the enzyme started to denature, and the activity

Figure 49

Effect of two different incubation time for the malathion solid-phase enzyme immunoassay on microtube immobilization. (□) and (⊕) represent 10 and 5 minutes incubation at room temperature for malathion assay. The absorbance was measured at 450 nm. Standard curve of malathion assay in microtube immobilization as plotted on semi-logarithm scale. The results were plotted as absorbance versus logarithm of malathion concentration.

□: $Y=0.372-0.140 \times \log(X)$, $r=-0.986$ ($X=0$ ng/mL to 100 ng/mL)

⊕: $Y=0.189-0.079 \times \log(X)$, $r=-0.902$ ($X=0$ ng/mL to 20 ng/mL)

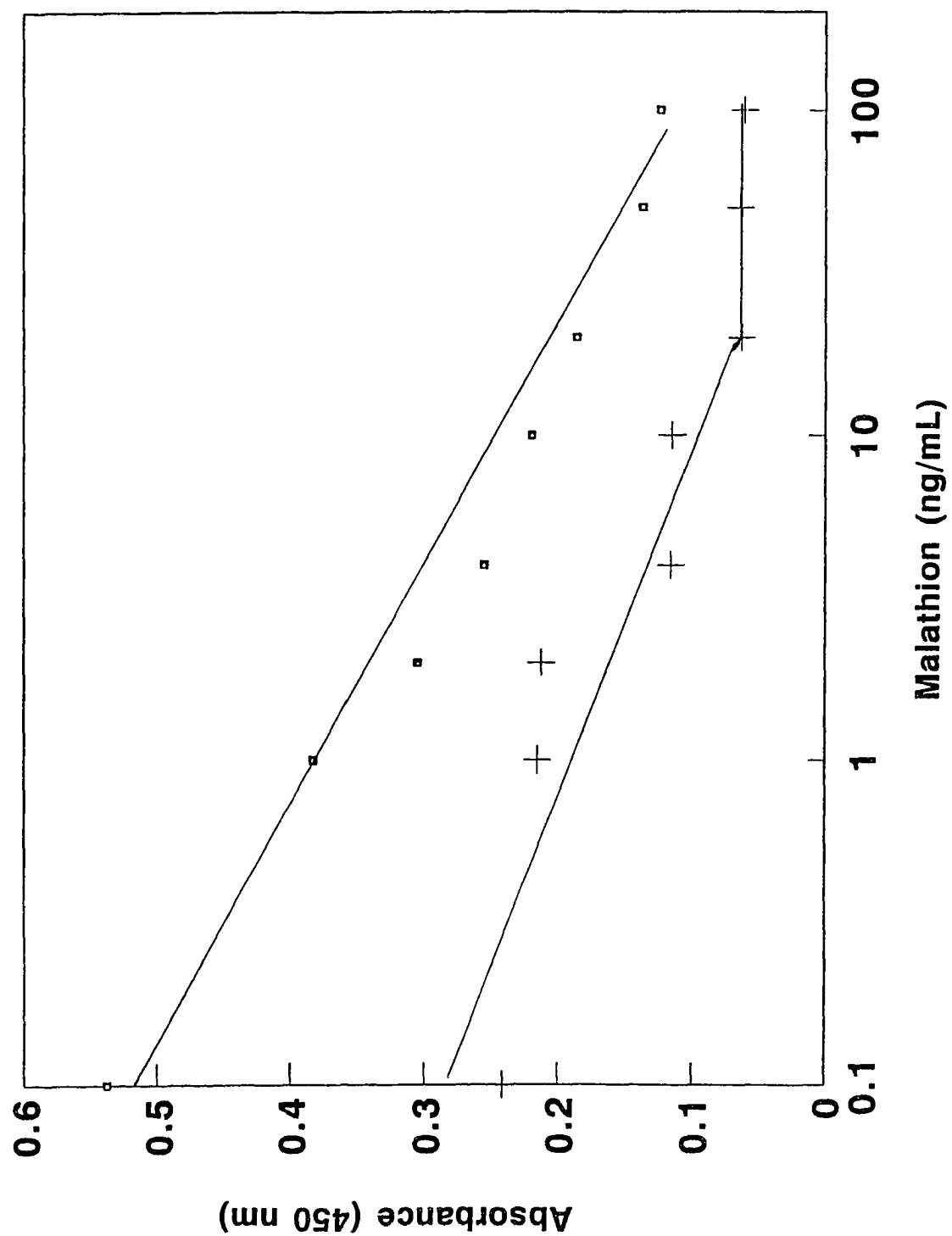


Figure 50

Effect of two different incubation time for the parathion solid-phase enzyme immunoassay on microtube immobilization. (□) and (+) represent 10 and 5 minutes incubation at room temperature for parathion assay. The absorbance was measured at 450 nm. Standard curve of parathion assay in microtube immobilization as plotted on semi-logarithm scale. The results were plotted as absorbance versus logarithm of parathion concentration.

□: $Y=0.915-0.239 \times \log(X)$, $r=-0.997$ ($X=0$ ng/mL to 100 ng/mL)

+: $Y=0.598-0.191 \times \log(X)$, $r=-0.998$ ($X=0$ ng/mL to 100 ng/mL)

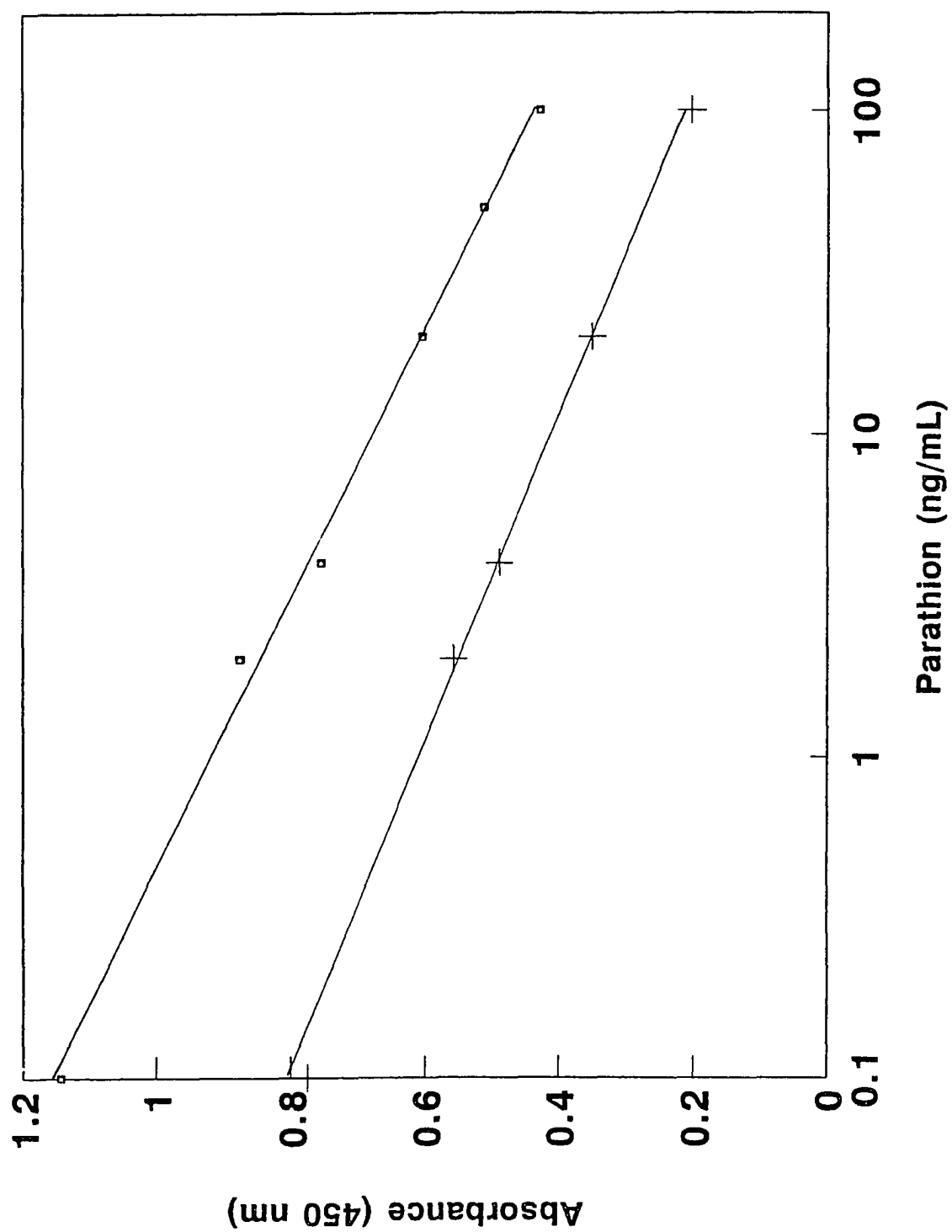


Figure 51

Effect of two different incubation time for the tamaron solid-phase enzyme immunoassay on microtube immobilization. (□) and (+) represent 10 and 5 minutes incubation at room temperature for tamaron assay. The absorbance was measured at 450 nm. Standard curve of tamaron assay in microtube immobilization as plotted on semi-logarithm scale. The results were plotted as absorbance versus logarithm of tamaron concentration.

□: $Y=0.897-0.308 \times \log(X)$, $r=-0.999$ ($X=0$ ng/mL to 100 ng/mL)

+: $Y=0.688-0.194 \times \log(X)$, $r=-0.968$ ($X=0$ ng/mL to 100 ng/mL)

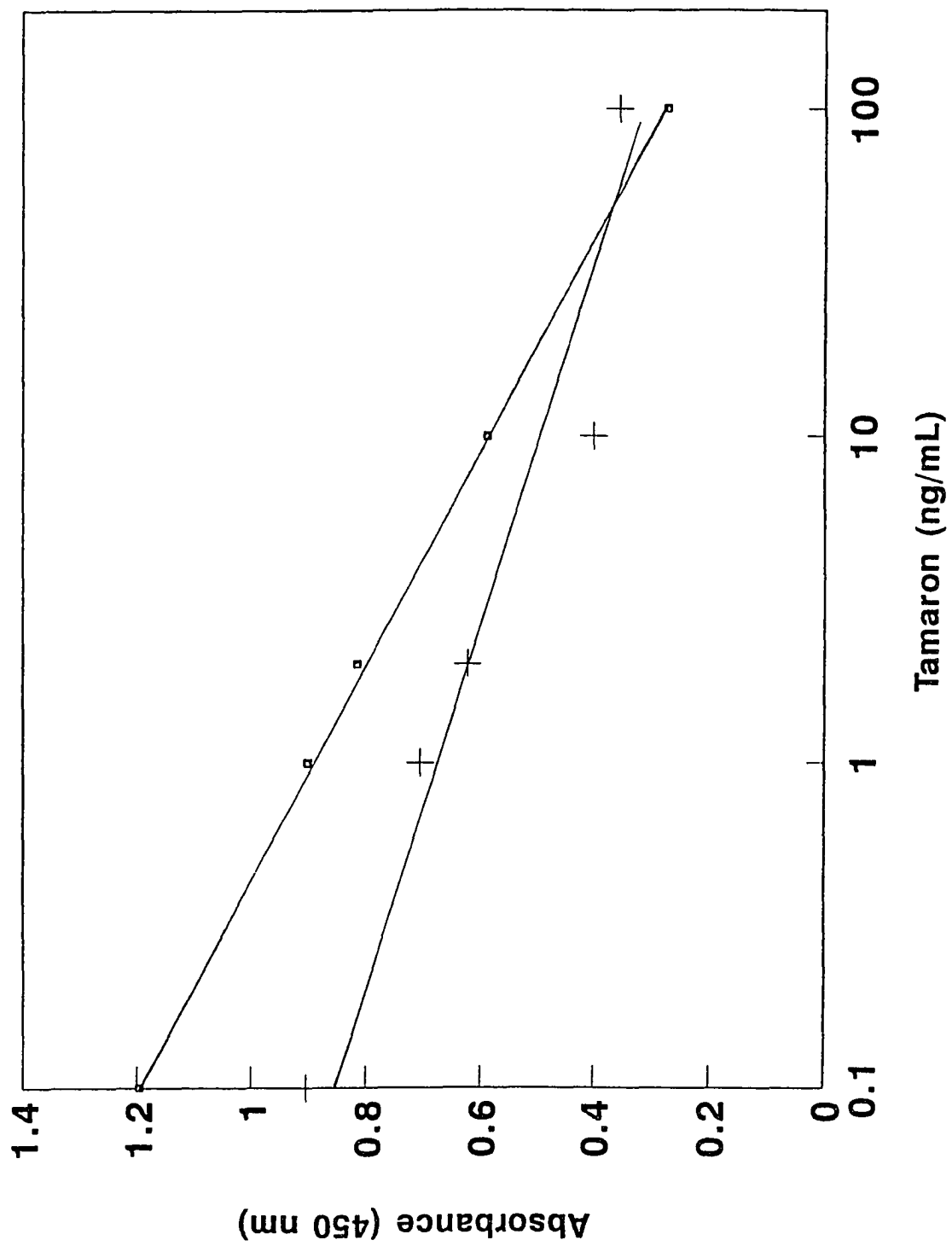


Figure 52

Effect of two different incubation time for the mevinphos solid-phase enzyme immunoassay on microtube immobilization. (□) and (+) represent 10 and 5 minutes incubation at room temperature for mevinphos assay. The absorbance was measured at 450 nm. Standard curve of mevinphos assay in microtube immobilization as plotted on semi-logarithm scale. The results were plotted as absorbance versus logarithm of mevinphos concentration.

□: $Y = 1.154 - 0.458 \times \log(X)$, $r = -0.990$ ($X = 0$ ng/mL to 100 ng/mL)

+: $Y = 0.980 - 0.571 \times \log(X)$, $r = -0.981$ ($X = 0$ ng/mL to 20 ng/mL)

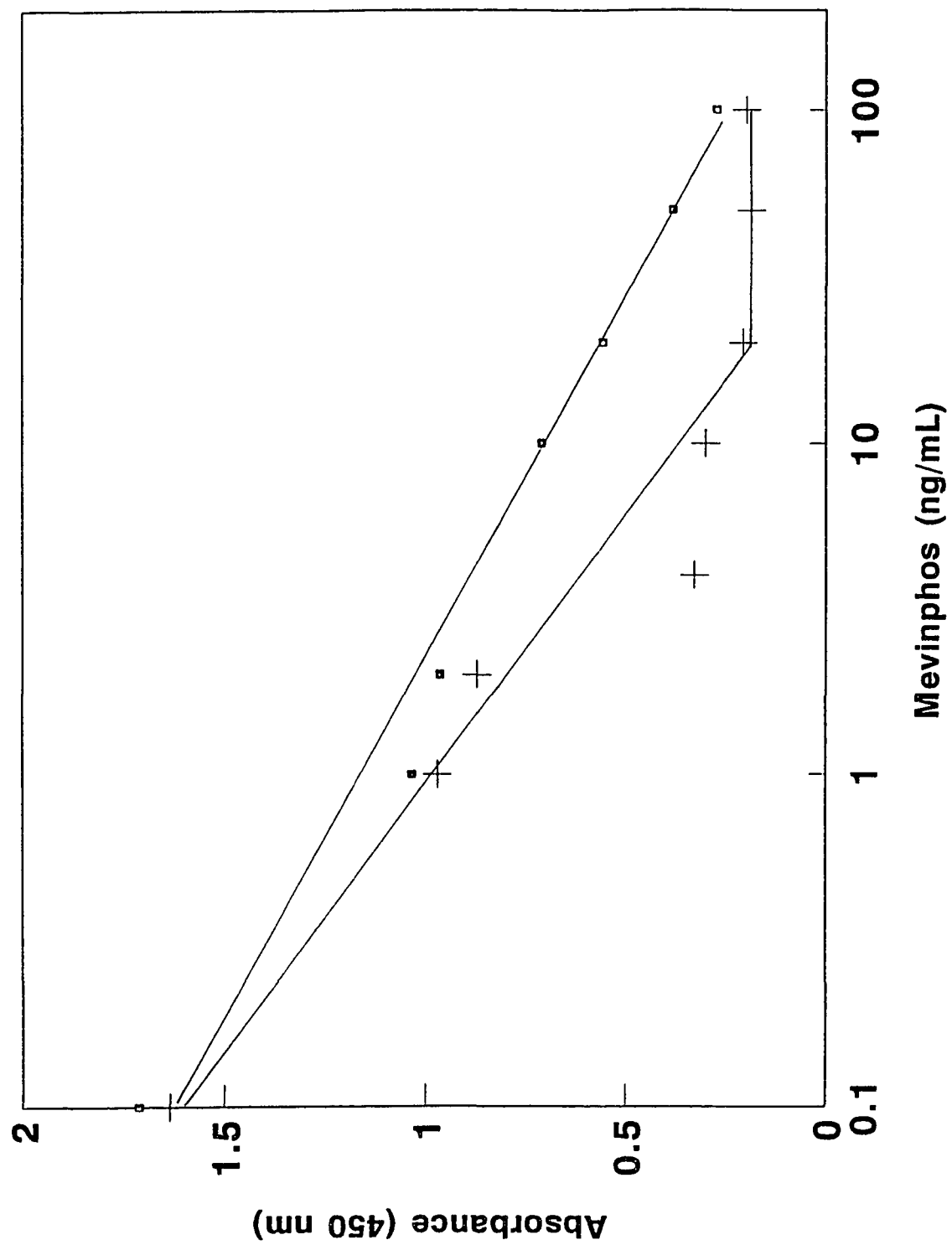


Figure 53

Effect of three different incubation temperatures for the malathion solid-phase enzyme immunoassay on microtube immobilization. (□), (⊕) and (*) represent 20°C, 30°C and 40°C for malathion assay. The absorbance was measured at 450 nm. Standard curve of malathion assay in microtube immobilization as plotted on semi-logarithm scale. The results were plotted as absorbance versus logarithm of malathion concentration.

□: $Y=0.494-0.098 \times \log(X)$, $r=-0.992$; ⊕: $Y=0.462-0.108 \times \log(X)$, $r=-0.972$

*: $Y=0.385-0.072 \times \log(X)$, $r=-0.973$

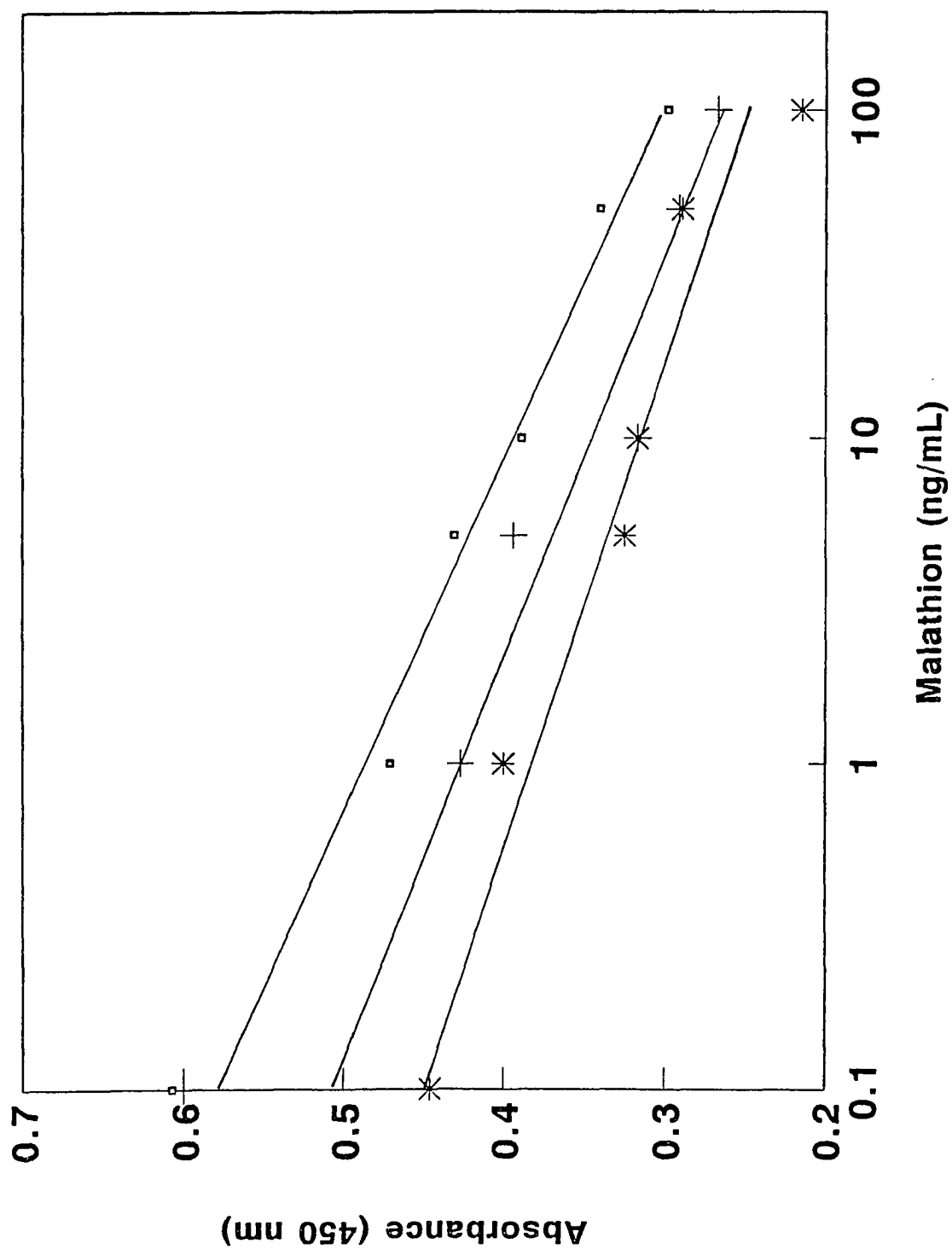


Figure 54

Effect of three different incubation temperatures for the parathion solid-phase enzyme immunoassay on microtube immobilization. (\square), ($+$) and (*) represent 20°C, 30°C and 40°C for parathion assay. The absorbance was measured at 450 nm. Standard curve of parathion assay in microtube immobilization as plotted on semi-logarithm scale. The results were plotted as absorbance versus logarithm of parathion concentration.

\square : $Y=0.601-0.192 \times \log(X)$, $r=-0.999$; $+$: $Y=1.018-0.170 \times \log(X)$, $r=-0.970$

*: $Y=0.273+0.007 \times \log(X)$, $r=-0.313$

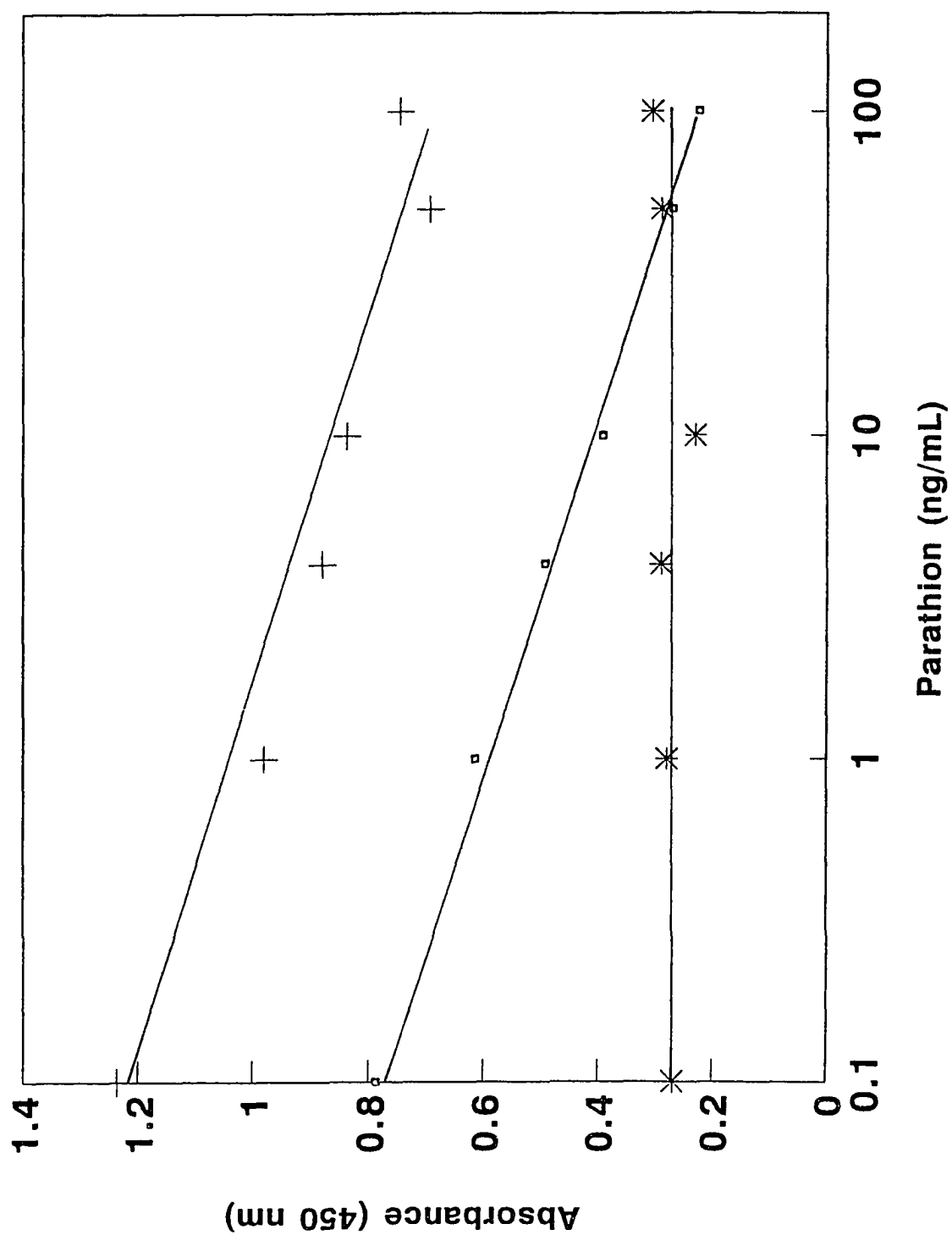


Figure 55

Effect of three different incubation temperatures for the tamaron solid-phase enzyme immunoassay on microtube immobilization. (□), (+) and (*) represent 20°C, 30°C and 40°C for tamaron assay. The absorbance was measured at 450 nm. Standard curve of tamaron assay in microtube immobilization as plotted on semi-logarithm scale. The results were plotted as absorbance versus logarithm of tamaron concentration.

□: $Y=0.676-0.215 \times \log(X)$, $r=-0.994$; +: $Y=0.659-0.174 \times \log(X)$, $r=-0.996$

*: $Y=0.687-0.228 \times \log(X)$, $r=-0.997$

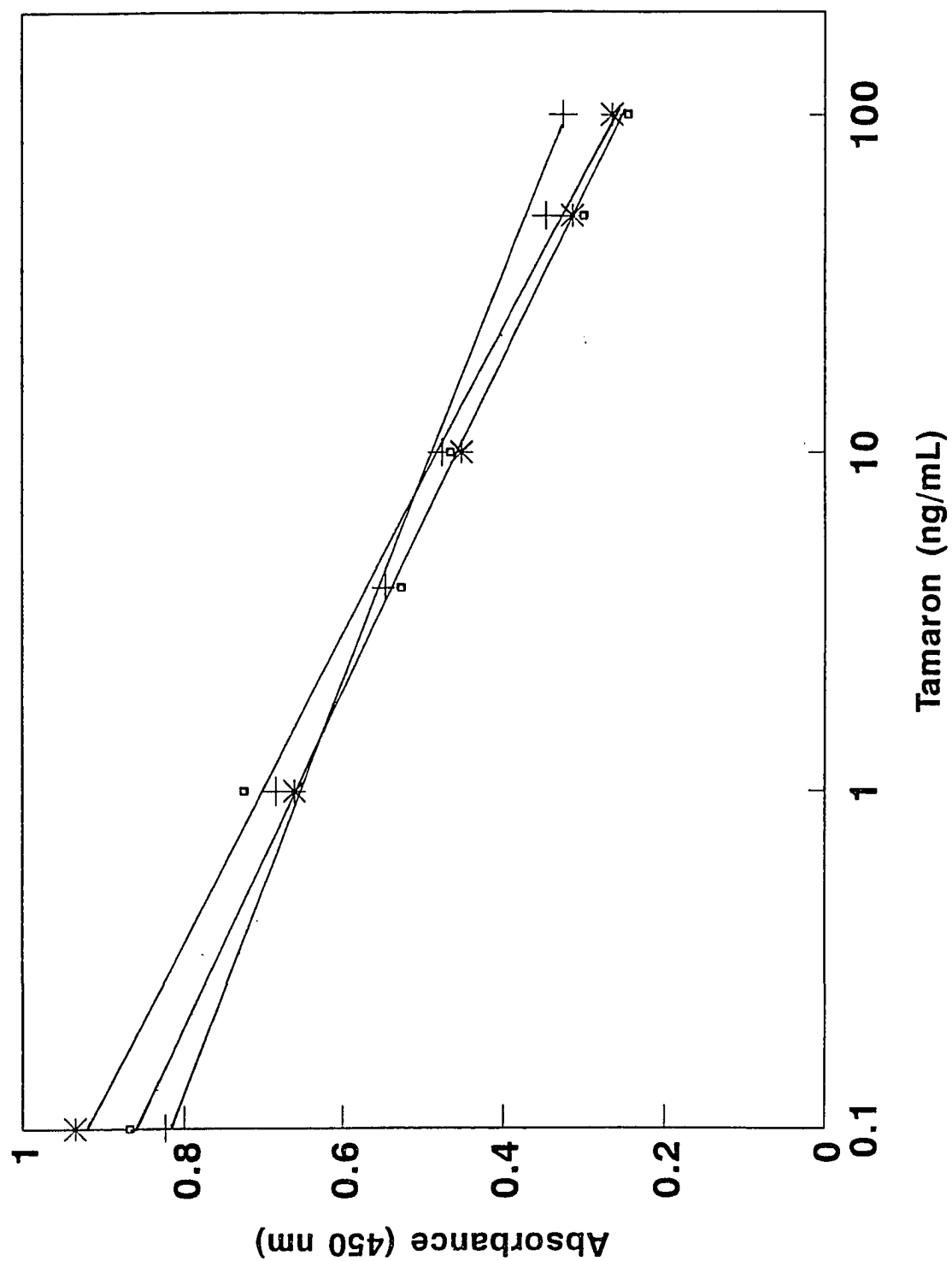
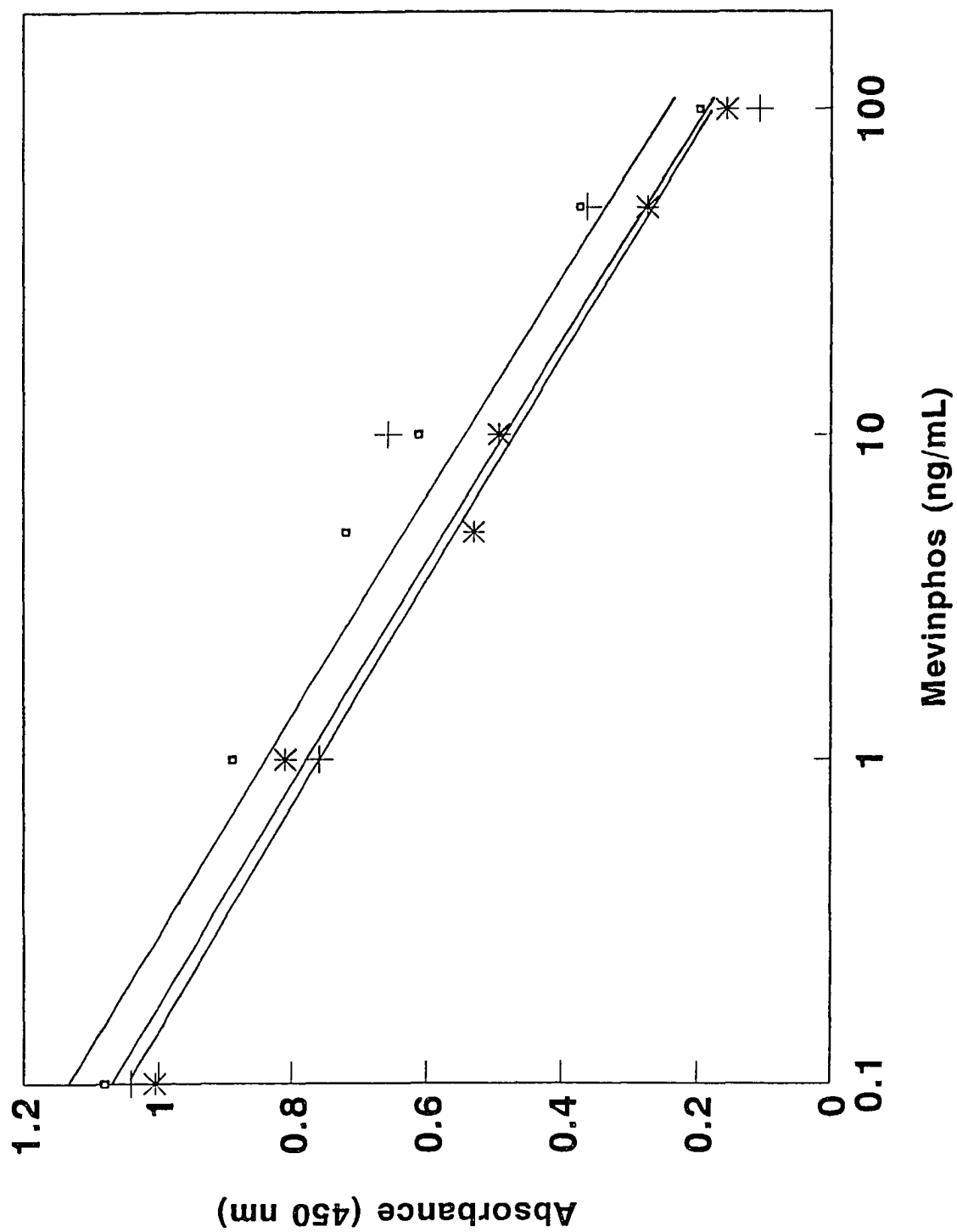


Figure 56

Effect of three different incubation temperatures for the mevinphos solid-phase enzyme immunoassay on microtube immobilization. (\square), (\dagger) and (*) represent 20°C, 30°C and 40°C for mevinphos assay. The absorbance was measured at 450 nm. Standard curve of mevinphos assay in microtube immobilization as plotted on semi-logarithm scale. The results were plotted as absorbance versus logarithm of mevinphos concentration.

\square : $Y=0.857-0.228 \times \log(X)$, $r=-0.983$; \dagger : $Y=0.792-0.279 \times \log(X)$, $r=-0.960$

*: $Y=0.754-0.286 \times \log(X)$, $r=-0.994$



decreased. The standard curves of 20°C and 30°C were parallel which indicated there is no significant difference in the separation, and the only difference was the enzyme activity increased. But the enzyme started to denatured at 40 °C; thus, the sensitivity decreased. Also the optimal concentration for parathion-HRPO was more dilute than the other three OP-HRPO; therefore the temperature is more critical especially close to the melting point of the enzyme.

5. Selection of the incubation solution

Four different solutions: deionized water; 10 mM sodium phosphate buffer, pH 7.4; 10 mM phosphate buffered saline (PBS) (10 mM phosphate buffer with 0.15 M saline), pH 7.4; and 10 mM glycine solution, pH 7.2; were studied as the solution system for the OP assays. The results obtained were plotted as absorbance at 450 nm versus concentration of the various OP.

In the parathion assay, shown in Figure 58, only the deionized water can be selected as the incubation solution. The polarity of the parathion structure may affect the assay performance. The side chain of the parathion structure contains an aromatic group which decreases the polarity of the compound; therefore, parathion can only give a higher sensitivity in a very low ionic strength condition. Since an enzyme cannot work in extreme pH conditions, a buffer is usually provided to maintain the pH range; therefore, the stock

parathion-HRPO was stored in 10 mM PBS. Although using deionized water as the incubation solution, the 150 fold dilution of parathion-HRPO provided sufficient buffer ability, and the lowered ionic strength was attained in comparison to phosphate buffer, PBS and glycine buffer.

In the malathion assay phosphate buffer and phosphate buffered saline gave better separation and with a sharper slope, with the regression coefficient of -0.12 and correlation coefficient of -0.969 for malathion assay shown in Figure 57. The results in Figure 60 showed that there was no significantly different sensitivity in the mevinphos assay between the incubation solutions of deionized water, 10 mM sodium phosphate buffer, 10 mM phosphate buffered saline (PBS). The similar results for both malathion and mevinphos assays can be explained due to the chemical structures of these two compounds. The side chains of malathion and mevinphos structures are both alkyl esters which are more polar than an aromatic group. They can tolerate the slightly higher ionic strengths of 10 mM phosphate buffer and 10 mM PBS.

In the tamaron assay deionized water gave the highest sensitivity as shown in Figure 59. Phosphate buffer and PBS both gave good separation within the concentrations of tamaron of 0 ng/mL to 100 ng/mL. Since the tamaron did not possess the highly hydrophobic portion, the assay can be performed in these low ionic strength conditions.

Figure 57

Effect of four different incubation buffers for the malathion solid-phase enzyme immunoassay on microtube immobilization. (□), (+), (*) and (■) represent deionized water, 10 mM phosphate buffer, pH 7.4, 10 mM phosphate buffer saline, pH 7.4 and 10 mM glycine buffer, pH 7.2 for malathion assay. The absorbance was measured at 450 nm. Standard curve of malathion assay in microtube immobilization as plotted on semi-logarithm scale. The results were plotted as absorbance versus logarithm of malathion concentration.

□: $Y=0.390-0.121 \times \log(X)$, $r=-0.969$; +: $Y=0.327-0.173 \times \log(X)$, $r=-0.985$

*: $Y=0.520-0.172 \times \log(X)$, $r=-0.997$; ■: $Y=0.708-0.001 \times \log(X)$, $r=-0.105$

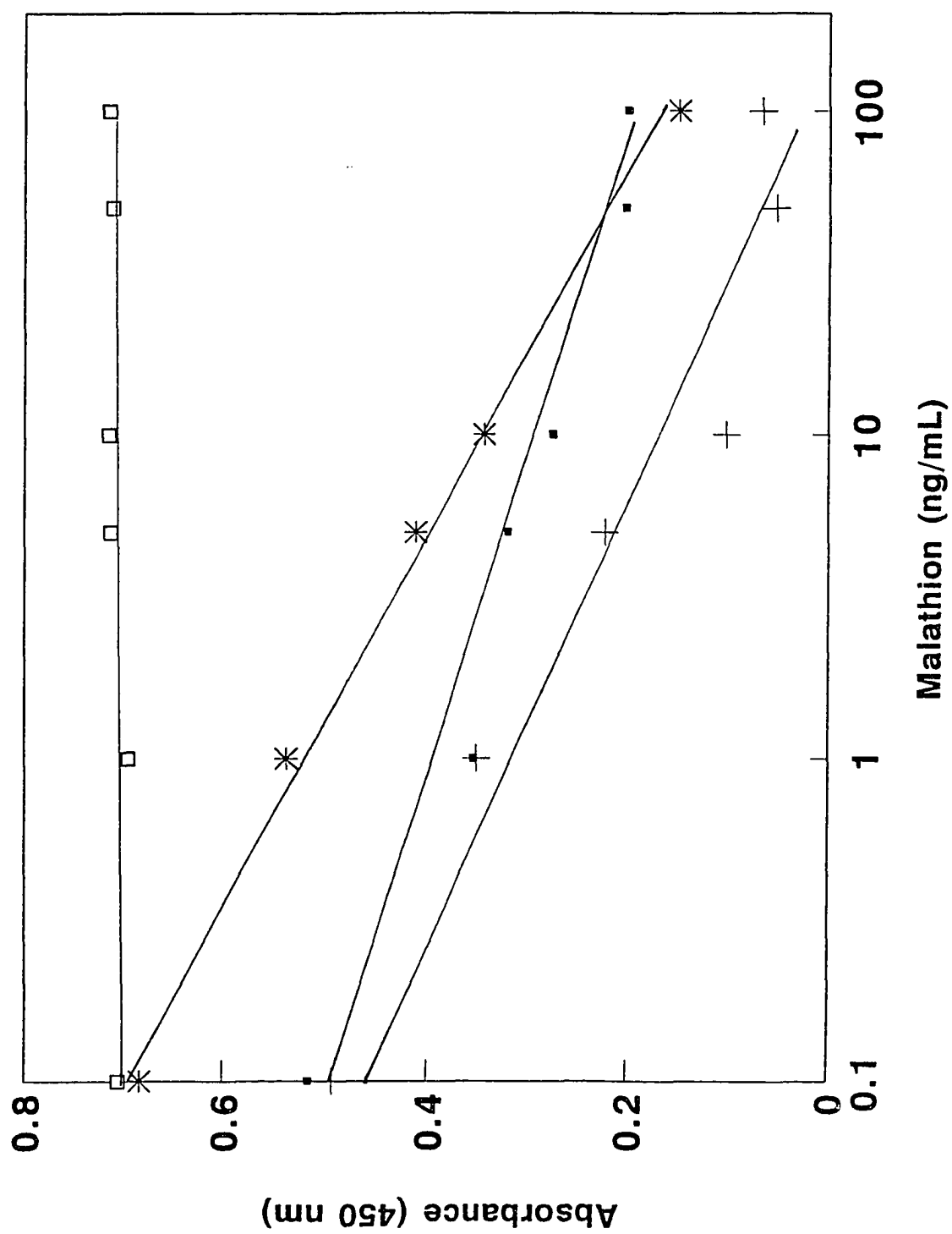


Figure 58

Effect of four different incubation buffers for the parathion solid-phase enzyme immunoassay on microtube immobilization. (□), (+), (*) and (■) represent deionized water, 10 mM phosphate buffer, pH 7.4, 10 mM phosphate buffer saline, pH 7.4 and 10 mM glycine buffer, pH 7.2 for parathion assay. The absorbance was measured at 450 nm. Standard curve of parathion assay in microtube immobilization as plotted on semi-logarithm scale. The results were plotted as absorbance versus logarithm of parathion concentration.

□: $Y=0.619-0.306 \times \log(X)$, $r=-0.999$; +: $Y=0.465-0.009 \times \log(X)$, $r=-0.214$

*: $Y=0.682-0.042 \times \log(X)$, $r=-0.811$; ■: $Y=0.814-0.023 \times \log(X)$, $r=-0.718$

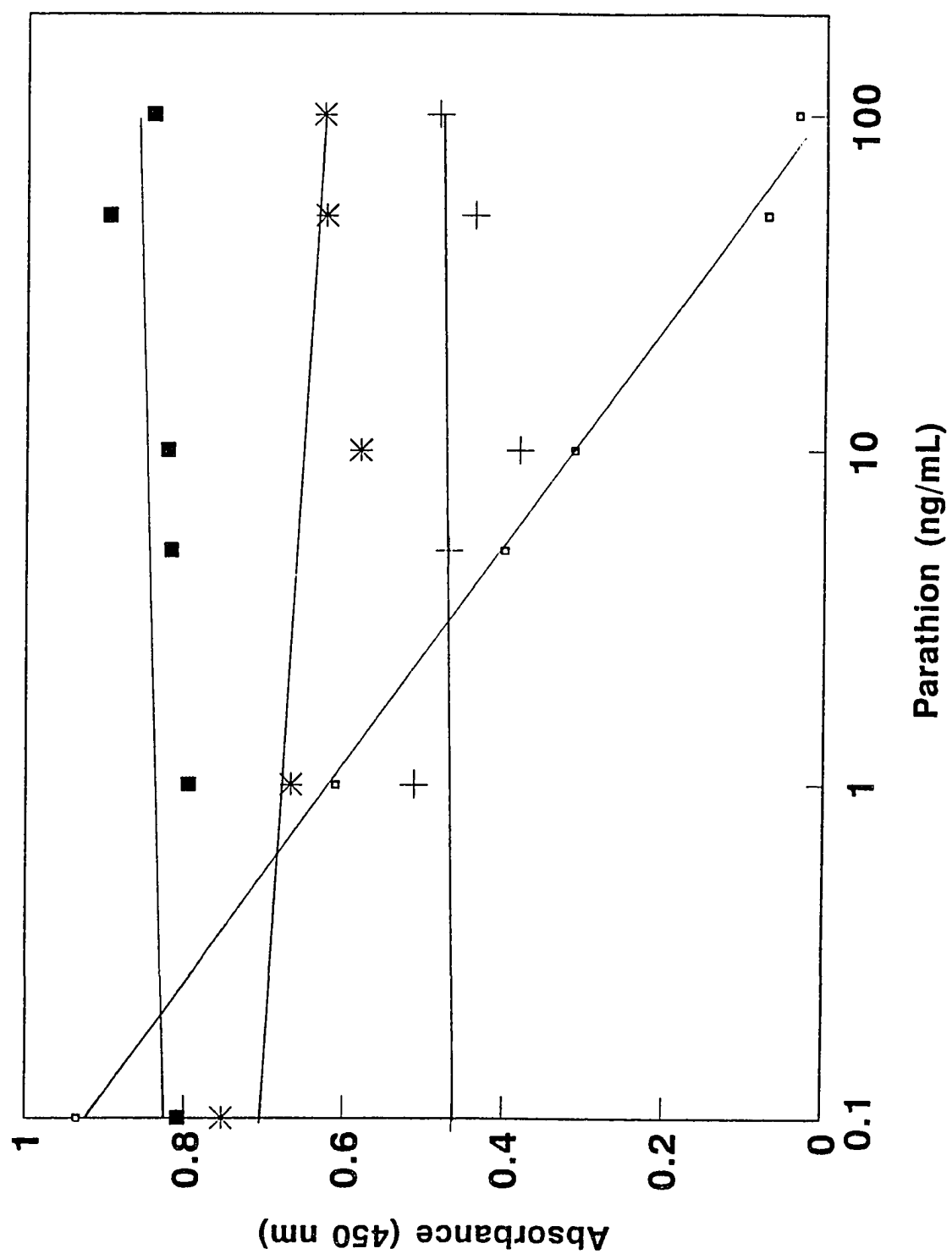


Figure 59

Effect of four different incubation buffers for the tamaron solid-phase enzyme immunoassay on microtube immobilization. (□), (+), (*) and (■) represent deionized water, 10 mM phosphate buffer, pH 7.4, 10 mM phosphate buffer saline, pH 7.4 and 10 mM glycine buffer, pH 7.2 for tamaron assay. The absorbance was measured at 450 nm. Standard curve of tamaron assay in microtube immobilization as plotted on semi-logarithm scale. The results were plotted as absorbance versus logarithm of tamaron concentration.

□: $Y=0.542-0.184 \times \log(X)$, $r=-0.991$; +: $Y=0.044-0.006 \times \log(X)$, $r=-0.222$

*: $Y=0.312-0.198 \times \log(X)$, $r=-0.998$; ■: $Y=0.149-0.030 \times \log(X)$, $r=-0.875$

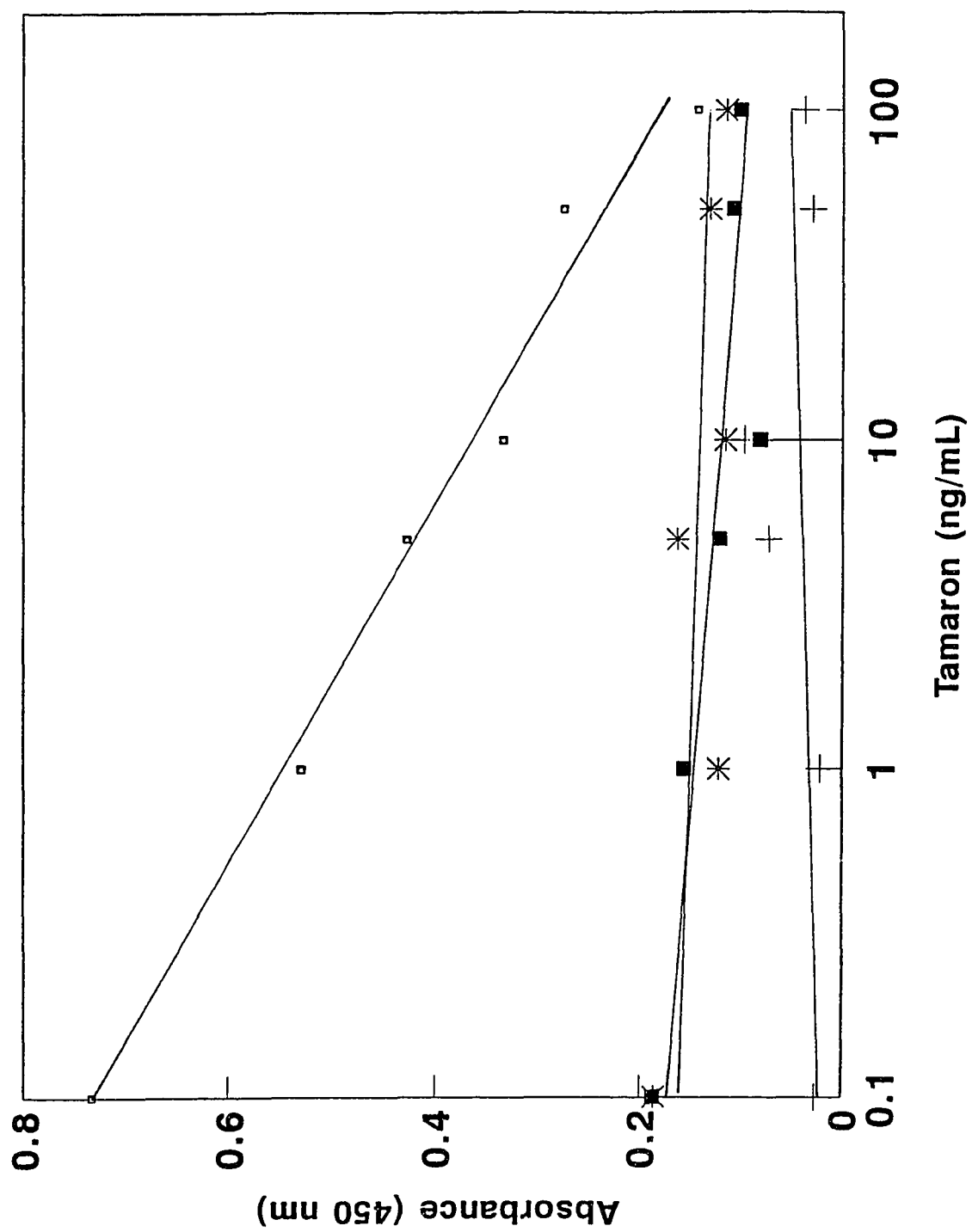
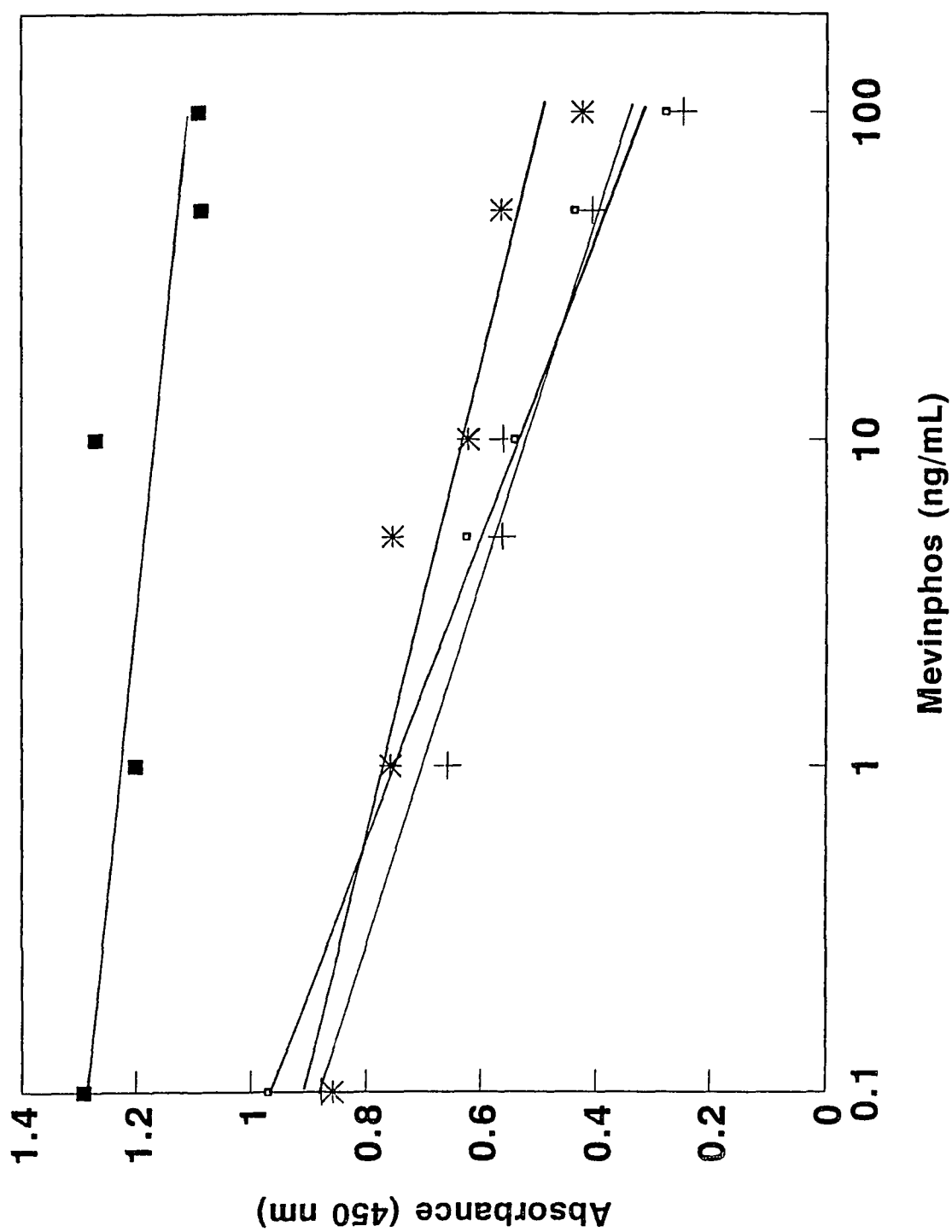


Figure 60

Effect of four different incubation buffers for the mevinphos solid-phase enzyme immunoassay on microtube immobilization. (□), (+), (*) and (■) represent deionized water, 10 mM phosphate buffer, pH 7.4, 10 mM phosphate buffer saline, pH 7.4 and 10 mM glycine buffer, pH 7.2 for mevinphos assay. The absorbance was measured at 450 nm. Standard curve of mevinphos assay in microtube immobilization as plotted on semi-logarithm scale. The results were plotted as absorbance versus logarithm of mevinphos concentration.

□: $Y=0.773-0.202 \times \log(X)$, $r=-0.989$; +: $Y=0.684-0.161 \times \log(X)$, $r=-0.972$

*: $Y=0.774-0.183 \times \log(X)$, $r=-0.951$; ■: $Y=1.232-0.054 \times \log(X)$, $r=-0.828$



6. Determination of pH condition for the OP assays

Since deionized water supplied a high sensitivity in the OP assays, and the EIA screening was designed for the environmental samples, the pH condition for the optimal OP assays are very important. The pH values for the samples from the environment were varied; therefore, the optimal pH condition needed to be investigated.

Three sets of standard solutions were made by dissolving the intermediate concentration (2000 ng/mL) of a specific OP stock solution as described in the method section in Chapter II, in three different pH conditions: acidic, pH 3.0; neutral, pH 6.8; and basic, pH 10.0. The pH was adjusted with HCl for acidic condition and NaOH for the basic condition. The results obtained from the enzyme immunoassay of the four OPs under the standard curve assay conditions described previously are shown on Figures 61-64. For all four OP assays, there was no detection of OP in acidic and basic conditions. Once the antibodies are kept in extreme pH conditions, the binding affinity to the antigen and antigen conjugated enzyme will not stay the same, causing the assay conditions for the competition enzyme immunoassay to change. Also the antigen will dissociate in the extreme pH conditions; thus, the pH condition is very important in the OP assays. It also suggests that the samples should be adjusted to a neutral pH before the assay is performed, and then the assay can be processed as usual.

Figure 61

Effect of different pH conditions for the malathion solid-phase enzyme immunoassay on microtube immobilization. (\square), ($+$), and (*) represent pH 3, pH 7 and pH 10 three conditions for malathion assay. The absorbance was measured at 450 nm. Standard curve of malathion assay in microtube immobilization as plotted on semi-logarithm scale. The results were plotted as absorbance versus logarithm of malathion concentration.

\square : $Y=0.128+0.003x\log(X)$, $r=0.884$; $+$: $Y=0.667-0.092x\log(X)$, $r=-0.993$

*: $Y=1.164+0.027x\log(X)$, $r=0.710$

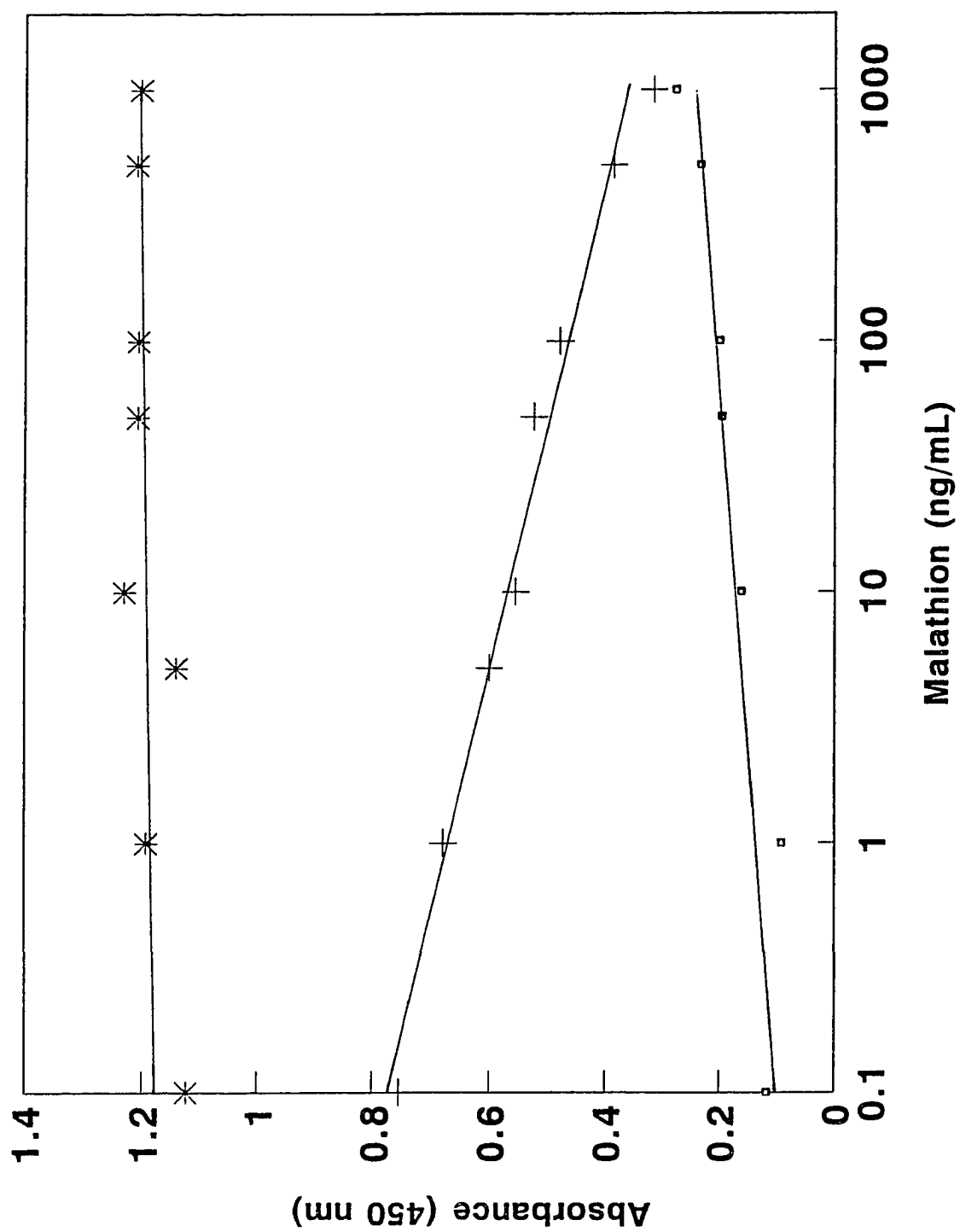


Figure 62

Effect of different pH conditions for the parathion solid-phase enzyme immunoassay on microtube immobilization. (\square), ($+$), and (*) represent pH 3, pH 7 and pH 10 three conditions for parathion assay. The absorbance was measured at 450 nm. Standard curve of parathion assay in microtube immobilization as plotted on semi-logarithm scale. The results were plotted as absorbance versus logarithm of parathion concentration.

\square : $Y=0.344-0.094 \times \log(X)$, $r=-0.403$; $+$: $Y=0.825-0.306 \times \log(X)$, $r=-0.993$

*: $Y=0.992-0.001 \times \log(X)$, $r=-0.025$

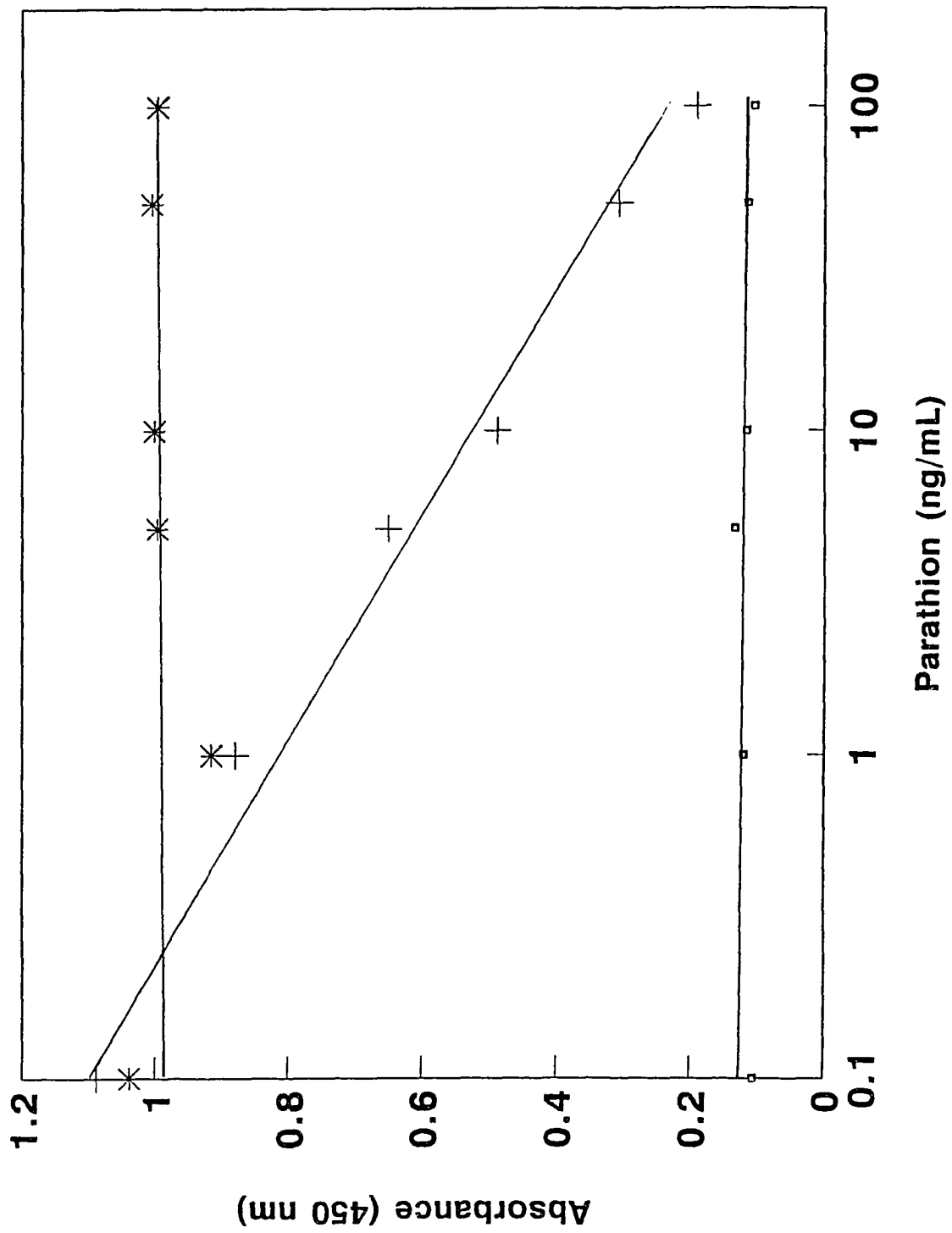


Figure 63

Effect of different pH conditions for the tamaron solid-phase enzyme immunoassay on microtube immobilization. (\square), ($+$), and (*) represent pH 3, pH 7 and pH 10 three conditions for tamaron assay. The absorbance was measured at 450 nm. Standard curve of tamaron assay in microtube immobilization as plotted on semi-logarithm scale. The results were plotted as absorbance versus logarithm of tamaron concentration.

\square : $Y=0.037+0.001 \times \log(X)$, $r=0.241$; $+$: $Y=0.582-0.210 \times \log(X)$, $r=-0.981$

*: $Y=0.743-0.040 \times \log(X)$, $r=-0.734$

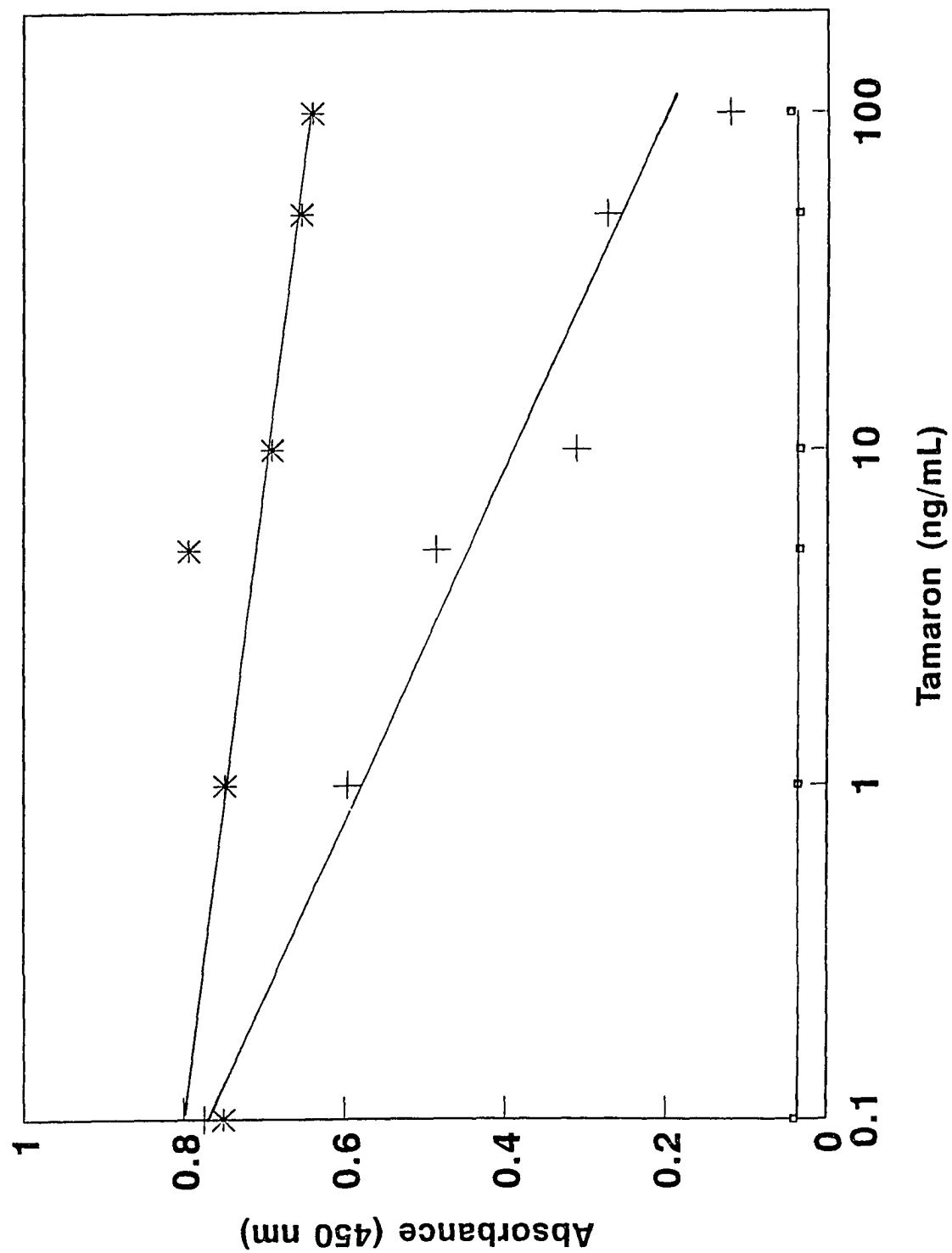


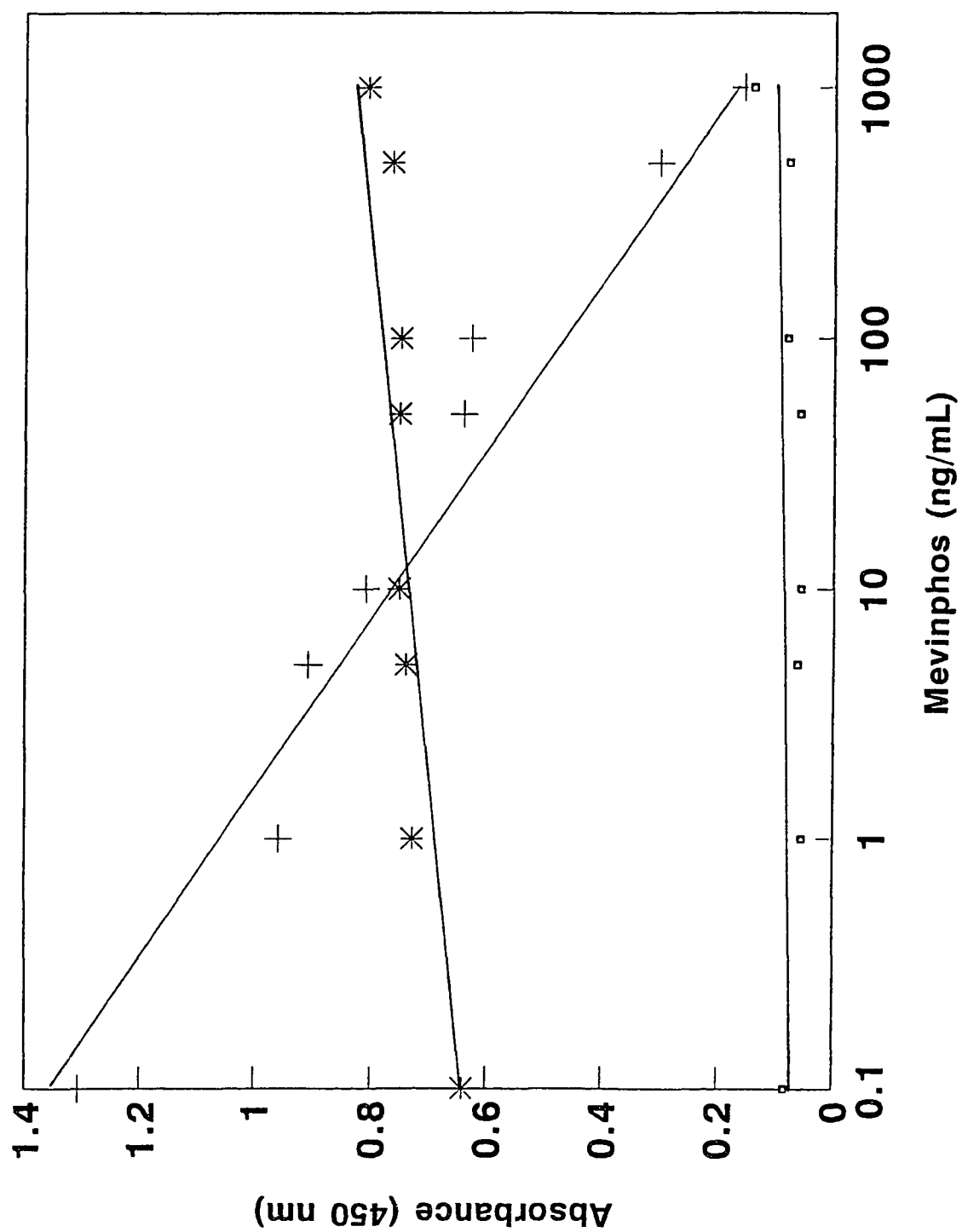
Figure 64

Effect of different pH conditions for the mevinphos solid-phase enzyme immunoassay on microtube immobilization. (\square), ($+$), and (*) represent pH 3, pH 7 and pH 10 three conditions for mevinphos assay. The absorbance was measured at 450 nm. Standard curve of mevinphos assay in microtube immobilization as plotted on semi-logarithm scale. The results were plotted as absorbance versus logarithm of mevinphos concentration.

\square : $Y=0.068-0.002 \times \log(X)$, $r=-0.166$; $+$: $Y=1.036-0.278 \times \log(X)$, $r=-0.953$

*: $Y=0.702+0.034 \times \log(X)$, $r=0.867$

- -



The standard curves obtained, shown in Figures 65-68, were plotted in a semi-logarithmic scale of OP concentrations versus the HRPO activity assayed at 450 nm. The correlation coefficients for these four enzyme immunoassays are -0.992, -0.993, -0.991 and -0.986 for malathion, parathion, tamaron and mevinphos assays, respectively.

The results of all the conditions studied for the OP EIA in microtubes in previous sections are summarized in Table 4.

7. Study of the relationship of the color development and enzyme-substrate-chromogen results

The linear relationship between color development time and the enzyme(HRPO)-substrate-chromogen reaction was investigated. In the OP competitive enzyme immunoassay, the enzyme activity of HRPO was terminated by the addition of 2 N sulfuric acid, which inactivated the enzyme by lowering the pH of the reaction mixture, with the concomitant conversion of the blue oxidized chromogen 3, 3', 5, 5'-tetramethylbenzidine (TMB), into a yellow colored compound due to the pH change of the structure of the oxidized TMB. The results shown in Figures 69-72 suggested that the intensity of the color is proportional to the length of developing time.

Figure 65

Standard curve of the malathion solid-phase enzyme immunoassay on microtube immobilization. The results were plotted as absorbance of peroxidase activity versus logarithm of malathion concentration. ($Y=0.398-0.159 \times \log(X)$, $r=-0.992$)

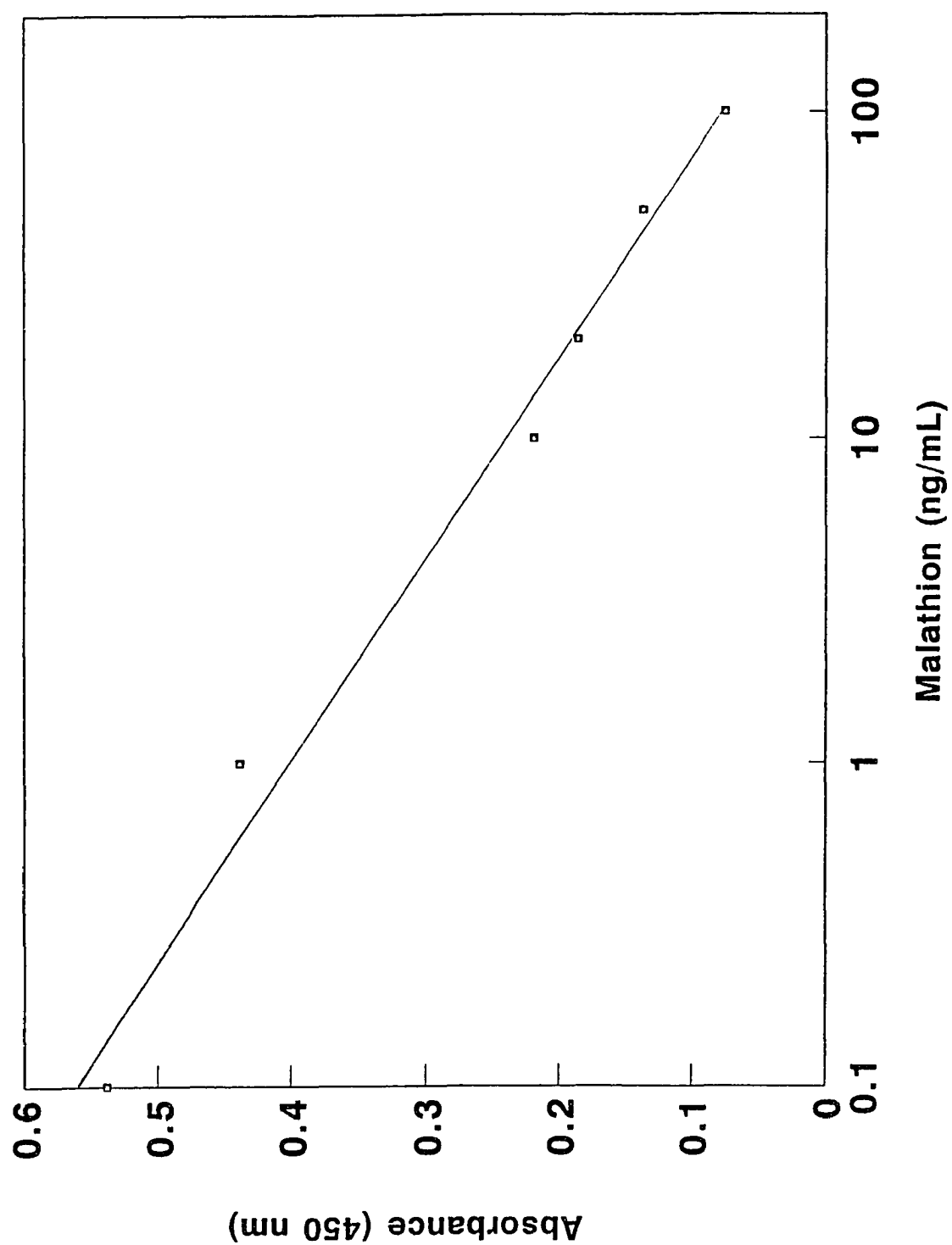


Figure 66

Standard curve of the parathion solid-phase enzyme immunoassay on microtube immobilization. The results were plotted as absorbance of peroxidase activity versus logarithm of parathion concentration. ($Y=0.751-0.256 \times \log(X)$, $r=-0.993$)

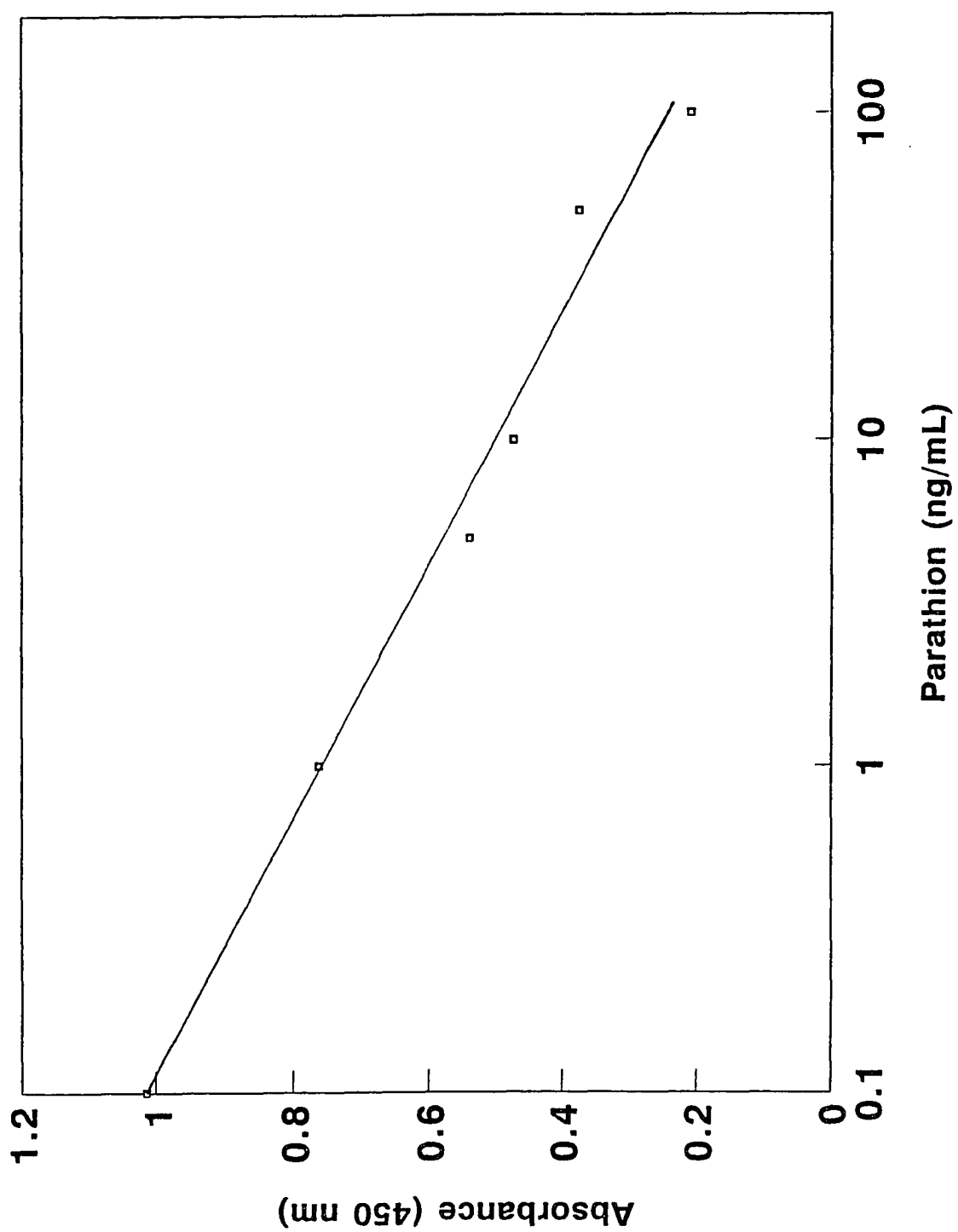


Figure 67

Standard curve of the tamaron solid-phase enzyme immunoassay on microtube immobilization. The results were plotted as absorbance of peroxidase activity versus logarithm of tamaron concentration. ($Y = 1.196 - 0.502 \times \log(X)$, $r = -0.991$)

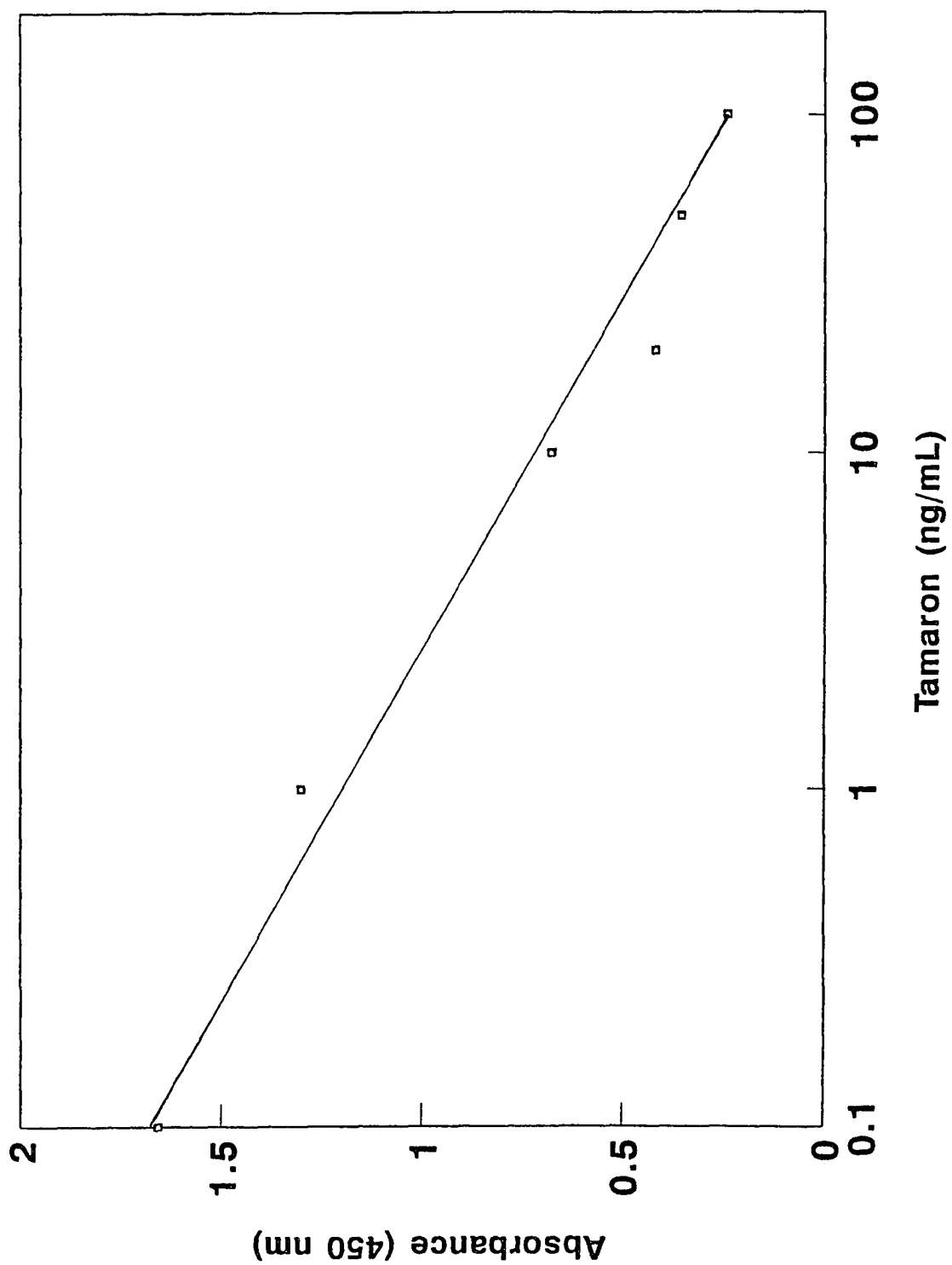


Figure 68

Standard curve of the mevinphos solid-phase enzyme immunoassay on microtube immobilization. The results were plotted as absorbance of peroxidase activity versus logarithm of mevinphos concentration. ($Y=0.639-0.309 \times \log(X)$, $r=-0.986$)

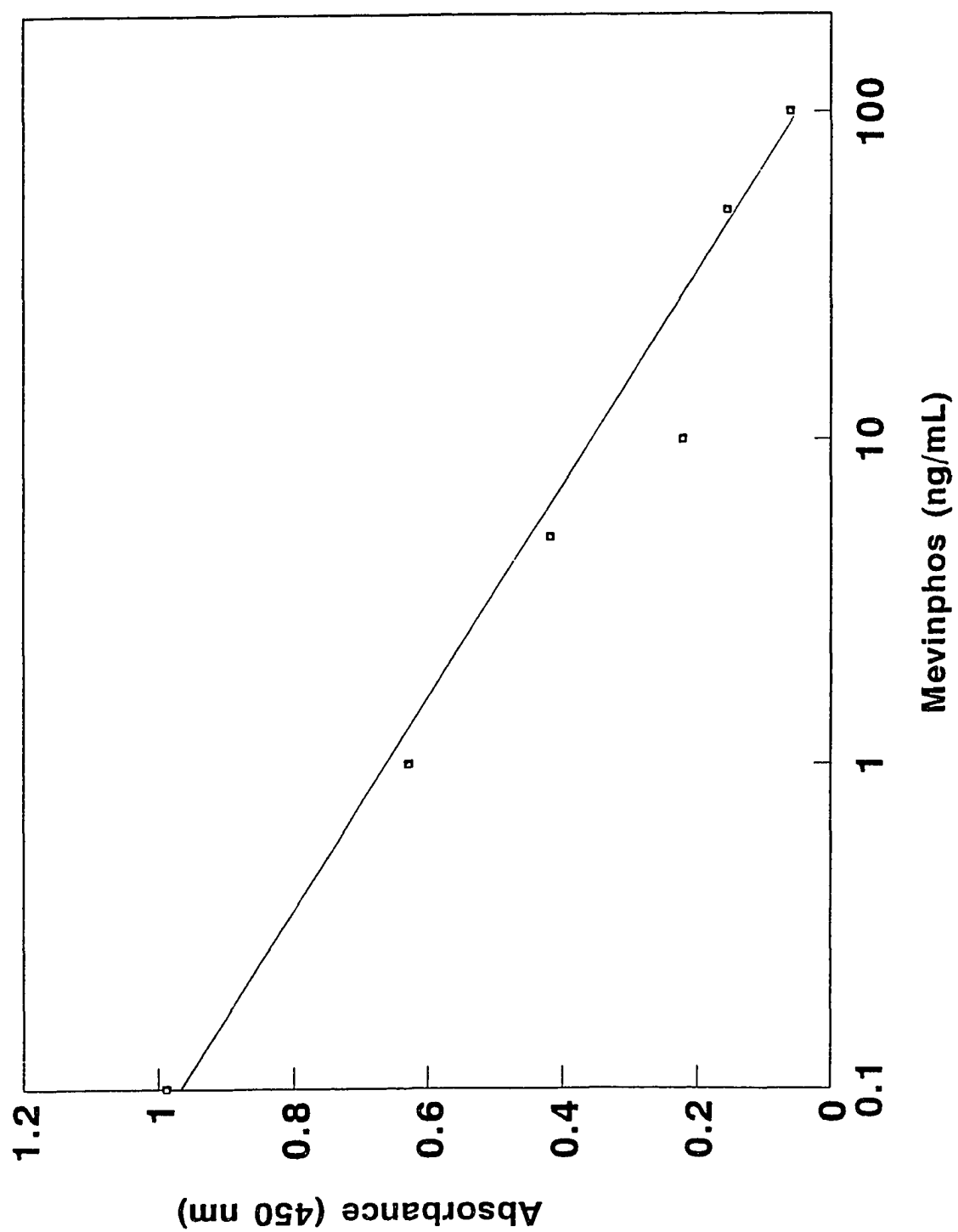


Table 4 Summary of the assay condition of the homogeneous enzyme immunoassay on microtube immobilization of the organophosphorus pesticides

	Malathion	Parathion	Tamaron	Mevinphos
Antibody concentration per tube (ng/tube) ¹	25	250	250	25
Volume of OP standard (μ L) ²	440	300	460	300
OP-HRPO concentration (mg/mL) ³	0.950	0.232	0.534	0.759
Volume of OP-HRPO (μ L) ⁴	10	50	10	50
buffer (water) (μ L) ⁵	50	150	30	150
Incubation time (min) ⁶	10	10	10	10
Color Developed time (min) ⁷	≤ 5	≤ 5	≤ 5	≤ 5
$\Delta OD_{450 \text{ nm}}$ ($A_{0 \text{ ng/mL}} - A_{100 \text{ ng/mL}}$)	> 0.5	> 0.5	> 0.5	> 0.5

1. the optimal antibody concentration suggested for microtube coating
2. the optimal volume suggested for the enzyme immunoassay of the organophosphorus pesticides
3. the optimal OP-HRPO concentration recommended for the enzyme immunoassay of the organophosphorus pesticides
4. the optimal OP-HRPO volume suggested for the enzyme immunoassay of the organophosphorus pesticides
5. the optimal buffer volume proposed for the enzyme immunoassay of the organophosphorus pesticides
6. the optimal incubation time suggested for the competitive reaction of organophosphorus pesticides and OP-HRPO
7. the optimal color development time required for enzyme-substrate-chromogen reaction

Figure 69

Color development time study for the malathion solid-phase enzyme immunoassay on microtube immobilization. The results of slopes generated from 2, 4, 6, 8 and 10 minutes enzyme-substrate-chromogen reaction were plotted on semi-logarithm scale for 0, 1, 5, 10, 50 and 100 ng/mL analyte concentration used for malathion assay. The absorbance was measured at 450 nm. The absorbance was measured at 450 nm.

$$Y=0.060-0.021 \times \log(X), r=-0.839$$

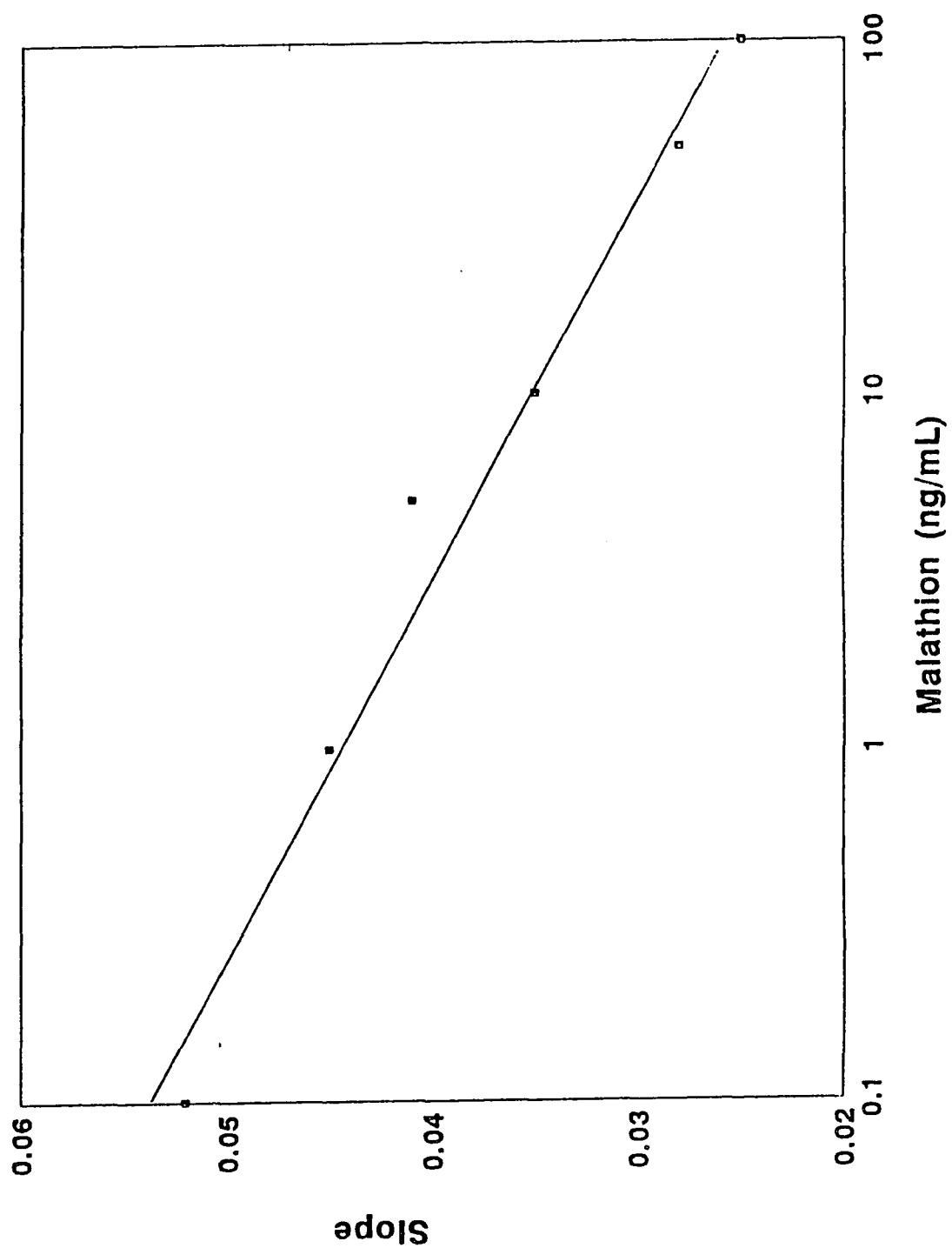


Figure 70

Color development time study for the parathion solid-phase enzyme immunoassay on microtube immobilization. The results of slopes generated from 1, 3, 5, 7 and 9 minutes enzyme-substrate-chromogen reaction were plotted on semi-logarithm scale for 0, 1, 5, 10, 50 and 100 ng/mL analyte concentration used for parathion assay. The absorbance was measured at 450 nm.
 $Y=0.075-0.032 \times \log(X)$, $r=-0.999$

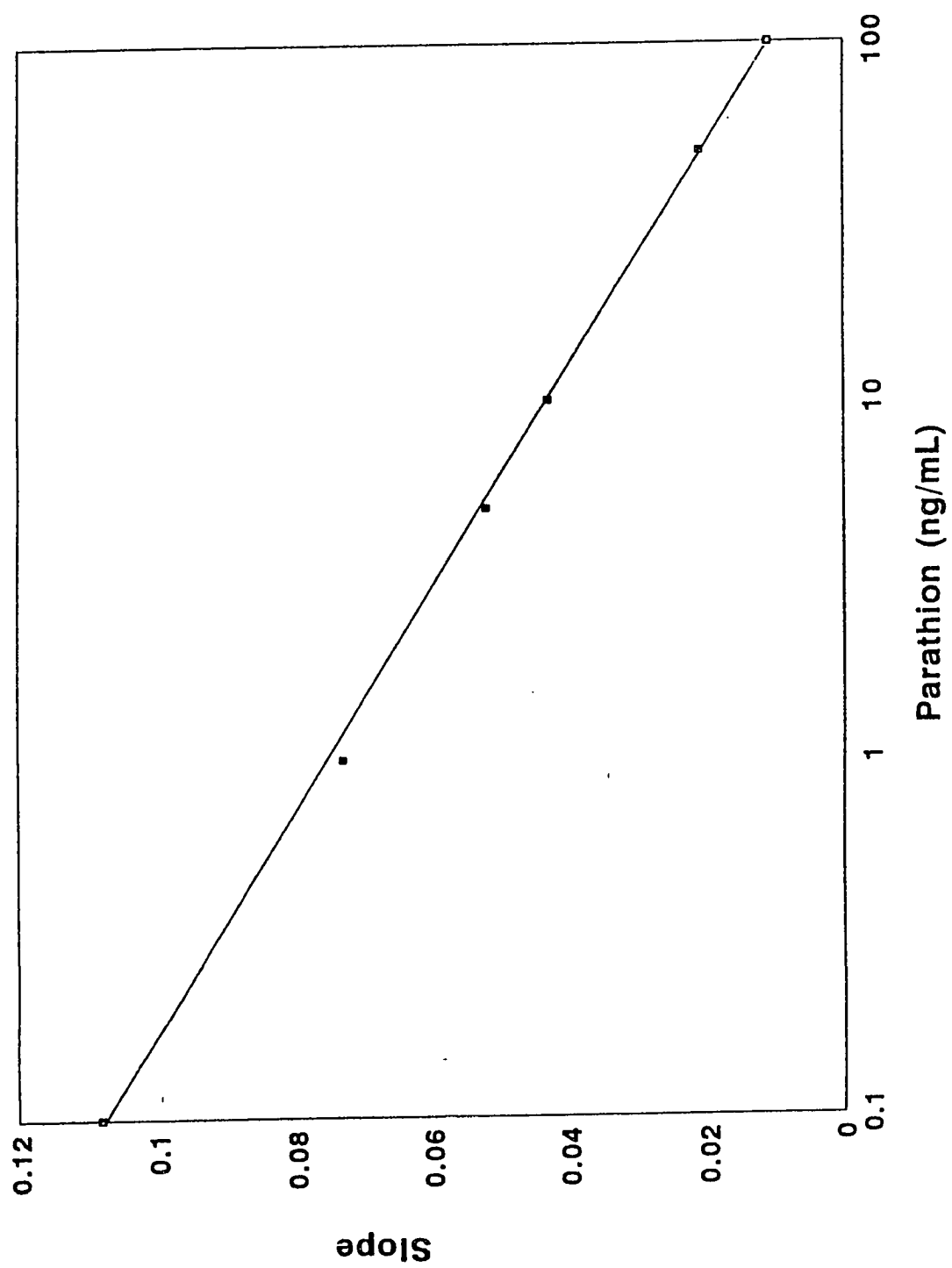


Figure 71

Color development time study for the tamaron solid-phase enzyme immunoassay on microtube immobilization. The results of slopes generated from 2, 4, 6, 8 and 10 minutes enzyme-substrate-chromogen reaction were plotted on semi-logarithm scale for 0, 1, 5, 10, 50 and 100 ng/mL analyte concentration used for tamaron assay. The absorbance was measured at 450 nm.
 $Y=0.007-0.003 \times \log(X)$, $r=-0.949$

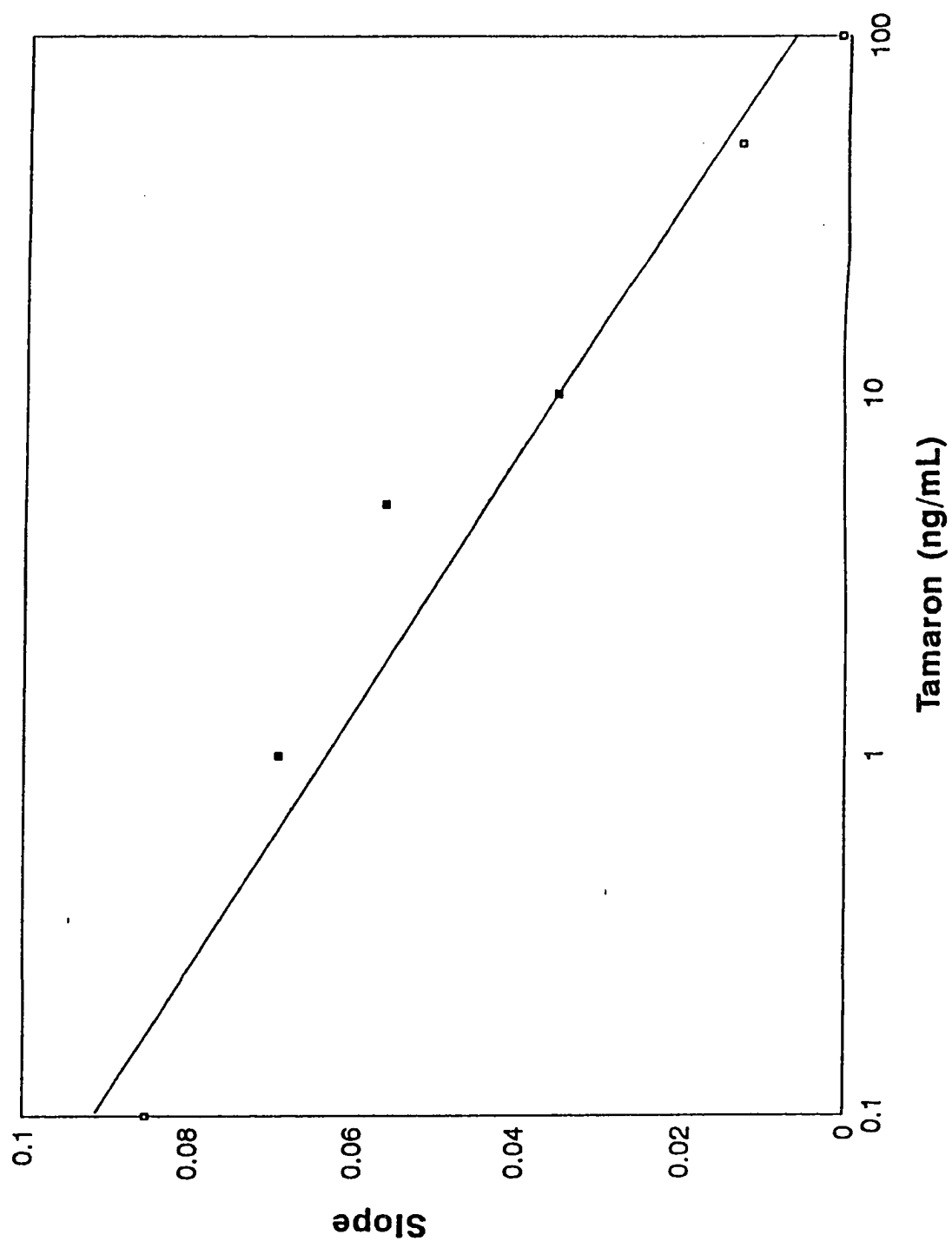
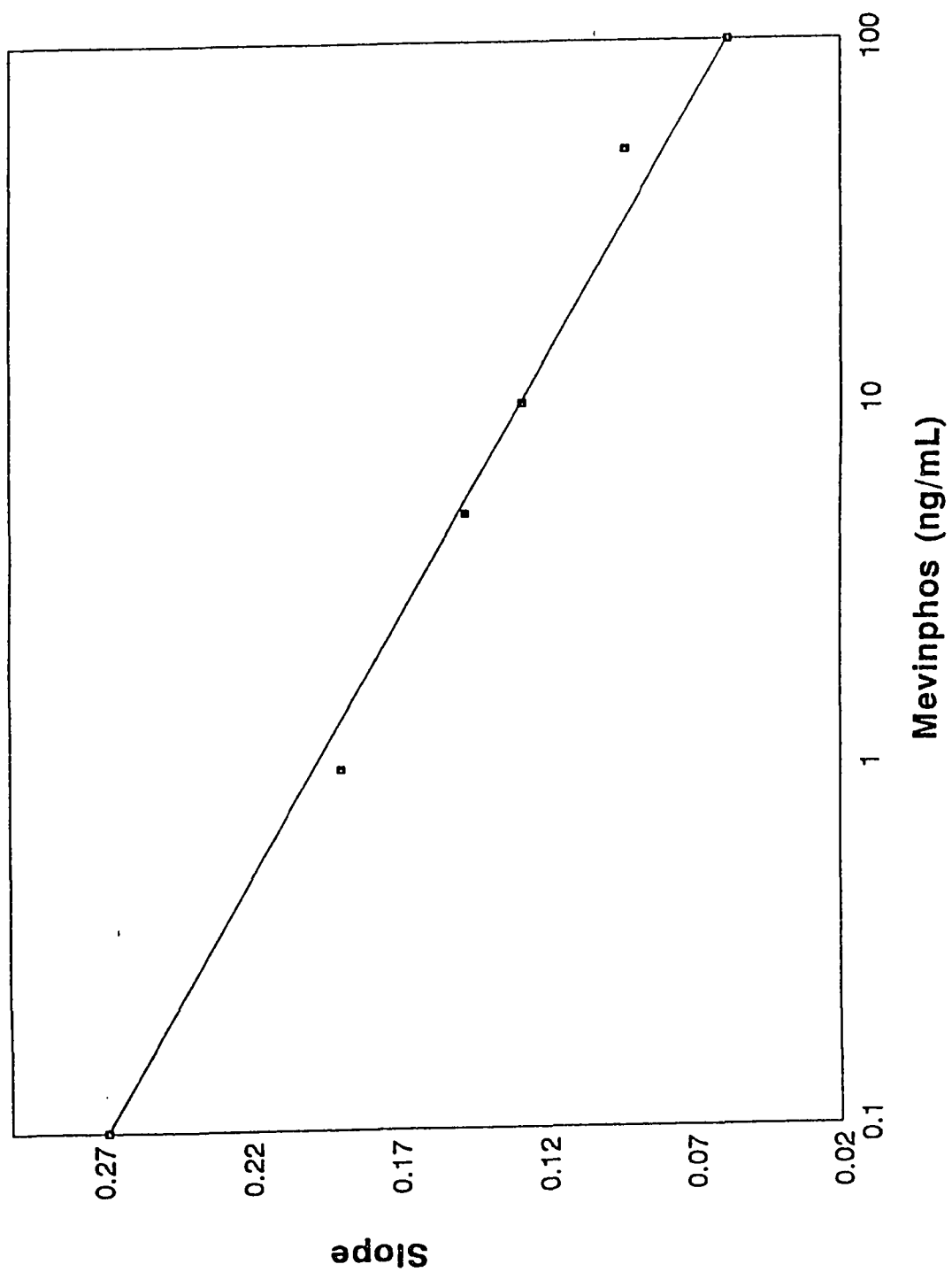


Figure 72

Color developing time study for the mevinphos solid-phase enzyme immunoassay on microtube immobilization. The results of slopes generated from 1, 2, 3, 4 and 5 minutes enzyme-substrate-chromogen reaction were plotted on semi-log scale for 0, 1, 5, 10, 50 and 100 ng/mL analyte concentration used for mevinphos assay. The absorbance was measured at 450 nm.
 $Y=0.205-0.006 \times \log(X)$, $r=-0.973$



F. Study of the performance characteristics

1. Study of limit of detection

The study to determine the limit of detection was performed by the use of a set of OP standards for the generation of the standard curves and twenty four replicates of a blank solution according to the previously established optimal conditions. The data (absorbance at 450 nm) for the blank samples were subjected to statistical analysis, and standard deviations of 0.064, 0.057, 0.036 and 0.069 were calculated for the twenty four replicates of the four blank solutions for malathion, parathion, tamaron and mevinphos, respectively. Following the recommendation of the International Federation of Clinical Chemistry (IFCC), the limits of detection equal $2.6 \times \text{S.D.}$, which are 0.166, 0.148, 0.094 and 0.179 for malathion, parathion, tamaron and mevinphos, respectively. From the standard curves, which were established in the same assays performed with the blank solutions, the limits of detections were calculated to be of 1.28, 0.99, 0.98 and 0.78 ng/mL for malathion, parathion, tamaron and mevinphos, respectively [75, 76].

2. Precision study

The precision study was performed by using two different concentrations of the standard solutions. Intra-assay coefficients of variation were assayed by utilizing 20 replicates of the same sample in a single experiment. The data obtained were then subjected to statistical analysis for the

calculation of the coefficients of variation. For the intra-assay precision study of the malathion assay, coefficients of variation of 18.6% and 16.6% were obtained for 5.0 ng/mL and 100.0 ng/mL, respectively. For the parathion assay, coefficients of variation of 35.7% and 8.8% were obtained for 1.0 ng/mL and 100.0 ng/mL, respectively. The coefficients of variation for 1.0 ng/mL and 100.0 ng/mL were 24.1% and 11.0% , respectively, in the tamaron assay; the coefficients of variation for the mevinphos assay were 34.0% and 5.0% for 1.0 ng/mL and 100.0 ng/mL, respectively. The results for the intra-precision studies are summarized in Table 5.

3. Study of cross reactivity

a. Study of the cross reactivity against other OPs

The assays developed were specific for each type of OP. Since these four types of OP have a high structural similarity to each other, the cross reactivity was determined to demonstrate the specificity of antibodies generated for the different OPs. The reactions were performed by running the other three kinds of OPs as the unknowns (at 100 ng/mL), and the results were compared to the remaining OP which was considered the "standard". All assays were performed under the same previously established optimal conditions. The absorbance readings of the unknowns can then be calculated into concentration according to the standard curve of the "standard OP" . The percentage of the cross reactivity was then calculated by dividing the "standard

Table 5 Precision study of total OP assays

	Malathion	Parathion	Tamaron	Mevinphos
Concentration (ng/mL)	5	1	1	1
n	20	20	20	20
Mean	0.171	0.112	0.137	0.103
Max	0.200	0.218	0.180	0.196
Min	0.138	0.070	0.066	0.060
S.D.	0.032	0.040	0.033	0.035
% C.V.	18.6	35.7	24.1	34.0

	Malathion	Parathion	Tamaron	Mevinphos
Concentration (ng/mL)	100	100	100	100
n	20	20	20	20
Mean	0.253	0.349	0.336	0.440
Max	0.281	0.394	0.417	0.479
Min	0.104	0.291	0.271	0.383
S.D.	0.042	0.031	0.037	0.022
% C. V.	16.6	8.8	11.0	5.0

100 ng/mL" by the calculated concentration for each OP multiplied by 100.

The results, illustrated in Table 6, show that malathion, parathion and mevinphos assays are more sensitive to all OPs with the percentage of the cross reactivity over 100%. Parathion showed the lowest cross reactivity, 5.0%, in the tamaron assay, but malathion and mevinphos had high cross reactivity to the same assay. The cross reactivity was most probably due to the antigen preparation. The antigens prepared for antibody production were similar by the addition of the six-carbon alkyl group as the bridge to conjugate the antigen and the BSA for anti-malathion, anti-tamaron and anti-mevinphos production; however, the antigen prepared for anti-parathion production was different since the modified parathion was directly conjugated to the BSA. The complete reactions were discussed in the antibody production section. Since tamaron is small and polar, the anti-tamaron was not sensitive to parathion but was to malathion and mevinphos.

The results indicated that these four different antibodies cannot distinguish the four different OP by the subtle difference of the structure except parathion to anti-tamaron gamma globulin.

b. Study of the cross reactivity of the metabolite analogues

Four metabolite analogues were chosen which were ethyl propionate (the metabolite of malathion), methyl isobutyrate (the metabolite of mevinphos), p-nitrophenol (the metabolite of parathion) and dimethyl phosphite,

Table 6 Specificity of anti-OP gamma globulin fraction against other OPs

To malathion assay:

Compound	Theoretical concentration (ng/mL)	Experimental concentration (ng/mL) ¹	% Cross reactivity ² Equivalent to malathion
parathion	100	620	100
tamaron	100	620	100
mevinphos	100	380	100

To parathion assay:

Compound	Theoretical concentration (ng/mL)	Experimental concentration (ng/mL) ¹	% Cross reactivity ² Equivalent to parathion
malathion	100	475	100
tamaron	100	3000	100
mevinphos	100	220	100

(Continued)

To tamaron assay:

Compound	Theoretical concentration (ng/mL)	Experimental concentration (ng/mL) ¹	% Cross reactivity ² Equivalent to tamaron
malathion	100	120	100
parathion	100	5	5
mevinphos	100	128	100

To mevinphos assay:

Compound	Theoretical concentration (ng/mL)	Experimental concentration (ng/mL) ¹	% Cross reactivity ² Equivalent to mevinphos
malathion	100	300	100
parathion	100	175	100
tamaron	100	162	100

1. For the absorbance readings obtained 100 ng/mL of organophosphorus compound were calculated to the equivalent concentrations according to the standard curve.
2. The cross reactivity was calculated by the percentage of experimental concentration to the theoretical concentration, 100 ng/mL.

(the metabolite analogue of general organophosphorus pesticides). The metabolites were prepared at 100 ng/mL and subjected to a study of the cross reactivity study according to the previously established optimal conditions. The percentage of the cross reactivity was calculated as the same manner as in the previous section. The cross reactivities of dimethyl phosphite were 12.2%, 3.3%, 3.5% and 150% for malathion, parathion, tamaron and mevinphos, respectively (Table 7). Low cross reactivity was shown with p-Nitrophenol in the parathion and tamaron assays, but it exhibited greater than 20% cross reactivity in the malathion and mevinphos assays. Methyl isobutyrate and ethyl propionate showed very low cross reactivity to the four types of OPs, with a cross reactivity of less than 1%.

G. Study of the validation of the EIA method

1. Water samples

Three kinds of water sources were chosen, deionized water, tap water and river water. The four types of organophosphorus pesticides were added to make the desired concentrations. The water samples were tested directly by EIA, but the samples for GC assay needed extra clean-up and extraction steps.

For GC assay, dichloromethane was used to extract the organophosphorus compounds from the water sources. Since the samples were

Table 7 Specificity of anti-OP gamma globulin fraction against the metabolites

To malathion assay:

Compound	Theoretical concentration (ng/mL)	Experimental concentration (ng/mL) ¹	% Cross reactivity ² Equivalent to malathion
dimethyl phosphite	100	12.2	12.2
p-nitrophenol	100	25.0	25
ethyl propionate	100	7.0E-1	0.7
methyl isobutyrate	100	9.0E-3	0.009

To parathion assay:

Compound	Theoretical concentration (ng/mL)	Experimental concentration (ng/mL) ¹	% Cross reactivity ² Equivalent to parathion
dimethyl phosphite	100	3.3	3.3
p-nitrophenol	100	3.5E-1	0.35
ethyl propionate	100	0.0	0
methyl isobutyrate	100	0.0	0

(Continued)

To tamaron assay:

Compound	Theoretical concentration (ng/mL)	Experimental concentration (ng/mL) ¹	% Cross reactivity ² Equivalent to tamaron
dimethyl phosphite	100	3.5	3.5
p-nitrophenol	100	4.5	4.5
ethyl propionate	100	1.5E-2	0.015
methyl isobutyrate	100	6.0E-3	0.006

To mevinphos assay:

Compound	Theoretical concentration (ng/mL)	Experimental concentration (ng/mL) ¹	% Cross reactivity ² Equivalent to mevinphos
dimethyl phosphite	100	150.0	150
p-nitrophenol	100	29.3	29.3
ethyl propionate	100	3.0E-3	0.003
methyl isobutyrate	100	0.0	0

1. For the absorbance readings obtained 100 ng/mL of metabolite analog was calculated to the equivalent concentrations according to the standard curve.
2. The cross reactivity was calculated by the percentage of experimental concentration to the theoretical concentration, 100 ng/mL.

extracted by dichloromethane, the recovery after the extraction should be considered. The samples with 1.0 $\mu\text{g/mL}$ of the OP were used to perform the percentage of recovery studies. The GC data of the dichloromethane extracted samples were then compared to those of the standard 1.0 $\mu\text{g/mL}$ sample, and the percentages of recovery were calculated.

The recoveries of dichloromethane extraction for malathion were 100%, 6.3% and 21.6% for deionized, tap and river water, respectively. The recoveries of dichloromethane extraction for parathion were 84.8%, 28.3% and 33.5% for deionized, tap and river water, respectively. The recoveries of dichloromethane extraction for tamaron were 11.5%, 29.9% and 6.5% for deionized, tap and river water, respectively. The recoveries of dichloromethane extraction for mevinphos were 28.6, 18.4% and 31.5% for deionized, tap and river water, respectively. The corrected concentrations analyzed by GC were with the percent recovery considered.

The samples which contained the organophosphorus pesticides spiked in the water sources were filtered first to get rid of the undissolved residue, and then assayed by EIA. The total OP concentrations in water samples generated by EIA method were compared to those obtained by GC method. Those data were also subjected to statistical analysis by linear regression, and the results generated are listed in Table 8.

**Table 8 Statistical data obtained for the comparison of
four organophosphorus compounds in water samples**

Deionized water:

OP compound	Intercept	Slope	Correlation Coefficient
malathion	-1.332	1.225	0.987
parathion	0.443	0.927	0.999
tamaron	5.624	0.680	0.951
mevinphos	2.859	0.775	0.981

Tap water:

OP compound	Intercept	Slope	Correlation Coefficient
malathion	1.361	1.109	0.988
parathion	-0.334	1.096	0.999
tamaron	3.792	0.975	0.983
mevinphos	0.755	0.780	0.998

Water from Elizabeth river:

OP compound	Intercept	Slope	Correlation Coefficient
malathion	-0.841	1.173	0.978
parathion	-1.768	0.974	0.969
tamaron	-1.412	1.182	0.912
mevinphos	1.379	1.033	0.994

2. Vegetable samples

Because the enzyme immunoassay is a colormetric measurement, lettuce and spinach were chosen as the sample matrixes to determine if two different concentrations of chlorophyll will interference with the colorimetric assay.

For GC analysis, 40 g of either sample was dissolved in 200 mL acetone before charcoal decolorization. The organophosphorus compounds were added to the charcoal decolorized extracts to make the desired concentrations, and then dichloromethane was used for the extraction, the same extraction procedure as for the water samples.

For the EIA screening, the 20 g vegetables were ground in 100 mL deionized water, and then the residues were filtered. The filtrate was either decolorized by charcoal or used directly as the solvent for the organophosphorus compounds which were added to make the desired concentration for the EIA screening. The results of the samples with or without the charcoal treatment assayed by EIA were compared to determine if there was any color interference.

The total OP concentrations in vegetable samples obtained by EIA method were compared to those obtained by GC method. Those data were also subjected to statistical analysis by linear regression, and the result obtained are listed in Table 9.

Table 9 Statistical data obtained for the comparison of four organophosphorus compounds in vegetable samples

Lettuce (w/o charcoal treatment for EIA):

OP compound	Intercept	Slope	Correlation Coefficient
malathion	-2.268	1.048	0.993
parathion	0.108	0.875	0.963
tamaron	1.582	0.538	0.998
mevinphos	-0.597	0.956	0.994

Lettuce (w/ charcoal treatment for EIA):

OP compound	Intercept	Slope	Correlation Coefficient
malathion	-3.096	0.646	0.963
parathion	3.271	0.780	0.992
tamaron	-1.921	0.653	0.949
mevinphos	0.238	1.089	0.996

(Continued)

Spinach (w/o charcoal treatment for EIA):

OP compound	Intercept	Slope	Correlation Coefficient
malathion	0.692	0.932	0.996
parathion	2.771	0.632	0.999
tamaron	3.323	0.851	0.997
mevinphos	6.453	1.284	0.991

Spinach (w/ charcoal treatment for EIA):

OP compound	Intercept	Slope	Correlation Coefficient
malathion	-0.985	1.284	0.998
parathion	-0.798	0.989	0.983
tamaron	-1.840	0.805	0.990
mevinphos	8.110	1.172	0.965

3. Reproducibility study

The reproducibility of the immunoassay in the detection of OP residues in water and vegetable samples is shown in Table 10. For both types of samples, the reproducibilities with the percent coefficients of variation (%CV) for malathion assay ranged from 31.1 to 5.02. The reproducibilities with the percent coefficients of variation (%CV) for parathion assay ranged from 51.6 to 5.18. The reproducibilities with the percent coefficients of variation (%CV) for tamaron assay ranged from 30.5 to 5.03. The reproducibilities with the percent coefficients of variation (%CV) for mevinphos assay ranged from 14.1 to 1.34. The higher the concentration of the sample the less the percent coefficients of variation was. The %CV of 31.1%, 51.6%, 30.5% for malathion, parathion and tamaron assays, respectively, may at first appear to be high; however, the sample containing 1.0 ng/mL OPs was below or close to the detection limit from the different sample sources.

Table 10 Reproducibility of the OPs immunoassay on OP-fortified water and vegetable samples

Malathion-fortified water samples

concentration (ng/mL)	1	5	10	50	100
n	6	6	6	6	6
% C.V.	31.1	18.9	10.8	5.02	5.55

Malathion-fortified vegetable samples

concentration (ng/mL)	1	5	10	50	100
n	8	8	8	8	8
% C.V.	18.6	7.22	11.0	6.09	6.16

Parathion-fortified water samples

concentration (ng/mL)	1	5	10	50	100
n	6	6	6	6	6
% C.V.	51.6	19.3	27.6	7.89	6.74

Parathion-fortified vegetable samples

concentration (ng/mL)	1	5	10	50	100
n	8	8	8	8	8
% C.V.	22.6	4.72	15.0	4.44	5.18

(Continued)**Tamaron-fortified water samples**

concentration (ng/mL)	1	5	10	50	100
n	6	6	6	6	6
% C.V.	21.4	14.7	11.5	5.43	7.23

Tamaron-fortified water samples

concentration (ng/mL)	1	5	10	50	100
n	8	8	8	8	8
% C.V.	30.5	41.7	12.4	4.02	5.03

Mevinphos-fortified water samples

concentration (ng/mL)	1	5	10	50	100
n	6	6	6	6	6
% C.V.	8.64	4.00	4.94	3.88	1.34

Mevinphos-fortified vegetable samples

concentration (ng/mL)	1	5	10	50	100
n	8	8	8	8	8
% C.V.	14.1	11.8	4.95	4.93	4.17

Chapter IV

DISCUSSION

Pesticide pollution is a major environmental problem. People use more pesticides to increase crop production, but the highly lipophilic pesticide residues such as organochlorine compounds can accumulate in the biota. Organophosphorus compounds (OPs) comprise one of the major classes of pesticides in use today. It is well accepted that the primary site of action of the OPs is at the cholinergic synapse. However, it has been suggested that OPs may have direct neural effects as well. For example, paraoxon, a metabolite of parathion, has severe effects on neurite extension and on tissue culture growth. It also disrupts the normal cell cultures by attacking the cellular proteins [77]. The exposure to OPs can inhibit enzymes or other proteins involved in the maintenance and regulation of the function and the integrity of cell membranes, as manifested by the cellular accumulation of lipids [78]. Many methods have been used for screening organophosphorus compounds in samples. The classical methods for analysis of water for contaminants, additives, or pesticides generally involve the use of techniques such as extraction with organic solvents, purification by column chromatography, and determination by liquid or gas chromatography. The early work of Ercegovich [79] described on the detection of pesticides by immunochemical means and indicated the potential usefulness of this method for routine assays. The use of immunoassays has been routinely

applied in clinical situations for the analysis of proteins, hormones, and drugs in blood and urine samples. The success these immunochemical procedures have achieved in the clinical area can be transferred to the area of pesticide determination in the environmental samples.

Immunochemical analytical methods are generally based on the principle of competition between an analyte and a labelled form of the analyte for a specific receptor, which consists of an antibody synthesized in an animal in response to the injection of a suitable form of the analyte. Thus the steps in immunoassay development involve the selection of the hapten, synthesis and characterization of the hapten, covalent binding of the hapten to carrier molecules such as proteins, immunization, purification and characterization of the antibody, development and optimization of the antibody based assay, development and optimization of the format, application to field samples, and validation [61].

A. Hapten preparation

Most of the OP pesticides are lipophilic, but the coupling reaction to protein is generally performed in aqueous solution, and the antibody production also takes place in an aqueous environment in the animal. Thus, the chemistry which links the hapten to the carrier molecule must be hydrolytically stable for a moderate period of time. There are several possible ways to attach a single

handle of hapten to a carrier protein which depend upon stearic properties plus hydrogen bonding and dipole-dipole interactions [80]. OPs which are highly lipophilic are dissolved in solvent first. Solubility is an important criterion in the selection of the solvent. For OPs, the solvent should be as non-polar as possible and contain no functional groups other than the one chosen for coupling. Dichloromethane is used to extract the OP from the market stocks since it is highly lipophilic. For the lipophilic hapten, very high concentrations of a co-solvent may improve the coupling.

Small molecules alone do not elicit an antibody response. Generally, a molecular weight of 10,000 daltons is required. OPs generally have a molecular weight around 300. Thus, they must be attached to a protein to form a conjugate which is termed the "immunogen". The initial task is to couple the analyte to a suitable carrier protein such as BSA or KLH [81]. Modification of the OP used in this study was performed because these OPs lacked the functional groups for coupling to a carrier protein. Adjustment of the pH can be used to perform this modification. For instance, the ester group can be modified into a carboxyl group for mevinphos and malathion by the change of pH, and the co-solvent environment can provide the conditions necessary for the separation of the reacted OP and from the unreacted OP. Reduction of a specific functional group is used for some antigen modifications. For example,

the nitro group of parathion is reduced into an amine group to promote the coupling.

The analyte, OP, must contain a functional group to permit attachment to a carrier protein [82]. A four to six-carbon bridge is considered optimal [83]. The point of attachment of the bridge to the analyte often has a profound effect on the specificity of the resulting antibody [84]. Structural changes in the vicinity of the bridge are not readily recognized; whereas, those changes occurring at more distant points are easily distinguished. A four to six-carbon chain with a functional group; such as -COOH , -NH_2 or -SH ; which can be covalently linked to the carrier protein, is usually chosen as the bridge. In the OP hapten design in the current study, 1,6-hexadamine was used as the bridge to link the OP to the carrier protein, BSA, for mevinphos and malathion, while adipic acid was used for tamaron .

The functional group of the hapten governs the selection of the method to be used to conjugate the hapten to the carrier directly. Two procedures routinely used for conjugation of carboxyl-containing haptens to proteins are the mixed anhydride procedure [85], shown in Figure 73, and carbodiimide procedure [86, 87], shown in Figure 74. Carbodiimide was chosen here to couple the hapten to the carrier protein in the reaction of modified mevinphos, malathion and tamaron. Haptens containing amine groups can be conjugated by

Figure 73

The mixed-anhydride procedure for conjugation of amine-containing hapten to protein.

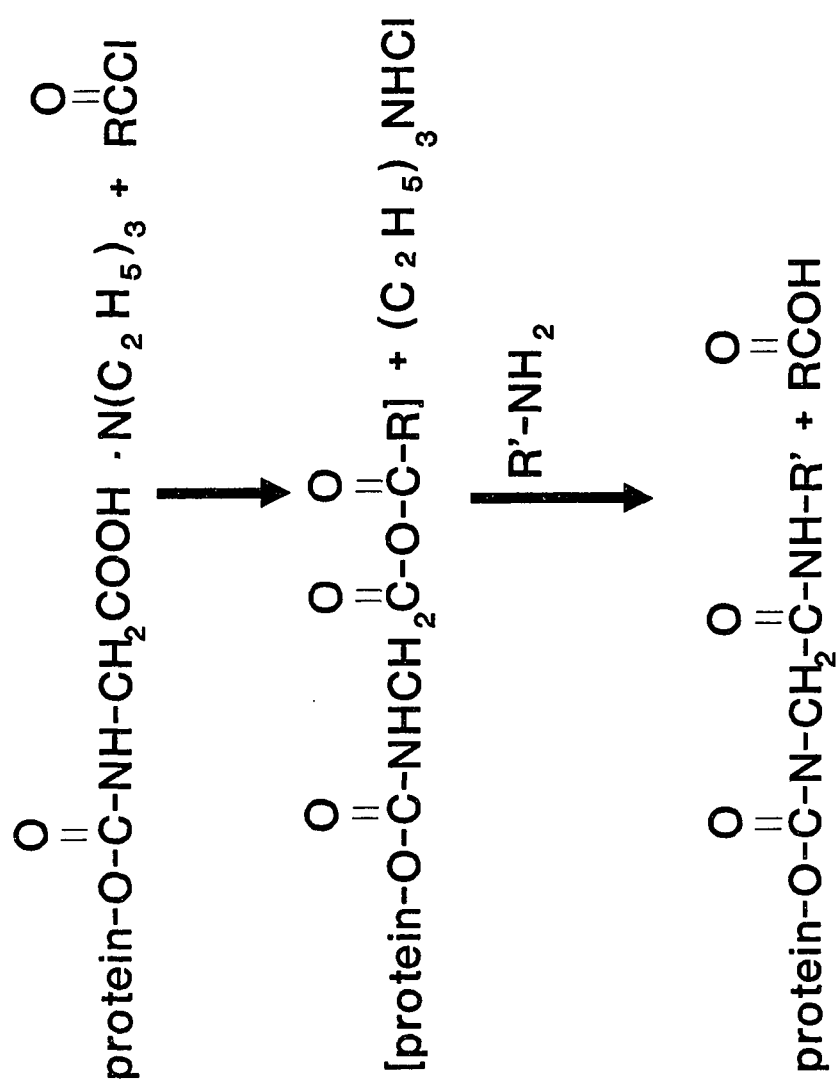
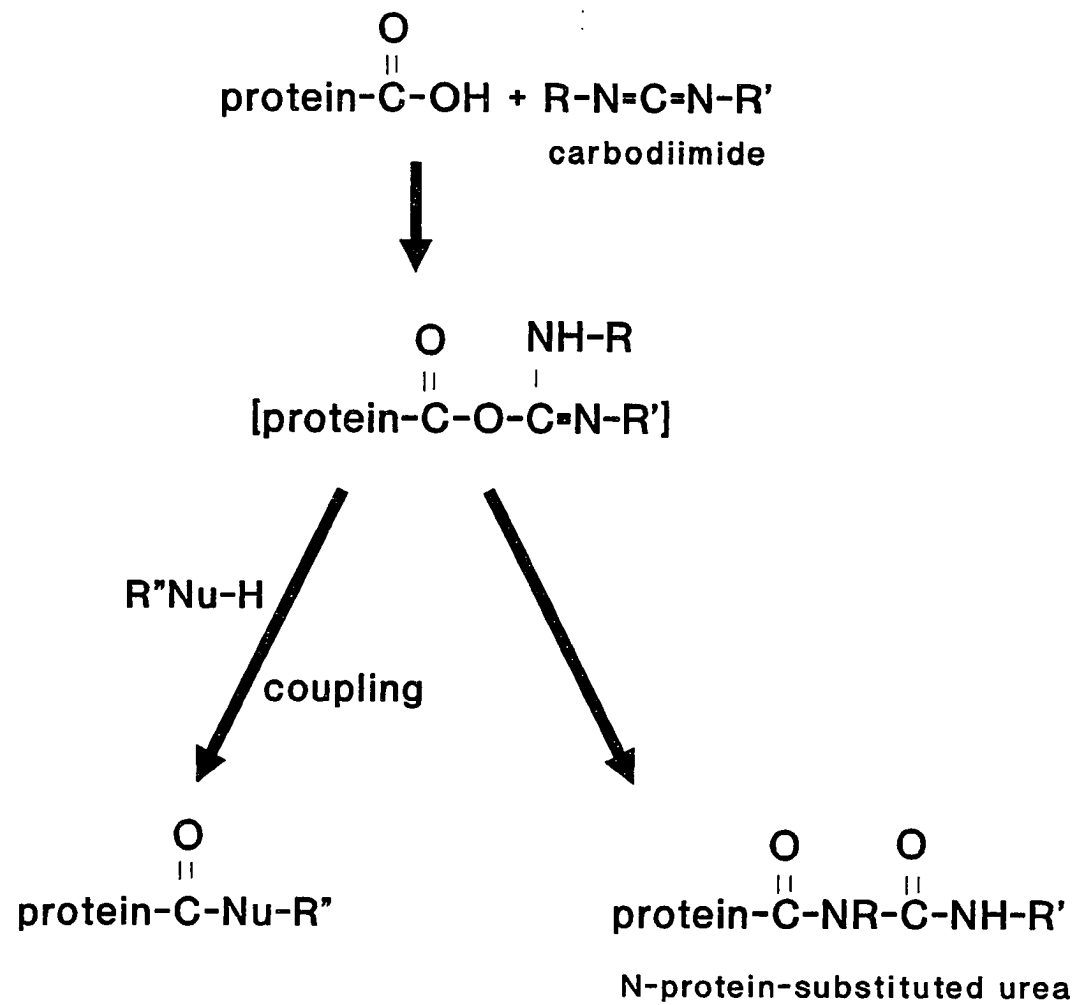


Figure 74

The carbodiimide procedure for conjugation of nucleophilic hapten to protein.



deoxidization [88]. Also the parathion nitro group was first reduced to an amine group and then conjugated to the carrier protein by deoxidization.

Both the competitive and noncompetitive immunoassay formats require either enzyme-labeled hapten or enzyme-labeled antibodies. The carbodiimide coupling procedure can be employed for the conjugation too.

B. Production and purification of antibody

Antiserum is readily obtained by the injection of the immunogen into a common laboratory animal such as rabbit, goat, or mouse. For the production of polyclonal antibody, the rabbit offers the advantages of being easy to care for and producing a moderate amount of serum, often with high titer, and is thus widely used. Monoclonal antibody technology, originated by Kohler and Milstein in 1975 [89], makes it possible to establish cell lines which produce a single desired antibody in vitro. Hybridomas require much more time, labor, and expense to prepare than polyclonal antisera, but each monoclonal antibody is a reagent with a single defined affinity and specificity, and it can be made in unlimited quantities as the hybridoma line can be maintained in culture or stored frozen in liquid N₂. Regardless of whether polyclonal sera or monoclonal antibodies are sought, the antibody response to a given antigen depends on the characteristics of the antigen, the animal's immune system, and the immunization schedule and methods. Protocols for the production of

antisera have been described in detail by Williams and Chase [90] and Hurn and Chantler [91]. For the production of polyclonal antibodies in rabbits, multiple intradermal injections were made along the footpads of the animal. The initial series of injections were followed by the booster injections several weeks later. The rabbit was bled after each boost, and the characteristics of the serum determined. The titer was determined, and it usually produced a higher titer response in the production of polyclonal antibodies than the production of monoclonal antibodies in mouse. The whole antiserum may be preserved by freezing or by lyophilization; the latter method can preserve the antiserum for at least one year.

After the serum was obtained from the rabbit, the serum must be purified, and the gamma globulin extracted before use. The general method to separate IgG from pooled serum is by ion exchange chromatography. The basis of ion exchange chromatography is the electrostatic attraction between oppositely-charged ions, one of which is an electrolyte and the other a synthetic resin polymer. DEAE-cellulose, a weakly basic anion exchange polysaccharide backbone, contains diethylaminoethyl positively charged functional groups associated with small mobile anion counter-ions. The counter-ion can be exchanged reversibly with other ions of the same charge, such as negatively-charged protein molecules, without physically changing the matrix. The electrostatic interactions taking place between the DEAE group of the resin and

the protein are an equilibrium process involving diffusion in the charged exchange site. Diffusion away from the exchange resin takes place upon elution with an appropriate buffer system. The rate of the movement of a given ion down the column is controlled by its ability to ionize and the ionic strength of the elution buffer. The protein ions held by electrostatic attraction on the resin are eluted differentially to yield the desired separation.

Serum proteins are separated electrophoretically into five different fractions. Albumin with the greatest negatively-charged surface migrates most rapidly towards the anode; whereas, the gamma globulin fraction migrates the least. It has been reported that the gamma globulin fraction could be obtained by using DEAE-cellulose with 0.01 M sodium phosphate buffer, pH 7.5, containing 0.015 M sodium chloride as the elution buffer system [68]. However, a simpler procedure which also had a better yield, utilized 5.0 mM sodium phosphate buffer, pH 6.5, as the buffer system for the elution of the gamma globulin fraction from the DEAE-cellulose ion-exchange column. By selecting a column buffer with the appropriate pH and ionic strength, the majority of the serum proteins from the whole anti-serum are bound to the DEAE-cellulose exchange column with the desired gamma-globulin fraction eluted straight from the column. The best eluent for the chromatographic separation of IgG from the antisera on DEAE-cellulose was found to be 5.0 mM sodium phosphate buffer, pH 6.5 [92]. The eluent fraction after

concentration was easily detected by electrophoresis, and the yield was calculated as percent of gamma globulin fraction present in the sample.

C. Immunoassay

There are several reported immunoassay for pesticides, some of which utilize radioimmunoassay techniques [93, 94]. Berson and Yalow developed radioimmunoassay, a powerful tool in clinical analytical chemistry [95]. Although RIA is a sensitive and precise analytical method, it has several disadvantages. Radiolabeling procedures, such as iodination, can sometimes produce molecular disruptions resulting in unstable compounds, which have a limited shelf life because of the isotope decay, and sometimes require extended counting times for accurate quantification. Rapid isotope decay, medical hazards and the requirement of expensive equipment led to the introduction of enzyme immunoassay. In 1971, enzyme immunoassay (EIA) was introduced independently by two research groups [96, 97]. In EIA, an analyte, an antibody to the analyte, or a nonspecific antibody is covalently linked to an enzyme and is used in some form of the specific binding reaction to measure the analyte concentration in a sample. The EIA relies on antibody binding for specificity and on the enzyme label for sensitivity through amplification. There are two general EIA methods used: one is homogeneous enzyme immunoassay and the other one is heterogenous enzyme immunoassay. The homogeneous

enzyme immunoassays include competitive enzyme immunoassay and non-competitive enzyme immunoassay. These two differ by which compound the enzyme is conjugated. The enzyme is conjugated to a hapten in the former assay and to the second antibody in the latter assay. In this research project, the competitive enzyme immunoassay was adopted. The basis of the competitive enzyme immunoassay for measurement of the analyte is the competition of the analyte and the conjugated hapten for the binding of the specific antibody to, based on the structural similarity between the analyte and the conjugated hapten. The interaction of the antibody with the hapten is used to either inhibit or enhance the enzymatic activity. The assay is performed with the test sample mixed with the enzyme-hapten conjugate and the specific anti-hapten antibody. If analyte is present in the sample, it competes with the labeled hapten for the limited number of antibody binding sites. Enzymatic activity can be correlated with the concentration of the analyte (unlabeled hapten).

Once the antibody against the OPs is obtained, it can be used in a variety of formats which can result in rapid, sensitive field procedures as well as highly-quantitative laboratory procedures. Each format has unique advantages in terms of speed, cost, sensitivity and other factors. All the formats used for pesticide analysis share three components: specific antibody, conjugated hapten, and target analyte. A number of analytical techniques can be used in the assay

detection system, including radioactivity, turbidity, polarization of light, visible or ultraviolet absorbance, fluorescence, phosphorescence, chemiluminescence, bioluminescence or electron spin resonance.

The first step for the immunoassay is to bind the desired antibody to the solid surface, which is polystyrene, in the general immunoassay formats. The adsorption of a bio-molecule to a polystyrene surface is due to intramolecular attraction (Van der Waals forces), to be distinguished from the other chemical bonds, such as covalent bonds and ionic bonds. The intramolecular attraction is based on the intramolecular electric polarities of which two types can be distinguished: alternating polarities and stationary polarities, dipoles.

Alternating polarities are developed when the molecules approach each other, thereby creating disturbances in each other's electron clouds. This causes synchronously alternating polarities in the molecules. That alternating polarities mediate binding is a common substance property, which is obviously stronger in larger molecules. Stationary polarities are developed while the molecules bind to each other simply by bedding dipole against dipole. The difference between these two polarities is that the attraction is inversely proportional to the seventh power of the distance for the alternating polarities; whereas, stationary polarity attraction is inversely proportional to only the second power of the distance [98, 99]. Hence the former one has weaker influence than the latter one. In general, ionic and covalent bonds are about 100 times stronger than the

Van der Waals force. However, among stationary polarity mediated bonds, the hydrogen bond takes up an exceptional position because it is up to 10 times stronger than the others due to the unique properties of water for specific biomolecules. Hydrogen bonds are also called hydrophilic bonds, as opposed to alternating polarity mediated bonds, which are called hydrophobic bonds. The alternating polarity mediated attraction is also called hydrophobic interaction.

Polystyrene is a common solid-phased support in ELISA as well as in many radioimmunoassays. In 1967, Catt and Tregear reported the adsorption of antibody to polymeric surfaces and developed a new method of solid-phase radioimmunoassay [100]. Cantarero reported the amount of protein binding varied for different proteins at a given input concentration and under constant conditions of time and temperature [93]. The maximum proportion of proteins absorbed did not correlate with the net charge of the protein at the adsorption pH. It was suggested that the adsorption of proteins to a surface such as polystyrene occurred through hydrophobic bonds and that charge played a minor role. A low concentration of antigen may not be detected if the concentration of antibody used for coating the microwells is either too high or too low. It is important, therefore, to find the optimal antibody concentration for microwell coating [101]. The optimal concentrations of purified gamma globulins from anti-malathion, anti-parathion, anti-tamaron and anti-mevinphos sera for the microwell coating were found to be 50 ng/mL, 500 ng/mL, 500

ng/mL and 50 ng/mL, respectively. The results from the immunoassay in microwells did not show a good response due to the smaller capacity of the microwells. A high ratio of analyte to the conjugated hapten is required by the huge size difference between enzyme-conjugated hapten and the OP analyte with molecular weights around 60,000 and 300, respectively. The microwells cannot provide sufficient capacity for the higher quantity of analyte competing with the conjugated hapten. The surface area of the microtube is 3.35 cm^2 and for microwell is 1.52 cm^2 . Microtubes provide 2.2 times the surface area for antibody binding than microwells; therefore, microtubes can provide a larger capacity for analyte and conjugated hapten to compete.

The ionic strength affects the OP assay. Most of the OPs are hydrophobic which provide less ionic strength and may have stronger reaction in low ionic strength condition. The results of the assay solution studies, shown in Figures 57-60, suggested a high concentration of salt increased the ionic strength in the assay condition and decreased the resolution of the OP assays. Enzymes tend to be denatured in extreme pH conditions; thus all the enzyme reactions are performed in a buffer. Deionized water was used in the OP assays; however, the diluted enzymes, organophosphorus-peroxidase (OP-HRPO), used was primarily stored in 50 mM PBS. Thus the reactions were actually performed in 20 μM , 33 μM , 20 μM and 100 μM PBS, pH 7.4,

condition for malathion, parathion, tamaron and mevinphos assays. That necessitated that the pH condition be investigated.

The lability of the protein structure makes it imperative that the pH be kept within certain limits and that the denaturing effects be avoided. The proteins, OP-HRPO or antibodies, are denatured at extreme pH conditions. Since deionized water gave the greatest absorbance change in the OP assays and the EIA screening was primarily designed for the environmental samples, which had various pH values, the optimal pH condition needed to be investigated. The structure of the protein may change and then interfere with the reaction. The results shown in Figures 61-64 explain the postulation that the pH is very important to the assay reaction, thus the pH of the samples needed to be adjusted to neutral before assay.

The structure of antigen governs the specificity of antibody produced. The high similarity of the antigens gives less diversity of the antibodies produced. The structures of the OPs are very similar; the only difference is on the side chain, the leaving group. Thus the cross reactivity of OPs would be proposed high. Table 6 shows that there is high cross reactivity between each. It demonstrates that the polyclonal antibody in the present preparation is not a specific antibody against the particular antigen, but that gives a good response to the whole OP family. This characteristic may provide a general method to screen the OPs in water or other sample sources.

Most OPs decompose rapidly in the environment. The half-life for the OPs in the environment is very short, around one to two weeks. OPs, the parent compounds, decompose into phosphite, and the side chain dissociates. Dimethyl phosphite, the major metabolite for the OPs, gives some cross reactivity since it is the main structure of the OP family. Nitrophenol, a metabolite of parathion, has some cross reactivity in screening for malathion and mevinphos. The reason may be due to the structural similarity to tyrosine, which is contained in most proteins, as in the carrier protein. Ethyl propionate and methyl isobutyrate, the metabolites of mevinphos and malathion, show no cross reactivity with the four OP assays. It proves that the antibody produced is targeted to the phosphite group not to the side chain. But because of the polyclonal characteristic, some of the antibody in the antibody serum conduct the specificity to the carrier protein; hence this may be the cause of the cross reactivity of p-nitrophenol.

The immunoassay showed a linear relationship between 0 to 100 ng/mL for all four OP assays which was observed between the logarithm of the OP concentration and the readings of the absorbance at 450 nm. The detection limit is much lower than the GC assay which is in ppm ($\mu\text{g/mL}$) range [49, 102, 103].

The precision of these immunoassay in the detection of OP residues is shown on Table 5. The percent coefficients of variation (%CV) ranged from

35.7% to 24.1% for parathion, tamaron and mevinphos at the concentration of 1.0 ng/mL; 18.6% for malathion at the concentration of 5 ng/mL, and 16.6% to 5.0% for malathion, parathion, tamaron and mevinphos at the concentration of 100 ng/mL. Better precisions, i.e. smaller CVs, were obtained at higher concentrations.

D. Sample preparation and analysis

Samples from the different sources for the general pesticide assays need to be cleaned in advance. Several methods were used to clean up the samples from soil, water, vegetable extracts, food and crops. The trace analytical process consists of a series of discrete steps, or unit processes. The processes generally for gas or liquid chromatography analysis include extraction, cleanup, modification, resolution, detection and measurement. The extraction removes the analyte from the matrix bulk; generally by mixing, grinding, or blending the sample with an extracting solvent. The cleanup step removes the extractable matrix components by some operations, such as liquid-liquid partitioning, column chromatography, Sep-pak C₁₈ cartridges solid-phase extraction [103], or forced volatilization. Modification is the optional step to convert the analyte to a derivative that is more amenable to detection and measurement than the parent analyte. Resolution separates the analyte, or analyte cluster, from potential interferences that survive cleanup, usually by gas

or high performance liquid chromatography. Detection usually obtains a response related to the amount of analyte present, such as an absorbance in spectrophotometry or peak in chromatography. Measurement is the last step which relates the response to the known standard, most commonly from an external standard of the pure analyte. For the pesticide assay, the pesticides generally have low to intermediate polarity. Mills in 1959 suggested a general procedure for pesticide assays which is to use an organic solvent extraction, petroleum ether-acetonitrile partitioning to remove lipids from fatty substances, and column chromatography with selective detection for quantification with the use of an external standard of the pesticide. This procedure has been used to analyze approximately 200 pesticides and their transformation products in a variety of foodstuff [104]. Although there is a lot of successful evidence in the GC or HPLC for pesticide analysis, there are still some drawbacks, such as high labor intensity.

Immunoassay is the easiest assay method for environmental assay. It was hypothesized that the natural constituents of samples would not interfere with the binding of an analyte to a specific antibody and that clean-up procedures need not be more rigorous than those used for conventional analyses. Immunoassay is particularly attractive because it can impact directly on all the steps in trace analysis. Antibodies can be used to extract analyte from the sample matrix thus potentially improving the recovery of the bound

residues. Less cleanup may be needed because of the specificity of the antibody-based determination, resulting in considerable time savings.

Chromatographic resolution may be bypassed for the same reason, lowering the instrumentation requirements.

The validation of EIA screening on water samples was performed. For the tap water and river water, longer time for the color to develop than for deionized water was observed. It is computed as the metal or salt concentration of these two sample sources interfering with the enzyme reaction or the antigen binding with the immobilized antibody; therefore, a mixed-ion resin deionization method was recommended for tap and river water to remove the excess ions before filter. A blank, the water with no OP present, must be run with each set of tests since it is used to determine the background value as the "stop indicator" (when the color has developed to an intense blue) for the color developing reaction. This may give a rough estimation of the result calculated because the result of the blank one obtained from test group may not be exactly the same as was obtained from the standard group. The validation study of the developed EIA compared to the GC assay on the water samples showed that the EIA screening was poorer corresponding to the standard than that of the GC assay, but the r (product-moment correlation coefficient) is close to 1 in most of the EIA screening on different water sources. The same results were shown on the vegetable assays. Lettuce and spinach were chosen for their different levels

of chlorophyll content. There was no significant difference with or without charcoal. Thus the vegetable matter does not interfere with the antibody-antigen reaction of the samples. The chlorophyll and/or other contents of the vegetable give little or no interferences in the reaction. Although the EIA screening results were poorer than GC analysis, the possibility of EIA as a screening test for the GC analysis is still feasible.

Immunoassay provides great potential in environmental analysis. The principal advantage over conventional approaches is that of cost-effectiveness, which stems from the inherent simplicity of the manipulations involved in the procedure. Once the antiserum has been developed, the remainder of the analytical process may be readily automated. Immunoassay does not possess the specificity that GC or LC provides, and the presence of an interferant in an unknown sample may not be detected. Thus, the immunoassay may be assigned a screening role in processing large numbers of samples, with confirmation of a statistically selected number of results by an established method.

List of References

1. Lauger, P., Martin, H., and Müller, P. Determination of DDT-DDT in the tissues, body fluids and excretion of the rabbit following oral administration. **Helv. Chim. Acta.** (1944) 27: 892.
2. Narahashi, T. Neuroactive agents and nerve membrane conductances. **Residue Rev.** (1969) 25: 275.
3. Gilman, A. P., Hallett, D. J., Fox, G. A., Allen, L. J. and Peakall, D. B. Effects of injected organochlorines on naturally incubated herring gull eggs. **Sci. Am.** (1978) 222: 72.
4. Matsumura, F. ed. **Toxicity of insecticides.** (1975) Plenum Press, New York.
5. Casida, J. E. Mode of action of carbamates. **Annul. Rev. Entomol.** (1963) 8: 39.
6. O'Brien, R. D. ed. **Insecticides, Action and Metabolism.** (1967) Academic Press, Inc., New York.
7. Aldridge, W. N. and Johnson, M. K. Side Effects of Organophosphorus Compounds: Delayed Neurotoxicity. **Bull. WHO** (1971) 44: 259.
8. O'Brien, R. D. ed. **Insecticides, Action and Metabolism.** (1960) Academic Press, Inc., New York.
9. O'Brien, R. D. Reaction of carbamates with acetylcholinesterase. **Ann. N. Y. Acad. Sci.** (1969) 160:204.
10. Saunders, B. C. ed. **Some Aspects of the Chemistry and Toxic Action of Organic Compounds Containing Phosphorus and Fluorine.** (1957) Cambridge Press, London.
11. Shrader, G. ed. **Die Entwicklung neuer Insektizide auf Grundlage organischer Fluor- und Phosphor-Verbindungen.** (1952) Monographie Nr. 62 zu Angewandte Chemie und Chemie- Ingenieur-Technik, Verlag Chemie, Weinheim.
12. Shrader, G., **German Patent 720577** (1942).

13. Schrader, G. ed. **Die Entwicklung neuer insektizider phosphorsäure-Ester** (1963) Verlag Chemie, Weinheim.
14. Schrader G. Zur Kenntnis neuer, wenig toxischer Insektizide auf der Basis von Phosphorestern. **Angew. Chem.** (1961) 73: 331.
15. Nishizawa, Y. New low toxic organophosphorus insecticide. **Bull. Agric. Chem. Soc. Jap.** (1960) 24: 744.
16. Harley, J. B., Grinspan, S., and Root, R. K. Paraquat suicide in a young woman: results of therapy directed against the superoxide radical, **Yale J. Biol. Med.** (1977) 50: 481.
17. Adrian, E. D., Feldberg, W., and Kilby, B. A. The cholinesterase inhibitory action of fluorophosphates. **Br. J. Pharmacol.** (1947) 2: 56.
18. Balls, A. K., and Jensen, E. F. Stoichiometric inhibition of chymotrypsin. **Adv. Enzymol.** (1952) 13: 321.
19. Metcalf, R. L., March, R. B., and Maxon, M. G. Substrate preferences of insect cholinesterases. **Ann., Entomol. Soc. Am.** (1955) 48: 222.
20. Wilson, I. B., and Bergmann, F. Studies on cholinesterase: VII The active surface of acetylcholinesterase derived from effects of pH on inhibitors. **J. Biol. Chem.** (1950) 185: 479.
21. Cunningham, L. W. Proposed mechanism of action of hydrolytic enzymes. **Science** (1957) 125: 1145.
22. Krupka, R. M. Chemical structure and function of the active center of acetylcholinesterase. **Biochem.** (1966) 5: 1988.
23. O'Brien, R. D. ed. **Toxic phosphorus esters: chemistry, metabolism and biological effects.** (1967) Academic Press, Inc., New York.
24. O'Brien, R. D. and Wilkinson, C. F. ed. **Insecticide chemistry and physiology.** (1976) Plenum Press, New York.
25. Hobbiger, F.: Reactivation of Phosphorylated acetylcholinesterase. In Koelle, G. B. ed. **Handbuch der Experimentellen Pharmakologie, XV.** (1963) Springer-Verlag, Berlin.

26. O'Brien, R. D. ed. **Toxic phosphorus esters.** (1960) Academic Press, New York.
27. Fukuto, T. R., and Metcalf, R. L. Structures and insecticidal activity of some diethyl substituted phenyl phosphates. **J. Agr. Food Chem.** (1965) 4: 930.
28. Damastra, T. Environmental chemicals and nervous system dysfunction. **Yale J. Biol. Med.** (1978) 51:457.
29. Metcalf, R. L., Francis, B., Metcalf, R. A., and Hanssen, L. Acute and delayed neurotoxicity of leptophos analogs. **Pestic. Biochem. Physiol.** (1983) 21: 57.
30. Davies, D. B. and Holub, B. J. Comparative effects of organophosphorus insecticides on the activities of acetylcholinesterase, diacylglycerol kinase, and phosphatidylinositol phosphodiesterase in rat brain microsomes. **Pestic. Biochem. Physiol.** (1983) 267: 281.
31. Johnson, M. K. The primary biochemical lesion leading to the delayed neurotoxic effects of some organophosphorus esters. **J. Neurochem.** (1974) 23: 785.
32. Abou-Donia, M. B., Patton, S. E., and Lapadula, D. M., in **Cellular and Molecular Neurotoxicity.** Narahashi, T. (ed.), (1984) Raven Press, New York.
33. Chow, E., Seiber, J. N., and McGillem, C. D., in **Spectral analysis : Prediction and extrapolation. CRC Critical Review in Bioengineering** (1986) 6:133.
34. Sennayake, N. and Karalliedde, L. Neurotoxic responses of organophosphorus insecticides. An intermediate syndrome, **N. Engl. J. Med.** (1987) 45:60.
35. Wecker, L., Kiauta, T., and Dettbarn, W. D. Relationship between acetylcholinesterase inhibition and the development of a myopathy. **J. Pharmacol. Exp. Ther.** (1978) 206:97.

36. Tular, S. M., **In Vivo and In Vitro Neurotoxic Effects of Organophosphate Exposure.** (1988) Ph. D. dissertation of the University of Georgia.
37. Luttgen, P. J. An outline of neurotransmitters and neurotransmission, part II. **J. Amer. Anim. Hosp. Assoc.** (1987) 23:663.
38. Giang, P. A., and Hall, S. A. Enzymatic determination of organic phosphorus insecticides. **Anal. Chem.** (1951) 23: 1830.
39. Holman, W. I. H. A new technique for determination of phosphorus by molybdenum blue method. **Biochem. J.** (1943) 87: 256.
40. Averell, P. R., and Norris, M. V. Estimation of small amounts of O, O-diethyl O,p-nitrophenyl thiophosphates. **Anal. Chem.** (1948) 20: 753.
41. Muir, D. C. G. and Solomon, J. Extraction and cleanup of fish, sediment and water for determination of triaryl phosphates by gas-liquid chromatography. **J. Ass. Off. Anal. Chem.** (1981) 64:79.
42. Suzuki, O., Hattori, and Asano, M., Z. Detection of malathion in a victim by gas chromatography/negative ion chemical ionization mass spectrometry. **Rechtsmed.** (1985) 94: 137.
43. Bardalaye, P. C. and Wheeler, W. B. Facile gas chromatographic method for the determination of residues of Bieldrin in pecan. **J. Chromatogr.** (1986) 369: 231.
44. Hattori, H., Suzuki, O. and Asano, M. Usefulness of gas chromatography/negative ion chemical ionization mass spectrometry for detection of an organophosphate pesticides in a victim. **Med. Sci. Law.** (1986) 26:263.
45. Bushway, R. J. High-performance liquid chromatographic determination of trace quantities of azinphos methyl and aziphos methyl oxon in various water sources by direct injection and trace enrichment. **J. Liquid Chromatogr.** (1982) 5: 49.
46. **Test Methods for Evaluation Solid Waste, Physical/Chemical Methods, SW846.** U.S. Government Printing Office, Washington, DC.

47. Liu, J.; Suzuki, O. Kumazawa, T. and Seno, H. Rapid isolation with Sep-Pak C₁₈ cartridges and wide-bore capillary gas chromatography of organophosphate pesticides. **Forensic Sci. Int.** (1989) 41: 67.
48. Omura, M, Hashimoto, K., Ohta, K., Ijo, J., Veda, S., Ando, K., Hiraide, H. and Kinae, N. Gas chromatography-electron capture detection method for determination of 29 organophosphorus pesticides in drinking water. **J. Assoc. Off. Anal. Chem.** (1990) 73: 276.
49. Prisloo, S. M. and De Beer, P. R. Gas chromatographic relative retention data for pesticides on nine packed columns:II. organophosphorus and organochlorine pesticides, using electron-capture detection. **J. Assoc. Off. Anal. Chem.** (1987) 70: 878.
50. Bowman, M. C. and Beroza, M. Gas chromatographic detector for simultaneous sensing of phosphorus- and sulfur- containing compounds by flame photometry. **Anal. Chem.** (1968) 10: 1448.
51. St. John, L. E. and Lisk, D. J. Determination of hydrolytic metabolites of organophosphorus insecticides in cow urine using an improved thermionic detector. **J. Agr. Food Chem.** (1968) 16: 48.
52. St. John, L. E. and Lisk, D. J. Rapid, sensitive residue determination of organophosphorus insecticides by alkali thermionic gas chromatography of their methylated alkyl phosphate hydrolytic products. **J. Agr. Food Chem.** (1968) 16: 408.
53. Bache, C. A., Lisk, D. J. Determination of organophosphorus insecticide residues using the emission spectrometric detector. **Anal. Chem.** (1965) 37: 1477.
54. Schomburg, C. J., Glotfelty, D. E. and Seiber, J. N. Pesticide occurrence and distribution in Monterey, California. **Environ. Sci. Technol.** (1991) 25: 155.
55. Watts, R. R. Chromogenic spray reagents for the organophosphate pesticides. **Residue Rev.** (1967) 18: 105.
56. Sherma, J. Chromatographic analysis of fungicides. **J. Chromatogr.** (1975) 113: 97.

57. Yuan, J. H., Lai, M. L., Lee, Y. C., Yang, J. T., Wen, K. L., and Hsieh, S. L. **A screening method for determining pesticide residues in vegetable.** (1989) Technical Report, Taipei Inst. Pathol.
58. Mendoza, C. E. Analysis of pesticides by the thin-layer chromatographic-enzyme inhibition technique. **Residue Rev.** (1974) 50: 43.
59. MacNeil, J. D., and Frei, R. W. **Analysis of Pesticide Residues.** Moye, H. A. ed. (1981) John Wiley, New York.
60. Newsome, W. H. Potential and advantages of immunochemical methods for analysis of foods. **J. Assoc. Off. Anal. Chem.** (1986) 69:919.
61. Jung, F., Gee, S. J., Harrison, L., Li, Q. and Hammock, B. D. Use of immunochemical techniques for the analysis of pesticides. **Pestic. Sci.** (1989) 26: 303.
62. Van Emon, J. M., Seiber, J. N. and Hammock, B. D., **Analytical Methods for Pesticides and Plant Growth Regulators: Advanced Analytical Techniques, Vol. XVII.** Sherma, J. ed. (1989) Academic Press, New York.
63. Bushway, R. J., Perkins, B., Savage, S. A., Lekousi, S. J. and Ferguson, B. S. Determination of atrazine residues in water and soil by enzyme immunoassay. **Bull. Environ. Contam. Toxicol.** (1988) 40: 647.
64. Eto, M., **Organophosphorus Pesticides: Organic and Biological Chemistry.** (1974) CRC Press, Cleveland.
65. Bellet, E. M., and Mendel B. Bicyclic phosphorus esters: High toxicity without cholinesterase inhibition. **Science** (1973) 182: 1135.
66. Myers, D. K., and Mendel, B. Investigations on the use of eserine for the differentiation of mammalian esterases. **Proc. Soc. Exp. Biol. Med.** (1949) 71: 357.
67. Brimfield, A. A., Hunter, K. W., Lenz, D. E., Benschop, H. P., Van Dijk, C., and De Jong, L. P. A. Structural and stereochemical specificity of mouse monoclonal antibodies to the organophosphorus cholinesterase inhibitor soman. **Molecular Pharmacol.** (1985) 28: 32.

68. Stanworth, D. R. A rapid method of preparing pure serum gamma-globulin. **Nature (London)** (1960) 188: 156.
69. Gebott, M. D. ed. **Beckman Microzone[®] Manual**. (1977) Beckman Instruments, Inc., Fullerton, CA.
70. Fiske, C. H., and Subbarow, Y. The colorimetric determination of phosphorus. **J. Biol. Chem.** (1925) 66: 375.
71. Damm, H. C., Besch, P. K., and Goldwin, A. J. **The Handbook of Biochem. Biophysics**. (1965) CRC Press, Cleveland.
72. Nisonoff, A. Conjugated and synthetic antigens:coupling of diazonium compounds to proteins. **Methods Immunol. Immunochem.** (1967) 120.
73. Sternberger, L. A., Cuculis, J. J., Meyer, H.E., Lenz, D., E. and Hinton, D. M. A vaccine against organophosphorus poisoning. **Army Science Conference Proceedings, Vol 3**. (1972) Office of Chief of Research and Development, Department of Army, Washington, DC 20310.
74. Napkane, P. K. and Pterre, G. B. Enzyme-labelled antibodies for the light and electron microscopic localization of tissue antigens. **J. Cell Biol.** (1967) 33: 307.
75. **International Federation of Clinical Chemistry**. **Clinical Chemica Acta**. (1979) 59: 337-346.
76. **International Federation of Clinical Chemistry**. **Clinical Chemica Acta**. (1979) 98: 145F-162F.
77. Strickland, R., Hardin, E. K., Shanon, L. M. and Horwitz, J. Peroxidase isoenzymes from horseradish roots. **J. Biol. Chem.** (1968) 243: 3560.
78. Kant, G. T., Kenion, C. C. and Meyerhoff, J. C. Effects of diisopropyl fluorophosphate (DFP) and other cholinergic agents on release of endogenous dopamine from rat brain striatum in vitro. **Biochem. Pharmacol.** (1984) 33: 1823.
79. Ercegovich, C. D. Analysis of pesticide residues-immunological techniques. **Adv. Chem. Ser.** (1971) 104: 162.

80. Nisonoff, A. ed. **Introduction to Molecular Immunology**. (1984) Sinauer Associates Inc., Sunderland.
81. Landsteiner, K. **The Specificity of Serological Reactions**. (1945) Harvard University Press, Cambridge, Massachusetts.
82. Newsome, W. H. Potential and advantages of immunochemical methods for analysis of foods. **J. Assoc. Off. Anal. Chem.** (1986) 69: 6.
83. Bermudez, J. A., Coronado, V., Mijares, A., Leon, C., Velazquez, A., Noble, P. and Mateos, J. L. Stereochemical approach to increase the specificity of steroid antibodies. **J. Steroid Biochem.** (1975) 6: 283.
84. Pratt, J., Solid immunoassay in clinical chemistry. **J. Clin. Chem.** (1978) 24: 1869.
85. Vaughan, J. R. and Osato, R. L. Preparation of peptides using mixed carboxylic acid anhydrides. **J. Am. Chem. Soc.** (1951) 73: 5553.
86. Goodfriend, T. L., Levine, L. and Fasman, G. D. Antibodies to bradykinin and angiotensin: A use of carbodiimides in Immunology. **Science (Washington)**. (1964) 144: 1344.
87. Kurzer, F. and Zadeh, K. D. Advances in the chemistry of carbodiimides. **Chem. Rev.** (1967) 67: 107.
88. Gee, S. J., Miyamoto, T., Goodrow, M. H., Buster, D. and Hammock, B. D. Development of an enzyme-linked immunosorbent assay for the analysis of the thiocarbamate herbicide molinate. **J. Agric. Food Chem.** (1988) 36: 863.
89. Kohler, G. and Milstein, C. Continuous cultures of fused cells secreting antibody of predefined specificity. **Nature (London)**. (1975) 256: 495.
90. Williams, C. A. and Chase, W. M. **Methods in Immunology and Immunochemistry**", vol. 1. Williams C. A. and W. M. Chase (eds). (1967) Academic Press, New York, New York.
91. Hurn, B. A. L. and Chantler, S. M. **Methods in Enzymology**. vol: 70. H. Van Vunakis and J. J. Langone (Eds). (1980) Academic Press, New York, New York.

92. Heftmann, E. **Chromatography (A Laboratory Handbook of chromatographic and Electrophrenic Methods.** (1975) Van Nastrand Reinhold, New York, New York.
93. Cantarero, L. A., Bulter, J. E. and Osborne, J. W. The adsorptive characteristics of proteins for polystyrene and their significance in solid-phase immunoassays. **Anal. Biochem.** (1980) 105: 375.
94. Engvall, E. and Perlmann, P. Enzyme linked immunosorbent assay, ELISA, III. Quantitation of specific antibodies by enzyme labelled anti-immunoglobulin in antigen coated tubes. **J. Immunol.** (1972) 109: 129.
95. Ercegovich, C. D., Vallejo, R. P., Getting, R. R., Woods, L., Bogus, E. R. and Mumma, R. O. Development of a radioimmunoassay for parathion. **J. Agric. Food Chem.** (1981) 29: 559.
96. Langone, J. J. and Van Vunakis, H. Radioimmunoassay for dieldrin and aldrin. **Res. Comm. Chem. Pathol. Pharmacol.** (1975) 10: 163.
97. Yalow, R. S. Radioimmunoassay: A probe for the fine structure of biologic systems. **Science** (1978) 200: 1236.
98. Esser, P. **Nunc Bulletin, No. 6.** (1988) Nunc Lab., Demark.
99. Cesbron, J. Y. and Capron, A. Platelets mediate the action of diethylcarbamazine on microfilaria. **Nature** (1987) 325: 533.
100. Catt, K. and Tregear, G. W. Solid-phase radioimmunoassay in antibody-coated tubes. **Science** (1967) 158: 1570.
101. Engvall, E. and Perlmann, P. Antibody production in mice: III. The suppressive effect of antibody on the initiation of secondary immune response. **Immunochemistry** (1971) 8: 871.
102. Van Weemen, B. K. and Schuurs, A. H. W. M. Immunoassay using antigen-enzyme conjugates. **FEBS Lett.** (1971) 15: 232.
103. Prisloo, S. M. and De Beer, P. R. Gas chromatographic relative retention data for pesticides on nine packed columns: I. organophosphorus pesticides, using flame photometric detection. **J. Ass. Off. Anal. Chem.** (1985) 68: 1100.

104. Ripley, B. D. and Braun, H. E. Retention time data for organochlorine, organophosphorus, and organonitrogen pesticides on SE-30 capillary column and application of capillary gas chromatography to pesticide residue analysis. **J. Ass. Off. Anal. Chem.** (1983) 66: 1084.